THE STABILITY OF WOOD RESIN COLLOIDS IN PAPER MANUFACTURE

UNIVERSITY OF TASMANIA

Roland Arthur Lee, BSc (Hons)

Submitted in fulfilment of the requirements

for the Degree of

Doctor of Philosophy

School of Chemistry

University of Tasmania

Hobart, Tasmania, Australia

April 2012

Declaration of originality

This thesis contains no material which has been accepted for the award of any other higher degree or graduate diploma in any other tertiary institution, and to the best of my knowledge, this thesis contains no material previously published or written by another person, except where due reference is made in the text of the thesis.

Statement of authority of access

This thesis may be made available for loan and limited copying in accordance with the Australian Copyright Act of 1968.

Statement of ethical conduct

The research associated with this thesis abides by the international and Australian codes on human and animal experimentation, the guidelines by the Australian Government's Office of the Gene Technology Regulator and the rulings of the Safety, Ethics and Institutional Biosafety Committees of the University.

Roland Arthur Lee 22 April 2012

Journal papers

R. Lee, K. Stack, T. Lewis, D. Richardson, G. Garnier, Study of pitch colloidal stability using a photometric dispersion analyser, APPITA Journal, 63 (2010) 387-391.

R. Lee, K. Stack, T. Lewis, D. Richardson, G. Garnier, Pitch deposition at the solid-liquid interface: effect of surface hydrophobicity/ hydrophilicity and cation specificity, Colloids and Surfaces A: Physiochemical and Engineering Aspects, 388 (2011) 84- 90.

R. Lee, K. Stack, T. Lewis, D. Richardson, G. Garnier, Effect of shear, temperature and pH on the dynamics of salt-induced pitch coagulation, Colloids and Surfaces A: Physiochemical and Engineering Aspects, 396, (2012) 106–114.

R. Lee, K. Stack, T. Lewis, D. Richardson, G. Garnier, Structure of wood extract colloids and effect of $CaCl_2$ on the molecular mobility**,** Nordic Pulp and Paper Research Journal, accepted for publication 20/1/12

Peer-reviewed conference papers

R. Lee, K. Stack, D. Richardson, T. Lewis, G. Garnier, Photometric Dispersion Analyser (PDA) to quantify pitch coagulation kinetics, 63rd Appita Annual General Conference, Melbourne, 2009, pp. 259-265.

R. Lee, K. Stack, T. Lewis, G. Garnier, D. Richardson, T. Van de Van, Measurement of pitch deposition by impinging jet microscopy: Effect of divalent salts, 64th Appita Annual General Conference, Appita, Melbourne, 2010, pp. 273-279.

R. Lee, K.S.D. Richardson, T. Lewis, G. Garnier, Aggregation studies of pinus radiata wood extractives under increased system closure., 65th Appita Conference & Exhibition, APPITA, Rotorua, New Zealand, 2011.

Abstract

Within the pulp and paper industry, the recycling of water to reduce water consumption leads to accumulation of colloidal material in the process water and greater risk of deposition. Resinous materials, arising from the wood extractives released during papermaking, form colloidal particles in solution that agglomerate and deposit onto the different surfaces within the mill. The formation of the resinous deposits, known as pitch, can be detrimental to the paper quality, process control and efficiency. A major factor in the colloidal stability of these substances is the presence of natural polymers originating from the wood and salts that accumulate in the process water as a result of increased system closure. To date, most work has looked at the stability of northern hemisphere woods. The work of this thesis explores the stability and formation of southern hemisphere *Pinus radiata* wood resins through the application of novel techniques. It investigates the factors that affect the stability of wood extractive colloids under varying conditions of ionic strength, ionic valency, shear, temperatures, pH, and mixtures of cations and wood polymers released from *Pinus radiata* thermomechanical pulp.

Electron paramagnetic resonance (EPR) was used to study model wood extractive colloids. Nitroxides were chosen as EPR probes to gain a greater understanding of the different interior vs. surrounding parts of the colloidal droplet in order to assess current proposed models of the structure of the wood extractive colloid. Additionally, salt was added to solution in order to understand the macroscopic environmental interactions that the colloid experiences. A revised model for the colloid structure has been proposed to better explain the behaviour of the wood extractive colloids.

Through the use of the photometric dispersion analyser (PDA), the coagulation kinetics for wood resins were determined. The coagulation kinetics allowed the stability factor (W) for the addition of various concentrations of salt to be determined with variation in a number of supernatant physiochemical factors (salt type, valency, temperature, pH, shear and simultaneous addition of multiple salts).

Coagulation of a colloidal wood extractive solution by a single salt was found to follow the Schultz-Hardy rule, with the critical coagulation concentration (CCC) for a salt strongly influenced by salt valency (z). Addition of trivalent salts indicates that the affinity of aluminium and iron salts for the colloidal wood resin surface is greater than their affinity for hydrating water molecules.

Changes in temperature and pH of an aqueous colloid suspension were observed to affect the concentration of salt required to destabilise the colloid, as expected from DLVO theory. An increase of the supernatant's pH resulted in an increase in the CCC for calcium. An increase in temperature

resulted in an increased CCC for all salts tested. The degree of variation in CCC with temperature was found to be valency dependant.

The stability of the colloidal wood resins was found to be highly dependent on the shear within the system. This aspect had not been reported before, particularly the effect of shear and metal ion valency. Increased shear within the system was found to decrease the CCC. The effect was found to be dependent on both the salt type and the valency of the metal ion. A change to the DLVO theory has been postulated to explain this. It is proposed that hydrodynamic forces need to be included in the relationship between the CCC and the counter ion charge: $CCC \alpha (\Omega z)^{-6\tau}$ or $CCC \alpha [z^{-6\tau} + \Omega]$; where $\Omega = f(G)$ and $\tau = g(G)$.

The addition of multiple salts simultaneously to solution (essential for industrial colloids) was explored. The interaction between multiple salts and the colloids resulted in complex behaviour, both in destabilisation and restabilisation of the colloid. A nonlinear decrease in the CCC was found. Restabilisation of the colloids was observed to occur at high salt concentrations when two salts of differing valency were added. This restabilisation is thought to occur as a result of charge reversal mechanism by which metal cations are adsorbed onto the colloid surface.

The coagulation kinetics for the addition of water-soluble wood polymers to the wood resins dispersions was determined in the same manner as the addition of salt through the use of the PDA. The interaction between the wood resin and the water-soluble wood polymer showed complex behaviour with two stages of destabilisation of the wood extractive colloids, separated by an apparently stable region. The behaviour was typical of aggregation by synthetic polymers: first, polymer bridging at low polymer additions caused colloid destabilisation with subsequent steric stabilisation of the colloids at medium concentration of the polymer, and then depletion flocculation was followed finally by depletion stabilisation at higher polymer concentrations.

The deposition rate of colloidal wood resin onto hydrophobic and hydrophilic model surfaces was measured at the solid-liquid interface by impinging jet microscopy (IJM) and the effect of cation specificity in solution on deposition was quantified. On both model surfaces, the wood resin deposition was slightly faster with calcium ions than with magnesium at the same salt concentration (800 mg/L). The rate of colloidal wood resin deposition on hydrophobic surfaces was far greater (up to a 2.5 times) than on hydrophilic surfaces for both salts. Film thinning, or spreading of the wood resin particles, occurred on the hydrophobic surfaces with calcium and to a lesser extent with magnesium salt. The formation of oil films has not been previously reported.

ACKNOWLEDGEMENTS

First, I wish to thank my supervisory team, Dr. Karen Stack, Dr. Trevor Lewis, Dr. Desmond Richardson and Professor Gil Garnier, for their exemplary help, support, guidance, patience and encouragement throughout my project. Without your help, I would not have had the tenacity to finish it.

I would also like to extend my gratitude to my international collaborators, Professor Theo Van de Ven, Professor Nicholas Turro, Associate Professor Steffen Jockusch and Professor Maria Ottaviani, for their help, expertise, inspiration and access to various pieces of experimental equipment. Further thanks must go to external and technical staff, for assistance with specific experimental techniques.

I would like to give a special thanks to Professors Emily Hilder and Gregory Dicinoski for their assistance in the finalization of this thesis. As well, to Professors Martin Hubbe and Anna Sunberg, I give my deepest appreciation for your attention to detail in the final review process.

Thank you to the University of Tasmania, the Australian Research Council and Norske Skog for providing funding, for the project itself as well as a post-research graduate scholarship (LP0882355).

I would also like to thank the members of the Pulp and Paper Research Group of the School of Chemistry at the University of Tasmania, particularly to my fellow research students and staff. As well, I extend my thanks to the Central Science Laboratory at the university, APPI, Monash University Chemical Engineering Department. All their help has been greatly appreciated.

Lastly, I would like to say thank you to my friends and family who have supported and encouraged me throughout this work.

CONTENTS

ABBREVIATIONS

Symbols given in equations defined in Appendix 1

BSA	Bis-trimethylsilyl acetamide
C	Concentration of water soluble wood polymers at equilibrium (mg/L)
CCC	Critical coagulation concentrations
DLVO theory	Derjaguin and Landau, Verwey and Overbeek theory
EPR	Electron paramagnetic resonance
G	Shear
K_L	Langmuir constant related to the affinity of the binding sites and the energy of adsorption (L/mg)
NMR	Nuclear magnetic resonance
PDA	Photometric dispersion analyser
Q	Amount of wood polymers adsorbed per unit mass of the wood resins (mg/g)
Q_m	Maximum adsorption capacity (mg/g)
Ratio	PDA signal (V_{rms} / V_{DC})
SAXS	Small angle x-ray scattering
TMCS	Trimethylchlorosilane
TMP	Thermo mechanical pulp
$T_{polymer}$	Time required for wood polymer solutions
T_{water}	Time required for distilled water
V_A	Van der Waals attractive forces
V_{DC}	Direct current (DC) voltage
V_{RMS}	Root mean square (RMS) value of the fluctuating (AC) signal
V_R	Electrostatic repulsion
W	Colloid stability ratio
η_r	Relative viscosity
Σ	Efficiency of coagulation

CHAPTER ONE

INTRODUCTION

Availability of fresh water is becoming a significant problem on a worldwide scale. The problem is particularly noteworthy in Australia, which is often identified as the driest inhabited continent [1]. It is crucial that reduction of water usage becomes a priority. Significant volumes of water are used in the pulp and paper industry from the pulping of wood chips through to the formation of the paper. World's best practice for water consumption in manufacture of mechanical paper grades is around 10 m^3 $tonne^{-1}$ of product [2]. Though the most water-efficient of Norske Skog's Australian mills operates at this level, climatic conditions are causing additional water shortages, and even further reductions would be welcome.

It is imperative for the industry to address general environmental concerns and the reduction of consumption for current and future pulp and paper mills. Norske-Skog Paper operates two pulp and paper mills in Australia, one at Albury in New South Wales and the other at Boyer in Tasmania. Both mills are located on major rivers, the Murray River and the Derwent River respectively, and both draw large volumes of water from their associated water systems. The Albury mill has a water usage of 10 m^3 per tonne of paper produced while the Boyer mill uses 30-40 m^3 per tonne of paper. Each mill has a target to significantly reduce water usage to bring them in accordance with world's best practice or better, in both economic and environmental terms.

One practical manner in which the reduction of fresh water may be achieved is increased recycling in the process water loop. However, increased recycling leads to a rise in the amount of organic and inorganic material present in the process water. Accumulation of organic and inorganic material has been shown to cause deposits, poor process control, loss of efficiency and product quality. Problems with extracted wood resin colloidal deposits and metal soap deposits already cost the pulp and paper industry in Australia an average of two to ten million dollars per annum in lost production. The situation will be greatly exacerbated with increased process water

recycling. This is particularly important for the Albury Paper Mill located in the Murray Darling Basin, where water quality and availability are significant environmental issues.

Currently in the mill, there are a number of different mechanisms that are used to facilitate the removal of the wood resins from solution. One example of this is the fixing of wood resin colloids to the wood fibres with the wood resins being accumulated onto the paper sheet. Fixation is achieved through the addition of synthetic polymers and other filler additives to the solution. However, there are a number of downstream issues associated with the de-adsorption of the wood resins to other surfaces such as printing presses, thus creating other deposition problems. To allow a greater degree of water recycling, additional work is now needed to understand the complex interactions that take place between these undesirable organic and inorganic materials. These include the factors that control formation and stability of the colloidal material that make up the major deposits in the mill.

Most of the studies investigating the factors affecting colloidal stability of both salt and dissolved organic extracts on wood resin deposition have been carried out on northern hemisphere wood, such as *Picea abies* (Norway Spruce). In the large scale plantations of Australia, *Pinus radiata* is the predominantly grown species and constitutes the basic fibre source for a number of substantial pulp and paper industries [3]. However, little is understood about the stability of wood resin in the presence of extracted wood polymers under the high ionic strength conditions typical of system closure, originating from southern hemisphere wood types, such as *Pinus radiata*. Due to the importance of *Pinus radiata* to the pulp and paper industry in Australia, this thesis will focus on the extractives from its thermo mechanical pulp (TMP).

1.2 AIMS

The major aims of this thesis are to:

1. Better understand the factors that result in destabilisation of the wood resin colloids from *Pinus radiata* under high levels of process recycling.

2. Investigate deposition of *Pinus radiata* wood resins onto different surfaces under hydrodynamic shear conditions.
3. Better understand the structure of the wood resin colloids.

1.3 APPROACH

The colloidal form of wood resins is exceptionally problematic as it is the cause of troublesome deposits. These result from the colloids becoming destabilised and aggregating unpredictably. To better understand the factors that result in the destabilisation of wood resin colloids, coagulation kinetics for the wood resins will be studied using a photometric dispersion analyser (PDA). The factors that will be investigated include:

- Addition of various metals ions at different valencies and determination of their critical coagulation concentrations (CCC);
- The effect of multiple salts present in solution simultaneously;
- The effect of different physiochemical factors such as pH, temperature and shear on the critical coagulation concentrations (CCCs) for various salts;
- The effect of dissolved wood polymers from *Pinus radiata* TMP under different ionic strengths.

In the mill, the wood resins are found to deposit onto most surfaces. There are a number of key factors involved in deposition, including hydrodynamic conditions in the region of the surface, and particle transport, adsorption and adhesion. It has been found that the form of the deposits on the surfaces, either calcium soaps or resinous deposits, affect their removal and the amount of material deposited. Impinging jet microscopy will be used to study the deposition behaviour of *Pinus radiata* wood resins under hydrodynamic conditions onto hydrophilic and hydrophobic surfaces.

A more detailed look at the colloidal structure building on the work by Qin et al. [4], Nylund et al. [5] and Vercoe et al. [6] will be undertaken to further develop an understanding as to why variation in the composition of the colloids results in changes in their stability. The internal

geometry of the wood resin colloids will be examined using electron paramagnetic resonance (EPR) by placing nitroxide probes of varying polarity within the colloid. Given the concentration of the probes compared to the wood resins, it is thought that no change in the structure will result. The coordination of the major components that are present in the wood resins (triglycerides, fatty acids and resin acids) in the macroscopic environment within the colloid will be investigated. In conjunction with the EPR measurements, surface tension measurements will be used to ascertain the compounds at the surface of the colloid.

CHAPTER TWO

LITERATURE REVIEW

2.1 WOOD RESIN

The wood resins extracted during the pulping process are made up of a number of different classes of compounds: resin acids, fatty acids, triglycerides and sterols, as shown in Table 2.1. Within the aqueous environment, these form a colloidal mixture that causes major downstream problems in the paper making industry.

Table 2.1: Extractives from Pinus radiata by GC [7]

Extractive	% Total Composition
Resin acids	58.8
Fatty acids	11.2
Esters as Triolein	7.6
Phenolics	5.2
Unsaponifiables (i.e. sterols)	16.3
Essential Oils	0.8

The relative composition of the wood extractives in the colloids changes with various growth variables, including the species, season, growth site, etc. The composition of the colloidal wood resins has been shown to have an impact on their stability in solution [8]. Table 2.2 shows the relative compositions of the wood resins from *Pinus radiata* and northern hemisphere spruce. From this, it is apparent that the wood resins derived from *Pinus radiata* have a much higher concentration of resins acids and lower triglycerides than the spruce extracts.

Table 2.2: Comparison of wood extractives from Pinus radiata and spruce.

Wood Source [a]	% Fatty Acids	% Resin Acids	% Triglycerides and steryl esters	References
P. radiata extract	10	53	37	McLean et al. [8]
Spruce	6	16	78	Qin et al. [4]

There are a number of different components that make up these classes, exemplified in Figures 2.1, 2.2, 2.3 and 2.4. As noted in Figure 2.1, the resin acids have a number of functional groups with a carboxylic head group. Nearly all have the same basic skeleton: a 3-ring fused system with the empirical formula $C_{19}H_{29}COOH$. The different types of resin acids differ in their degree of saturation.

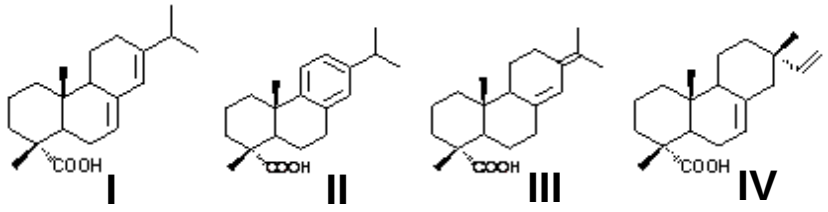

Figure 2.1: Examples of resin acids present in wood resin colloids. I: Abietic acid, II: Dehydroabietic acid, III: Neoabietic acid, IV: Isopimaric acid.

On the other hand, the fatty acids present in the wood resin colloids are made up of a carboxylic acid (head) with a long un-branched aliphatic chain (tail) (Figure 2.2). The tail can be partially unsaturated depending on the type of fatty acid, as shown in Figure 2.2.

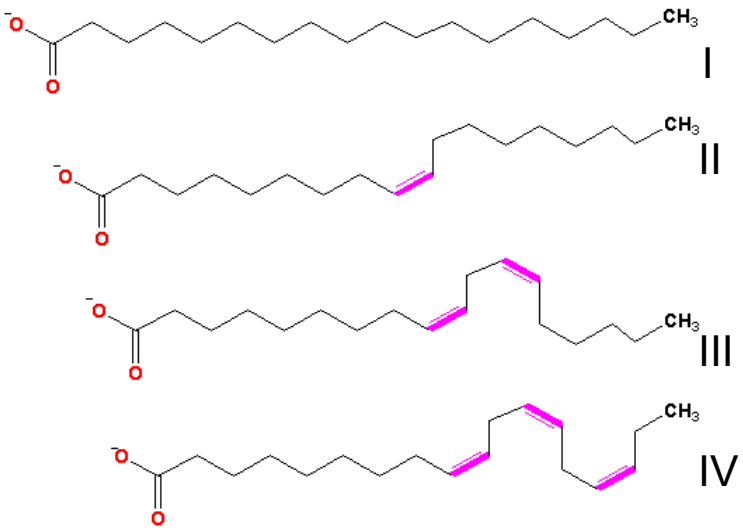

Figure 2.2: Examples of fatty acids present in wood resin colloids. I: Stearic acid, II: Oleic acid, III: Linoleic acid, IV: Linolenic acid.

The third main class of compounds that make up the wood resins are the triglycerides. They are comprised of straight chain fatty acids esterified at the carboxylic head group to a glycerol backbone, as shown in Figure 2.3. The fatty acids shown can be replaced to represent any fatty acid present in wood resins.

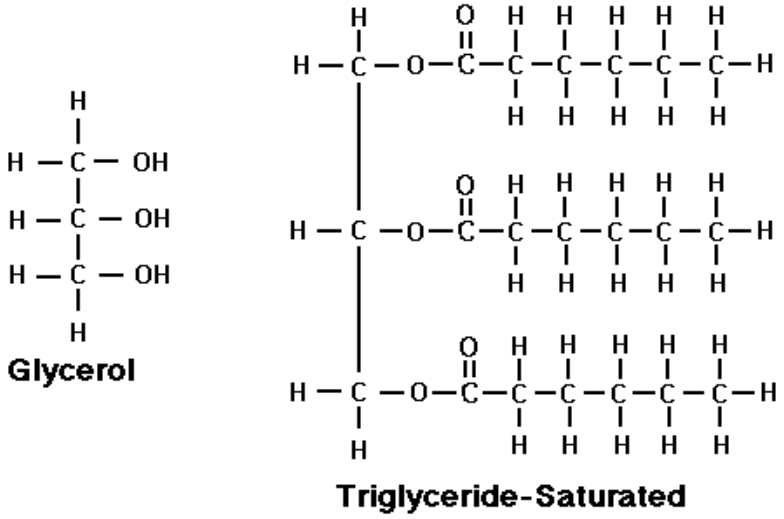

Figure 2.3: Example structure of triglycerides present in wood resin colloids.

The fourth main class of compounds that make up the wood resins are the sterols and sterol esters. The sterols and sterols esters have a main skeleton similar to that seen for the resin acids with varying numbers of fused rings and side changes with a hydroxyl head group, as shown in Figure 2.4. The formation of the sterol ester occurs with the esterification of the hydroxyl group to phospholipids or, in plants, with carbohydrate (replacing the R group in Figure 2.4 (II)).

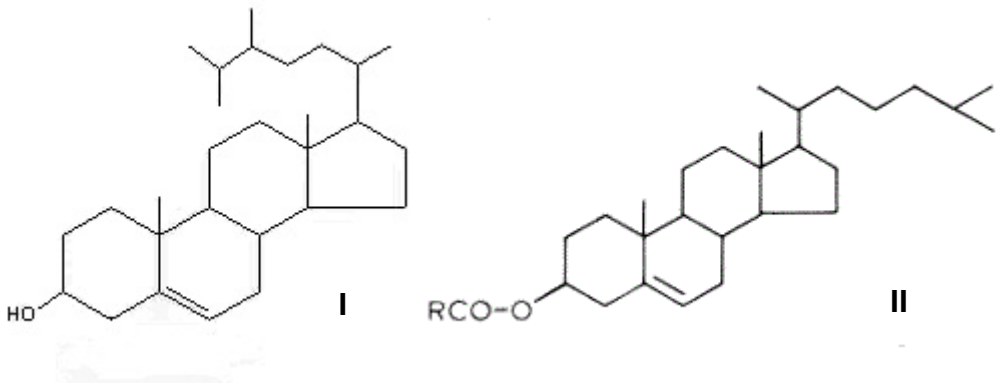

Figure 2.4: Example structure of sterols (I) / sterol esters (II) present in wood resin colloids.

For both the resin acids and fatty acids, the compounds have characteristics of a hydrophobic tail and a hydrophilic head [9]. The hydrophilic head group on both acid groups allows the compounds to be solubilised at higher pH due to deprotonation [9]. The pK_as of the resin acid and the fatty acid components are in the 6.8-7.3 and 7.4-9.9 range, respectively [10]. The pK_as for the fatty acids has been shown by Kanicky and Shah[11, 12] to be dependent on the "tail" length (increasing size results in increasing pK_a)[12] and degree of saturation (decreasing saturation results in increasing pK_a)[11], McLean et al. [9] pointed out that this occurs up to the critical micellar concentration (CMC) at which point the colloidal pK_a takes effect and the pK_a for the fatty acids becomes constant[9], Kanicky et al. indicated that the pKa for the fatty acids becomes a constant above a certain chain length [11]. The pK_a for the resin acids is noted to increase with reduction of the double bonds associated to the side chain on the furthest fused ring from the carboxylic acid group[8].

On the other hand, with the triglycerides and phytosterols (sterols / sterol esters), the solubility is greatly reduced, and the compounds are commonly hydrophobic in nature. The triglycerides are a common form of energy storage in plants and animals [13]. In plants, the sterols and sterol esters are commonly referred to as phytosterols and a range of different types are commonly found – they are amphipathic lipids. These compounds act as a structural component in the cell membrane[13].

The relative composition of the wood extractives is found to differ with wood type [14-17], growing site [17] and season [18, 19]. For example, southern hemisphere *Pinus radiata* contains significant amounts of resin acids in contrast to the northern hemisphere spruce which contains only very small amounts of resin acids and significant amounts of triglycerides [20]. Qin et al. [4] showed that the ratio of the component compounds that make up the TMP wood resins from northern hemisphere spruce is 5.5: 2.5: 0.25: 1.25: 0.5 (triglycerides: sterol esters: sterols: resin acids: fatty acids). In contrast, the relative abundances for the various colloidal components for southern hemisphere *Pinus radiata* (Table 2.1) show that the resins extracted from the *P. radiata* is much lower in the non-polar components (triglycerides and sterol esters) and higher in the relative concentration of the resin acids as shown in Table 2.2.

Numerous researchers have demonstrated that the relative composition of the wood extractives plays a major role in their colloidal stability [8, 21-24]. The variation in the stability of the wood resins may result from the different pK_as of the component resin acid (7.1-7.3), saturated fatty acid (7.1-10.2) and unsaturated fatty acids (6.8-8.3) [10]. McLean suggests that the variation in the stability of the colloids with composition is related to the solubility of the components through pH and temperature of the solution [17, 23].

McLean also indicates with changes in pH, there is a change in the interactions within the wood resins that lead to deposition as a result of variation in the physiochemical properties of the components [23]. Additionally, if the colloidal system becomes primarily resin acid or triglycerides, then deposition will occur as a consequence [25]. This indicates that it is not merely a result of the properties of the components within the colloid.

Sundberg et al. [26] showed that the phase distribution of the wood resin components is dependent on the pH. They report that at pH 3, no resin or fatty acids are dissolved in the water phase. As the pH increases, the resin acids are incorporated into the dissolved phase at lower pH than fatty acids. Fatty acids of shorter chain length and greater unsaturation dissolve more than their saturated counterparts. The concentration of NaCl was noted to have a dampening effect on the dissolution of the resin and fatty acids. Contrary to the work by McLean et al. [23], the phase distribution as a function of temperature did not show any large differences [26].

The work conducted by MacNeil et al. [27], looking at the phase distribution of fatty acids and resin acids in the deinking processes of paper recycling, indicates that as the pH increased the resin acids were at least partially dissolved even at high calcium ion concentrations. Dehydroabietic acid, noted to have the highest solubility, is also not precipitated to the same degree as other resin acids in the presence of calcium. On the other hand, the calcium concentration was found to impact the solubility of the fatty acids, rendering them practically insoluble at higher concentrations [27].

It has been noted previously by Odberg et al. [28] and Palonen et al. [29] that the fatty acids and resin acids commonly found in the wood resins act as surfactants under the conditions of the mill. Odberg et al. [28] point out that the solubility of the un-saponifiable components increases

in the presence of different acids. The solubility of the different components on addition of salt to solution changes with concentration. Odberg also showed that there is a large increase in size of micelles formed as the concentration of NaCl in solution increases. On the other hand, Palonen et al. [29] showed increased solubilisation of sodium oleate at low concentrations of NaCl addition, as a result of reduced repulsive forces. The solubilisation decreases as the NaCl concentration increases as the salt concentration increases to the point the agglomeration predominates. For sodium abiete, there is a continuous decrease in the solubility with the addition of sodium chloride. The micelles of the mixed oleate and abieate were found to be highly stable in solution and more stable than the micelles formed from the pure components [28, 29].

2.2 STRUCTURE OF WOOD RESIN COLLOIDS

Qin et al. [4], Nylund et al. [5] and Vercoe et al. [6] proposed similar models for the colloid structure for both Southern hemisphere *Pinus radiata* and northern hemisphere spruce wood extracts. The proposed models of the wood extractive colloid show the particles are made up of an inner hydrophobic core consisting of the non-polar components, such as steryl esters and triglycerides, and an outer layer of resin acids and fatty acids (as seen in Figure 2.5). The outer layer determines the surface properties of the resin particles [30-32]. An average-sized colloidal droplet of spruce TMP was proposed to have a diameter of 0.24 μm for the interior domain and the thickness for the outer film is less than 0.01 μm [4, 33, 34].

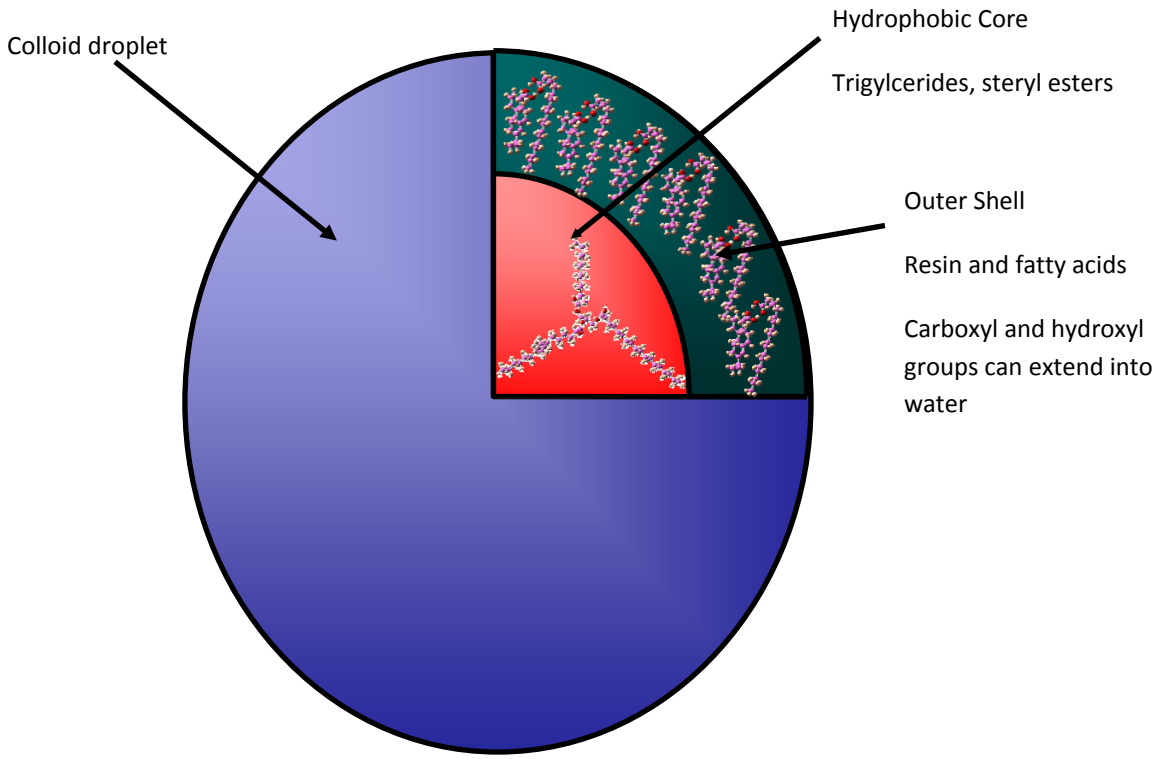

Figure 2.5: Model of the wood resin colloid, with non-polar core containing triglycerides and a polar shell made up of fatty acids and resin acids [6].

Nylund et al. [5] showed with the use of surface tension measurements that the carboxylic acid head groups of the resin acids and fatty acids orientate to the solution on account of the extensive acid-base reaction between the colloid and the supernatant solution. However, the microstructure of the outer polar shell is not elucidated, and the effect of the triglycerides on the surface properties is unexplored.

2.2.1 TECHNIQUES TO STUDY COLLOID STRUCTURE

A number of techniques are available to investigate the structure of colloids, such as nuclear magnetic resonance (NMR)[35, 36], small angle x-ray scattering (SAXS) [37-39] and electron paramagnetic resonance (EPR) [39-41]. EPR has been used to study the colloid structure of

pharmaceuticals[42, 43], reverse micelles [44] and various other micelles/vesicles[45]. EPR has been used not only to study the colloid substructure but also the molecular mobility, polarities and changes in viscosity within the colloid[41].

The approach taken by many researchers is to assess the changes to the base free spin EPR spectra for a free radical spin probe. Weber et al. [41] noted that it was possible, by analysis of spectra obtained from both frozen micelle solutions (at or below the melting point of the solvent) and free solutions of micelles, to gain information about the mobility of ions in the electrical double layer, core of the colloidal particles and the bulk solution. In the fluid solution, the viscosity for micelle cores may be up to 30 times that for the water and close to the surface the viscosity is increased by factors between 10 or 20 greater than the water. These viscosities change with the surfactant's chain lengths and the atomic number for the counter ion. Furthermore, it was noted that the mobility within the micelles decreases with an increase in the atomic number of the counter ion [41].

In frozen micelle solutions, it is seen that there is no significant movement in the core of the micelle up to the macroscopic melting point. However, in the electrical double layer associated with the colloid, mobility is noted at temperatures > 240 K [41]. This is explained by the local high concentration of ions in the double layer depressing the melting point. This and similar techniques for the elucidation of the microenvironments of emulsions have been used by numerous other groups [42-44, 46, 47]. Zielinska [48] used this to assess the polarity and the viscosity for microemulsions of *N*-alkyl-*N*-methygluconamides as water-in-oil, oil-in-water with *n*-alcohols or *iso*-alcohols as co-surfactants.

Gandini [39] found with the combination of SAXS and EPR that it is possible to estimate the diffusion of compounds into the core of micelles and the average polarity, by monitoring the nitroxides in the surfactant 3-(*N*-hexadecyl-*N*,*N*-dimethylammonium) propane sulfonate (HPS) colloids in the presence of porphyrins. For all porphyrins, a decrease in the mobility was observed indicating greater packing of the porphyrin-HPS micelles. The utilisation of SAXS in this allowed the elucidation of the micellular structure of porphyrin/HPS colloids, which was found to be quite similar to that observed for pure HPS colloids. It is also noted that changes to

the pH are not seen to affect the features of either the core or the polar shell of HPS micelles significantly [39].

Griffiths [48] used 16-DOXYL stearic acid methyl ester as an insoluble spin probe. As a result of this insolubility, the probe was incorporated into the micelles, reflecting the hydrophobicity of the microenvironment within the internal region of the colloids. It was noted that changes to the compounds that make up the colloidal particles affect the spin freedom of the probes, however this was not affected by changes to the pH. From work with small angle neutron scattering (SANS), it was noted that the presence of the spin probe had no effect on the structure or size of the particles. Other such investigation with the use of EPR spin probes have been conducted looking at the structure of various colloidal materials, it has proved to be a powerful tool in such investigations. While the choice of spin label is highly important to understanding the different colloidal regions, few interactions between the colloidal substances and EPR spin probes are known to result in changes in variation to the colloidal structure, partially as a result of the small concentrations used and the stability of the nitroxides utilised [41, 44-46, 49-55]. Although this is a very useful technique for structural and viscosity changes within the micelle and the electronic double layer, it is important to note that the interpretation of results is not trivial [52, 56].

When changes occur in the macroenvironment, its effect on the microenvironment where these probes exist will then affect the spectrum's amplitude, peak width and shape. The changes to these specific spectrum characteristics can be interpreted in order to better understand alterations to the microscopic environments within the colloid [57-60].

2.3 FACTORS AFFECTING COLLOIDAL STABILITY OF WOOD RESINS

Problems occur when wood resin deposits onto the moving parts of the paper machine and cause catastrophic breaks of the paper sheet moving at speeds up to 2000 m/min. Increased water recycling being undertaken by many pulp and paper mills only aggravates the problem by

increasing the concentration of wood extractives and substances, such as dissolved organic compounds and inorganic salts, that affect colloidal stability in the process water.

2.3.1 STABILITY OF COLLOIDS - THEORY

Appendix 1 gives relevant information on symbols used in the following theoretical equations.

Destabilisation of the particles occurs as the salt concentration in solution increases, resulting in reduction in the electrostatic repulsion (V_R) between the particles and manifestation of the van der Waals attractive forces (V_A). Where the repulsive forces and the attractive forces equal each other, every interaction between particles results in permanent attachment. This point is termed the critical coagulation concentration (CCC) [61, 62]. The CCC can be considered a thermodynamic value, which is a function of the system composition. Using the classical DLVO theory (Equation 2.1), the colloidal stability and coagulation can be predicted from the interaction potential (V) between two colloids[61, 62]:

$$\mathbf{V = V_A + V_R} \qquad \textbf{Equation 2.1}$$

where the attractive potential (van der Waals attraction) (V_A) for small interparticle distances for equal spheres is:

$$V_A = -\frac{Aa}{12H} \qquad \textbf{Equation 2.2}$$

and the electrostatic repulsive potential (V_R) is:

$$V_R = \frac{32\pi\varepsilon a k_B^2 T^2 \gamma^2}{e^2 z^2} \exp[-\kappa H] \qquad \textbf{Equation 2.3}$$

where A denotes the Hamaker constant, z is the charge of the counter-ion, T is the temperature in Kelvin, a is the radius of the colloidal spheres, ε is the permeability of the dispersion medium, k

is the Boltzmann constant, e is the electron charge, H is the shortest distance between the Stern layer of two particles; κ and γ are defined by:

$$\gamma = \frac{\exp[ze\Psi_d / 2k_BT] - 1}{\exp[ze\Psi_d / 2k_BT] + 1}$$ **Equation 2.4**

$$\kappa = \left(\frac{2e^2 N_A c z^2}{\varepsilon k_B T} \right)^{1/2}$$ **Equation 2.5**

where c is the electrolyte concentration, N_A is Avogadro's number and 1/κ is the Debye length representing the double layer thickness. At the CCC, as defined above V =0, giving the following;

$$V = V_R + V_A = \frac{32\pi\varepsilon a k_B^2 T^2 \gamma^2}{e^2 z^2} \exp[-\kappa H] - \frac{Aa}{12H} = 0$$ **Equation 2.6**

and

$$\frac{dV}{dH} = \frac{dV_R}{dH} + \frac{dV_A}{dH} = -\kappa V_R - \frac{V_A}{H} = 0$$ **Equation 2.7**

From which κH=1 [61]; therefore,

$$\frac{32\pi\varepsilon a k_B^2 T^2 \gamma^2}{e^2 z^2} \exp[-1] - \frac{Aa\kappa}{12} = 0$$ **Equation 2.8**

Giving

$$\kappa_{(coagulation)} = \frac{443.8\varepsilon k_B^2 T^2 \gamma^2}{Ae^2 z^2}$$ **Equation 2.9**

Substituting Equation 2.5 for κ gives

$$CCC = \frac{9.85 \times 10^4 \varepsilon^3 k_B^5 T^5 \gamma^4}{N_A e^6 A^2 z^6}$$ **Equation 2.10**

At high potentials (typically 100mV) γ limits to 1, and at low potential it limits to $ze\zeta_d/4k_BT$. Equation 2.10 can then be simplified as:

$$CCC \propto \frac{1}{z^6}$$ **for high potentials** **Equation 2.11**

$$CCC \propto \frac{\Psi_d^4}{z^2}$$ **for low potentials** **Equation 2.12**

Equation 2.11 is known as the Shultz-Hardy rule[61, 62].

2.3.2 COAGULATION RATE - THEORY

The rate of coagulation of colloidal particles depends not only on the frequency of collision between particles but also on the particles having sufficient energy to overcome the repulsive energy barrier to coagulation. The rate of coagulation between two particles is given by the second order kinetic equation[61]:

$$\frac{dn}{dt} = -k_2 n^2$$ **Equation 2.13**

The energy barrier to coagulation can be reduced to zero with the addition of electrolytes which compress the electrical double layer. Assuming rapid coagulation to be diffusion-controlled (no energy barrier), the Smoluchowski equation gives the particle number as[61]:

$$n = \frac{n_o}{1+8\pi a D n_o t}$$ **Equation 2.14**

where n_o is the initial number of colloids. Combining Einstein's diffusivity equation ($D = k_BT/6\pi\eta a$) in Equation 2.13 and 2.14 and integrating yields the kinetic constant for fast coagulation (k^*):

$$k^* = \frac{4k_B T}{3\eta}$$ **Equation 2.15**

The colloid stability ratio, W, can be defined as [62]:

$$W = \frac{\text{Number of collisions between particles}}{\text{Number of collisions that result in coagulation}}$$ **Equation 2.16**

Following the addition of a salt to a solution, the growth of the colloids is proportional to the efficiency with which the colloids interact and form permanent attachments to each other. This allows us to find the stability factor (W) for a given addition of salt as follows[63]:

$$W = \frac{1}{\sigma} = \frac{k^*}{k_i}$$ **Equation 2.17**

where σ is the efficiency of coagulation. This can be expressed in terms of rate constants from the experimental results, where k* is the rate of fastest coagulation and k_i is the coagulation rate of interest. The efficiency of coagulation (σ) is proportional to the salt addition through V_R (Equation 2.3) as shown below[63]:

$$\frac{1}{\sigma} = 2\int_0^\infty \frac{\exp\left(V_R / k_B T\right)}{\left(u+2\right)^2} du$$ **Equation 2.18**

u is the dimensionless separation distance (u=2h/d, h is the separation distance, *d* is the diameter of the particle), k_B is the Boltzmann constant and T is the temperature. Gregory [63] points out that this calculation of σ is inappropriate for particle collisions that are a result of fluid motion, as it only takes into account thermal energy.

Reerink and Overbeek summarise[62]: "When there is no repulsion every collision of two colloid particles lead to coagulation (rapid coagulation). When the repulsive energy is not zero

only a fraction 1/W of collision leads to coagulation (slow coagulation)". Reerink and Overbeek also approximated the rate of coagulation as follows [61, 62]:

$$W \approx \frac{1}{2\kappa a}\exp\left[\frac{V_{\max}}{k_B T}\right] \qquad \textbf{Equation 2.19}$$

which can be rearranged to the following at 25℃ :

$$\log\ W = -x_1 \log c + x_3 \qquad \textbf{Equation 2.20}$$

where c is the electrolyte concentration and k_1 and k_3 are constants. This equation indicates that the log of stability for the colloid suspension is expected to vary linearly with the log of the salt concentration (stability curves).

The stability curves are used to give information about the colloids themselves, the point at which they intersect the x-axis is the CCC for the addition of the specific electrolyte to the colloidal solution.

The colloidal stability of a suspension is governed by the attractive and repulsive forces that exist between the particles that are defined by the Derjaguin and Landau, Verwey and Overbeek (DVLO) theory [64-66]. The particle surface charge, pH, ionic strength and additives that adsorb onto the particles all influence colloidal stability [67-70]. Furthermore, the shear [71-74] and temperature [8, 75-77] that the supernatant solution are subjected to will influence the rate of coagulation. Van de Ven and Mason [78] found the efficiency of coagulation is related to the shear rate of the system approximately proportional to $G^{-0.82}$. This is neglected in many of the studies on the collision rate and efficiency [73, 79-83]. Little or no work has been completed re-examining the experimental critical coagulation concentrations as a function of the shear [78, 84-86]. Furthermore, the effect of the type of salt and the valency on van de Ven's proposed shear perturbation is unreported. This is essential in understanding the effect that increasing electrolyte levels have on colloidal stability under non-ideal flow conditions.

2.3.3 CRITICAL COAGULATION CONCENTRATION

Past studies have focused largely on the effect of salt addition and stabilising polymers arising from synthetic polymers or from naturally occurring wood polymers that are extracted during the pulping process [67-70] on the wood resin colloid stability. The critical coagulation concentrations of salt required to aggregate wood resin dispersions found by various researchers (each under different shear conditions) are summarised in Table 2.3. However, it is noted that the pH and the salt valency greatly affect the concentration of salt required to destabilise the colloids [67-70].

Table 2.3: Salt concentrations necessary to destabilise wood resin dispersions reported by various researchers.

pH	NaCl	$CaCl_2$	$AlCl_3$	Reference
5	150mM	25mM		Sihvonen [68]
	200mM	10mM	0.02mM	Sundberg [69]
5.5	100mM			Mosbye [67]
6.4	600mM			Mosbye [67]
8	500mM	25mM		Sihvonen [68]

Sundberg et al. [69] noted that dispersions made from extracted wood resin behaved similarly to the colloids that occur within the mill process water streams [69]. It is noted by Sihvonen et al. [68] that the pH of the supernatant solution plays an important role in the stability of the wood resin colloids becoming more stable at higher pH. The critical coagulation concentration (CCC) for northern hemisphere spruce on addition of sodium ions to a colloid dispersion changes from 150 mM at pH 5 to 500 mM at pH 8 [68].

Interestingly, from comparison of the work by Sihvonen et al. [68] with the previous work completed by Sundberg et al. [69], it is apparent that the CCC varies even at the same pH [68]. The variation is a possible result of the changes in experimental method. With regard to the work completed by Sihvonen et al. [68], the samples underwent agitation for a short period of

time before concentration testing was completed [68]. In comparison, the method utilised by Sundberg et al. [69] tests the stability during continuous agitation.

It has also been found that at very high salt concentrations restabilisation of colloids may occur [87]. This restabilisation has not been reported before for colloidal wood resins. Dishon et al. [87] showed from atomic force microscope (AFM) measurements that the force between silica surfaces in NaCl, KCl and CsCl aqueous solutions have three distinct regions of destabilisation, stabilisation and destabilisation. As ion concentration increases, the electrostatic double layer repulsion is suppressed, resulting in the domination of the van der Waals attractive forces between the surfaces. At even higher salt concentrations, repulsion re-emerges because of surface charge reversal by excess adsorbed cations. The force curves were found to be practically identical for the three salts independent of their concentration [87].

2.3.4 SURFACE CHARGE

The surface charge of wood resin colloids is a result of the components that make up the outer layer of the colloid (Figure 2.5). As the pH of the solution increases, the carboxylic acid head groups of the fatty acids and resin acids are de-protonated (Figure 2.6) [9, 26]. The equilibrium is dependent on the concentration of hydroxide or hydrogen ions present in solution.

Figure 2.6: The effect of hydroxide ions on the carboxylic acid head groups

As the concentration of de-protonated head groups on the surface of the colloid increases, the effective charge of the colloid also increases [8]. The charge on the surface of the colloid

causes a redistribution of the dissolved ions adjacent to the colloid [61, 88], as shown in Figure 2.7.

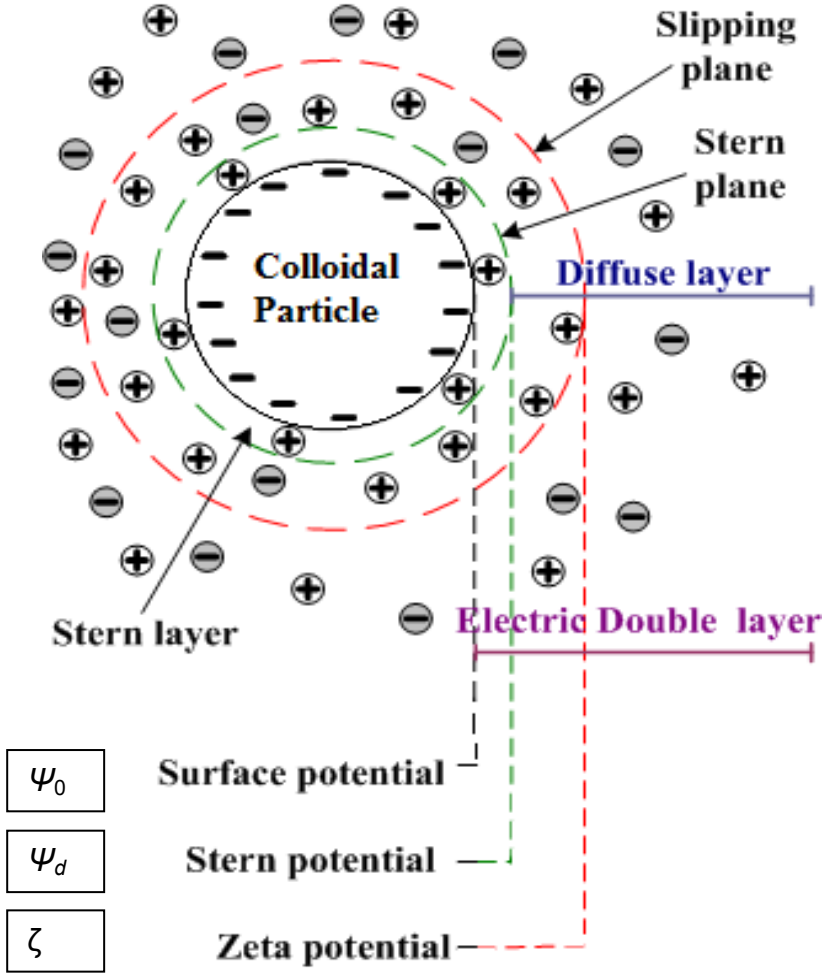

Figure 2.7: Electrical double layer associated with colloidal particle [88].

Surface charge can also result from ion adsorption onto the surface of the colloid. Some hydrolysed metal ions can be adsorbed very strongly, which can determine the resulting surface charge [89, 90].

Sundberg et al. [69] showed that as the pH of the colloidal solution increases, the electrophoretic mobility of the wood resin particles also increases. This increase in electrophoretic mobility indicates an increase in the surface charge of the particle. The change in the electrophoretic mobility was noted at low pH to increase dramatically up to pH 7. Following this, the change was noted to plateau [69].

2.3.5 TEMPERATURE

McLean et al. showed that at different temperatures of 20 and 50℃, the component that is responsible for the deposition changes between fatty acids and resin acids [8]. At 20 ℃, deposition is the result of an interaction between the fatty acids and resin acids, whereas at 50℃, it is resin acid alone that is responsible for the amount of deposition [8].

Contrary to the work by McLean et al. [8], Sundberg et al. [26] indicates that the phase distribution as a function of temperature did not show any large variation. This indicates that the changes in the deposition of the colloids may result from either changes in the colloidal viscosity or the thermal energy of the system [91]. This variation could be the result of differences in experimental method resulting in surface deposition.

2.3.6 SHEAR

One of the pre-requisites for particle-particle agglomeration is governed by the process by which the particles come together, which is related to the shear within the system [71-74]. The effect of shear on the rate of coagulation of colloidal particles has been shown to be dependent on a number of colloidal factors [61, 71-74, 91], including the radius of the particle and the concentration of particles in solution [72]. Back observed that the rate of shear for the system causes an increase in the accumulation of wood resin on surfaces, which reaches an optimum at about 1000 rpm (for a flat bladed propeller in a baffled Britt jar). An additional increase in the rate of stirring results in a decrease of the accumulation of resins on surfaces [92].

At higher shear rates, Hubbe et al. [93] observed that the decrease in the accumulation of wood resins can be associated with the tearing of the wood resin colloids into finely divided droplets.

2.3.7 RESTABILISATION OF WOOD RESIN COLLOIDS DUE TO THE ADDITION OF WOOD POLYMER

During the pulping process, there are a number of naturally occurring water-soluble wood polymers, which are extracted from the wood along with the wood resins. These extracted wood polymers are made up of a number of different constituents. The more common are neutral O-acetyl-galactoglucomannans, lignin, lignans, hydrophilic acids and colloidal fibre fragments [94]. These dissolved organic polymers have been shown for northern hemisphere woods to stabilise the colloidal wood resin in solution [95].

Most of the studies investigating the effect of dissolved organic extracts on wood resin deposition have been carried out on northern hemisphere wood [56-59, 85, 89, 90], such as *Picea abies* (Norway Spruce) [96, 97], *Populus tremula* (aspen) and *Pinus sylverstris* (pine wood) [98]. However, little is understood about the stability of wood resin in the presence of extracted wood polymers under the high ionic strength conditions typical of system closure, originating from southern hemisphere wood types, such as *Pinus radiata* [99, 100].

Sundberg [95] found that dissolved substances in unbleached thermomechanical pulp (TMP) stabilised wood resin colloids more efficiently than O-acetyl-galactoglucomannans and galactans, which are the main polysaccharides released in unbleached TMP. This suggests that other water-soluble material released from the pulp is also contributing to stabilisation of wood resins.

The water-soluble wood polymers comprise a mixture of several different organic compounds, primarily a mixture of hemicelluloses and pectins. Fengel and Wegener [101] summarised the polysaccharides in various woods, including both softwood, such as *Pinus radiata*, and hardwood species, such as *Eucalyptus regnans*. For both soft- and hardwoods, it was indicated that they contain acetyl groups attached to the polysaccharide backbone. This

attachement typically occurs to the xylans in hardwoods and to the mannans in softwoods. With the use of mass spectrometry and NMR, McDonald et al. showed that, for softwoods, hemicellulose present in *Pinus radiata* is a complex branched polymer sugar of galactomannan, xylan, arabinan and galactan. Furthermore, the acetyl substitution occurs at position 3 on the mannose residue [102, 103]. This is also shown for northern hemisphere spruce (*Pices abies*) by Hannuksela et al. with the substitution occurring at every tenth mannose in the back bone [104]. This acetylated formation was shown to be reactive to the bleaching process in the pulp and paper industry [105].

It has been found that changes in the chemical structure of hemicellulose occur on bleaching and alkali treatment [22, 95, 105-107]. Alkaline peroxide bleaching of TMP causes deacetylation of O-acetyl-galactoglucomannans, adsorption of dissolved galactoglucomannans on the fibres and release of polygalacturonic acid from fibres. The result is a decrease in mannose and glucose in the dissolved organics in the water phase and an increase in galactouronic acid compared to unbleached TMP [70, 108, 109].

Sundberg [95] showed a variation in the effect of the extracted wood polymers on the stability of the wood resin colloids, between unbleached TMP and those from bleached TMP. With unbleached TMP, wood polymers showed greater effectiveness in stabilising wood resins against NaCl and $CaCl_2$. The wood polymers extracted from bleached TMP provided some stability against aggregation of wood resins with NaCl but not $CaCl_2$. This indicates that the acetylation of the hemicellulose and chemical makeup of the branch or substitution group are important in the stabilisation properties of polysaccharides released in pulping [22, 95, 105-107].

Interestingly, de-acetylated and O-acetyl-galactoglucomannans are both effective stabilisers, while polygalacturonic acid provided stability of wood resin with NaCl but caused aggregation with $CaCl_2$ [95]. Contrary to the work by Sundberg [95], Otero [105] found that the polysaccharides from peroxide-bleached TMP were more effective against wood resin deposition than polysaccharides from unbleached TMP water. It was noted that a carbohydrate/wood resin ratio of 1.0 was needed to reduce wood resin deposit formation with unbleached TMP polysaccharides, while a ratio of 0.5 was needed for bleached TMP polysaccharides. These results are additionally affected by the concentration of salt present in solution. Johnsen [70]

found a carbohydrate/wood resin ratio of 4.0 was needed to stabilise wood resin against aggregation at high NaCl concentrations (up to 1000 mM).

2.3.8 TECHNIQUES FOR THE STUDY OF COLLOIDAL STABILITY

Colloidal stability has been studied with the use of numerous instrumental methods as shown in Table 2.4. Many of these techniques have been utilised to investigate the flocculation stability of the particles. With respect to the stability of the wood resin in solution, the critical coagulation concentrations (CCC) of various salts common in white water were studied (Section 2.3.3). Most commonly, the CCC studies for wood resins were conducted with the use of turbidity variations. Stability of the wood resins was reported with respect to the concentration of salt added [67-69]. Coagulation kinetics is a more accurate measure for determination of the CCC [61].

The photometric dispersion analyser (PDA) has been found to be a useful research tool to study colloidal aggregation in a wide range of applications including oils, clay dispersions and fillers and fines [77, 110-116].

Work by Hopkins et al. [113], in a study of flocculation under heterogeneous turbulence, noted that it was possible to look at both the growth and the distribution of sizes of colloids. Furthermore, it was noted that with an increase in primary particle concentration, the floc growth, mean size and variance are seen to increase. This is also the case in the event that the coagulation mechanism was switched from charge neutralisation to sweep floc [113].

It is noted that in the ratio distribution curves a number of regions exist: growth, steady-state, peak, and lower steady-state [113]. Furthermore, it is seen that the variation in these regions is proportional to the homogeneity of the colloidal flocs. This proportionality results in the distribution for the flocs being reduced with increases in the velocity gradient (G) due to greater particle collision rates with increased shearing rates [113]. These results hold well in comparison to those seen by other researchers in the field [77, 110-112, 117].

Table 2.4: Methods used for determination of colloidal stability.

Method	**Parameters measured**	**References**
Jar test	Hindered settling rate, supernatant turbidity, sludge volume, deposition, flocculation	[118]
Turbidity	Relative number of particles (flocculation and deposition)	[67-69, 119]
Photometric dispersion analysis	Fluctuations in relative number of particles, particle distribution, floc structure	[77, 110-116]
Centrifugal sedimentation	Flocculation and particle size distribution	[68, 69]
Static light scattering	Average scattered light intensity	[120]
Dynamic light scattering, photon correlation spectroscopy	Particle size	[120-126]
Non-imaging reflectance scanning laser microscopy Focused beam reflectance measurement	Distribution of chord lengths of particles	[127-129]
Backscattered laser light	Floc size from frequency analysis	[130]
Coulter counter	Distribution of particle size	[131]
Flow cytometry	Concentration, size distribution, flocculation	[132, 133]
Electron microscopy	Emulsion imaging, flocculation	[134, 135]
Ultrasound velocity scanning	Volume fraction of suspension as a function of height	[136]

For the major regions in the PDA curves, there are a number of calculations that can give information into the floc variation and growth. The slope of the initial growth region indicates the rate at which the flocs develop. In a similar manner, the PDA can be used to analyse the aggregation rates and dynamics of coagulation, as reported by Ching et al. [114]. The time-weighted ratio variance provides an indication of the severity of floc breakup as well as a measure of floc structural differences. According to Hopkins et al. [113] a small variation in signal signifies a tighter floc size distribution and a more homogeneous, dense, and less porous floc structure.

It is noted by Fernandes et al. [116] that PDA allows the average diameter for the particles or droplets to be found and thus the optimum dosage of flocculating agent, in spite of the inability to attain quantitative interpretations in terms of size distribution with the PDA.

Poraj-Kozminski et al. [115], working with alkyl ketene dimer (AKD) and precipitated calcium carbonate (PCC), were able to correlate the initial growth slope for coagulation and the maximum final value for ratio to time curves for different additions of AKD with variation to the floc growth. This then allowed the optimal addition of flocculent to be found. Above 10 mg_{AKD}/g_{PCC}, Poraj-Kozminski et al. [115] observed that the growth and maximum size for the flocs is unchanged, whereas below this, there is a dampening of the growth rate and maximum floc size reached.

2.4 COLLOIDAL WOOD RESIN DEPOSITION

It is noteworthy that the unstable wood resins can be found to adsorb onto many surfaces in the mill [18, 137, 138]. For particle-surface interactions, there are numerous significant factors involved in deposition, such as hydrodynamic conditions in the region of the surface, and particle transport, adsorption and adhesion [139, 140]. Furthermore, deposition rate will be affected by the particle-surface attractive and repulsive forces, similar to those noted previously for particle-particle interactions [61]. As before, these forces of attraction and repulsion are influenced by the particle charge, pH, ionic strength and additives that adsorb onto the particles

[67-70]. However, added to this, the surface-liquid interface itself will be affected by these changes separately from the colloidal particles [61].

It has been indicated by Qin et al. [4, 33, 34] that when a droplet of water was introduced to a surface covered with colloidal components, the wood resin contact angle and wettability is dependent on its chemical composition and surface [4, 33, 34].

A number of the techniques for the determination of colloidal stability/flocculation have been utilised to determine the extent that colloids deposit onto surfaces, as noted in Table 2.4. Many of these studies into colloidal deposition have been conducted to consider their deposition with respect to the initial concentrations [8, 31, 33, 141-144]. It is possible to determine the deposition kinetics with the use of impinging jet microscopy [140].

Through deposition measurements, McLean et al. [23] noted that the major contributing interactions within the wood resins that result in deposition change with the pH of the supernatant solution. This change is a result of variation in the physiochemical properties of the components [23]. Furthermore, it was found that if the colloidal system is primarily either resin acid or triglyceride, then deposition occurs [25].

Vahasalo and Holmbom [133] found that the adsorption of the wood resins to mill surfaces influences the stability of added coating particles. Through a sequence of wood resin deposition tests conducted on laboratory scale using flow cytometry (FCM), they found that wood resin deposition is the main cause of the aggregation of coating particles [133].

Dai and Ni [145] noted that the deposition of wood resins was influenced by the pH and the type of the metal ion present in solution. The effect of decreasing the pH was found to be detrimental to the deposition of the colloids, resulting in a greater accumulation of deposits. With respect to the effect of the metal ions, it was noted that the valency had a larger effect than the type of metal added to solution [145].

CHAPTER THREE

MATERIALS AND METHODS

3.1 WOOD PULP

Thermo-mechanical pulp (TMP) from *Pinus radiata* was collected from the primary refiners at Norske Skog's Boyer mill in Tasmania. The pulp was freeze dried and then soxhlet extracted with hexane to remove wood resin extractives. The TMP fibres were stored at -24°C until required, pre and post extraction.

3.2 EXTRACTED COLLOIDAL WOOD RESIN PREPARATION

Wood resin colloidal dispersions were prepared in two ways using variations on methods developed by both Sundberg et al. [69] and Stack et al. [146].

For the first type of wood resin colloids, denoted "wood resins", the *Pinus radiata* pulp was freeze dried and soxhlet extracted for 8 hours with hexane. The hexane was removed by rotary evaporation and the resulting wood resin ("wood resins") was stored at -24°C until required.

Aqueous wood resin dispersions of about 100 mg/L concentration were prepared by dissolving the extracted wood resin in acetone (99.5% purity, Chem.- Supply) and adding to distilled water with a concentration of 1 mM KNO_3, and pH adjusted to 5.5. Dialysis of the dispersion was performed using cellulose membrane tubing with a molecular mass cut off of 12,000 amu (Sigma-Aldrich D9402-100FT), to remove acetone. The wash water, containing 1 mM KNO_3 at pH adjusted with HNO_3 (0.5M, BDH) to 5.5, was changed every hour for the first 5 hrs and after 24hrs.

The second type of wood resin colloids, denoted "designer pitch", were prepared by dissolving model components (Oleic acid (tech grade, Sigma-Aldrich, impurities of other fatty acids), trilinolenin (practical grade, Sigma-Aldrich, impurities of other triglycerides) and Abietic acid (tech grade, Fluka, impurities of other resin acids)) in acetone (99.5% purity, Chem-Supply) and then adding distilled water at 1 mM KNO_3 and pH adjusted to 5.5. The dispersion was dialysed using cellulose membrane tubing with a molecular mass cut off of 12,000 amu (Sigma-Aldrich D9402-100FT), to remove acetone. The wash water was pH adjusted with HNO_3 (0.5 M, BDH) to 5.5, changed every hour for the first 5 hrs and after 24 hrs. The three components (resin acids, fatty acids and triglycerides) used to simulate the colloids are shown in Figure 3.1.

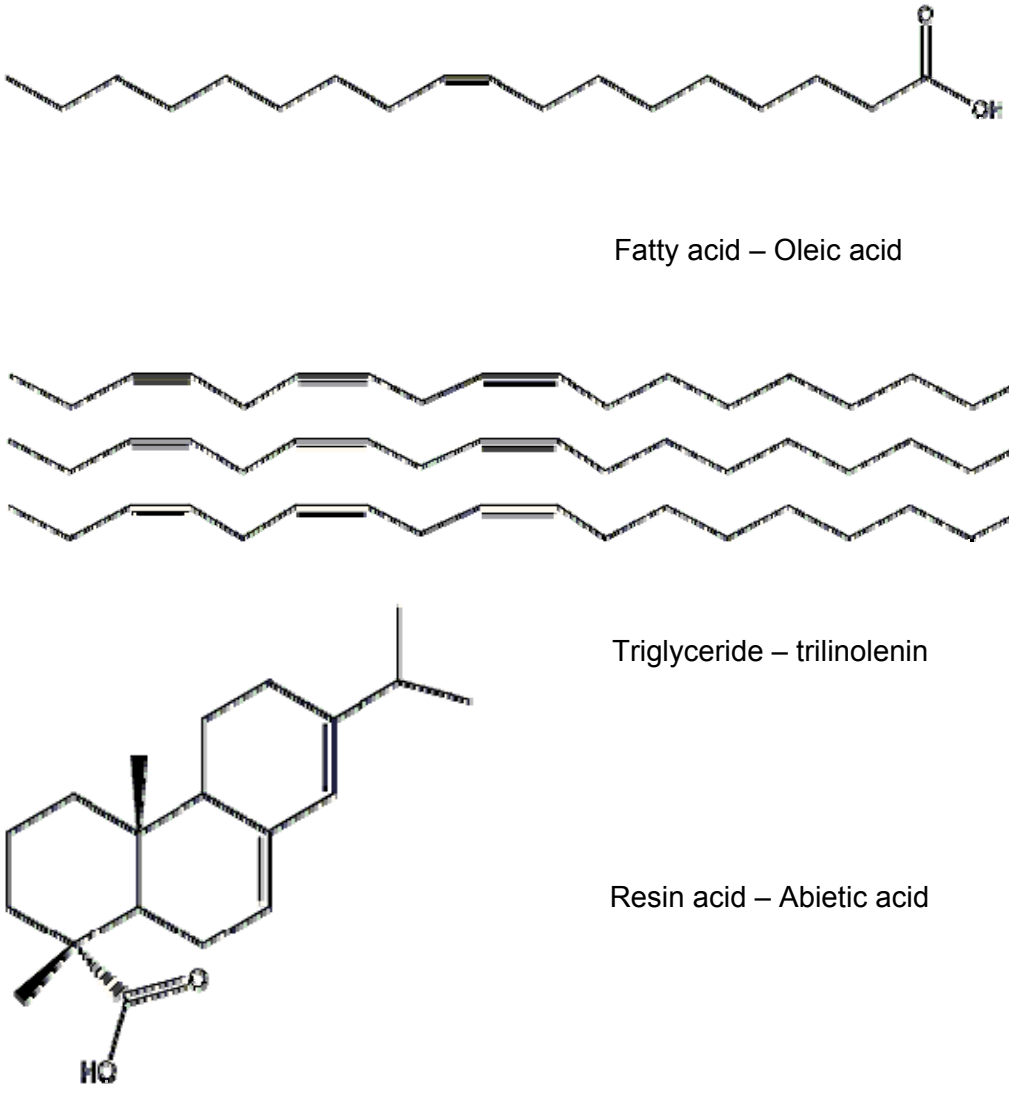

Figure 3.1: Chemical structure of model compounds of wood extractive components.

3.3 WOOD RESIN ANALYSIS - GC

The wood resin dispersions were pH adjusted to below pH 3.5 with 5 % HNO_3. To the acidified dispersions, samples were spiked with 100 uL of an internal standard of Heptadecanoic acid (C17), pentadecanoic acid (C15), Cholesteryl stearate (CS) and 1,3-dipalmitoyl-2-oleoyl-glycerol (DOG). These were added to dispersions and the sample was shaken. The wood resins were extracted from the aqueous colloidal dispersions using 2 mL of tertiary-butylmethylether (*t*-BME) (HPLC Grade, 99.8 % purity, Ried-el Haen). The samples were shaken for 30 sec to dissolve the wood resins; following agitation, the samples were then centrifuged at 500 G to separate the organic and aqueous layers. The t-BME layer was pipetted off into the GC vials and extracted wood resins were air blown to dryness. They were then silylated as per McLean et al. [8], 100 µL of pyridine (99% purity, Sigma-Aldrich) and 100 µL of N,O-bis(trimethylsilyl)-acetamide (BSA) (98% purity, Sigma-Aldrich) were added to blow dry sample extracts. The resulting solution was placed in the oven for 20 minutes at 60ºC. The GC vials were cooled to room temperature and 800 µL of toluene was added.

The silylated samples were analysed using a Varian 3800 GC-FID with a Varian 8400 auto sampler. Separation of wood resin components was achieved with a 15 metre Phenomenex® 100 % polydimethylsiloxane (ZB-1, 15 m × 0.53 mm ID × 0.15 µm FT) Zebron™ capillary GC column.

GC data was analysed using the Varian Star 5.5 software package. Retention times and FID response factors were assessed with a standard solution containing the internal standard solution (C17, C15, CS and DOG) and known concentrations of oleic acid, dehydroabietic acid and triolein. The oleic acid response factor was utilised for fatty acids, dehydroabietic acid for the resin acids and triolein was used for the triglycerides. Figure 3.2 shows typical GC chromatogram for the standard solution. Table 3.1 gives the GC program conditions for colloidal wood resin analysis.

Table 3.1: GC analysis conditions.

Parameters	**Description**
Injector temperature	90 ºC for the first 1.5 minutes following injection, increase to 325 ºC at a rate of 180 ºC/min
Oven/column temperature	90 ºC for the first 2.0 minutes following injection increase to 320 ºC at a rate of 15 ºC/min
FID temperature	360 ºC
Carrier gas	Ultra high purity helium
Constant column pressure	3.0 psi
Corresponding linear velocity	54.8 cm/s

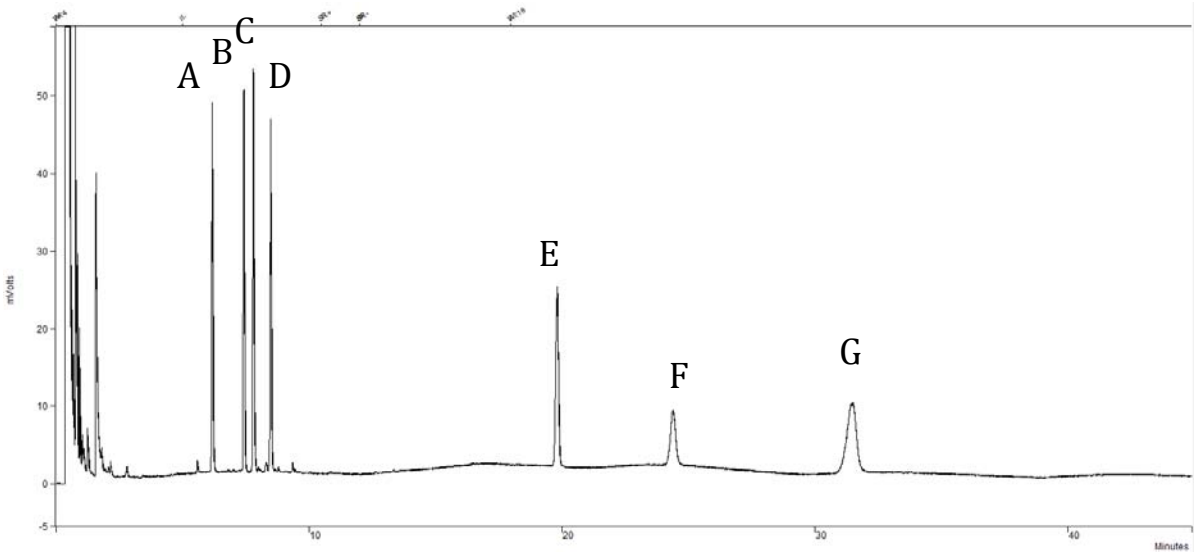

Figure 3.2: GC chromatogram of standard. A) Pentadecanoic acid (C15), B) Heptadecanoic acid (C17), C) Oleic acid (FA), D) Dehydroabietic acid (RA), E) Cholesteryl stearate (CS), F) 1,3-dipalmitoyl-2-oleoyl-glycerol (DOG), G) Triolein (TG).

3.4 PREPARATION OF EXTRACTED WOOD POLYMERS

Extracted wood polymers were obtained using the soxhlet extracted pulp from *Pinus radiata* TMP following the procedure of Johnsen [147]. The pulp was stirred in water to 2% consistency at 70°C for 3 hours; repeating this process five times after filtering out the wet wood fibre. The solution was then concentrated by evaporation using air, and filtered through 0.45 μm nylon filters (Micro Analytix Pty Ltd). This dispersion was dialysed for 24 hours in 1mM KCl and pH adjusted to 5.5 to remove unwanted material. Dialysis was conducted using cellulose membrane tubing (Sigma D-9402, 76mm wide, >12,000 MW).

3.5 LIGNIN ANALYSIS OF WOOD POLYMERS

For lignin analysis, the sample was prepared by performing a 1 in 10 dilution of the wood polymers solution with distilled water. UV absorbance at 205 nm was measured using a Shimadzu UV-160 spectrophotometer with 1 cm quartz sample cell and an extinction coefficient of ε=110.0 L g^{-1} cm^{-1} [16]. The lignin concentration was determined using the Beer-Lambert law (Equation 3.1).

$$A = \varepsilon l c \qquad \textbf{Equation 3.1}$$

where c is the concentration of the sample and l is the path length.

3.6 METHANOLYSIS AND GAS CHROMATOGRAPHY (GC) OF WOOD POLYMERS

Analysis of the sugars from the wood polymers and its composition was undertaken using similar methodology to the method of Sundberg et al. [98, 148]. Changes to the methodology

were implemented to improve cleavage of the wood polymer backbone with the use of the Radley's reactor. Acid methanolysis reagent was prepared by adding 14 mL acetyl chloride to 86 mL of dried methanol. This operation was done carefully in an ice bath. The resulting acid methanolysis reagent was stored at -24 °C.

Wood polymer samples (2.0 mL) were weighed and freeze-dried overnight. Methanolysis reagent (3 mL) was added to the dry samples and solutions were allowed to stir for 5 hours at 70 °C in Radley's reactor (heater stirrer) with 12 reaction vessels (sealed test tubes containing magnetic stirrer bars). Following the reaction time, samples cooled to room temperature and 100 µL of pyridine was added to neutralise the solution. To each sample, 4 mL of dry methanol solution containing 0.1 g/L sorbital was added. 1.0 mL of the resulting solution was removed and blown to dryness.

The dried samples were silylated with 100 µL of pyridine and 300 µL of bis-trimethylsilyl acetamide (BSA) and heated at 60°C for 20 minutes. All samples were made up to 1.0 mL with toluene. Sorbitol was used as the internal standard for quantification. Sugar retention times and peak assignments were found from standards of mannose, glucose, galactose, glucouronic acid and galactouronic acid. Standards methylated and silylated in the same method described for the samples.

The concentration of the silylated monomeric sugars was analysed using programmed injection temperature on-column high temperature gas chromatography with a flame ionisation detector using a Varian 3800 GC equipped with a Varian 8400 auto sampler. 1 µL samples were injected onto a Phenomenex® 100% polydimethylsiloxane (15 m × 0.53 mm I.D. × 0.15 µm FT) Zebron™ capillary GC column. The injector temperature was held at 90°C for the first 0.5 minute after injection and then increased to 260°C at a rate of 200°C/min. The column oven temperature was held at 90°C for the first 1.5 minutes after injection and then increased to 130°C at a rate of 20°C/min. The FID temperature was held at 290°C for the duration of approximately 24 minutes. Ultra high purity helium was used as the carrier gas and a constant flow rate of 3.0 ml/min. GC data was analysed using the Varian Star software package.

3.7 WOOD POLYMERS ANALYSIS - NMR

All NMR experiments were carried out using a VARIAN 400MHz Nuclear Magnetic Spectrometer. Pre-saturation of the water peak was carried out prior to each NMR analysis. Studies were done in aqueous media with D_2O as the internal standard. For *DOSY* NMR experiments, the sample concentration and salt type were kept constant with a stimulated echo sequence with self-compensating gradient schemes and convection compensation was employed.

3.8 WOOD POLYMERS ANALYSIS - SEC

High performance size-exclusion chromatography was carried out on a Waters – 2695 separation unit with Aqua Pore OH – 100 um lot 1817 (USA Brownlee labs) column at 50°C. This column was found to be suited to the size range of the extracted wood polymers in the crude sample and gave sufficient separation. The standards were made to a concentration of 500 mg/L and the sample to 800 mg/L. The volume of injected sample was about 50 μL, with the detection of the samples by a differential refractometer detector (Waters 410). The eluent was de-ionised distilled water at a flow rate of 0.8 mL/min. The signal was recorded and processed by Empower Pro software (Waters Assoc.).

Molecular weight calibration of this system was achieved using, D (+) galactose (BDH Chemicals Ltd.) and a set of fractionated dextran standards (5,220 Da, 11,600 Da, 23,800 DA, and 48,600 Da, Sigma-Aldrich).

3.9 TOTAL CARBOHYDRATES OF WOOD POLYMERS

Total carbohydrate concentration was determined using the Orcinol method [149]. Orcinol reagent was prepared by dissolving 0.2 g of orcinol in 100 mL of concentrated sulphuric acid. The samples were prepared by performing a 1 in 25 dilution of the wood polymer sample

with distilled water. Calibration curves were prepared using glucose solutions in distilled water at concentrations of 0, 10, 30, 60 and 100 mg/L.

Wood polymer samples (1.00 mL) were pipetted into a teflon test tube and made up to a final volume of 3 mL with orcinol reagent. During the orcinol reagent addition, solutions were cooled with cold water. The solution was then placed in an 80 °C water bath for 15 minutes, finally allowed to cool to room temperature. Sample absorbance was measured with a Shimadzu UV-Vis 160 at 540 nm immediately after cooling. Glucose standards and blank were treated in the same manner as the samples.

3.10 PDA WOOD RESIN AGGREGATION ANALYSIS

A Photometric Dispersion Analyser (PDA 2000, Rank Brothers, Cambridge, UK) was used to monitor the changes in aggregation of the wood resin colloidal dispersions. A Cole Palmer Masterflex L/S peristaltic pump and 3 mm tubing were used to circulate the suspension. The instrument was initially calibrated with distilled water and the DC gain control was adjusted to give a DC value of 10 V [113, 150]. Figure 3.3 represents the schematic of the experimental system.

The PDA measures turbidity fluctuations of a flowing suspension under controlled shear conditions. The PDA signal is the ratio of the root mean square (rms) measured as the AC voltage, to the DC voltage; this is plotted as a function of time. Three replicates are measured for each condition. The PDA signal was smoothed using a 40 point moving average.

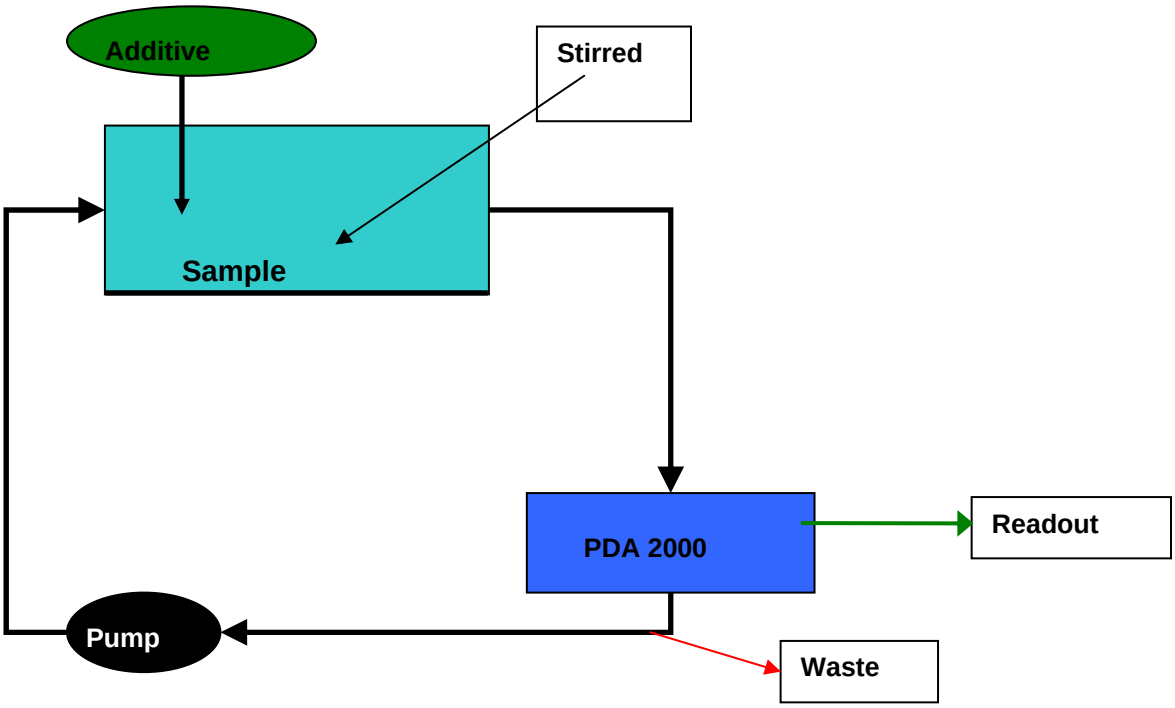

Figure 3.3: Schematic representation of the wood resin dynamic coagulation apparatus using a PDA as detector.

Peristaltic pump flow rate was set at 70mL/min and stirring of the sample occurred with a variable speed stirrer using a (4 cm diameter) flat impeller. The pump and sample vessel are connected with 2mm tubing to the PDA cell tubing of 1mm. Total sample added was constant at 200 mL.

All electrolytes used in the experiments were dissolved in distilled water as stock solutions. Constant volumes were added to the sample solution with desired concentration of stock solutions, such that the final volume had the required concentration of salt. Salts of KCl, $CaCl_2$, and KNO_3 were purchased from BDH at 99.8% purity. $MgCl_2$, $Al_2(SO_3)_4$ and $FeCl_3$ (99.8%) were obtained from Merck.

3.11 HYDROPHOBIC CONVERSION OF GLASS SLIDES

Microscope glass slides (CANEMCO & MARIVAC Frosted End Microscope Slides 75 x 25 mm) were immersed in a 50/50 solution of trimethylchlorosilane (TMCS) (≥99% Sigma-Aldrich) and pyridine (≥99% Sigma- Aldrich) at 60°C for 12 hrs, removed and cleaned with hexane (99.8% Sigma- Aldrich) and air dried.

3.12 ADSORPTION METHOD

Colloidal wood resins were adsorbed onto the surface of hydrophobised cover slips for 24 hrs. Adsorbed mass of wood resins was determined via the change in the solution concentration with the use of the established GC method. The resulting surfaces were placed into dissolved wood polymer solutions at various concentrations (wood polymer concentrations were determined with the orcinol method) and allowed to stand for 24 hrs. The difference in the concentration of wood polymers was determined to be the mass of wood polymers adsorbed to the wood resins surface. It was assumed that complete coverage of the surfaces occurred and the surface area for the wood resins was determined to be the surface area of the cover slips.

3.13 PARTICLE SIZE ANALYSIS

The instrument background was taken with distilled water. 6.85 mM $CaCl_2$ was introduced to a stirred wood resin solution in a Britt jar (as total distribution of sample was relevant, no mesh was utilised in the procedure). Stirring was constant at 1000 RPM. The particle size distribution of the wood resin colloids was measured with a Micrometrics Saturn 5200 Laser Particle Size Analyser. The solution was centrifugally pumped through the sample cell at 9 L/min. Particle size measurements were made through exposures of a solid state 658 nm diode laser at ten different anguler positions. Deconvolution of the data was carried out with Mie theory using a sample refractive index of 1.463/0 and 0.983 density(g/cm^3). Particle size distribution was taken from samples collected every 5 minutes.

3.14 CONTACT ANGLE MEASUREMENTS

The contact angle measurements were conducted with the use of a Data Physics OCA 20. A 10 μL drop of water was placed on the surface and the contact angle assessed with SCA20 software. This procedure was the same for the contact angle of wood resin with the model surfaces (glass slides and hydrophobised glass slides). A 100 μL drop of pure extracted pitch, prior to formation of the wood resin colloids, was introduced to the model surfaces and the contact angle of the wood resin on the surface was determined.

3.15 IMPINGING JET

The dialysed wood resin colloidal dispersion was made up to salt concentration of 20 mM with the desired salt and stirred for 10 min to allow particles to aggregate. The h/r (where h is the distance between the collector plate and the confiner plate and r is the radius of the inlet, as shown in Figure 8.1) ratio within the jet was kept at 1.7 for all experiments, with a constant flow rate of 70 mL/min through the impinging jet.

Magnification of 100 times objective was achieved with an Autoplan microscope. Images were captured with the use of an IMI tech Han series digital camera and interpreted with the use of Image Jay.

3.16 EPR PROCEDURES

EPR spectra were recorded on a Bruker EMX spectrometer operating at X band (9.5 GHz) using 1 mm (inner diameter) glass tubes as sample containers. All nitroxide probes used in EPR experiments were obtained from Columbia University.

The nitroxide Surfactant-NO (Figure 3.4) was synthesised analogous to a previous procedure [151]. Non-polar-NO (Figure 3.4) was synthesised from 1,4-dimethylnaphthalene following a route described in [152-154].

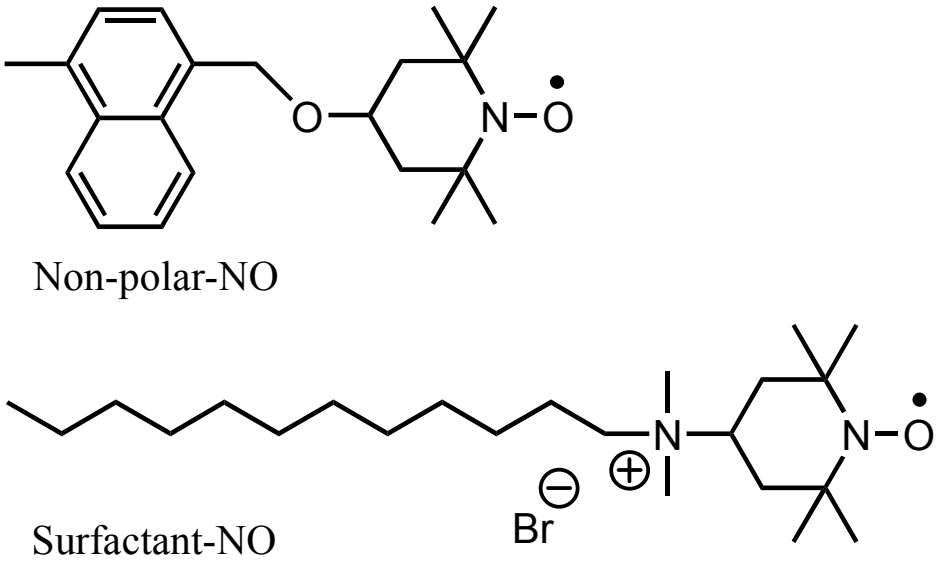

Figure 3.4: Chemical structure of nitroxide probes used.

The EPR spectra were computed by using the computation program by Budil and Freed [155] which takes into account the relaxation process and therefore allows the EPR line shape to be correctly computed.

3.17 SURFACE TENSION MEASUREMENTS

Hydrophobised slides were dipped for 10 min into acetone solution of model wood resin components or extracted wood resins, removed from the solution and either placed into H_2O or allowed to air dry.

An Analite surface tension meter (based on the Wilhelmy plate method) was used to measure the surface tension of water with the coated glass slides. The force on the coated length

of glass slide due to the adhesion of water to the coating substances (wood resin, resin acid, fatty acid or sylated glass) was determined via:

$$\gamma = \frac{F}{2L \cdot \cos\theta}$$ **Equation 3.2**

If we assume complete wetting θ= 0 therefore:

$$F = \gamma \times 2L$$ **Equation 3.3**

Where F is the force of adhesion (mN), L is the length of the slide (40mm), and ɣ is the surface tension (mN/m).

3.18 SURFACE CHARGE MEASUREMENT

Excess 0.055 M HCl was added to 200 mL of solution (colloidal wood resins suspension or wash water at the same concentration of salt) to reduce the pH below 2.47. The solution was then titrated with 0.01 M NaOH with the pH taken following every addition of base to solution. In Figure 4.13, the variation in the pH between salt solution with and without wood resins present in solution is shown. The variation in the volume of NaOH required to reach a given pH is equivalent to the charge on the particle via:

$$s\sigma = \frac{-\Delta V \bullet c \bullet f}{w}$$ **Equation 3.4**

where *s* is the surface area (m^2g^{-1}), σ is the surface charge (Cm^{-2}), ΔV (dm^3) is the difference in titre volumes, *c* is the concentration of NaOH ($mol.dm^{-3}$), *f* designates faraday's constant (96 485 $Cmol^{-1}$) and *w* is the dry weight of pitch (g).

Potentiometric titrations were conducted in temperature controlled jacketed vessel and nitrogen was bubbled through the solutions to reduce dissolved CO_2 in solution. End point for the pH change due to the addition of NaOH was determined as a stable pH for 30 sec.

3.19 IZON ZETA POTENTIAL MEASUREMENT

As colloidal wood resins are known to aggregate at high salt concentrations, it was decided to work at a reduced molarity (Izon's standard electrolyte is 0.1 M) and use a non-ionic surfactant to keep the particles from aggregating. Background solution was made up of potassium chloride tris buffer 0.05 M pH 8.5 and trace amounts of Tween (non-ionic surfactant) with low shear and no sonication. Calibration particles of CPC200B ("Izon Certified" carboxylated polystyrene particles produced by Bangs Laboratories and certified by Izon for size and concentration) and CPN200A (NIST traceable) non-functionalised polystyrene particles were used. The CPC200B particles were analysed using two Zeta Sizers to give an average zeta potential of -30mV. The standard qNano system with NP200 nanopore (100nm to 400nm+ sensing range), was utilised to find the zeta potential for the wood resin particles.

3.20 TOTAL CARBOHYDRATES OF WOOD POLYMERS

Total carbohydrate concentration was determined using the Orcinol method [143]. Orcinol reagent was prepared by dissolving 0.2 g of orcinol in 100 mL of concentrated sulphuric acid. Samples preparation required a 1 in 25 dilution of the wood polymer with distilled water. Calibration curves were prepared using glucose solutions at concentrations of 0, 10, 30, 60 and 100 mg/L. 1 mL of wood polymer sample was pipetted into teflon test tubes and made up to 3 mL with orcinol reagent. During the orcinol reagent addition, solutions were chilled. Samples were placed in an 80°C water bath for 15 minutes and allowed to cool to room temperature prior to analysis. Sample absorbance was measured with a Shimadzu UV-Vis 160 at 540 nm immediately after cooling.

CHAPTER FOUR

COLLOIDAL WOOD RESIN STRUCTURE AND SURFACE CHARGE

This chapter looks at the use of Electron Paramagnetic Resonance (EPR) to study model wood extractive colloids. The nitroxides were chosen as EPR probes to achieve a greater understanding of the different regions of the colloid in order to assess the current proposed models of the structure of the wood extractive colloid. Additionally, salt was added to solution in order to understand the macroscopic environmental interactions that the colloid undergoes.

Furthermore, the surface charge of the particles is explored with the use of potentiometric titration measurements. The surface charge of the particles plays a significant role in determining the stability of the colloids in solution.

4.1 INTRODUCTION

Electron Paramagnetic Resonance (EPR) has been used to elucidate microenvironments of emulsions, micelles and other colloidal systems [51, 54, 156-159]. The most common approach is the examination of the changes to the spectra for the free radical spin probe as the colloidal matrix is changed. Free spin radical nitroxide probes in aqueous solution show an isotropic three-line spectrum that is characteristic of highly mobile nitroxide radicals [41]. When changes occur in the macroenvironment, its effect on the microenvironment where these probes exist will then influence the spectrum's amplitude, peak width and shape. The changes to these specific spectrum characteristics can be interpreted in order to better understand alterations to the microscopic environments within the colloid [43, 46, 47, 52, 53, 160-162].

4.1.1 ORIGIN OF AN EPR SIGNAL

The electron spin resonance/electron paramagnetic resonance (ESR/EPR) spectroscopic technique uses transitions induced between Zeeman levels of paramagnetic systems in a static magnetic field [57-59]. Compounds with unpaired electrons and hence a magnetic moment, are capable of interacting with the magnetic field and give characteristic spectra. The spectrum is dependent on the macroscopic environment of the ions [60].

The electron has a magnetic moment and spin quantum number s = 1/2, with magnetic components $m_s = +1/2$ and $m_s = -1/2$ [57-59]. In the presence of an external magnetic field with strength B_0, the electron's magnetic moment aligns itself either parallel ($m_s = -1/2$) or antiparallel ($m_s = +1/2$) to the field, each alignment having a specific energy, as shown in Figure 4.1. The parallel alignment corresponds to the lower energy state, and the separation between it and the upper state is $\Delta E = g_e \mu_B B_0$, where g_e is the electron's so-called g-factor and μ_B is the Bohr magneton. This equation implies that the splitting of the energy levels is directly proportional to the magnetic field's strength, as shown in Figure 4.1 [57-59].

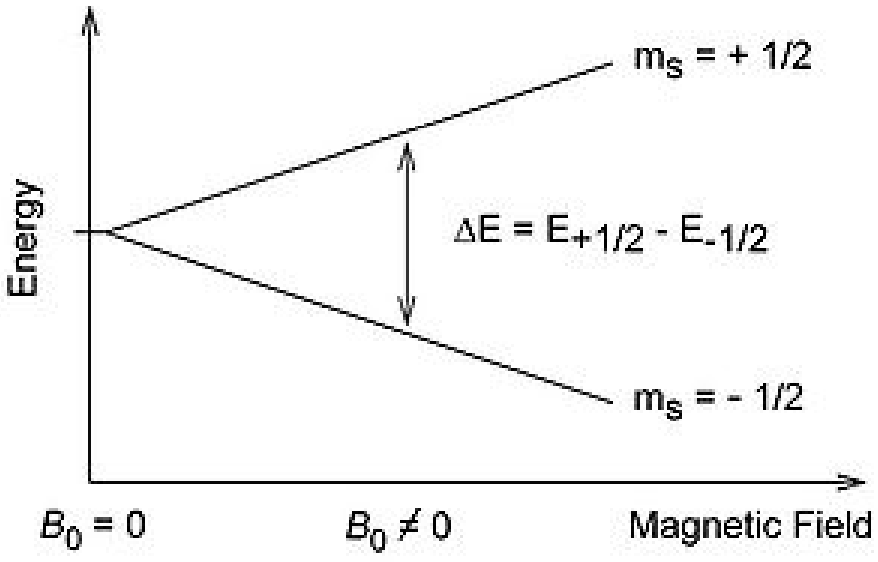

Figure 4.1: Zeeman levels of paramagnetic systems in an increasing magnetic field.

In principle, EPR spectra can be generated by either varying the photon frequency incident on a sample while holding the magnetic field constant, or doing the reverse. In practice, it is usually the frequency which is kept fixed. A collection of paramagnetic centers, such as free radicals, is exposed to microwaves at a fixed frequency. By increasing an external magnetic field, the gap between the $m_s = +1/2$ and $m_s = -1/2$ energy states is widened until it matches the energy of the microwaves, as represented by the double-arrow in Figure 4.1 [57-59]. At this point, the unpaired electrons can move between their two spin states. Since there are typically more electrons in the lower state, there is a net absorption of energy, and it is this absorption which is monitored and converted into a spectrum. Note that while two forms of the same spectrum are presented in the Figure 4.2, most EPR spectra are recorded and published only as first derivatives [57-59].

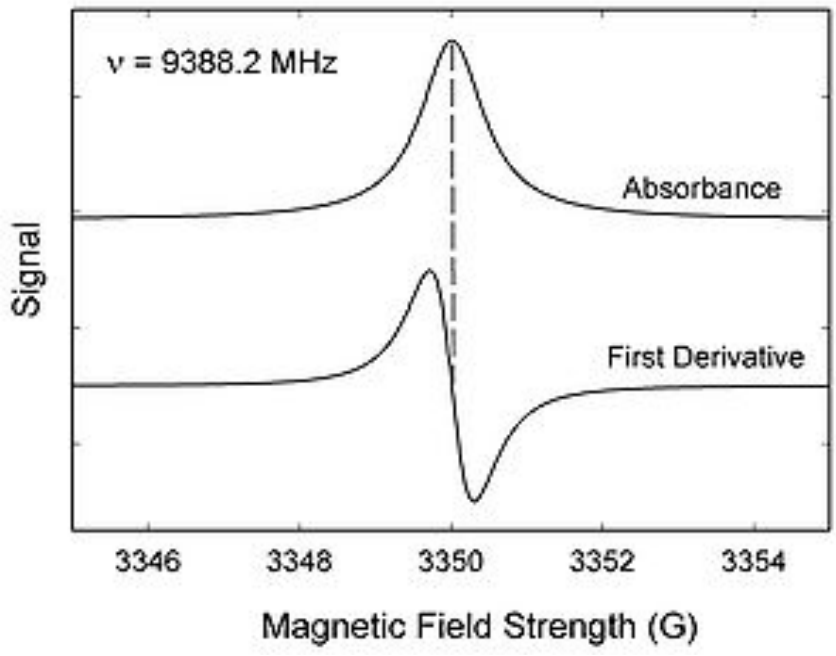

Figure 4.2: EPR signal for a free electron.

Because of electron-nuclear mass differences, the magnetic moment of an electron is substantially larger than the corresponding quantity for any nucleus, so that a much higher electromagnetic frequency is needed to bring about a spin resonance with an electron than with a nucleus, at identical magnetic field strengths [57-59]. In NMR spectra, the magnetic field strength is kept constant and the radio frequency is varied, resulting in the spectra. For the EPR, this is reversed and the magnetic field strength is varied to a constant radio frequency [57-59].

The EPR spectrum for the unpaired electron associated to nitroxide in solution typically shows three lines, which result from hyperfine coupling of the electron with the nuclear spins of the ^{14}N nitrogen atom. Nuclei individually associated with the electron spin system often have a magnetic moment "*I*" which also has certain allowed orientations ($2I + 1$) [60]. The hyperfine coupling for the ^{14}N nitroxide atom has three spin states ($I = 1$) [60].

The line width is sensitive to the mobility of the nitroxide label. A nitroxide that is rapidly tumbling shows sharp lines, while the spectrum becomes more anisotropic with concomitant line-broadening when the motion slows down.

At high local concentrations of radicals in solution, the EPR spectra can be influenced by Heisenberg spin exchange. Heisenberg spin exchange is a dynamic isotropic effect due to the collision of radicals at high local concentration. An increase in the local concentration of radicals will result in an increase in the spin-spin exchange and is related to the formation of aggregates of nitroxides in suspension. Nitroxides with a long chain carbon tail also behave as surfactants, and therefore, tend to aggregate in solution at a critical micelle concentration [163].

4.1.2 SURFACE CHARGE AND ZETA POTENITAL

The surface charge of wood resin colloids results from the chemical composition of the outer layer primarily made of resin and fatty acids [4-6]. As the suspension pH increases, the carboxylic acid head groups for the fatty acids and the resin acids are de-protonated, which increases the colloidal charge [9, 26] in a non-linear fashion [10]. Surface charge can also result

from ion adsorption onto the colloid. Some hydrolysed metal ions can be adsorbed very strongly, which can determine the resulting surface charge [89, 90].

With the use of electrophoretic mobility, Swerin and Odberg [164] show that up to pH 5 the electrophoretic mobility of the wood resins increases and then plateaus at a electrophoretic mobility of about -1.75 (μm/s)/(V/cm) up to a pH of 10 with little or no variation. On the other hand, Sihvonen et al. [68] found electrophoretic mobilities of -3.08 x 10^{-14} and -4.28 x 10^{-14} m^2 s^{-1} V^{-1} for wood resins at pH of 5 and 8 at 25°C, respectively [68], which corresponds to zeta potential (ς) of -39 and -55 mV. These experimental colloidal wood resin zeta potential values seem rather high for the low carboxyl surface density expected from wood resins. The electrophoretic mobilities found by Sihvonen et al. [68] are significantly higher than those of Swerin and Odberg [164].

4.2 RESULTS AND DISCUSSION

4.2.1 COLLOIDAL STRUCTURE OF WOOD RESINS

In order to assess the proposed models of the wood resin colloids in relation to the coordination of the triglycerides, fatty acids and resin acids within the colloid and the alterations pertaining to the addition of salt to the supernatant solution, a series of experiments were undertaken to assess the changes to the EPR spectra of nitroxides when placed within model wood resin colloids. Two different probes, the surfactant type Surfactant-NO and Non-polar-NO (Figure 3.4), were chosen to obtain a better understanding of the different regions within the wood extract colloid. The total concentration of the nitroxide probes was kept at 2 mM for all experiments. At this low concentration, it is assumed that changes in colloid structure due to the presence of the probe are minimal. As noted in Chapter 2.2.1, the choice of spin label is important in understanding different molecular environments within the colloid. It is reported that few interactions between the colloidal substances and EPR spin probes result in changes in colloidal structure at these relative low concentrations. [41, 44-46, 49-55]. Due to its non-polar nature, it was predicted that the Non-polar-NO would more readily move with the non-polar components of the colloid, therefore allowing for the analysis of the triglycerides' and steryl esters' interactions within the

colloidal mixture as well as the effect other components have on their mobility. In contrast, Surfactant-NO was expected to interact with the colloid in a similar manner as the fatty acids because of its polar head group and surfactant type tail. Taking into account these predictions, the interaction of the fatty acids and the bulk components within the colloid could then be determined. From this, an idea of the colloidal shell microstructure could be built, and the interaction between the fatty acids and the supernatant solution could be better understood.

4.2.2 CORE OF THE WOOD RESIN COLLOIDS

The spectrum obtained from the addition of Non-polar-NO to abietic acid, a resin acid found in wood resins and often used as a model compound for the resin acid group, is shown in Figure 4.3. The spectrum depicts a characteristic isotropic three-line EPR spectrum of a freely rotating nitroxide [165]. The presence of the EPR spectrum shows that nitroxides are still present in solution following dialysis. Given their respective molecular masses, if free in solution they would be removed through the dialysis with 12,000 amu cellulose tubing.

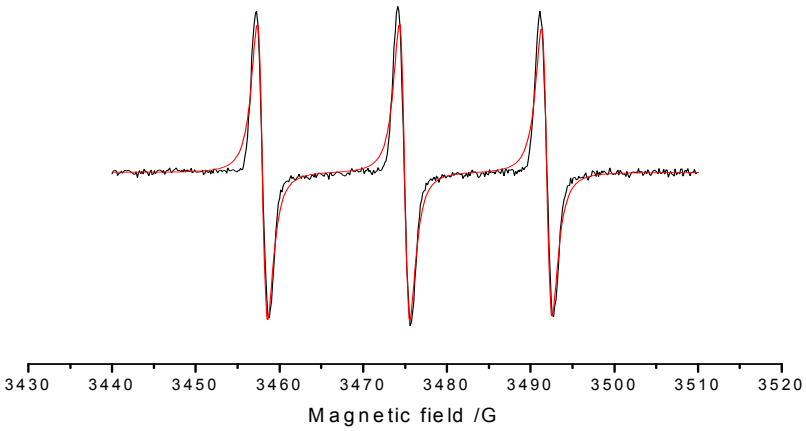

Figure 4.3: Experimental (black) and computed (red) EPR spectrum of Non-polar-NO at the center a colloid made up of resin acids only (T1) (Colloidal make up and relevant spectrum details can be found in Table 4.1).

Figure 4.4 shows the EPR spectra of the Non-polar-NO in the presence of wood resin colloids with different amounts of triglyceride. As given in Table 4.1, the main parameters extracted from the EPR spectral analysis are:

(a) the g_{ii} components of the **g** tensor for the coupling between the electron spin and the magnetic field;

(b) the A_{ii} components of the coupling tensor between the electron spin and the nuclear nitrogen spin, **A**, for comparison purposes the average value $<A_N>= (A_{xx} +A_{yy} +A_{zz})/3$, whose increase is related to an increase in environmental polarity of the radicals, is reported;

(c) the correlation time for the rotational motion of the probe, τ. The Brownian diffusion model ($D_i=1/(6\tau_i)$) was assumed in the computation. In this case, the main component of the correlation time for motion is the perpendicular one, τ_{perp}, which is thereafter termed, for

simplicity, τ. An increase in this parameter corresponds to a decrease in the radical mobility which, in turn, reflects the interactions of the radical with environmental molecules.

In cases where there is more than one spectral component, each component was subtracted from the experimental spectrum and their relative percentage contribution was obtained from double integration of each component.

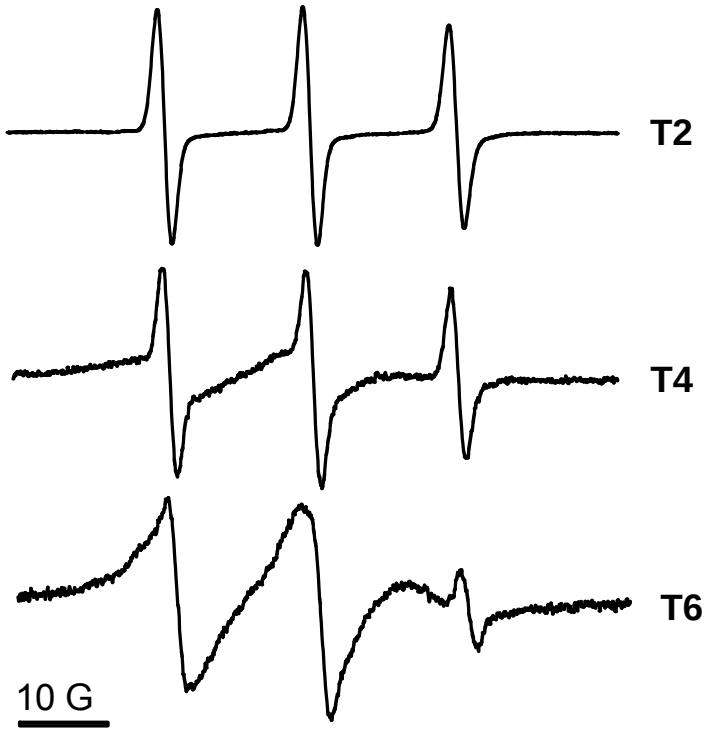

Figure 4.4: EPR spectra of Non-polar-NO in wood resin colloids with variation in the concentration of triglycerides (colloidal makeup and relevant spectrum details can be found in Table 4.1).

At higher amounts of triglyceride, a new spectral component is evident with broader line width and smaller coupling constant A_N. The broader line width is an indication of reduced mobility of the nitroxide and the smaller coupling constant shows that the nitroxides are located

in a less polar environment. In the sample with the maximum amount of triglycerides (T6), about half of the non-polar nitroxides reside in a highly viscous (τ = 0.42 ns), less polar environment (A_N =15.8 G). The nature of this environment will be discussed later.

Table 4.1: Colloidal makeup and rotational correlation times determined by EPR for Non-polar-NO due to changes to the concentration of triglycerides at pH 5.5.

Non-polar-NO	Resin acids (mg/L)	Fatty acids (mg/L)	Triglycerides (mg/L)	τ (ns)	$\langle A_N \rangle$ (G)	%
T1	50	0	0	0.009	17.0	100
T2	50	16	52	0.7	16.3	21.5
				0.009	17.0	78.5
T4	50	16	250	0.53	15.8	31.5
				0.009	17.0	68.5
T6	50	16	1500	0.42	15.8	44.0
				0.009	17.0	56.0

Due to its nature, the Non-polar-NO would more readily move with the non-polar components of the colloid, such as triglycerides and steryl esters. Following the addition of triglycerides to the colloid, it is observed that there is a reduction in the mobility of the Non-polar-NO at the colloidal core on the initial addition of triglycerides to the colloid followed by an increase in the mobility of the nitroxide. This result likely occurred because of changes in the viscosity of the macroscopic environment. The EPR studies indicate that the colloidal shell formed by the resin acid in solution has a relatively large interior volume in which the molecular mobility of the nitroxide radical is not affected by the abietic acid.

4.2.3 SHELL OF THE WOOD RESIN COLLOIDS

EPR experiments with Surfactant-NO were performed as it was expected that this surfactant-type nitroxide would interact with the colloid in a similar manner as the fatty acids. Therefore, the influence of the fatty acids on the colloid structures could be probed with Surfactant-NO. Figure 4.5 shows representative EPR spectra of Surfactant-NO in the presence of different colloid compositions. Table 4.2 shows the spectral components extracted from the EPR spectra in Figure 4.5.

The presence of Surfactant-NO nitroxides within the sample following dialysis indicates that they have penetrated the colloids that are formed from abietic acid. Furthermore, as there was no line broadening or amplitude reduction, as noted for Surfactant-NO when placed in a colloid of resin acid, it can be assumed that its mobility is unaffected by the presence of resin acid in solution. In previous work, surfactant-type nitroxides similar to Surfactant-NO have been observed to form micelles in solution [166]. As a result of nitroxide being moved into close proximity to each other via this aggregation process, Heisenberg spin exchange was noted [167]. However, for the spectra of Surfactant-NO within resin acid, no spin-spin exchange is seen, and as such, aggregates of the surfactant type nitroxide (Surfactant-NO) are not present in solution.

On addition of fatty acid to the colloid, a depression of the signal is noted in Figure 4.5 (F2), which could be the result of spin-spin interaction. Furthermore, as shown in Figure 4.5, the addition of triglycerides to the colloid at low concentrations of fatty acid (F3) increases the magnitude of the signal. This is a result of the reduction in the amount of spin-spin exchange occurring, which indicates a reduction of the local concentration of nitroxide in the colloid. It is also noted from the spectrum that, following the addition of triglycerides, there is no line broadening due to reduction in the mobility of the Surfactant-NO within the colloid. As such, the triglycerides do not have any effect on the rotational motion of the nitroxides of Surfactant-NO, which is in sharp contrast to the Non-polar-NO.

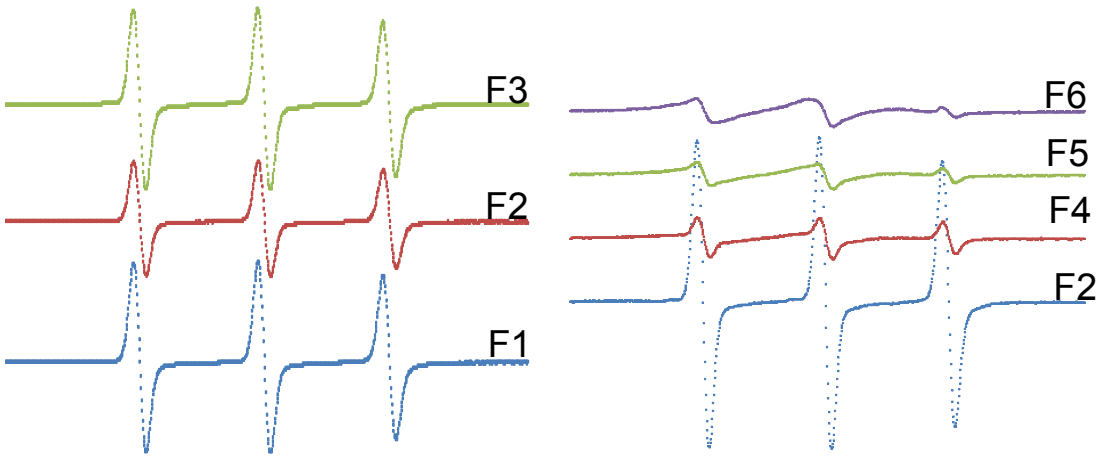

Figure 4.5: Addition of Surfactant-NO to colloid of varying makeup prior to solution (colloidal makeup and relevant spectrum details can be found in Table 4.2).

The spectra of Samples F4-F6 at higher concentrations of fatty acids contain a second spectral component with lower mobility, which was extracted from the experimental spectra by subtraction of the spectrum at high mobility (F1). Figure 4.6 shows a representative example of the subtracted spectrum for F6.

In Figure 4.5, the reduced signal height observed for the addition of fatty acids (F2) to the colloid intensifies when more fatty acid is added to the colloid (F4-F6). As such, the signal reduction may be due to Heisenberg spin exchange, precipitation, separation or self-aggregation of the Surfactant-NO. However, as the Surfactant NO concentration is kept below the critical micelle concentration, it is unlikely due to separation or self-aggregation. At high local concentrations of radicals in solution, the EPR spectra can be affected by Heisenberg spin exchange. Heisenberg spin exchange is a dynamic isotropic outcome of the collision of radicals at high local concentration. An increase in the local concentration of radicals will result in an increase in the spin-spin exchange and is related to the formation of aggregates of nitroxides in suspension or within a microenvironment in the existing colloid [163].

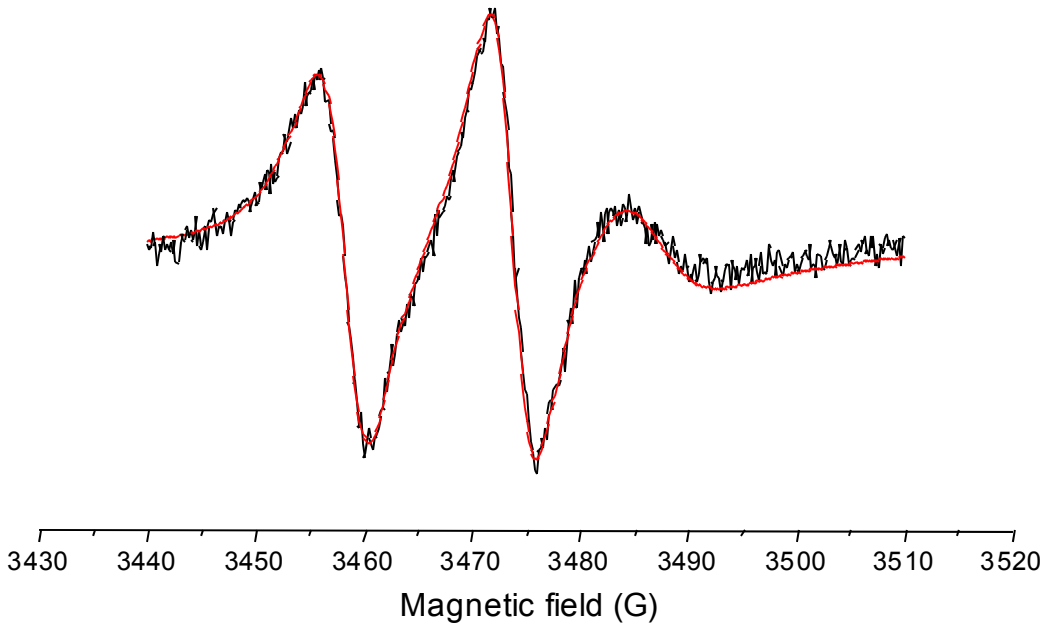

Figure 4.6: Subtracted EPR spectrum (black) of the low mobility component of Surfactant-NO at high concentrations of fatty acids within the colloids (colloidal makeup and relevant spectrum details can be found in Table 4.2). This spectrum was generated by subtraction of a 19% contribution of spectrum of F1 from spectrum F6. The red line shows the simulated spectrum.

From the EPR spectrum, it is evident that the Surfactant-NO nitroxide is residing within the fatty acids and is not interacting with the resin acids. Therefore, fatty acids are assumed to exist as an independent shell within the colloid, separate from resin acids.

Table 4.2: Colloidal makeup for the addition of Surfactant-NO to the colloids at pH 5.5.

Surfactant-NO	Resin acids (mg/L)	Fatty acids (mg/L)	Triglycerides (mg/L)	τ (ns)	$\langle A_N \rangle$ (G)	%
F1	50	0	0	0.05	16.7	100
F2	50	16	0	0.05	16.7	100
F3	50	16	52	0.05	16.7	100
F4	50	400	52	2.65	16.1	35.5
				0.05	16.7	64.5
F5	50	790	52	2.47	15.9	67.0
				0.05	16.7	33.0
F6	50	1180	52	2.47	15.9	81.0
				0.05	16.7	19.0

4.2.4 MAKEUP OF WOOD RESIN COLLOIDAL SHELL OUTER LAYER

In order to ascertain if the fatty acids make up the outer layer of the colloid or if they are mixed with the resin acids, interactive force measurements were performed. For these experiments, hydrophobic (silylated) glass cover slips were coated with the colloidal components and the interaction of the coating substance (resin acid, fatty acid, wood resin or silylated glass) with water was assessed with the use of the Analite Surface Tension meter based on WIlhemy plate method. Figure 4.7 presents the adhesion forces between water and different components of wood resin that have been deposited onto a hydrophobic glass surface. Both the resin acids and fatty acids are more hydrophilic than the hydrophobic glass, as is noted from their higher interactive force with the solution. However, the resin acids notably have a higher affinity for the water with an interaction of about 0.0065 N. In contrast, the fatty acids have an interaction of about 0.004 N. The surface interactive force of the pure resin acid with water is the same as that

displayed by both the combined resin and fatty acids and the extracted wood resins (real wood resin) on the surface. The similarity in the surface interactive force between the pure resin acid on hydrophobic glass and the combined mixtures of fatty acids and resin acids indicate that the outer surface of the wood resin colloids is pure resin acid.

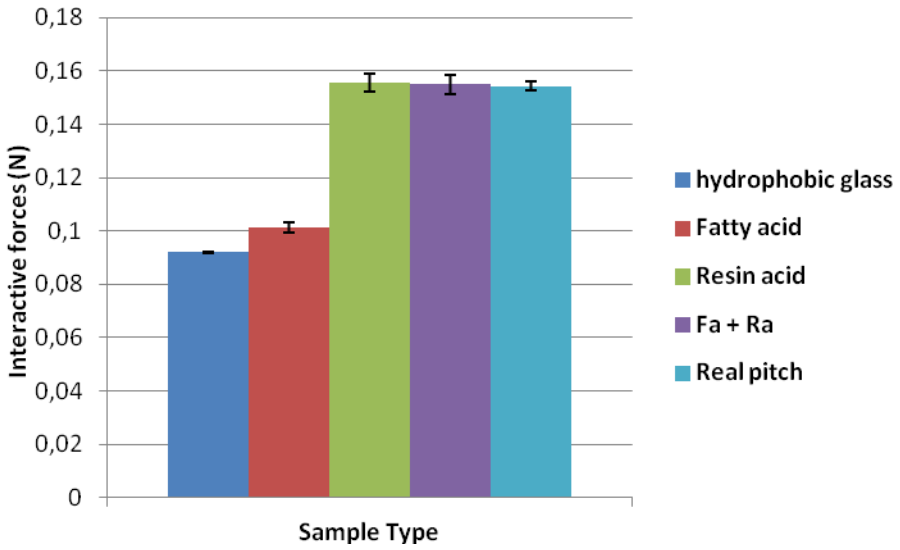

Figure 4.7: Surface interactive force between wood resin, resin acids, fatty acids or sylated glasswith distilled water.

4.2.5 IMPROVEMENTS PROPOSED FOR COLLOIDAL STRUCTURE OF WOOD RESINS

The presence of free-moving fatty acids, as shown in Figure 4.5, suggests a change in current colloidal models of wood extractive colloids. It is proposed that the model for the colloidal structure needs to be adapted in order to account for this mobile fatty acid phase separation from the resin acid shell of the colloid. From the forces of interaction of component compounds plated onto hydrophobic surfaces with distilled water, it is observed that the outer layer is made up of resin acids. Therefore, as shown in Figure 4.8, a new proposed model for the colloidal structure is made up of a bilayer of resin acids and fatty acids with a hydrophobic core of triglycerides and other hydrophobic components of the wood extracts. Similar lateral phase

separations have been noted in lipid-lipid bilayers and biological membranes [168-170]. Previous work by Longo et al. [169] indicated that this lateral phase separation can result in mixtures in which the lipid chain length varies by as little as 6 CH_2 groups.

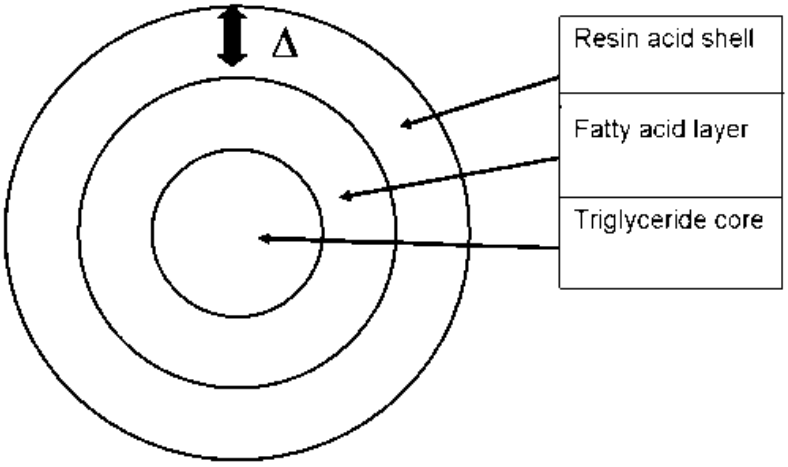

Figure 4.8: Proposed structure for the colloid (Figure not to scale; Shell thickness is undetermined and dependant on triglyceride concentration).

Even though it is proposed that resin acids and fatty acids exist in a bilayer as opposed to a monolayer, there is still interaction between the two. As shown in Figure 4.8, the interaction of the fatty acids' shell is termed Δ and is dependent on the ratios of fatty acids to resin acids and the concentration of triglycerides in the colloid's centre.

$\Delta \propto$ [Fatty Acid]

$\Delta \propto 1/$ [Triglycerides]

Due to the mobility of the fatty acid layer, the changes to the interaction of the fatty acids and the resin acids will affect the colloidal interface with the supernatant solution and thus the stability of the colloid in solution, as shown in Figure 4.9.

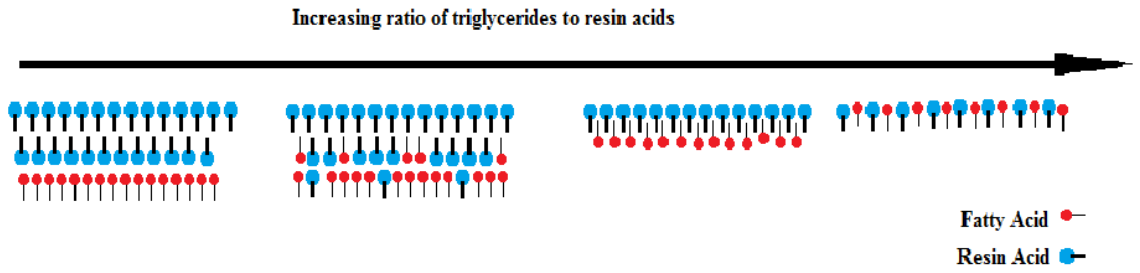

Figure 4.9: Proposed colloidal shell structural changes on increasing triglycerides to resin (figure not to scale; shell thickness is undetermined and dependant on triglyceride concentration).

Figures 4.8 and 4.9 show that the proposed modifications to the colloidal structure can explain the changes to the stability attributable to variations in the component ratios. As a result of alterations to the concentration of triglycerides within the colloidal core, the fatty acids will vary their association with the resin acid shell. It has been previously shown by McLean [17] that the percentage of wood resin remaining in solution is dependent on the ratio of resin acids to triglycerides. As the ratio increases, the percentage of the total colloid remaining in solution increases. The new model proposes that with increases in triglycerides to resin acids, there will be an increase in the interaction of fatty acids and resin acids. As a result of greater interaction, there will be proportional changes to the surface chemistry of the colloid, resulting in a greater stability of the wood resin colloids in solution.

The pKa for the different fatty acids increases with chain length [8] and the degree of saturation (greater saturation results in increased pKa). A reduction in the polarity of the carboxylic acid head group with the chain length and reduced double bonds occurs. It is thought that the reduction of polarity in the fatty acid will result in greater separation between the resin acid and fatty acids within the colloid.

4.2.6 CHANGES IN MICROENVIRONMENTS ON ADDITION OF Ca^{2+} TO SUPERNANT SOLUTION

The addition of salt to the supernatant solution greatly affects the stability of the colloidal wood resins. As was noted by McLean [17], the changes in the composition of the wood resins greatly affects this stability. To understand how this phenomenon occurs, $CaCl_2$ was added to the wood resins suspensions and the changes in the molecular mobility of the different nitroxide radicals were observed.

Table 4.3 shows the colloidal makeup and relevant spectral details for EPR experiments using Non-polar-NO for samples containing $CaCl_2$ in the supernatant solution. In general, the parameters (τ, A_N, and %) extracted from the EPR spectra with increasing triglyceride concentration follow the same trend as in the absence of salt (see Table 4.1). With increasing concentration of triglyceride, a new spectral component appears where Non-polar-NO resides in a less polar environment with increased viscosity, as shown by the coupling tensor (A_N) in Table 4.3.

Table 4.3: Colloidal makeup and relevant spectrum details for the variation in EPR signal, for Non-polar-NO due to changes to the concentration of triglycerides following the addition of 2 mM of $CaCl_2$ to solution at pH 5.5.

Non-polar-NO + $CaCl_2$	Resin acids (mg/L)	Fatty acids (mg/L)	Triglycerides (mg/L)	τ (ns)	$<A_N>$ (G)	%
TB1	50	0	0	0.02	17.0	100
TB2	50	16	52	0.73	16.2	18.5
				0.02	17.0	81.5
TB4	50	16	246	0.44	15.8	45.0
				0.02	17.0	55.0
TB6	50	16	1510	0.19	15.6	49.5
				0.02	17.0	50.5

As was noted by other groups, viscosity within the microenvironments present in the colloid can be influenced by alterations to the makeup of the colloid or solution. Variations in the colloid's viscosity will result in changes to the mobility of nitroxides and therefore its spectrum. Figure 4.10 shows the effect that the addition of triglycerides to the colloid has on the molecular mobility for the Non-polar-NO, or the time it takes for the molecules to reorientate themselves within their microenvironments. As previously noted by Weber et al. [41], viscosity of the microenvironment increases as the correlation time increases. On addition of triglycerides to the colloid, there is an incorporation of the Non-polar-NO into a non-polar phase. As noted previously, an increase rotational mobility (τ) corresponds to a decrease in the radical mobility which, in turn, reflects the interactions of the radical with environmental molecules. As such, the rotational mobilities for the nitroxides in Figure 4.10 and 4.11 show an increase in the rotational mobility thus indicating a reduction in their mobility within the molecular environment. Following the initial decrease in mobility, it is observed that as the concentration of triglycerides in the colloid increases, the mobility of molecules in the centre of the colloid begins to increase as well. These increases are proportional to changes in the viscosity for the colloidal core.

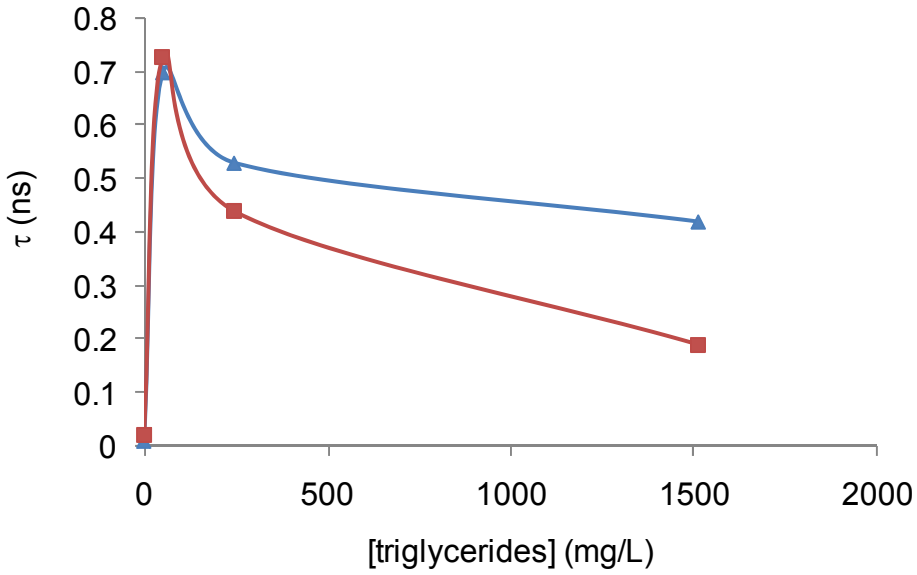

Figure 4.10: Variation in the mobility of Non-polar-NO nitroxide radicals in the center of the wood resin colloids due to 2 mM $CaCl_2$ in the supernatant solution (with 2 mM $CaCl_2$ and without $CaCl_2$).

Figure 4.11 shows the effect of the fatty acid concentration on the mobility of the surfactant NO probe in the absence and presence of $CaCl_2$. It can be seen that the mobility of the Surfactant-NO is not influenced by the addition of salt to solution until very high concentrations of fatty acids are present.

As a result of the head and tail configuration of the Surfactant-NO and the EPR's ability to "see" only the radical associated to the "head" group of the molecule, it is summarised that the head of the nitroxide is in a free movement region at low concentrations. This free movement of the head groups is unaffected by changes to the resin acid concentration or the salinity of the solution, as shown by the free movement of the nitroxide within a colloid made exclusively of the resin acid. However, as the ratio of fatty acids to resin acids increases, the mobility of the nitroxide follows the same trend as that shown by the Non-polar-NO, which indicates a filling of the shell as shown by the rate of molecular reorganisation shown in Figure 4.11.

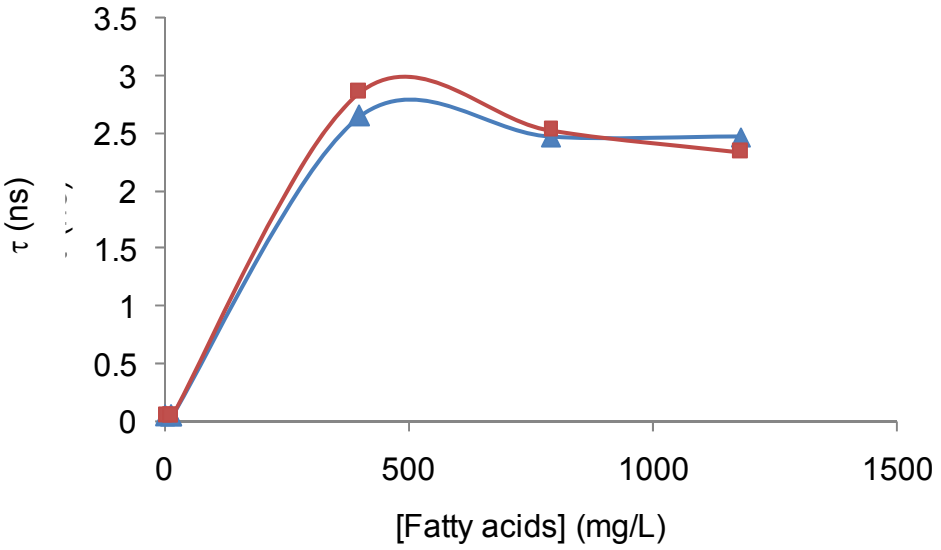

Figure 4.11: Mobility of Surfactant-NO nitroxide radicals in the fatty acid shell of the wood resin colloids with ($CaCl_2$) and without addition of $CaCl_2$ = 2mM.

The addition of salt, such as $CaCl_2$, to the supernatant solution is assumed to only affect the surface of the colloid in contact with solution. Depending on the rate of coagulation, salt should also influence the rate at which different components within the colloid can move. It is thought that the outer shell of the colloid will be most affected. However, as noted from transmittance microscope images shown in Figure 4.12, the colloid is seen to undergo changes in the size distribution on the addition of electrolytes to solution (scale for colloidal particle samples shown in Figure 4.12 can be noted from the scale bar shown in Tb 6). It can be seen in Figure 4.15 that particle size change is less apparent at high trigyceride concentration (T6 and Tb6). This occurs even though no macroscopic changes to the colloidal shape (spherical shape is retained) are observed.

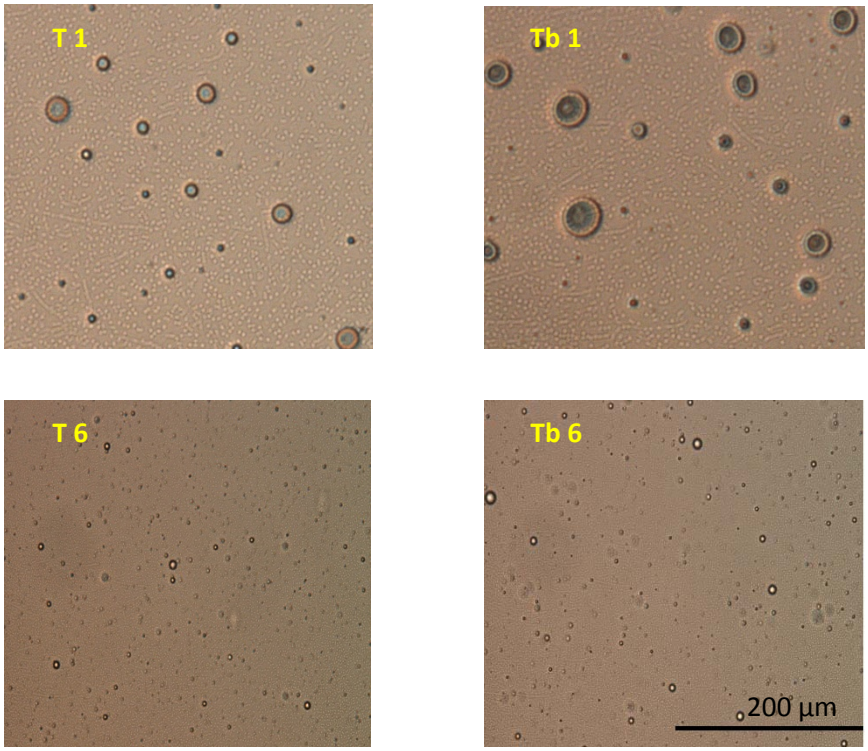

Figure 4.12: Transmittance microscope image of model wood resin colloidal particles at 40x zoom, Left: no electrolytes in solution (T 1, T 6), and to the Right with 2 mM $CaCl_2$ in supernatant solution (Tb 1, Tb 6). Composition for colloids in images T 1 and T 6 given in Table 4.1, and for Tb 1 and Tb 6 are in Table 4.3 at pH 5.5. (Scale given in Tb6 for all microscopic images).

Interestingly, from Figure 4.9, it can be seen that the molecular mobility at the colloid's centre is affected by changes to the supernatant with the addition of salt. Although there is variation in the colloidal size distribution in solution, the colloid is not seen to undergo macroscopic changes in colloidal shape (spherical shape is retained) on addition of salt to the supernatant solution (Figure 4.12). There is an indication that colloidal morphology is not a factor in the mobility of the molecules. It is proposed that the effect of salt on the molecules' mobility in the colloidal centre is due to the movement of metal resinates to its core, in this case calcium resinates. These resinates are a result of the resin acids' carboxylate groups acting as ligands, binding with the metals in solution and forming non-polar complexes. Due to the soft

nature of the colloids, the resulting complexes can move so that they are present in the non-polar region of the colloids, which results in the reduction of the final colloid's viscosity. This is further indicated by the decrease in the coupling tensor (A_N), shown in Table 4.3, as a result of the decrease in the microscopic environment's polarity on the addition of the salt to the supernatant solution.

4.2.7 SURFACE CHARGE

The colloidal surface charge of the wood resins was determined through potentiometric titration measurements to better understand the stability of the wood resins in solution. The potentiometric titrations measure the effect of variation in the pH on the surface charge of the wood resins. The variation in the volume of NaOH required to reach a given pH, between the colloidal suspension and a blank water solution, is used to calculate the charge on the particle using the following equation:

$$s\sigma = \frac{-\Delta V \bullet c \bullet f}{w} \qquad \textbf{Equation 4.1}$$

where s is the surface area (m^2g^{-1}), σ is the surface charge (Cm^{-2}), ΔV (L) are the titre volumes, c is the concentration of NaOH (mol.L), f is Faraday's Constant (96 485 $Cmol^{-1}$) and w is the dry weight of wood resin (g).

Figure 4.13 shows a titration curve for the addition of NaOH to dialysis water and to a colloidal wood resin solution. The difference between the two curves is proportional to the charge of the particles in solution from Equation 4.1.

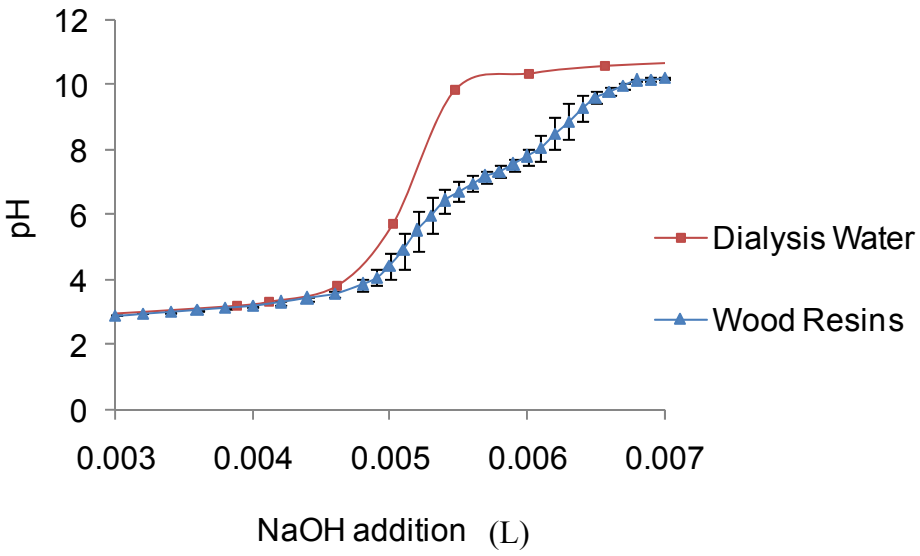

Figure 4.13: Variation in the pH with the addition of NaOH.

The titration curve for the wood resin suspension is noted to have a similar curve to a titration curve for a weak, diprotic acid, with a step occurring between pH 6.5 and 8. This step correlates to the pK_as for the resin acids and the fatty acids, similar curves for the colloidal resin acids and fatty acids have been shown by McLean et al. [10]. McLean et al. also showed that for the colloidal acids, the step type curve shown in Figure 4.13 will generally occur, and they have postulated that the pK_a for these insoluble materials being measured is a pK_a of the colloids and not the true molecular pK_a.

4.2.8 DIFFICULTIES EXPERIENCED IN SURFACE CHARGE DETERMINATION.

For the determination of the colloidal surface charge, there are a number of variables that need to be taken into account, particularly with regard to the surface charge of the wood resins. The colloidal suspension and the wash water solutions will require different volumes of the acid to reach the lower limit pH. For this starting pH, it is important that the two solutions start at the

same value as this will determine the initial variation in the surface charge. As shown in Figure 4.14, through constant volume additions of acid, variation in the starting pH of the water solution occurs. This results in reproducibility problems.

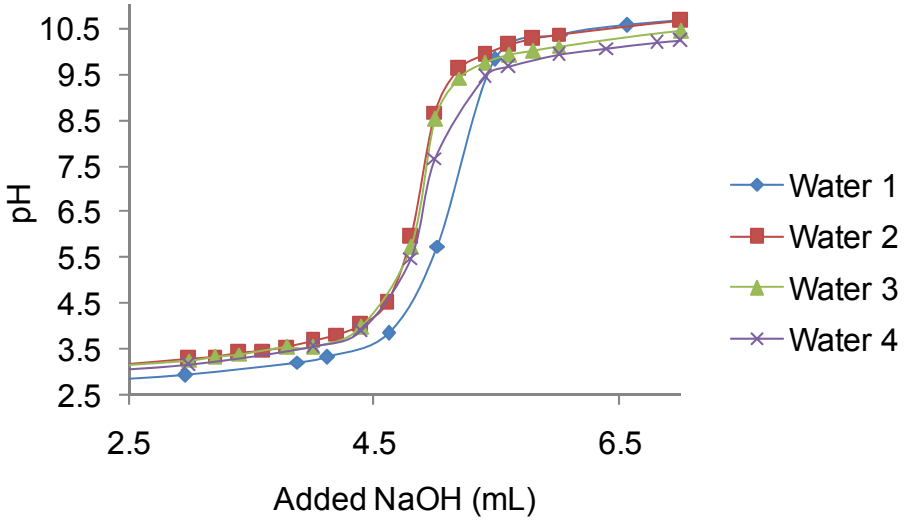

Figure 4.14: Addition of NaOH to dialysis water, 4 replicates indicating variation in pH with constant initial volume additions of 0.2% HCl.

Low salt concentrations in solution result in large variability in the determination of the pH. Low solution ionic strength can result in poor pH determination, and the variability is a result of the low conductivity of solution.This can result in pH values that are low by comparison to the true solution pH. Furthermore, the response of the pH probe to the addition of compounds to solution that result in changes in the pH can be slow as a result of the low conductivity. In Figure 4.15, there are large changes in the titration curve for the wash water at 1 mM KCl as a result of the low ionic strength.

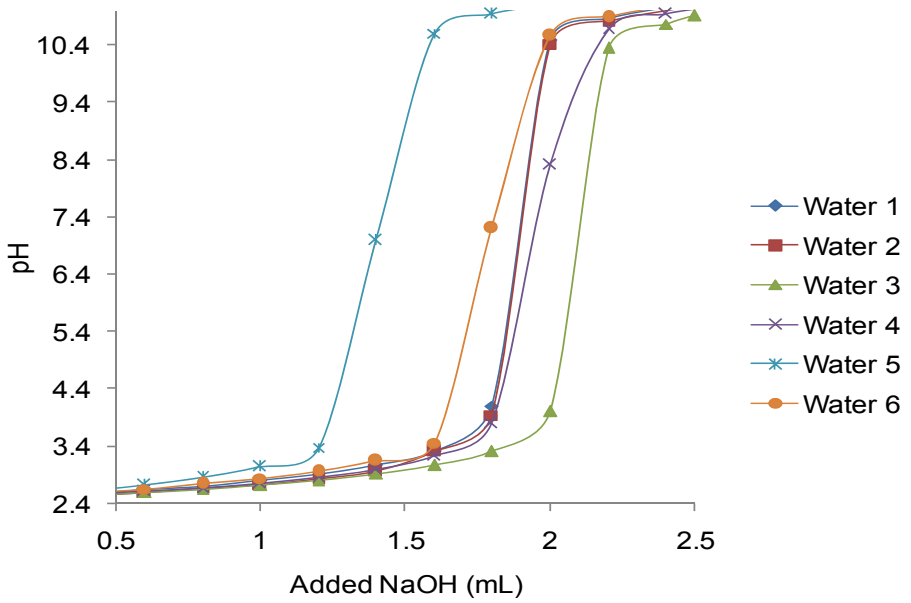

Figure 4.15: Variation in the pH with the addition of NaOH to dialysis water, 6 replicates at low ionic strength.

For the determination of the wood resin surface charge, there is a difficulty directly as a result of the wood resins composition and the form that they take in solution. The wood resin dispersions are well known to change in their stability in solution as a result of changes in composition resulting in surface chemistry changes. Each wood resin dispersion will vary in composition to some extent. Furthermore, the colloidal particles that are formed by the wood resins in solution are not the typical hard spheres, they form a soft colloid (forming oil at room temperature) in solution that can undergo molecular reorganisation and even a low composition changes with variation in the solution pH. These colloidal physiochemical factors can result in a number of problems including the fouling of the pH probe and variability in the charges as a result of the composition changes.

4.2.9 COLLOIDAL WOOD RESIN SURFACE CHARGE.

Table 4.4 gives the colloidal wood resin surface charges determined by potentiometric titration. These are similar in magnitude to those found by Kuys, Zhu et al. and Herrington et al. [171-173] for the surface charge of wood fibres through the same technique. This is to be expected as the surface charge for the wood resins and the wood fibres have previously been shown to have surface charges of similar magnitude [147]. Johnsen [147] points out that the surface of the wood resins has a higher anionic charge density than the cellulose wood fibres [147]. Conversion from C/g to C/m^2 was calculated based on the mass of wood resins added to solution. The density of the wood resins and the volume per droplet calculated from the average particle size distribution allows the surface area for the colloidal suspension to be determined.

Table 4.4: Surface charge of wood resin particles with 40 mM KCl.

pH	**particle charge (Cg^{-1})**	**particle charge (Cm^{-2})**
3	-55.7± 10	-7.4± 1.4
4	-68.5± 13	-9.1± 1.7
5	-79.9± 9.0	-10.7± 1.2
5.5	-81.3± 11	-10.8± 1.4
6	-87± 14	-11.6± 1.8
7	-92.8± 12	-12.4± 1.6
8	-97± 9	-12.9± 1.2

Herrington et al. [173] show that the surface charge can be used to approximate the surface potential for the colloidal particles as follows:

$$\sigma = \left(2nk_BT\varepsilon\right)^{\frac{1}{2}} 2\sinh\left(\frac{ze\psi_d}{2k_BT}\right)$$ **Equation 4.2**

Work completed by Izon on the *P. radiata* wood resins, with the use of the standard qNano system with NP200 nanopore (100 nm to 400+ nm sensing range), indicate that the zeta potential for the wood resin particles is -10 mV at a pH of 5.5. By comparison, Sihvonen et al. [68] measured electrophoretic motilities for pine wood resin dispersions at pH of 5 and 8 respectively of -3.08 x 10^{-14} and -4.28 x 10^{-14} m^2 s^{-1} V^{-1} [68]. This corresponds to zeta potential (ς) of -39 and -55 mV. These values for the zeta potential are much higher than those found with the use of the qNano system. However, Izon utilised a surfactant to prevent aggregation of the colloidal wood resins. It is unknown what effect the addition of the non-ionic surfactant will have on the surface potential of the wood resins.

Furthermore, the colloidal surface charge at pH 3 is unreported prior to this work. Gantenbein et al. [174] reported an electrophoretic mobility for the wood resins at pH 4 of -0.525 × 10^{-8} $m^2V^{-1}s^{-1}$. It is thought that given the consistency in the presence of this charge that it represents a true surface charge on the colloidal wood resins at pH 3, as a result of the initial dissociation of the hydrogen ions associated to the carboxylic acids.

On addition of high concentrations of salt to the wood resin dispersions, many significant problems were experienced. In Figures 4.16, 4.17 and 4.18, the effect of the addition of various concentrations of sodium, calcium and aluminium, respectively, on the wood resin surface charge is shown. The results for the addition of salt to the wood resin colloids are felt to have a number of major issues. For both the addition of sodium (Figure 4.16) and calcium (Figure 4.17), there is an apparent drop in the surface charge. This drop is expected and is probably the result of specific ion adsorption, however, the decrease in the surface charge is not continuous. It is postulated that the inconsistency in this drop in the colloidal wood resin surface charge is a result of molecular reorganisation within the colloid due to formation of metal resinates during deprotonation of the surface active carboxylic acids.

For the addition of sodium to a 100 mg/L wood resin suspension (Figure 4.16), there is an apparent decrease in the surface charge on the addition of 100 mM of sodium such that at pH 5.5

the surface charge is about 15 Cm^{-2}. On addition of 400 mM, however, this surface charge increases again, becoming 37.5 Cm^{-2}.

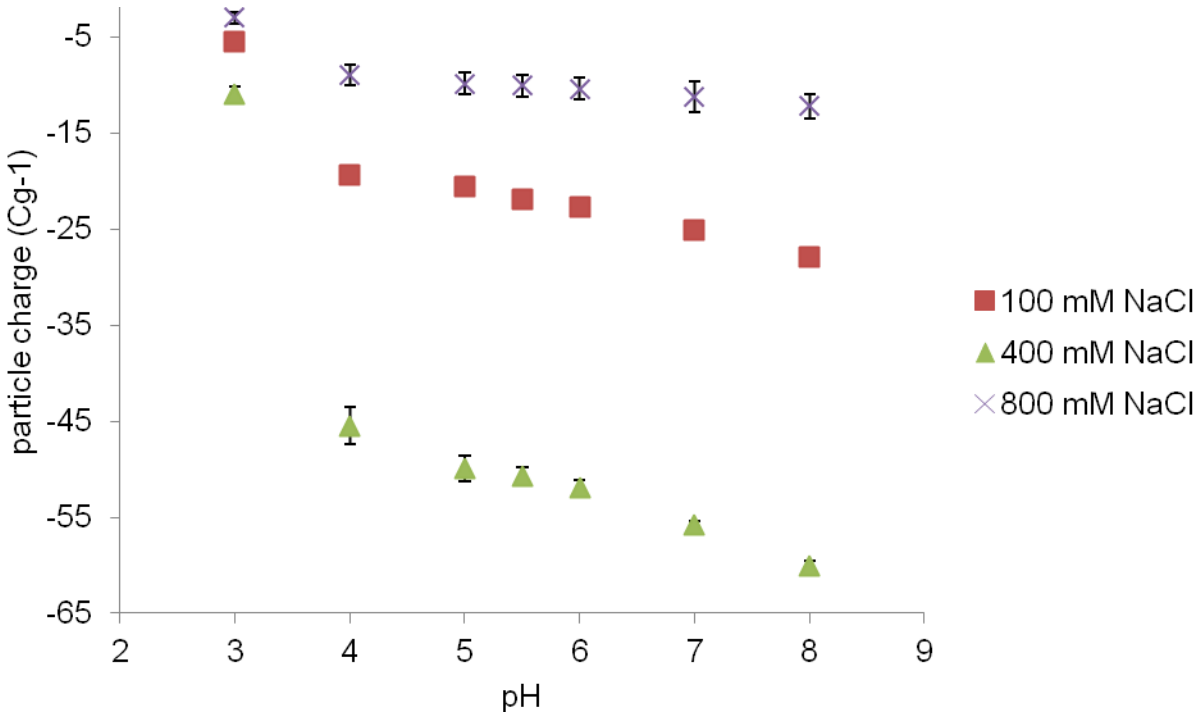

Figure 4.16: Variation in wood resin surface charge with supernatant pH on addition of NaCl to the 100 mg/L colloidal wood resins suspensions at various concentrations.

On the other hand, for the addition of calcium to the colloidal wood resins (Figure 4.17), the addition of 4 mM calcium to solution results in the reduction of the surface charge on the colloidal wood resins. However, on addition of 8 mM to the wood resins, the surface charge of the colloid increases.

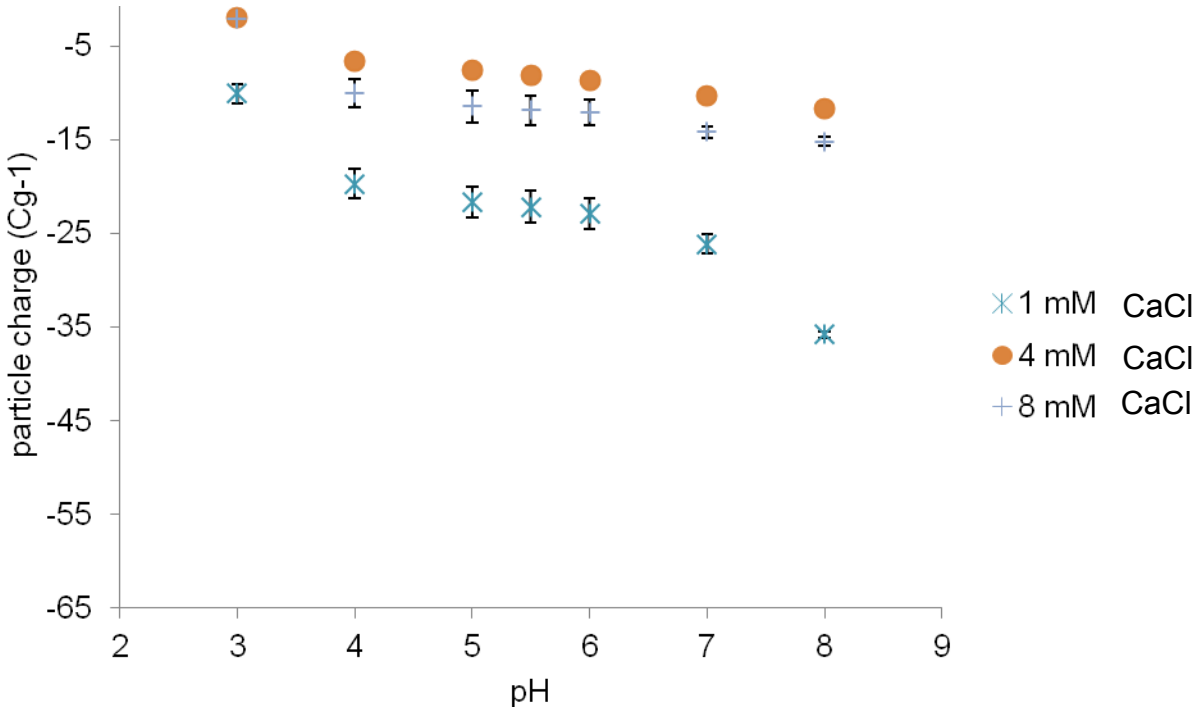

Figure 4.17: Variation in wood resin surface charge with supernatant pH on addition of $CaCl_2$ to the 100 mg/L colloidal wood resins suspensions at various concentrations.

As seen with the addition of calcium, the addition of aluminium to the wood resins led to an inconsistency in the results obtained due to the apparent charge reduction at lower addition of aluminium, as shown in Figure 4.18.

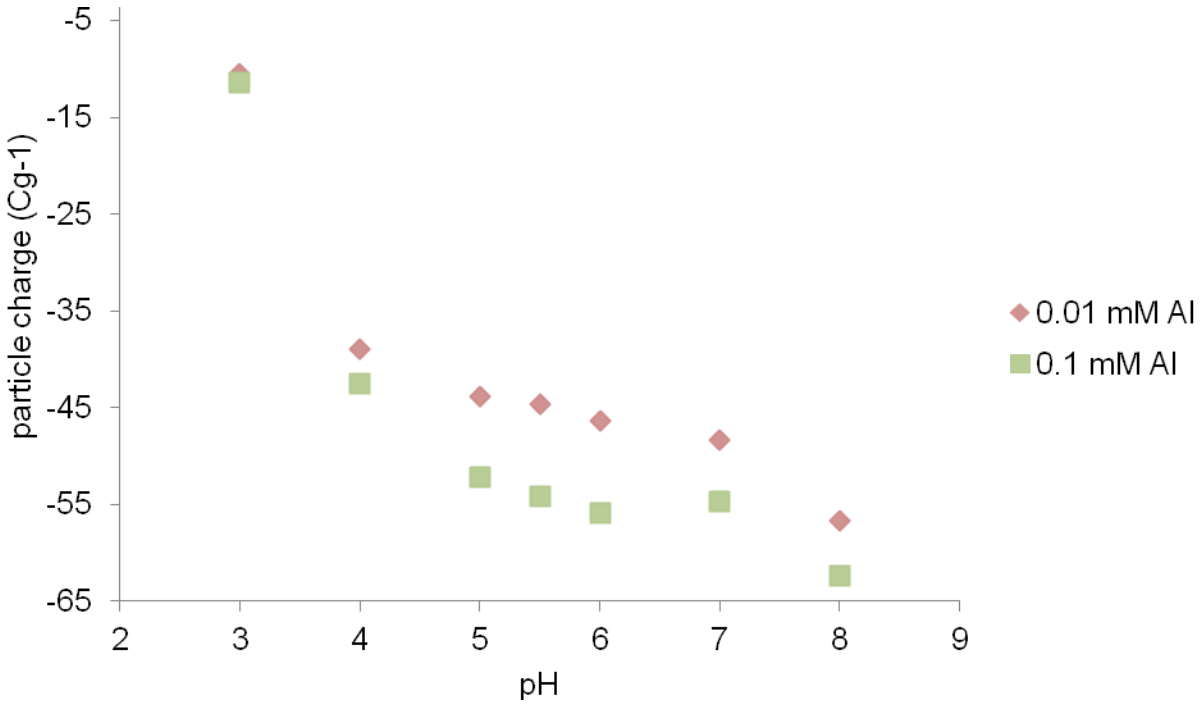

Figure 4.18: Variation in wood resin surface charge with supernatant pH on addition of $Al_2(SO_4)_3$ to the 100 mg/L colloidal wood resins suspensions at various concentrations.

One possible explanation of this is that the inconsistencies in the surface charges obtained for the wood resins on addition of salt to the dispersion arise from the destabilisation of the colloids and deposition to the surface of the pH probe. As noted previously, the deposition of the wood resins and changes in the wood resin composition can result in poor reproducibility and pH depression due to the coating of the electrode surface. Consequently, the results for the addition of salt at high concentration to the wood resin dispersions are not thought to be representative of the true colloidal surface charge. However, electrode fouling was noted at very low salt concentrations at low pH. The endpoint for change in pH due to the addition of sodium hydroxide to solution was determined as the stable pH. These pH values were stable for 30 seconds, see Chapter 3.18. It is postulated that the odd sequence in the charges determined for the addition of the various salts and concentrations of salt are the result of the reorganisation of the various fatty acid and resin acid species, possibly as a result of the formation of metal resinate species. Results are included to give a general idea as to the effect of pH on the surface

charge of the colloidal wood resins in order to better understand their stability in solution. However, these are best to be taken as a broad notion for the charge and a basis for the changes in surface charge with pH, but not as absolute values.

4.3 CONCLUSION

According to the EPR spectra, the triglycerides and other non-polar components of the colloid sit within its core, as proposed by both the Qin and Vercoe colloidal structure models.

In regard to the colloidal shell, an improved model is proposed to account for the fatty acids' formation of a mobile phase apparently separate from the resin acid shell. The interaction of the fatty acids with the supernatant solution is dependent on the concentration of both the fatty acids and non-polar components. It is proposed that the reduction of polarity in the fatty acid will result in greater separation between the phases within the colloid, indicating that unsaturated fatty acids will have a greater interaction with the aqueous solution outside the colloid. From the current experiment, it is not possible to determine if there is a separation of the fatty acids of trygicerides from the bulk colloid at the very high concentrations.

The addition of electrolytes to solution affects the mobility of molecules at the colloidal core. However, the mobility of the fatty acid mobile phase is unaffected by this addition. It is proposed that this is a result of the movement of metal resinates to the colloid's centre affecting the viscosity of the microscopic environment within the core of the colloid.

The surface charge of the wood resin colloids was found to increase with the pH of the solution. Comparison between the zeta potentials found with the use of the qNano system show large reduction in the zeta potential by comparison to the zeta potentials reported for the northern hemisphere wood resins. This variation may be a result of the differences in composition. However, given the increased percentage of resin acids in *Pinus radiata,* a greater charge than the spruce wood extracts would be expected. The surface charges determined from potentiometric titrations show good correlation in their magnitude to the potentials found on the wood fibres of both northern hemisphere spruce and *Pinus radiata*.

CHAPTER FIVE

COAGULATION KINETICS AND COLLOIDAL STABILITY: EFFECT OF SALT ADDITION

This chapter looks at the effect of the ionic strength of the process water on the wood resin colloids separate from the other aqueous materials. Coagulation is reviewed as a function of salt type, salt valency and multiple salts present in solution simultaneously. Through this, a better understanding of how to control and predict behaviour of the resinous material can be achieved.

5.1 INTRODUCTION

The stability and aggregation of colloidal particles is important to many industrial processes (paint, food, petrochemical, pharmaceutical, mineral processing and papermaking etc.) [77, 175, 176]. It is well established that colloidal stability is governed by the attractive and repulsive forces between the colloidal particles as discussed in Chapter 2, Section 2.3.

The DLVO theory describes the total energy between two particles (V) as they approach one another as a function of the electrostatic repulsion forces (V_R) and the van der Waals attractive forces (V_A) [61, 88]. The addition of salt to the colloidal suspension results in the compression of the electrical double layer, reducing the electrostatic repulsion forces that inhibit the coagulation of the particles [61, 88]. This effect increases with salt concentration. The Shultz-Hardy rule predicts that at a critical concentration of salt in solution, the repulsive forces will be completely screened, and the van der Waals attractive forces will predominate. The outcome being every interaction between particles resulting in permanent attachment [61, 88].

5.1.1 ORIGIN OF THE PDA SIGNAL

The photometric dispersion analyser (PDA) has been found to be a useful research tool to study colloidal aggregation [116, 177]. It also offers potential as an on-line sensor. The PDA measures the turbidity variations of a moving colloidal suspension. The instrument measures the direct current (DC) voltage (V_{DC}), which corresponds to the average transmitted light intensity and the root mean square (RMS) value of the fluctuations in intensity of light transmitted (V_{rms}), which indicates aggregation of the suspension. The ratio (R) of V_{rms} / V_{DC} has been shown to be a function of the particle concentration and particle size [116, 177] and has been used to measure the degree of aggregation of colloidal particles. More importantly, it has been found to be unaffected by contamination of the optical surfaces or drift in the electronic components [177].

As noted, it is possible with the PDA to monitor aggregation/dissociation rate for particles and from these determine the stability ratio (W). The stability ratio is measured from the coagulation rate of the particles from experimental results, as per Equation 2.17. However, there are a number of challenges and difficulties involved in the measurement of soft colloidal suspensions.

5.2 RESULTS AND DISCUSSION

5.2.1 PDA SIGNAL

The PDA was used to study aggregation kinetics of wood resin colloids. Figure 5.1 shows a typical PDA ratio output with time for colloidal wood resins from *Pinus radiata*. In this experiment, 625 mM KCl was added to aqueous suspension of undialysed hexane extracted wood resins. The curve obtained is typical of other colloidal systems [113]. It shows three distinct regions: an initial region with a positive slope, rising to a peak, and then tailing off. The slope of the initial growth region indicates the rate at which flocs develop/aggregate. The peak represents the steady state between aggregation and disruption of the aggregates. Most reported studies find that the ratio output maintains a constant value after the peak while some indicate that a lower steady state is reached representing the balance between floc formation and floc

breakup induced by shear [113]. In Figure 5.1, the trace continues to decrease to a level lower than the starting value. This could reflect a change in particle concentration, a disruption of aggregates as the weak salt-induced flocs are broken down by shear to a lower equilibrium size, or a change in the internal structures of the wood resin particles with time. The signal as ratio (R) takes into account both the V_{DC} and V_{rms} signals and internally corrects for the changes in the light scattering efficiency [177]. The time-weighted variance in the output provides an indication of the variations in the homogeneity of the colloidal flocs and can be used to measure the floc structural differences and the effect of changes in solution on the floc variation. Small variations in signal indicate a tighter floc size distribution and a more homogeneous, dense and less porous floc structure.

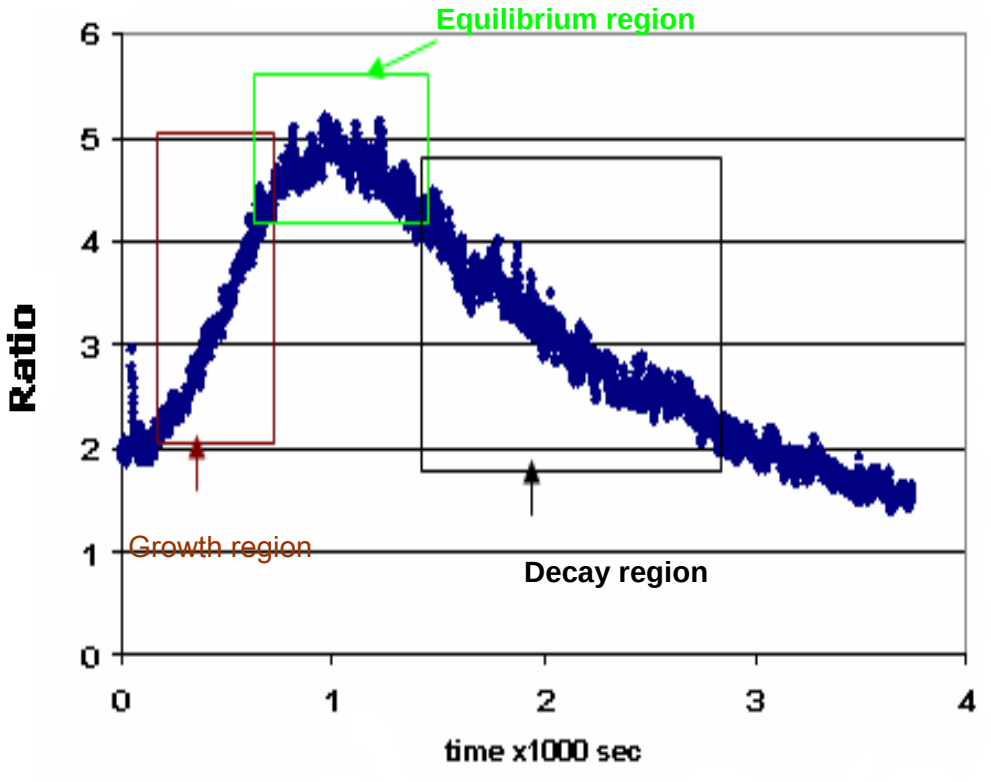

Figure 5.1: PDA Ratio output signal for an aqueous suspension of undialysed hexane-extracted colloidal wood resins (100 mg L^{-1}) with 625 mM KCl.

The wood resin concentration in the PDA suspensions was monitored over a period of time. Figure 5.2 shows clearly that the concentration of wood resin colloids in solution was

decreasing throughout the PDA experiment. This decrease in concentration is most likely due to deposition of wood resins onto the tubing and/or sample vessel of the PDA apparatus.

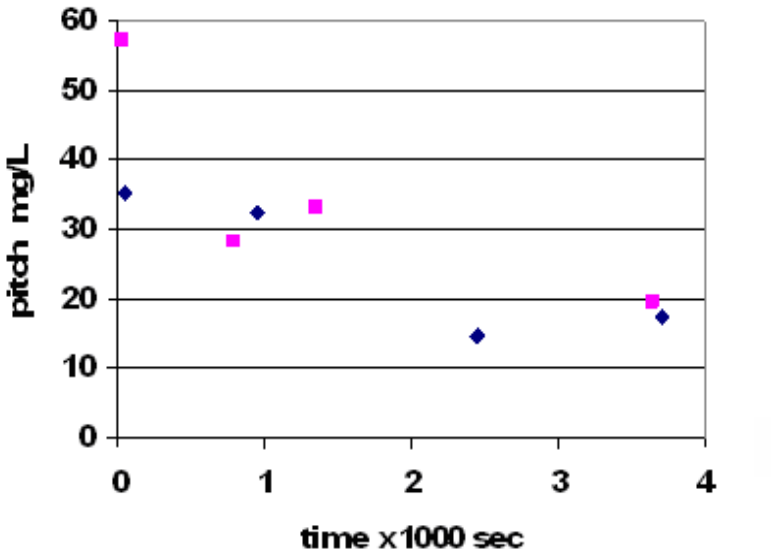

Figure 5.2: Change in wood resin concentration and effect of initial concentration during PDA measurements of aqueous suspensions of undialysed hexane-extracted wood resin with 625 mM KCl.

5.2.2 REPRODUCIBILITY AND CONTAMINANTS

During the initial stages of experimentation with the wood resin dispersions, a problem was encountered with reproducibility of results. The signal response was found to increase with repeated measurements of the same solution in the apparatus. It was found that conditioning of the tubing was required prior to measurement to ensure reproducible and reliable results. It appeared that the hydrophobic tubing material and sample vessels were absorbing wood resins prior to the PDA detector and a period of time was needed to condition these surfaces. To prepare the apparatus, a suspension of a colloidal wood resin sample was allowed to pass through the tubing for a period of 12 hours until the signal response became more reproducible. No further conditioning was required during experimentation unless changes in

tubing or other components were made. Reducing the tubing length was also found to increase reproducibility and reduce the conditioning time required. Figure 5.3 shows the variation in the signal due to conditioning after six consecutive runs of one sample.

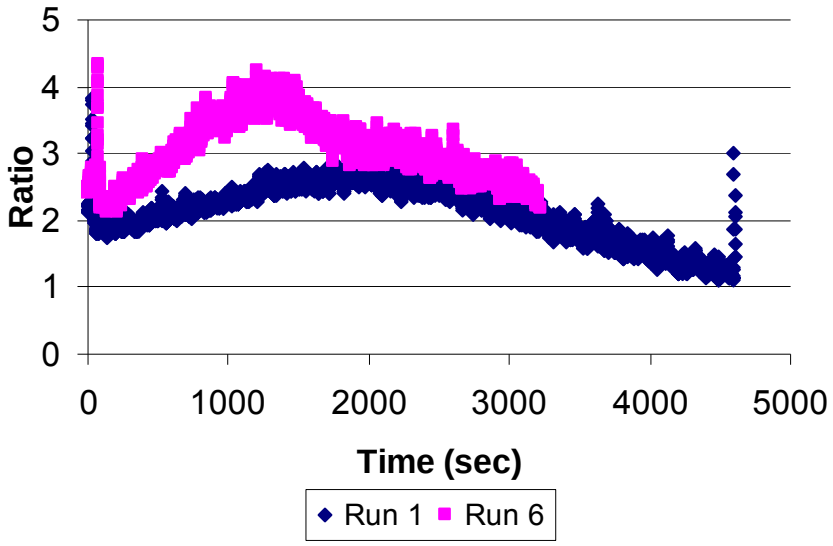

Figure 5.3: Effect of conditioning of tubing on PDA output for addition of 625 mM of KCl to a solution of 100 mg/L of wood resin.

5.2.3 FACTORS AFFECTING PDA SIGNAL

During the experiments, several other factors were found to affect the behaviour of the colloid in solution and thus the PDA signal. These included the concentration, flow rate and stirring of the colloidal wood resin sample. Figure 5.4 shows the effect of wood resin concentration and flow rate (controlled by the pump speed) on the signal variance and response. It is noted that as the concentration of wood resin colloids in solution increases, the signal response of the PDA also increases. Furthermore, the increase in flow rate from 20 mL/min to 60 mL/min enhanced the response to the changes in concentration of particles. This is thought to be the result of changes to the shear experienced by the colloid.

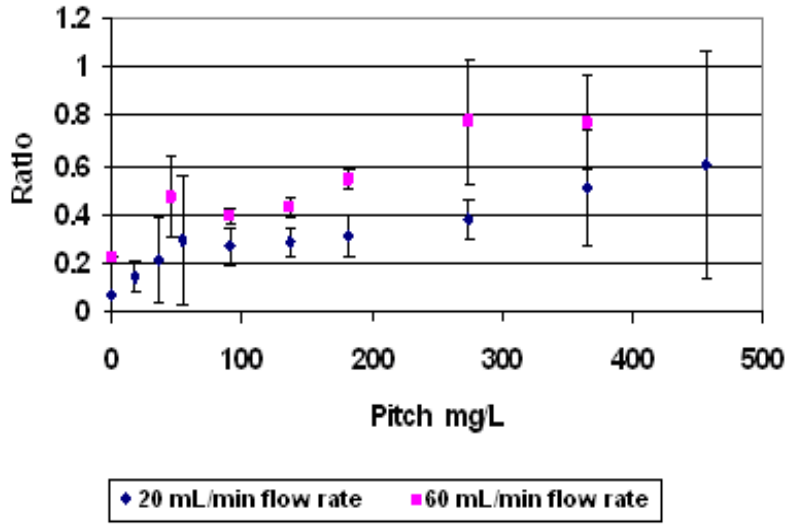

Figure 5.4: Effect of wood resin concentration in 1 mM KCl solution, on PDA Signal Ratio at 20 mL/min and 60 mL/min flow rate. (Error bars are 1 standard deviation)

Within the system, it is noted that there are two sources of shear: the first is the result of pump flow rate and the second is the result of stirring within the sample vessel. Figure 5.5 shows the output signal for both a stirred and unstirred sample at the same concentration of wood resin (91 mg/L) and electrolyte (625 mM KCl at t = 500 sec). The initial slope for the growth of colloids on addition of salt was greater with continuous stirring. The plot also indicates that under continuous shear conditions, the flocs reach a maximum size and then stabilise at this size, as indicated by the plateau region in Figure 5.5. On the other hand, it could be argued that the particles formed change their density and form smaller, denser flocs in solution with a stable region resulting from the change in refractive indices. However, given that the particles are liquid under these conditions, changes in density are unlikely unless there are changes in the colloidal makeup. The formation of the lower plateau level for the wood resin colloid sample with delayed stirrer turn on (Figure 5.5) is postulated to result from reformation of the colloidal particles in solution giving smaller, tighter flocs. The two spikes in the PDA curve following the initiation of stirring are possibly caused by larger flocs breaking away from the paddle under the shear conditions.

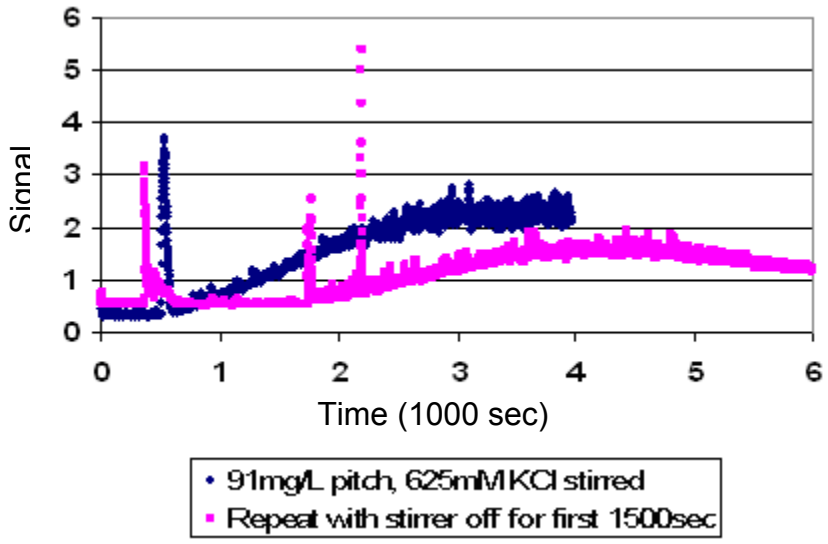

Figure 5.5: Effect of stirring on PDA ratio output signal.

As a result of the variability of the PDA signal due to these physiochemical conditions, it was noted that the wood resin concentration, sample stirring and pump flow rate are variables that must be controlled for all experiments if comparison between samples and quantification of coagulation rates are to be carried out.

5.2.4 CONVERSION OF PDA SIGNAL TO STABILITY FACTOR.

The effect of variation in the concentration of $CaCl_2$ added to colloidal wood resin dispersions is shown in Figure 5.6. Coagulation studies were performed using dialysed wood resins, as they are a better analog for the colloidal particles present in the mill. As the concentration of salt added to solution increases, the slope of the growth region and the final signal strength for the PDA both increase. The slope for the growth region is a measure of the rate of coagulation of the particles and is used to calculate the stability factor (W) using Equation 2.16 and 2.17.

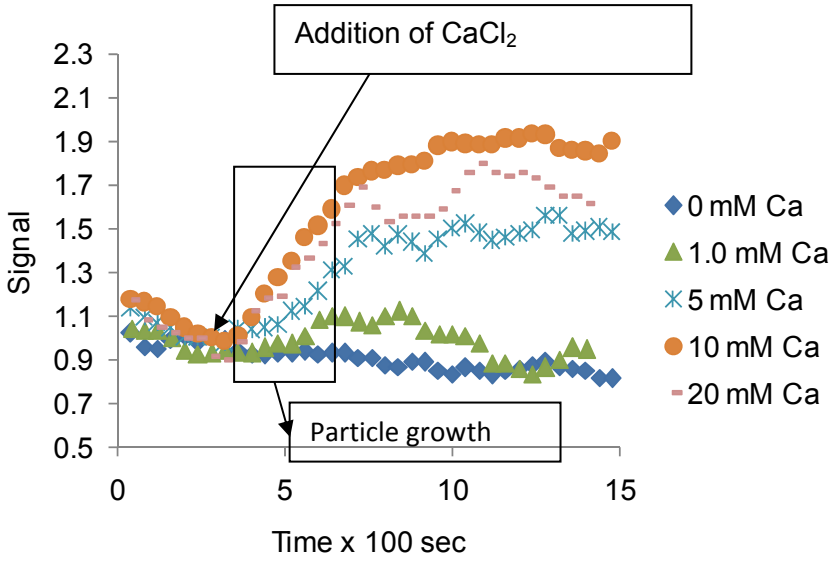

Figure 5.6: Effect of $CaCl_2$ concentration on the coagulation kinetics of dialysed wood resins (100 mg/L) measured by PDA.

Figure 5.7 shows in more detail the growth region for the PDA curves (variation in PDA signal following addition of calcium to colloidal wood resins) in Figure 5.6. The slope of the trend lines plotted through each of the PDA occurs at different salt concentration additions. Table 5.1 shows the calculated stability factors (W) for the results in Figure 5.7. The steepest slope was taken to be the slope for the 10 mM $CaCl_2$ curve. At concentrations in excess of 10 mM of $CaCl_2$, the rate of coagulation remained constant or decreased, as shown in Figure 5.7, which was interpreted as indicating complete coagulation.

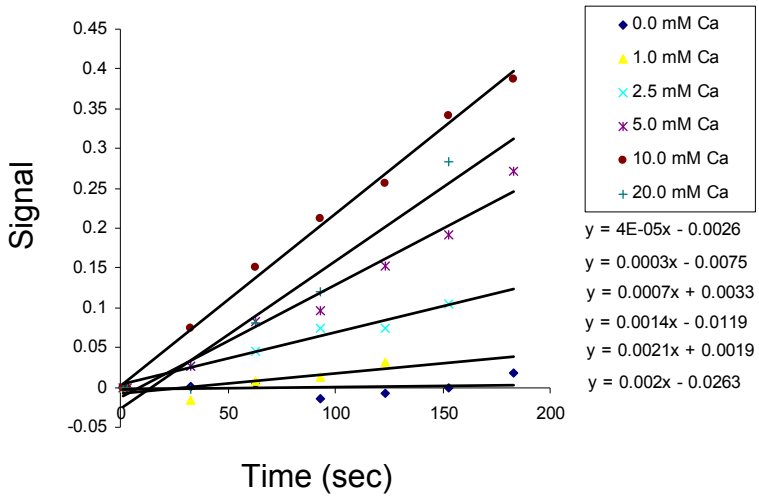

Figure 5.7: Growth region for the addition of $CaCl_2$ to dialysed wood resin dispersion (extracted from Figure 5.6) (with trend lines and trend equations in ascending order).

Table 5.1: Calculated stability factors from coagulation rate for the addition of $CaCl_2$ to 100 mg/L wood resin dispersion (the slope is obtained for the results in Figure 5.7 and W is calculated using Equation 2.16).

[$CaCl_2$]	**Log c**	**Slope**	**W**	**Log (W)**
0	N/A	0.00004	52.5	1.72
0.1	-1	0.0002	10.5	1.02
1	0	0.0003	7	0.85
2.5	0.40	0.0007	3	0.48
4	0.60	0.00113	1.885	0.28
5	0. 70	0.0014	1.5	0.18
10	1	0.0021	1	0
20	1.3	0.002	1.05	0.02

A plot of log W against log salt concentration (Figure 5.8) defines the colloidal stability of the system. At low salt additions, the system has a high value for log W and is said to be

stable. As salt is added and aggregation of the colloids occurs, the system becomes unstable. Stability curves for each electrolyte were obtained by plotting log W against the log of the salt concentration (Figure 5.8) as per the Reerink and Overbeek approximation (Equation 2.20). Inverse sigmoidal curves with three distinct regions are observed in Figure 5.8:

1. an initial flat region at low salt concentration (a stability zone);
2. a region in which Log W decreases rapidly (a transition zone of colloidal instability); and
3. a region in which Log W is 0 at higher salt concentration (complete aggregation of the colloid).

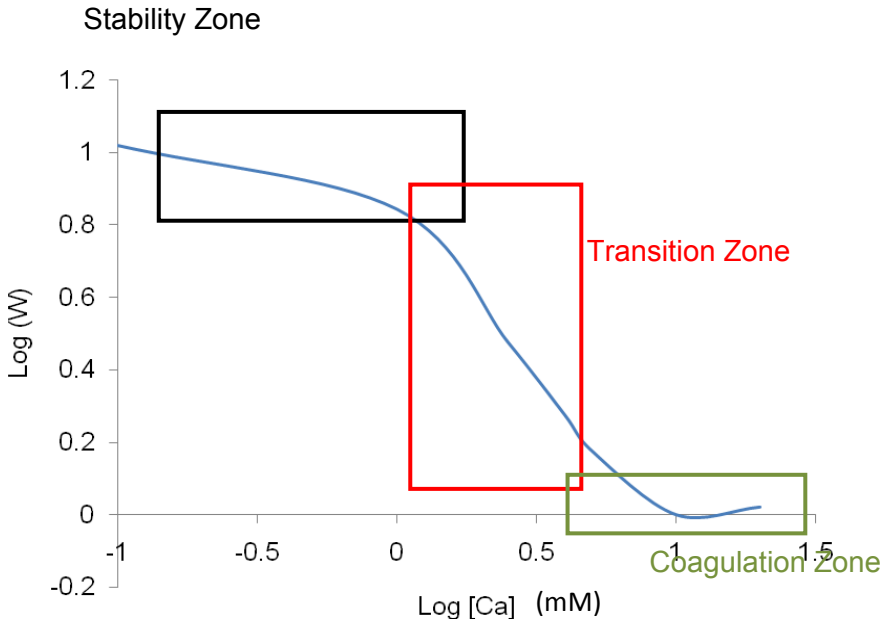

Figure 5.8: Stability ratio curve for the addition of $CaCl_2$ to an aqueous suspension of 100 mg/L dialysed colloidal wood resin.

The critical coagulation concentration (CCC) for a particular salt is determined by fitting a straight line to the relatively linear "transition zone" shown in Figure 5.8 for the stability ratio

curve for that salt and extrapolating to the x-axis. As shown in Figure 5.9, the critical coagulation concentration for Ca^{2+} under the experimental conditions used in Figure 5.8 (pH 5.5, stirring rate 500 rpm, wood resin concentration 100 mg/L) was estimated from the equation for the line of best fit to be 7.8 mM. This method was used to calculate the CCC for all other salts.

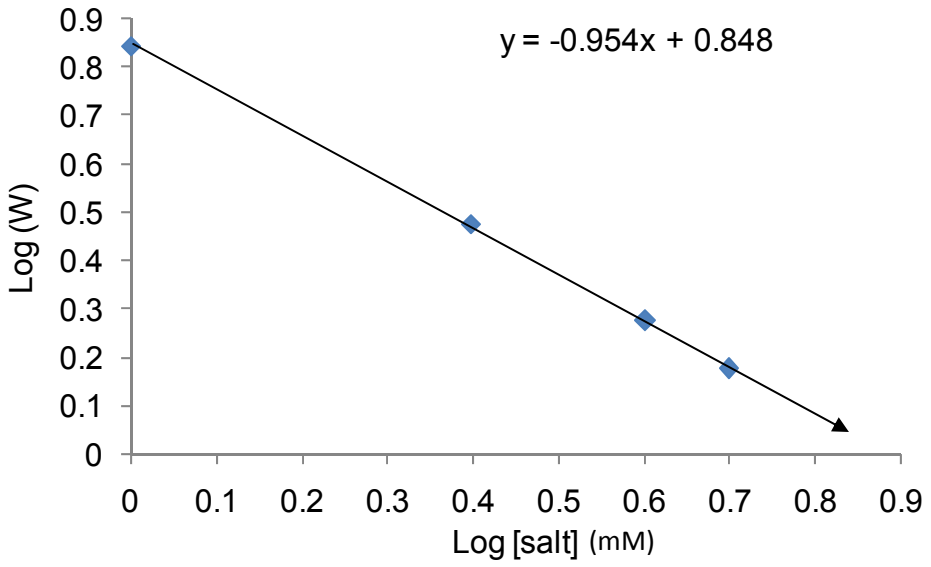

Figure 5.9: Transition region for the stability ratio curve of $CaCl_2$ to colloidal wood resin (Figure 5.8).

5.2.5 EFFECT OF SINGLE SALTS ON COAGULATION OF WOOD RESINS

Salt-induced coagulation experiments were performed with monovalent (NaCl and KCl), divalent ($MgCl_2$) and trivalent ($FeCl_3$ and $Al_2(SO_4)_3$) metal salts. Figure 5.10 shows stability factor (W) curves for the various salts.

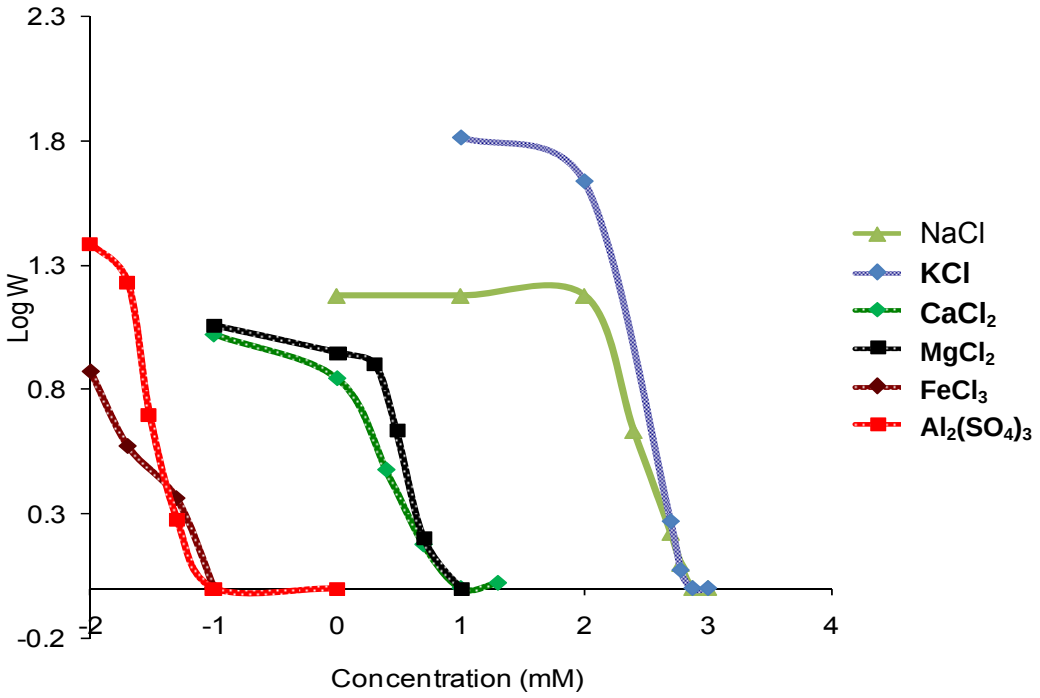

Figure 5.10: Wood extractive stability curves under dynamic conditions for various electrolytes (pH 5.5, 23℃ and 500 rpm).

Table 5.2 summarises the critical coagulations for each salt, determined by extrapolating the linear transition regions in Figure 5.10 to the x–axis as discussed in 5.2.4. Error in the result is calculated on the basis of the average standard deviation in the three replicates for each salt concentration.

The results in Figure 5.10 and Table 5.2 show a strong dependence on the salt valency. As the salt valency increases, the CCC decreases. Slight differences in the CCC's for the different cations of the same valency are observed. The transition in the curves and the CCC values for the monovalent electrolytes occurs at a concentration around two orders of magnitude higher than that of divalent salts and similarly for the trivalent ions.

Table 5.2: Wood extractive critical coagulation concentration (CCC) under dynamic conditions of different electrolytes at pH 5.5.

Salt	z	CCC (mM)	Error (mM)
NaCl	1	720	36
KCl	1	670	33
$CaCl_2$	2	7.8	0.3
$MgCl_2$	2	6.5	0.4
$Al_2(SO_4)_3$	3	0.065	0.003
$FeCl_3$	3	0.075	0.005

This result is similar to values reported for divalent calcium salts [67-69]. Swerin [164] noted that if colloidal wood resin was stabilised only by electrostatic means then coagulation should occur at a few mM $CaCl_2$. Previous studies quantified the wood resin coagulation critical concentration as a function of pH and salt valency. Mosbye [67], Sundberg [69] and Sihvonen [68] tested wood resin stability by adding electrolyte to a colloidal suspension centrifuged to 500 G. The reported CCC's are presented in Table 2.3.

Literature suggests that the CCC is a function of the type of salt and pH. Although no exact comparison is possible between the CCC's of this work (Figure 5.10 and Table 5.2) and those previously reported (due to different pH, shear conditions), the values do not appear to be in good agreement. However, this could be a result of the different pH, shear conditions (reviewed in Chapter 6) or makeup of the wood resins. The comparison of the results presented in this work with those shown in Table 2.3 raise questions as to the effect of dynamic shear conditions on the value of the critical salt coagulation (CCC) which will be explored in Chapter 6.

Practical application

Within the white water at the Albury paper mill, sodium levels in the process water circuit can vary between 8.7 and 17.4 mM (200-400mg/L). With regard to calcium, soluble levels can vary between 2 and 3.8 mM (80- 150 mg/L). Aluminium is unknown for the Albury site but has been found for the Tasman mill to be 0.04 mM at an upper limit. By comparing these mill values with the CCC values determined, it can be concluded that sodium concentrations in the mill are not a concern, where as, on the other hand, calcium and aluminum are. As the amount of recycling of water increases, the concentration in the mill will approach the determined CCC's resulting in poor process control.

The addition of other additives to the solution will affect this critical coagulation concentration. Additives to the pulp and paper can be used to remove the wood resin particles in a number of different ways. A popular method of wood resin removal from the system is to attach the particles to the paper mat with the use of highly charged cationic polymers or through the use of retention aids. Recently, however, it has been noted that there is a limit to the amount of wood resins that can be attached to the fibre surface before detrimental effects to the paper quality result [16]. Deposition of resin acids onto the customers' printing presses arising from transfer from the paper surface has been found to be a problem. Other methods of wood resin removal that are utilised are screw press systems and flotation, however, each of these comes with their own drawbacks that are not part of this work.

Correlation to Shultz-Hardy rule

The Shultz-Hardy rule predicts variation in the critical coagulation concentration (CCC) to the sixth power of the cation valency (z), for high surface potentials where the gamma function of the DLVO theory limits to 1. For the low surface potentials observed on the surface of the colloidal wood resins, the gamma function in the DLVO theory is expected not to limit to 1 and the relationship will shift to a z^{-2} relationship. A linear relationship between the Log CCC and Log cation valency was obtained (as per Equation 2.20), as shown in Figure 5.11. The slope of the graph is -8.2.

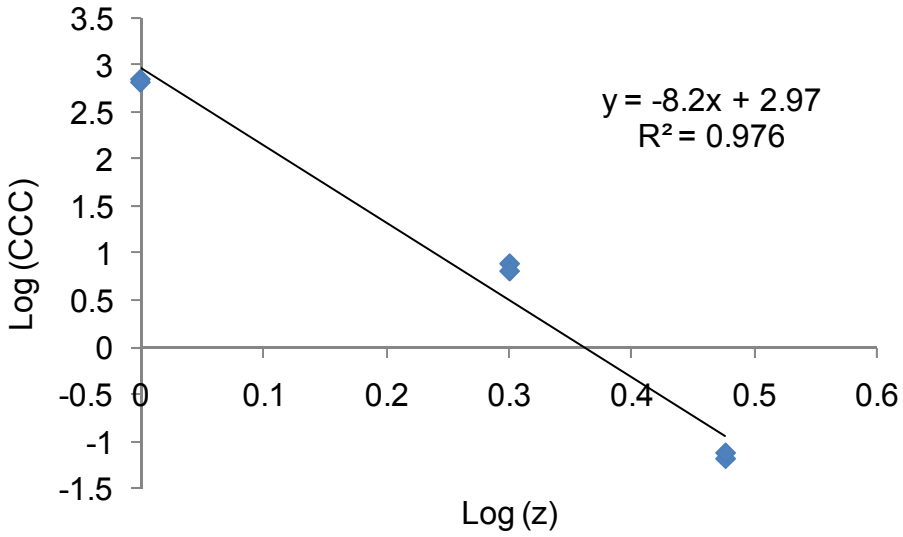

Figure 5.11: Effect of salt valency on the wood resin critical coagulation concentration (CCC) assuming Fe^{3+} and Al^{3+}; pH 5.5 at 23^{o}C and 500 RPM.

It is debatable whether or not the slope of the relationship in Figure 5.11 fully supports the DLVO theory, which predicts a slope of –2 at these surface potentials. The destabilisation effect of metal ion addition for the multivalent ions can be impacted by other side reactions within the solvent.

The result for the trivalent ions is a little surprising because these ions should exist in a number of hydrated forms of varying charge and not strictly in a trivalent form at the pH investigated [178, 179].

Formation of polynuclear metal hydrolysis species and correlation to Shultz-Hardy rule

Conversely, it can be argued that the relationship shown in Figure 5.11 does not support the Shultz-Hardy rule, and the greater than expected dependence of the CCC on the metal ion valency is a result of formation of polynuclear aluminium and iron species. The 3+ ions of both aluminium and iron form poly-nuclear metal oxy-hydroxide species in solution.Among these is an aluminium (or iron) dimer which is a 4+ species [180, 181]. Similar 4+ polynuclear ions of

aluminium have been shown at this pH range by Matijevic et al. [182]. Matijevic et al. postulated the polynuclear formation from the coagulation of silver iodide and silver bromide. Noting that below pH 4, it forms the mononuclear +3 free ion in solution, and between pH 4.75 and pH 7, the coagulation of the silver sols changes which is a result of the formation of the polynuclear species [182]. Above pH 7, the CCC increases again, indicating further hydrolysis resulting in polynuclear species of decreased charge [182]. On fitting the CCC data to these 4+ species, it was found that a very good relationship occurs, as shown in Figure 5.12.

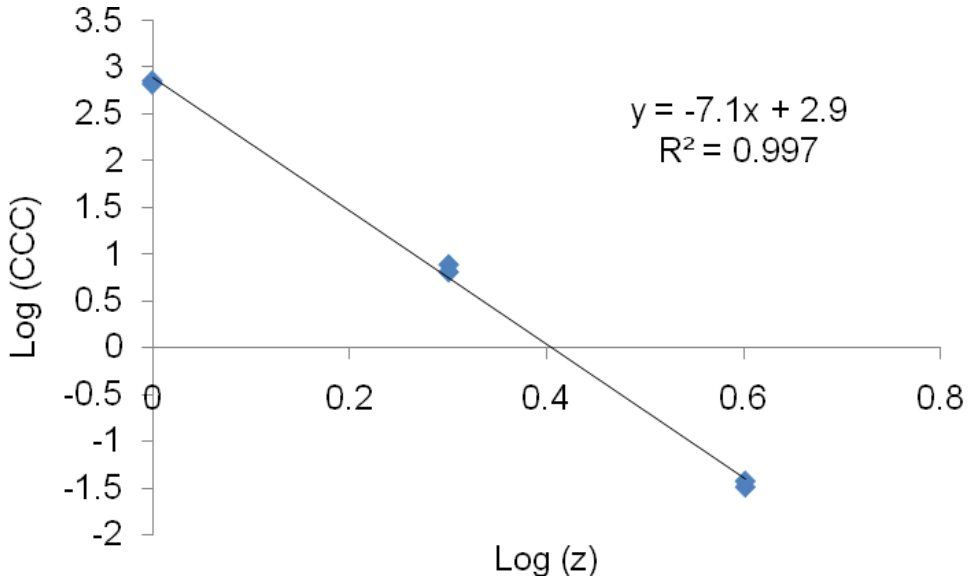

Figure 5.12: Effect of salt valency on the wood resin critical coagulation concentration (CCC) assuming Fe^{4+} and Al^{4+}; pH 5.5 at 23°C and 500 RPM.

Comparison between Figure 5.11 and 5.13 shows an improved correlation if the iron and aluminium species are assumed to be 4+ polynuclear hydroxide ions. The plot of log (CCC) against log (cation valency) for the polynuclear aluminium and iron species (Figure 5.13) yielded a linear plot with a slope of -7.1. This indicates that the change in the CCC is proportional to $z^{-7.1}$, not $z^{-8.2}$ shown in Figure 5.11. This variation in the CCC with the cation charge is higher than

expected and may still result from specific ion adsorption, the dynamic conditions used during coagulation and/or lowering of the Stern potential.

The deviation from classical DLVO theory and the Shultz-Hardy rule for the variation in the CCC with respect to the charge on the cation shown in Figures 5.11 and 5.12 may also result from changes in the coagulation regime between orthokinetic and perikinetic (this is explored further in Chapter 6). Furthermore, it is noted that aluminium in solution is well known to form larger, more highly-charged species, such as the Keggin ion in solution [181] and other polynuclear species [61, 88, 183]. Such polymeric species have been postulated from Al NMR spectra [181, 187]. However, due to the interactions with the wood resin surface and formation of various metal resin soap structures that would equilibrate with the metal ions quickly in solution, it is thought that such species are unlikely.

5.2.6 SIGNAL VARIANCE

Wood resin colloids can be considered as "soft colloids" capable of molecular reorganisation with changes to the environment. The variance in the PDA output signal is an indication of the floc homogeneity in solution as they pass the detector, with larger fluctuations indicating greater variance in particles in the system [113]. The time-weighted variance in the raw ratio signal values is shown in Figure 5.13.

The dependence of the floc structure on the salt type, concentration and valency was observed. The trend in the floc homogeneity from most homogeneous to least homogeneous was found to be Na > Mg > K > Ca= Al > Fe. The fluctuations in the variance can have two explanations: the first being that the aggregate size distribution becomes narrower as the counter ion charge decreases, or the smaller signal variance could result from the floc structure formed on the addition of the salts to solution being tighter.

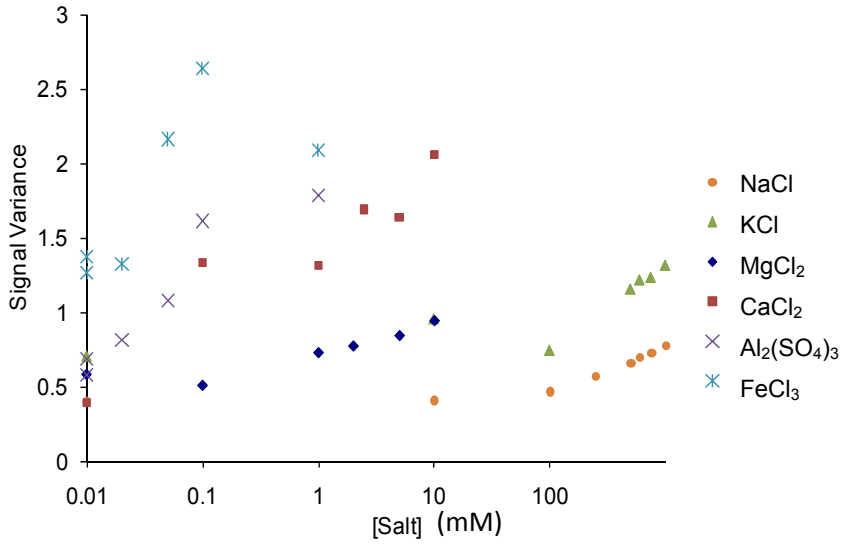

Figure 5.13: Comparison of signal variance for NaCl, KCl, $MgCl_2$, $CaCl_2$, $Al_2(SO_4)_3$ and $FeCl_3$.

5.2.7 VARIATION OF SLOPE OF LOG W AGAINS LOG C

Reerink and Overbeek [62] proposed that the slope of the transition regions in the log W curves (Figure 5.10) is a function of the primary particle size of the colloid, the charge of the cation and the Stern potential (ψ_d) [62]. These are related via the following:

$$\frac{dLog(W)}{dLog(c)} = \frac{-2.15\times10^{7} a\gamma^{2}}{z^{2}} \qquad \textbf{Equation 5.1}$$

Where c is the concentration of electrolyte, a is the radius of the particle, z is the charge on the cation and γ is given by;

$$\gamma = \frac{e^{j/2}-1}{e^{j/2}+1} \qquad \textbf{Equation 5.2}$$

where:

$$j = \frac{ze\psi_d}{k_B T}$$ **Equation 5.3**

e is the charge on the electron, ψ_d is the Stern potential, k_B is the Boltzmann constant and T is the temperature in Kelvin. Reerink and Overbeek noted that there was little or no difference in the values obtained for the zeta potentials and the Stern potentials calculated in this manner [62].

In Figure 5.14, the effect of different salts on the slope of the stability factor linear transition region is shown, with respect to the cation charge.

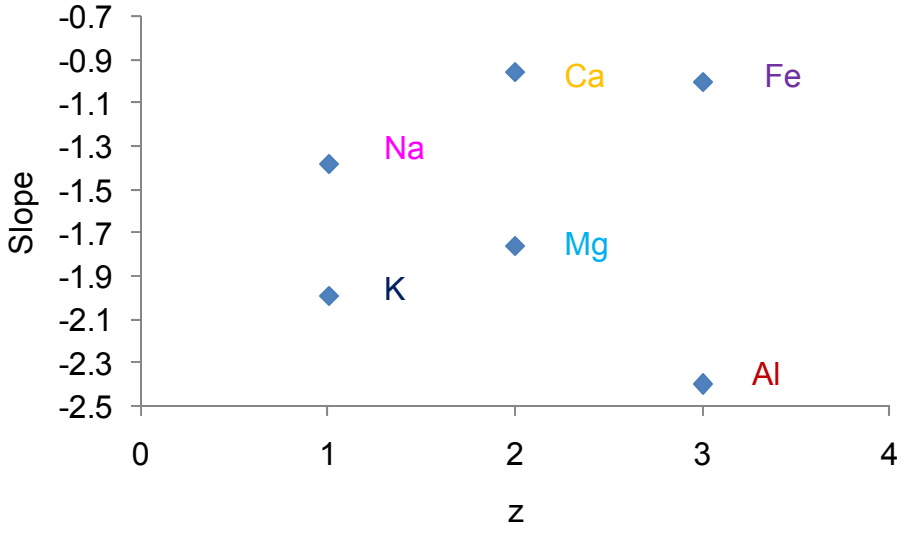

Figure 5.14: Slope changes for log (W) [salt] curves with respect to the counter ion charge.

Given that all primary particles can be assumed to be of a similar distribution, the variation in the slopes for the addition of salt should indicate changes in the agglomeration mechanism due to the varying salt effects [62]. Unlike the variation with the signal and the CCC's, there is a large variation between the different salts of the same valency. There is no obvious trend in their effect on the coagulation that may be associated with adsorption of the different metal ions to the surface influencing the colloidal surface charge.

With the use of Equation 5.1, the calculated ψ_d is shown in Figure 5.15. However, this equation does not consider differences in the salt type (which will lead to different charge densities, hard / soft acids / bases characteristics) but only the salt valency. Furthermore, it does not take into account the potentially determining ion. This is the ion at the surface of the colloidal particle that causes the surface charge or potential. As such, the assumption is that the salts of the same valency and changes in the potentially determining ion will result in the same effect on zeta potentials. This is known to not be the case for many salt types, with the surface charge affected by the potential determining ion (for wood resins, the carboxylic acid head groups of the fatty acids and resin acids) and the differential adsorption of metal ions to the colloidal surface as a result of their different chemical interaction. The variation in the adsorption of the different metal ions to the colloidal surface affects the success of interactions between colloids and with surfaces. Within the pulp and paper industry, the primary variation in this is the effect on the colloidal wood resins when treated with Mg^{2+} as opposed to Ca^{2+} differs (this is discussed further in Chapter 8). The results in Figure 5.13, 5.14 and 5.15 clearly show that there are variances between metals of the same charge and so highlight a deficiency in the traditional theory.

Table 5.4: Calculation of colloid zeta potentials from the slopes of log (W) curves using equation 5.1.

Salt	Z	Slope	ɣ	$1/\psi_d$ (mV)	ψ_d (V)	ψ_d (mV)
Na	1	-1.379	0.345	-81.73	-0.012	-12.2
K	1	-1.989	0.414	-70.88	-0.014	-14.1
Ca	2	-0.955	0.574	-106.23	-0.009	-9.4
Mg	2	-1.756	0.778	-77.23	-0.013	-12.9
Al	3	-2.398	1.363	-52.17	-0.019	-19.2
Fe	3	-1.000	0.880	-99.95	-0.010	-10.0

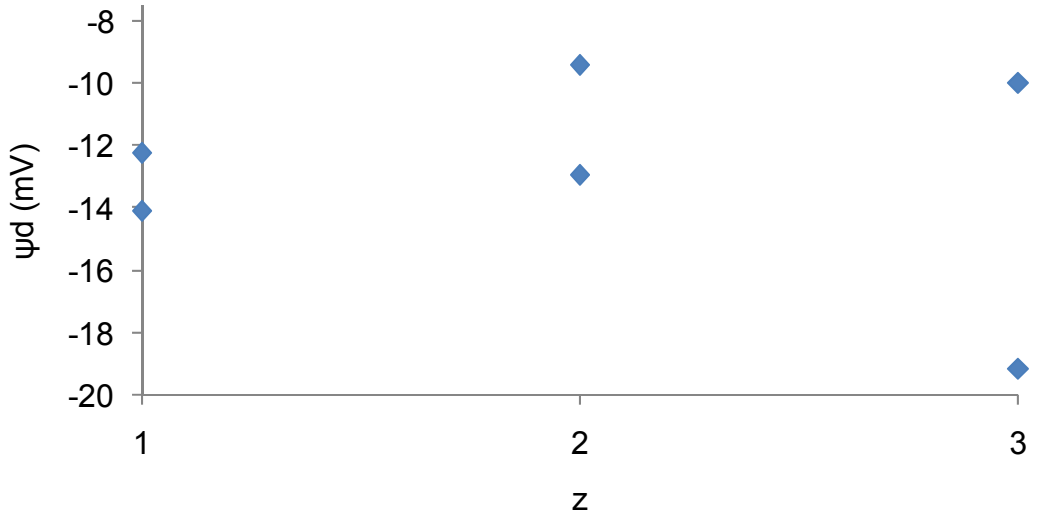

Figure 5.15: Calculated wood resin colloid ψ_d from the converted slopes for various cations (assuming Al^{3+} and Fe^{3+}).

Comparison of the zeta potentials calculated as per Equation 5.1, shown in Figure 5.15, with those determined with the use of the Izon qNano system given in Chapter 4, Section 4.2.9, show similar results with the calculated zeta potentials between -10 mV and -20 mV. However, in comparison, Sihvonen et al. [68] indicate large differences in the surface charge on the particles. At pH 5, the electrophoretic mobility's shown by Sihvonen et al. [68] convert to a zeta potential (ς) of -39 mV for wood resins derived from northern hemisphere spruce. This value is much greater than those calculated for the *Pinus radiata* wood resins from the log (W) slopes. However, given that the wood resins in the present study are derived from *Pinus radiata* not spruce, and thus have different composition and particles size, these zeta potentials give a reasonable estimate for the colloids under consideration in this thesis. This indicates that the zeta potentials calculated in this manner are reasonable approximations but cannot be taken as absolute values.

It is interesting to note from both Figure 5.15 and Table 5.4 that there is variation in the calculated slopes within each valency. This variation within the valencies seems to indicate a reduction in the charge at the surface of the wood resin colloids as a result of specific ion

adsorption for the addition of Ca^{2+} and Fe^{3+}, with greater affinity for the Ca^{2+} over the Mg^{2+}. However Al^{3+} appears to interact with the surface in some other manner resulting in an increase in the zeta potential. This may result from changes in the nucleation of the aluminium in solution, resulting in the formation of higher apparent ionic charge as noted previously. Furthermore, it could result from the formation of various aluminium metal resinates that conform to the surface of the colloid in various sheet-like adsorbed structures [186].

The surface charge calculated from Equation 5.1 is dependent on the charge of the cations. In Figure 5.16, the charge of the counter ion is assumed to be 4+ (as per section 5.2.5). At the higher cation charge, the surface charge for the wood resin increases, which is most apparent for the addition of aluminium. For aluminium, this is calculated to be -19 mV and increases to -27 mV when polynuclear. The change in the surface charge for the addition of iron is not as dramatic as noted for the aluminium.

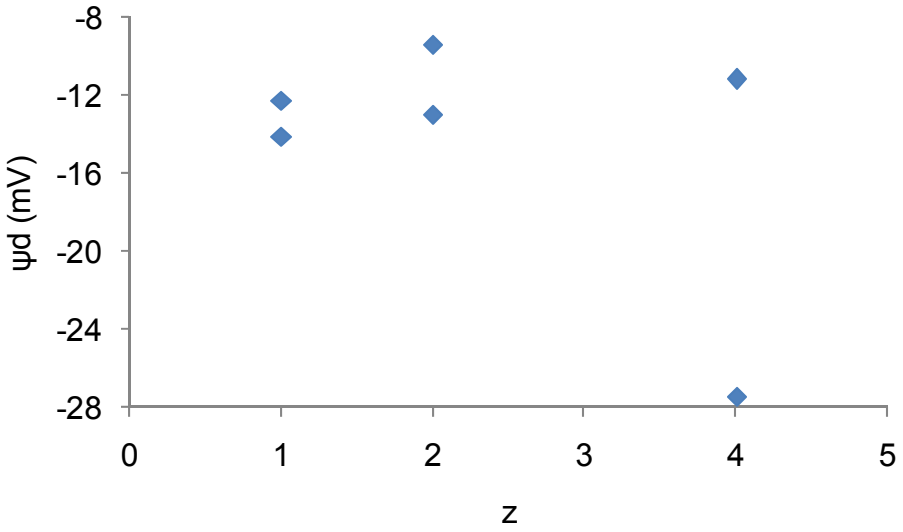

Figure 5.16: Calculated wood resin colloid ψ_d from the converted slopes for various cations (assuming Al^{4+} and Fe^{4+}).

5.3 COAGULATION WITH MULTIPLE SALTS

In the industrial process, a number of electrolytes of varying valency are present in the process water at any time [146, 184]. Therefore, it is important to understand how these salts interact with each other and the colloids.

5.3.1 EXPERIMENTAL EFFECT OF MULTIPLE SALTS.

The effect of multiple salts on the stability of the wood resin colloids was investigated using the PDA. Metal ions, either divalent Ca or trivalent Al, were simultaneously added with a constant 150 mM monovalent Na to a 100mg/L colloidal wood resin solution. The results of the divalent and trivalent salts indicate a similar coagulation response to when a single salt was added.

Figure 5.17 shows the PDA signal response of the coagulation of the wood resin colloids to the addition of varying concentrations of Al^{3+} salt to wood resins in 150 mM NaCl. Similarly, stability experiments were also performed on the addition of varying concentrations of $CaCl_2$ in 150 mM NaCl.

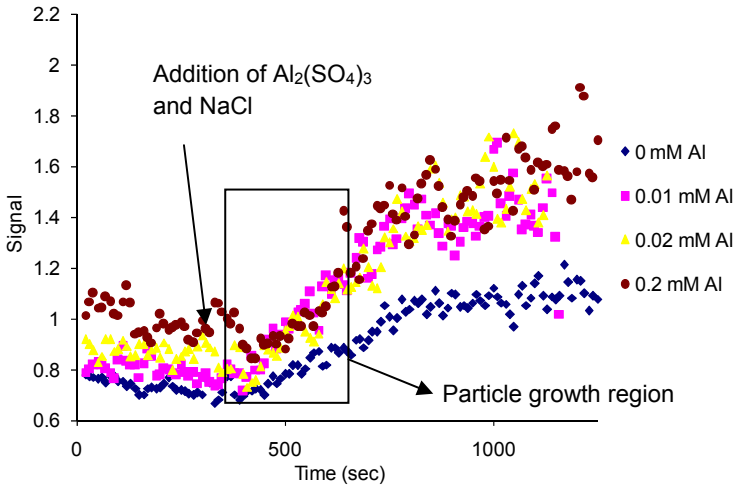

Figure 5.17: PDA response to the addition of various concentrations of $Al_2(SO_4)_3$ in 150 mM Na^+ under dynamic conditions to wood resin colloids (pH 5.5, 23^{o}C and 500 rpm).

The slope of the PDA response curves for addition of multiple salts to the colloidal dispersion was used to determine the stability ratio (W).

In a second set of related experiments, divalent Ca or trivalent Al, in a range of concentrations of monovalent Na solution, were added to a 100 mg/L colloidal wood resin solution. Figure 5.18 shows the effect of varying the concentrations of both NaCl and $CaCl_2$ on the stability ratio (log W). The results indicate that as the levels of the electrolytes increase, the colloids are destabilised, and the stability curve's minimum shifts to the left as the concentration of the second salt (Na) increases. It is noted that restabilisation of the colloids occurs as the concentration of the multivalent salt increases above the CCC.

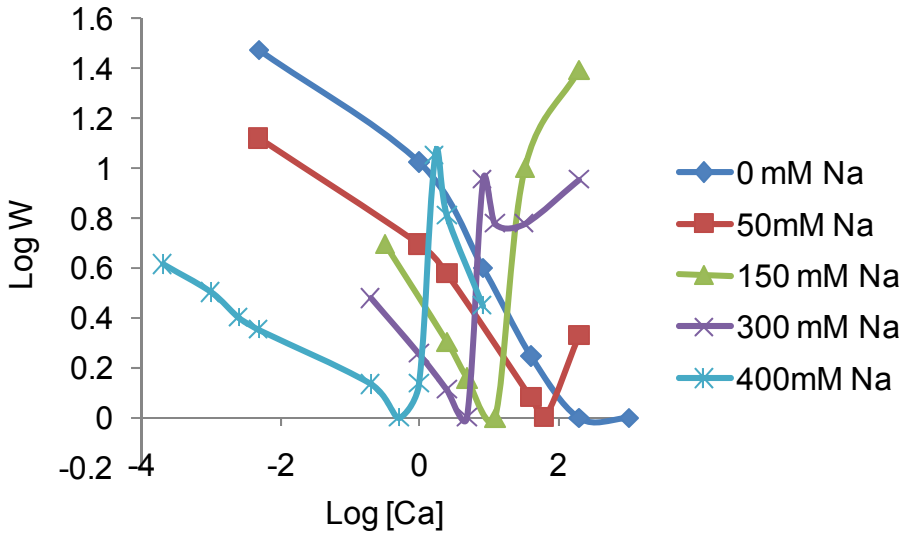

Figure 5.18: Wood resin stability curves under dynamic conditions for various concentration of Ca^{2+} in a number of Na^{+} solutions (pH 5.5, 23°C and 500 rpm).

By plotting log W as a function of $\log[Al_2(SO_4)_3]$, the variation in the wood resin stability curves with the addition of $Al_2(SO_4)_3$ at a number of NaCl concentrations can be seen. As was observed in the case of $CaCl_2$ addition, the stability of the colloids decreases at low

concentrations of aluminium in NaCl and then passes through a maximum in the rate of coagulation of the particles, as shown by the minimum in the log [Al] vs log W plot (Figure 5.19). Restabilisation of the colloidal particles occurred at high addition of $Al_2(SO_4)_3$ for all samples.

The apparent restabilisation of the colloid at addition of high levels of multiple salts has not been previously reported for colloidal wood resins, though it has for other colloidal systems. Dishon et al. [87] showed from atomic force microscope (AFM) measurements that the force between silica surfaces in NaCl, KCl and CsCl aqueous solutions have three distinct regions. As ion concentration increases, the electrostatic double-layer repulsion is reduced with compression of the electrical double-layer, and the Van der Waals attraction forces predominate. It was further found by Dishon that as the salt concentrations were further increased, repulsion re-emerges because of surface charge reversal by excess adsorbed cations. There are a number of limitations to the DLVO theory, with regard to the effect of the electrolyte. The electrolyte interaction with the surfaces, and thus destabilisation of the colloidal particles, is assumed to occur through indifferent electrolyte screening of the surface charge. The results shown in Figures 5.18 and 5.19 indicate that the DLVO theory does not apply to these systems as a result of the adsorption of metal to the potential-determining hydroxide ions at the colloidal surface, resulting in surface charge reversal.

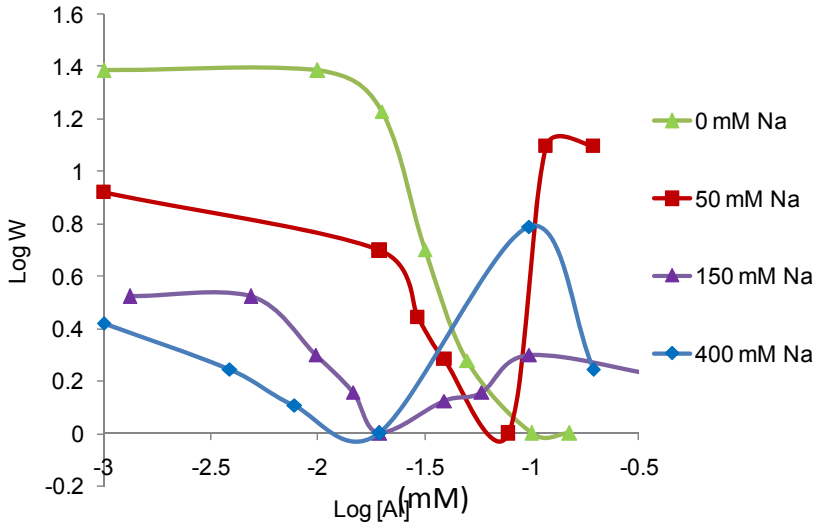

Figure 5.19: Wood resin stability curves under dynamic conditions for various concentration of Al^{3+} in a number of Na^{+} solutions (pH 5.5, 23^{o}C and 500 rpm).

5.3.2 VARIATION IN THE CCC WITH MULTIPLE SALTS PRESENT

Table 5.5 summarises the changes in the CCC values for the colloidal wood resins with the addition of sodium and calcium salts as well as sodium and aluminium salts, respectively. The critical coagulation concentration (CCC) was determined by extrapolating the slope of the linear transition to the origin in the stability curve in Figure 5.18 and 5.19, in the same manner as the destabilisation of the colloids due to single salts.

Table 5.5: The critical coagulation concentrations for calcium and aluminum at different sodium concentrations. As before (Section 5.2.5) the error in the CCC results is calculated from the standard deviation in the rates of coagulation.

[Na] mM	CCC [Ca]	Error (mM)	CCC [Al]	Error (mM)

	(mM)		(mM)	
0	7.8	0.3	0.07	0.003
50	6	0.2	0.06	0.005
150	3	0.2	0.02	0.002
300	2	0.1		
400	0.9	0.04	0.01	0.0007
720	0		0	

The effect of sodium ion concentration on the CCC for Ca^{2+} and Al^{3+} is shown in Figures 5.20 and 5.21. Intuitively, the effect of the second salt on the CCC is predicted to be simply additive – where if half the CCC for a monovalent salt is added to solution with varying divalent salt concentrations, the newly predicted CCC will be half the original CCC for the divalent salt. Figure 5.20 and 5.21 show that the critical coagulation concentration for calcium and aluminium decrease in a non-linear way with the addition of sodium.

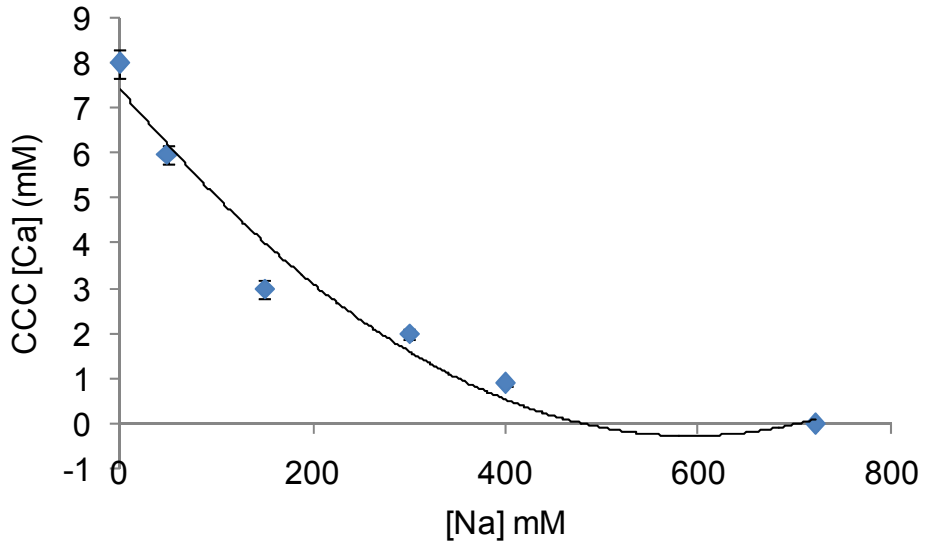

Figure 5.20: Effect of the presence of a second salt in solution on the critical coagulation concentration for Ca.

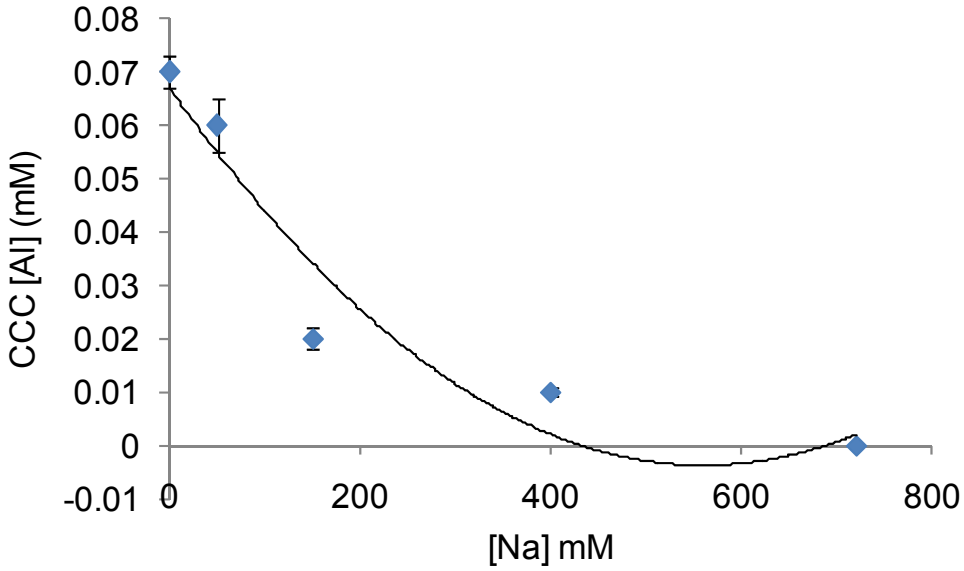

Figure 5.21: Effect of the presence of a second salt in solution on the critical coagulation concentration for Al.

The coagulation of the colloidal particles is attributed to the suppression of double-layer repulsion upon addition of positively charged salt ions, resulting in the dominance of the van der Waals attractive forces between the particles. Formerly, there has been no characterisation of the stability of wood resin colloids on addition of multiple salts to solution. As such, comparison of the resulting CCC's from the addition of the second electrolyte to the mixture is not possible.

Deviation from an expected linear relationship between the CCC and total salt concentration (multivalent salt plus monovalent sodium) (Figures 5.20 and 5.21) may result from non-DLVO effects, such as the adsorption of the ions onto the colloid surface, influencing the surface charge and from solvation effects [185] where hydrating water molecules are released (especially in the case where they are weakly bound to the cation). The precipitation of the

multivalent ion onto the surface is enhanced in some manner by the presence of the sodium ions in solution, resulting in greater deviation with increasing sodium concentration.

Furthermore, the apparent restabilisation of the colloids to coagulation (Figures 5.18 and 5.19) is not accounted for by classical DLVO theory. It is not observed for the colloidal destabilisation due to single salts within the concentration range added. As a result of the afore-mentioned work by Dishon et al., this is currently being attributed to the adsorption of positive ions onto the surface and a charge reversal possibly driven by the entropy associated with the release of hydrating water molecules (especially in cases where they are weakly bound to the cation). Therefore, the indication is that the deviation for the relationship between the CCC's, for the multivalent salts and the concentration of the added monovalent sodium to the colloidal wood resins, is attributed to the specific ion adsorption of the multivalent salt and not to the solvent effects as the latter should be constant for all additions. This specific ion adsorption of the aluminium and calcium on to the colloidal surface is obviously influenced by the addition of the monovalent Na ions to the solution, causing the deviation from DLVO theory.

However, although it is postulated that the multivalent ion present in solution is facilitating the charge reversal, the specific mechanism used by the sodium ion to facilitate this is unknown (charge reversal is not seen for the addition of single salts to solution). It is postulated that the multivalent salt is forming a polymeric soap structure, similar to the keggin ion [186] (keggin ions have been found to be stable polymeric ions over pH ranges from pH 3 to pH 7 [187]) that is solubilised in the presence of the sodium, resulting in colloidal interactions similar to that seen for the addition of polymers to colloidal suspensions.

It may also be postulated that the addition of the sodium to solution results in a decrease in the required concentration of the multivalent ions to transition between the different types of destabilisation/ flocculation. It is noted in Figures 5.18 and 5.19 that at the higher concentrations of sodium with the multivalent salts, following the restabilisation of the wood resins, there is an apparent second destabilisation. This indicates possibly 4 zones of stability: at low concentrations, the wood resins colloids retain charge; at medium concentrations, charge neutralisation occurs; then through to charge reversal as the concentration of the multivalent increases; and there is a possible zone of sweep flocculation [91]. For sweep flocculation, the

dosages concentrations for multivalent ions are greater than their solubility. Flocculation is thought to occur as a result of incorporation of the colloidal particles into the growing hydroxide precipitate [91].

5.3.3 MULTIPLE SALT - VARIATION OF SLOPE OF LOG W AGAINST LOG C

Figure 5.22 shows the effect that the change in the concentration of NaCl has on the slope of the stability factor linear transition region. Results shown in Figures 5.22 are extracted from Table 5.5 for the respective CCC values for the different salts.

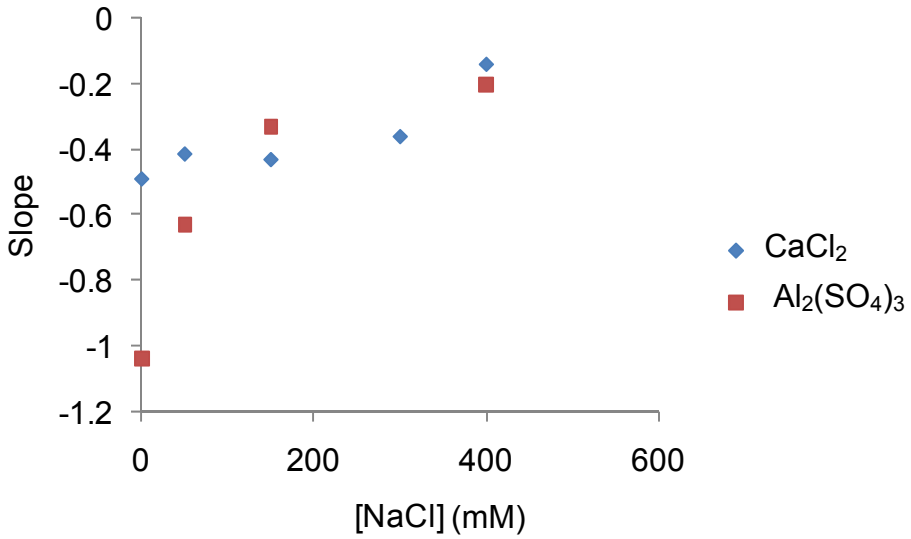

Figure 5.22: Variation in log (W) [salt] curves for the addition of multiple salts to wood resin dispersions with respect to the concentration of [NaCl] (at the CCC for the respective salts, see Table 5.5).

The slope for this region is noted to increase as the concentration of NaCl increases. This variation does not appear to be linear, particularly for the simultaneous addition of aluminium

and sodium, and may result from changes in the agglomeration mechanism. There is a large difference in the change of the slopes of aluminium and calcium additions with sodium concentration increase. This difference between the transition region slopes is indicative of changes in the surface charge or coagulation manner due to the different cation - colloid reactions [62].

In Figure 5.23, the changes in the calculated zeta potentials (Equation 5.1) are shown. Figure 5.23 indicates that as the concentration of the sodium added increases, there is a reduction in the zeta potential associated with the colloidal wood resin surface. For the addition of aluminium, the apparent variation in the calculated zeta potential appears to be very close to linear in its effect. This linearity is not as apparent for the addition of calcium with sodium.

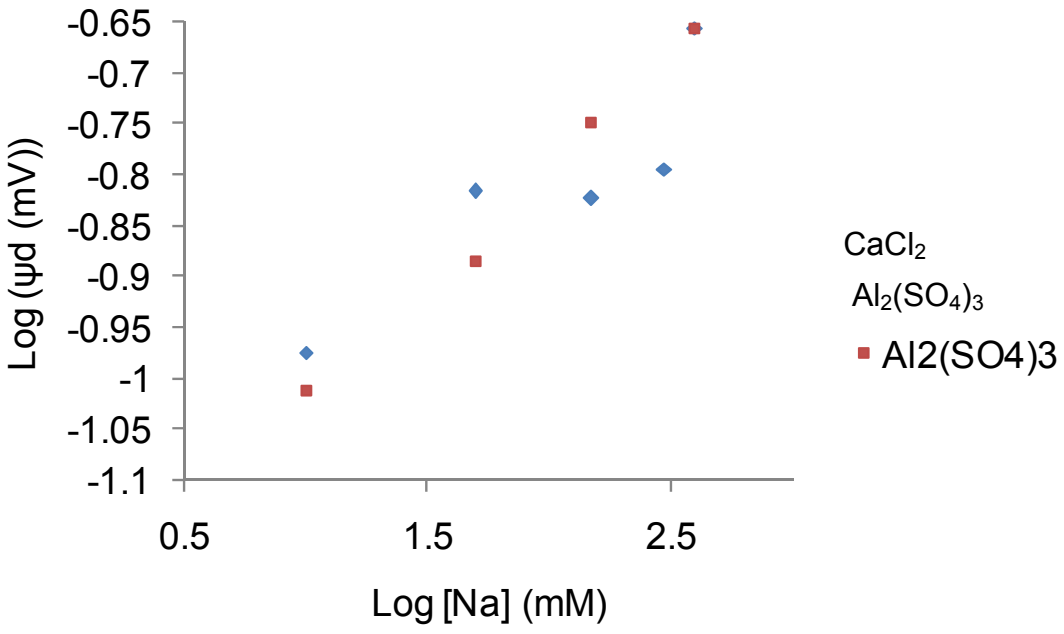

Figure 5.23: Variation in log ψ_d for the addition of multiple salts to wood resin dispersions with respect to the log [Na] (at the CCC for the respective salts, see Table 5.5).

5.4 CONCLUSIONS

Coagulation kinetics of wood resins with variation in the salt type, valency and simultaneous addition of multiple salts were investigated. The critical coagulation concentration for the wood extracts from *Pinus radiata* at pH 5.5 for the cations tested were found to be 670 mM for K^+, 720 mM for Na^+, 6.5 mM for Mg^{2+}, 7.8 mM for Ca^{2+}, 0.065 mM for Al^{3+} and 0.075 mM for Fe^{3+} for single salt additions (at 23°C and pH 5.5).

At the low surface potentials found for the wood resins, the Shultz-Hardy rule predicts variation of the critical coagulation concentration (CCC) to be proportional to the second power of the cation valency (z). There is, however, considerable deviation from this expected relationship and instead it was found that CCC is proportional to $z^{-8.2}$. Under the conditions of this experiment, the multivalent ions of both Al^{3+} and the Fe^{3+} are expected to be present as various hydroxide species and their interaction with the surface is expected to increase. From the coagulation kinetics experiments, it is evident that for both the polynuclear hydroxide species aluminium and iron, the polynuclear ions are postulated to take the form $Al_2(OH)_2^{4+}$. The resulting CCCs appear to fit well with this postulation.

The effect of multiple salts on the system was assessed and shown to initiate a reduction in the CCC for a given salt. The change in the CCC is not simply additive, i.e. if Na at half the CCC is added to solution and Ca is varied, the new CCC is not equal to half the original CCC for Ca. This is shown for both the divalent and trivalent ions.

On addition of multiple salts to a concentration above the CCC, there is a notable restabilisation of the colloid in solution. This effect is not apparent for the addition of single salts to solution.

Both the deviation from the expected simple additive behaviour and the restabilisation of the wood resins on the addition of multiple salts to solution could result from specific ion adsorption to the surface and/or shift in the concentrations of multivalent ions required to undergo sweep flocculation. The restabilisation of the colloids may result from solubilisation of the multivalent ion surface adsorbed species in the presence of the sodium ions in solution.

CHAPTER SIX

FACTORS INFLUENCING THE CCC AND COAGULATION RATE

The stability of colloids and thus the critical coagulation concentration (CCC) is influenced by a number of different supernatant solution physio-chemical characteristics, as shown by the DLVO theory, Equations 2.1 – 2.10. From Equation 2.10, it is evident that the charges on the colloids (through the pH of the solution), the temperature of the solution, as well as the salt valency all influence the CCC. It is also thought that because coagulation is occurring in a dynamic system, the CCC may be affected by the shear in the system through changes in the efficiency of coagulation.

In Chapter 2, the reported values for the critical coagulation concentrations of salt required to aggregate wood resin dispersions were summarised (Table 2.3). It was observed that the pH and salt valency influence the CCC for different salts [67-70]. It was also shown that for the same valency and pH, there is a discrepancy between the different reported CCC's. This chapter explores in more detail the differences in the CCC's, and the effect of pH, temperature and shear.

6.1 INTRODUCTION

As previously noted, wood resins form soft colloidal droplets within solution which coagulate and produce depositions under industrial conditions. This causes numerous downstream issues [188-193], partially due to changes in salt and shear conditions.

It is well understood that an increase of electrolyte in solution instigates destabilisation and coagulation of colloids and the manner in which it occurs [61, 62, 65, 68, 75, 91, 145, 194-197]. However, there are two pre-requisites for particle-particle agglomeration to occur.

The first is accounted for by the change in the concentration of electrolyte reducing the energy barrier between particles, allowing particle-particle interaction to result in stable attachment [61, 91]. This permanent attachment can be affected by variation in a number of the other physiochemical parameters of the colloidal solution. Wood resin charge increases as pH increases due to the ionization of the carbonyl groups of the resin and fatty acids, as indicated in Chapter 4. Solubilisation, especially of resin acids, begins at pH 7 and becomes significant at pH of 8 and higher [8, 26].

The second requirement for coagulation to occur is related to the ability of the solution to bring particles into contact with one another. This can be varied by changes in the kinetic energy of the system through the temperature of the solution or through applied shear. Through PDA measurement, Kang et al. [77] showed the response of Kaolin clays to the addition of ferric nitrate and that the rate of coagulation is affected by the supernatant solution temperature. As the temperature of the solution decreases, there is a marked decrease in the rate of particle-particle interaction. This finding of a decrease in the rate of coagulation was shown again by Xiao et al. [198] with the addition of Al^{3+} to solution. They demonstrated that the change in the temperature altered the rate of coagulation of the particles but that the hydrolysis of the alum species was not affected by the change in the temperature [198]. Kang et al. [77] also demonstrated that the rate of coagulation of the particle is greatly influenced by the pH of the solution. As the pH increases, there should be a decrease in the concentration of Fe^{3+} in solution as a result of hydrolysis to stable $Fe(OH)_n^{z-}$ species.

The shear within the system has been shown to be another factor that influences the rate of particle-particle interaction [61, 71-74, 91]. Sato et al. [84] measured the absolute rates of initial coagulation for polystyrene latex particles as functions of KCl concentration and shear rate and determined that the point of CCC shifts to higher value with increased shear. Furthermore, a plot of the slope of capture efficiency (the efficiency by which particle-particle interactions result in permanent attachment) against ionic strength in the slow coagulation regime decreases with increasing shear [84].

Van de Ven and Mason [78] found that the efficiency of coagulation, or capture efficiency, is related to the shear rate of the system approximately proportional to $G^{-0.82}$. This is

neglected in many of the studies on the collision rate and coagulation efficiency [73, 79-83]. As such, little or no work has been completed re-examining the experimental critical coagulation concentrations of particles as a function of the shear within the system [78, 84-86]. As well, the effect of the type of salt and the valency is unreported, which is essential in understanding the influence that increasing electrolyte levels have on colloidal stability under non-ideal flow parameters.

A better understanding of this matter is crucial, seeing as most mills worldwide are using water recycling processes which result in additional accumulation of electrolyte and colloidal material. However, other influencing factors, such as the temperature of the solution, the pH of the supernatant and the shear experienced, are required to understand the effects the electrolyte-induced coagulation and the critical coagulation concentration for the colloidal wood resins.

For particle-particle interaction that is the result of fluid motion, Kusters et al. [72] give the following expression for the efficiency of coagulation (σ):

$$\sigma = \left(\frac{R_c}{\pi a^2} \right)^{3/2} \qquad \textbf{Equation 6.1}$$

Where R_c is the capture cross-section and *a* is the radius of the particle. However, this calculation of the efficiency of coagulation does not take into account the forces of attraction and repulsion. Kusters et al. also relate the efficiency of coagulation, the radius of two interacting particles (a_i and a_j), the number concentration of aggregates (*n*) and the shear (*G*) to the rate of coagulation of the particles *m*:

$$m = 1.294 \sigma G \left(a_i + a_j \right)^3 n_i n_j \qquad \textbf{Equation 6.2}$$

This expression for the rate of coagulation of particles indicates that when a change in shear occurs, there will be a proportional variation in the rate of coagulation.

Kusters et al. [72] equations for the rate of coagulation and the coagulation efficiency (Equations 6.1 and 6.2) do not take into account the concentration of salt. Furthermore, these

equations suggest that shear will affect the coagulation rate and not the efficiency of coagulation. This would indicate that the repulsive forces from the DLVO theory are present in orthokinetic coagulation and the rate of coagulation will be independent of salt addition.

The efficiency of coagulation has been defined in terms of both repulsive forces (electric double-layer repulsion) and attractive forces (van der Waals attraction) by van der Ven and Mason [199] as follows:

$$\sigma = xC_R C_A \qquad \textbf{Equation 6.3}$$

x is a constant determined from experimentally obtained values at different conditions of flocculation using non-linear regression analysis. C_R accounts for the contribution of electric double-layer repulsion and C_A takes care of van der Waals attraction. Specific forms of C_R and C_A were obtained from the trajectory analysis of the coagulating colloids. According to van der Ven et al. and Agarwal S. [199, 200], C_R and C_A take the following forms:

$$C_R = \frac{2\pi E_C \varepsilon \psi_0^2 (\kappa H)}{3\eta G a^2} \qquad \textbf{Equation 6.4}$$

where E_C is the dielectric constant, η is the viscosity of the solution, and Ψ_o is the surface potential.

$$C_A = \frac{A}{36\pi\eta G a^3} \qquad \textbf{Equation 6.5}$$

Shear affects both attractive and repulsive forces in the Equations 6.4 and 6.5.

6.2 RESULTS AND DISCUSSION

6.2.1 EFFECT OF TEMPERATURE ON THE CCC FOR WOOD RESINS

An increase in the temperature of the wood resin colloidal solution was found to result in a shift of the stability curve to the right and an increase in the CCC, as shown in Figure 6.1. This outcome was expected from the DLVO theory and matches up with previous results for the wood resin colloids [8, 26].

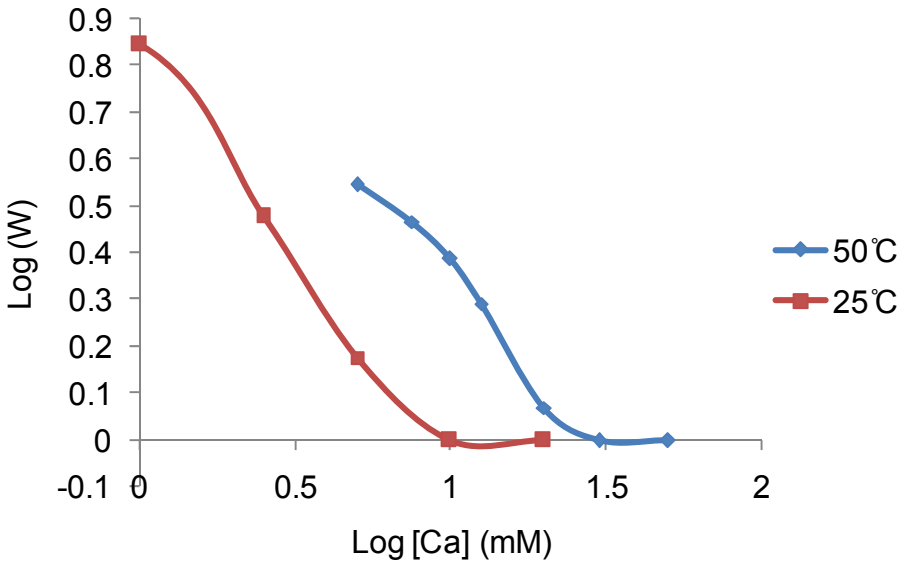

Figure 6.1: Effect of variation in temperature on stability curves for the addition $CaCl_2$ to wood resin dispersions.

Table 6.1 indicates that for different valencies there is variation in the response with an increase in the temperature of the solution. For Na^+ and Ca^{2+}, the change in the CCC is great; however, little or no change is noted for Al^{3+}. This variation in the effect of temperature on the effect of the salt may be a result of two different mechanisms. Firstly, they may be destabilising the colloids with Na^+ and Ca^{2+} acting as indifferent electrolytes and Al^{3+} through specific ion

adsorption. Furthermore, the increase in wood resin temperatures can also affect the interactions of the wood resin particles, both with other particles and the metal ions present in solution, resulting in variations in the surface structures formed [181]. Changes to the rate of formation and structure of various metal resinates at the colloidal surface affects the tackiness of the colloidal particles. On the other hand, it could be influenced by the charge on the counter ion (z) as Na^+ and Ca^{2+} were added as chloride salts and Al^{3+} was added as a sulphate salt.

Table 6.1: Effect of temperature on the CCC for colloidal wood resins to the addition of Na, Ca and Al to solution.

Temperature	**Na^+(mM)**	**Ca^{2+}(mM)**	**Al^{3+}(mM)**
25	720	8	0.07
50	1600	24	0.09

Temperature is expected to influence the critical coagulation concentration. As more thermal energy (KT) is provided to the system, electrostatic repulsions increase ($V_r \alpha T^2$, Equation 2.3), the double layer thickness increases ($1/\kappa \alpha T^{0.5}$, Equation 2.5) and so does the CCC (CCC αT^5, Equation 2.10). This is observed in Figure 6.1 and Table 6.1. However, the valency dependency of the CCC should not be affected by temperature. This dependency for the destabilising cation valency is represented on a logarithm scale in Figure 6.2 for two temperatures: 25°C and 50°C; the slope is relatively unaffected by temperature, as expected.

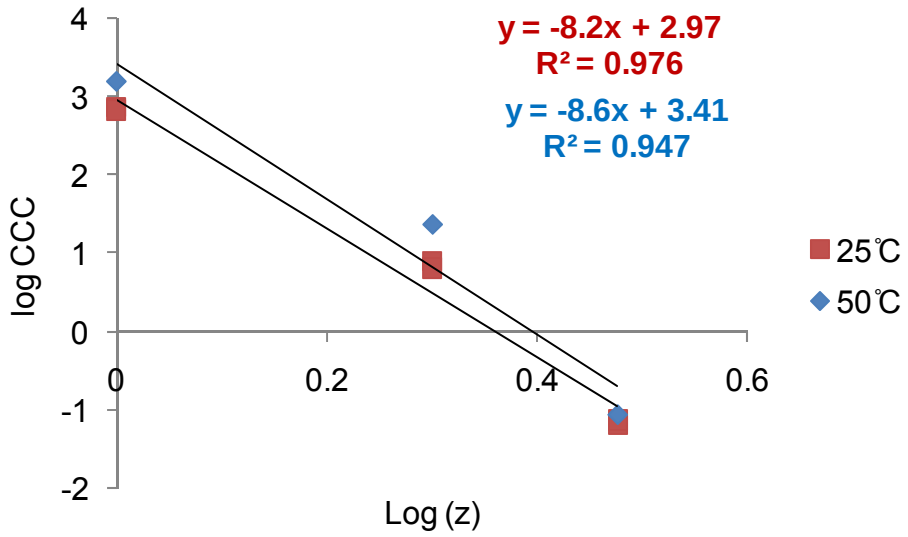

Figure 6.2: Variation of the CCC with respect to the valency of the destabilising ion. Equations for lines of best fit appear in the same order as legend (assuming Al^{3+} and Fe^{3+}).

As it was difficult to maintain a precise constant temperature within the experimental setup, an average of 50 ℃ was assumed. Figure 6.3 shows actual temperature changes that occurred during the PDA measurements.

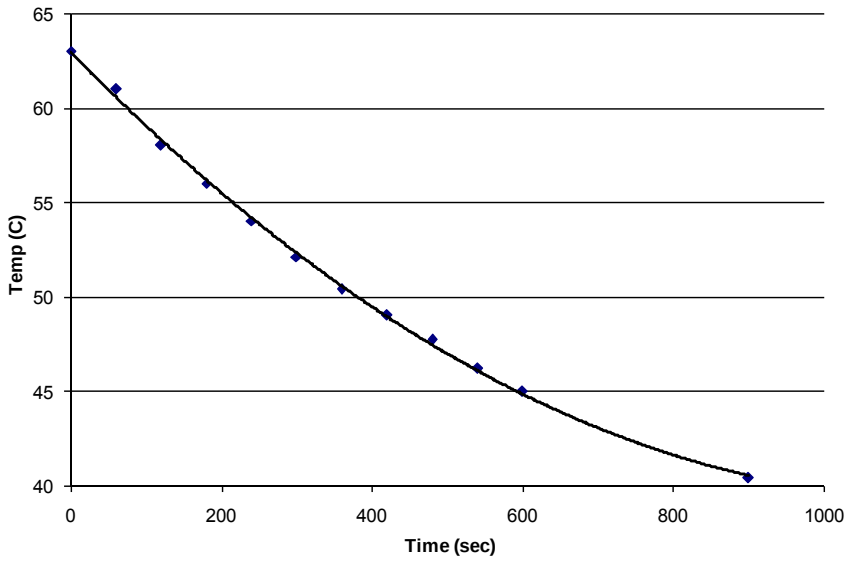

Figure 6.3: The variation in the reaction temperature over the coagulation time.

In Chapter 5, it is postulated that the aluminium and iron form polynuclear metal hydroxides in solution. In Figure 6.2, it is assumed that the Al and Fe ions are free in solution and carry a 3+ charge. In Figure 6.4, the correlation is shown for the two temperatures with the charge on the Al and Fe assumed to be 4+. Comparison between Figures 6.2 and 6.4 indicates that there is improved correlation with respect to the Shultz-Hardy rule at the higher cation charge, suggesting that these polynuclear species are present even under the increased temperatures.

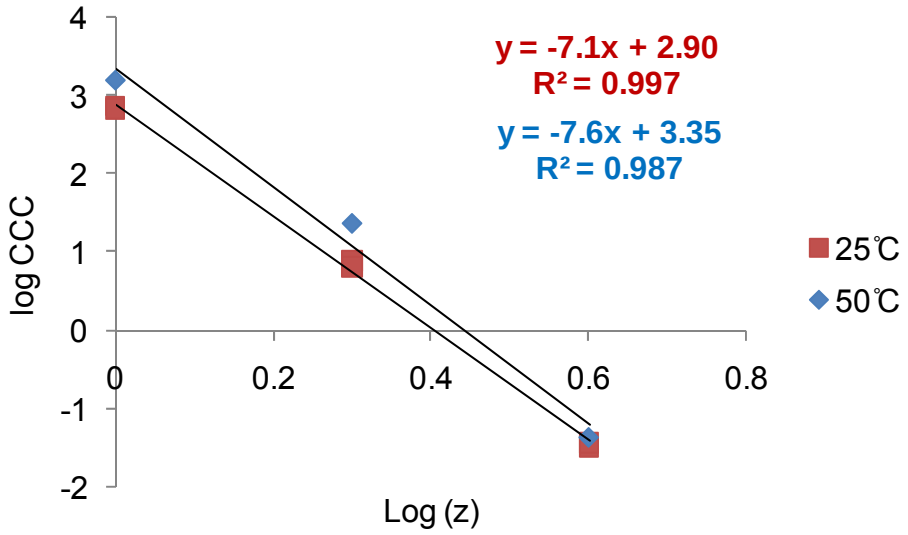

Figure 6.4: Variation of the CCC with respect to the valency of the destabilising ion. Equations for lines of best fit appear in the same order as legend (assuming Al^{4+} and Fe^{4+}).

Increases in temperature affect many chemical reaction equilibriums. It has been found previously that the relative concentration of the hydrolysed aluminium species increases with temperature [201, 202]. However, at the higher temperature if a higher charge is assumed (eg +5), this correlation improved further. $Al_3(OH)_4^{+5}$ species have been proposed previously on the basis of coagulation data [91].

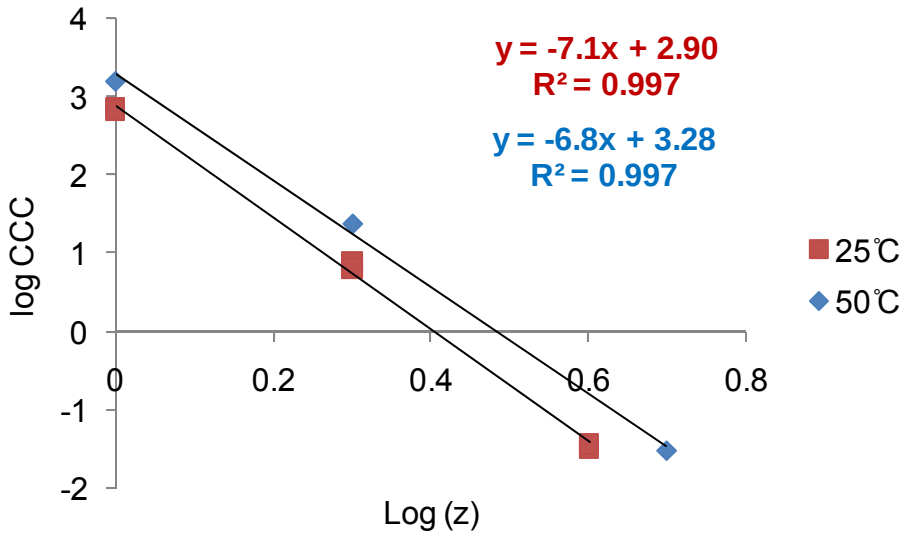

Figure 6.5: Variation of the CCC with respect to the valency of the destabilising ion. Equations for lines of best fit appear in the same order as legend (assuming Al^{4+} and Fe^{4+} at room temperature and shifting to Al^{5+} and Fe^{5+}).

6.2.2 TEMPERATURE - VARIATION LOG W VS. LOG C SLOPE

In Figure 6.6, the effect that the counter ion charge in the supernatant solution has on the stability factor linear transition region slope is shown.

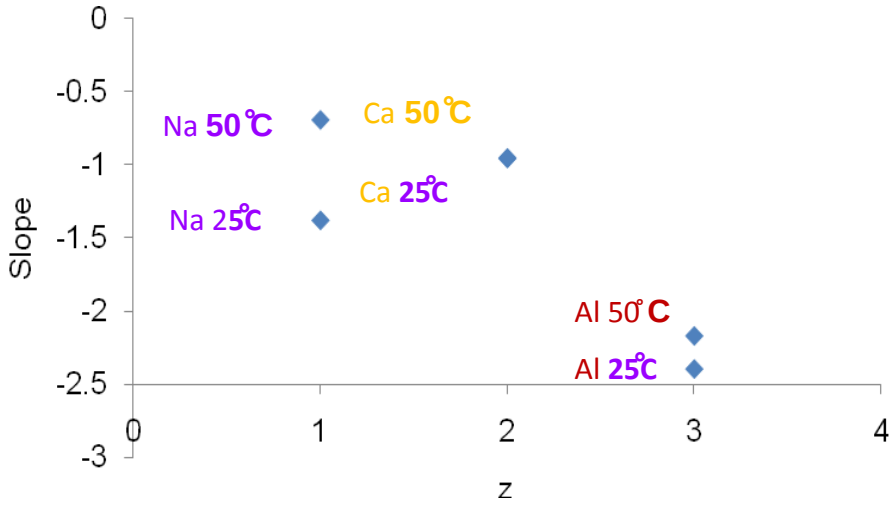

Figure 6.6: Variation in slope of log (W) [salt] curves with respect to the counter ion charge for room temperature and 50 ℃.

It is observed that with an increase in temperature, the slope of the linear transition region increases for both sodium and aluminium. However, there is no discernible change in the slope of the calcium log W curve. Nevertheless, the CCC results for the addition of calcium to the wood resin dispersions indicate that there is a variation in the ionic effect on the colloidal stability. If destabilisation occurs as a result of surface adsorption of calcium, then as the temperature increases, the equilibrium between the adsorbed calcium species and the dissolved species changes.

With the use of Equation 5.1, the slopes for the transition regions in the log (W) curves was converted to the approximate zeta potentials, as shown in Table 6.2. It is noted that the increase in the supernatant solution temperature results in a reduction of the zeta potential for the addition of sodium to the colloidal wood resins. However, for both calcium and aluminium, the addition to solution results in an increase in the calculated surface charge. The reduction in the zeta potential for the addition of sodium is contrary to the expected increase in the electrical double-layer from DLVO theory. On the other hand, the calcium and aluminium results support both the

DLVO theory and the CCC changes with temperature. As discussed previously in Chapter 5, on comparison of the Stern potentials for the variation in the temperature shown in Figure 6.6 and Table 6.2 with those determined with the use of the Izon qNano system given in Chapter 4, Section 4.2.9, there is great similarity in the results with the calculated zeta potentials between -10 mV and -20 mV. There is still large variation with regard to the results extracted from work by Sihvonen et al. [68] with regards to electrophoretic mobility. As noted previously, the zeta potentials calculated from the slope of the log W curves are reasonable approximations but cannot be taken as absolute values.

Table 6.2: Calculation of stern potentials for the change in the solution temperature from log (W) curves slopes with the use of Equation 5.1.

Salt	**z**	**Slope**	**ψd (V)**	**ψd (mV)**
Na (25°C)	1	-1.4	-0.012	-12.2
Na (50°C)	1	-0.69	-0.01	-10.0
Ca(25°C)	2	-0.96	-0.009	-9.41
Ca (50°C)	2	-0.95	-0.01	-9.93
Al(25°C)	3	-2.4	-0.019	-19.2
Al (50°C)	3	-2.2	-0.02	-19.8

6.2.3 EFFECT OF pH ON STABILITY OF COLLOIDAL WOOD RESINS

The effect of solution pH on the dynamic stability of a colloidal wood resin suspension was investigated upon salt addition. Figure 6.7 presents the log W-log concentration for a wood resin suspension mixed at 500 rpm and 25^{o}C upon $CaCl_2$ addition, under a range of pH from 3 to 8. Distinct stability curves were measured. It was observed that as the pH increases, the curve shifts to the right toward higher stability. Wood resin solubility and foaming become issues at pH

higher than 8. The critical coagulation concentration was measured as a function of pH by extrapolation of the linear decrease slope to log W=0 (Figure 6.7). The results reported in Table 6.3 show that the CCC increases with pH. Experimental error also increases with pH because the results are affected by the wood resins' higher deposition/adhesion at higher pH and by higher dissolution (foaming). The error in the CCC was calculated in the same manner as previously (Section 5.2.5).

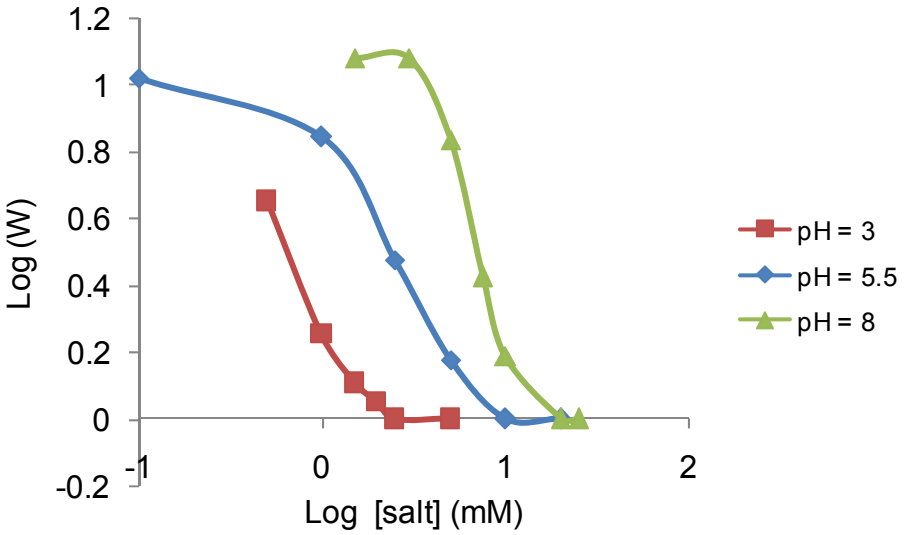

Figure 6.7: The effect of pH and salt concentration on the stability ratio (W) of colloidal wood resins destabilised by addition of $CaCl_2$. (500rpm).

Table 6.3: Effect of pH on wood resin CCC for $CaCl_2$ addition.

pH	**CCC (mM)**	**Error (mM)**
3	1.6	0.2
4	1.7	0.4
5.5	7.8	0.3
7	8.8	0.4
8	12	0.6

6.2.4 VARIATION IN CCC WITH RESPECT TO THE SOLUTION pH

The relationship between pH and CCC for the addition of calcium to solution is shown in Figure 6.8. The curve is flat at pH lower than 4 and then increases sharply at pH ranging from 4 to 8. Standard deviations are very small. For comparison, the pK_a's of the resin acid and the fatty acid components are in the 6.8-7.3 and 7.4-9.9 range, respectively [10]. Significant dissolution of the resin acid and fatty acid components are expected above pH 6 and 8 [10], which notably influences the composition and charge of the wood resin colloids. Sundberg et al. [40] calculated a pK_{lw}, for the pH at which 50% of the acid was dissolved in the water phase and found the pK_{lw} values varied from 5.3-7.2 for the resin acids and 7.3-9.5 for the fatty acids. These regions correspond reasonably well to the two regions in Figure 6.8. MacNeil et al. [27] further demonstrated that calcium significantly affected the phase distribution of the resin and fatty acids in the wood resin colloids, where dehydroabietic acid was less affected by calcium addition than the other resin acids, and fatty acids were precipitated with the addition of calcium salts.

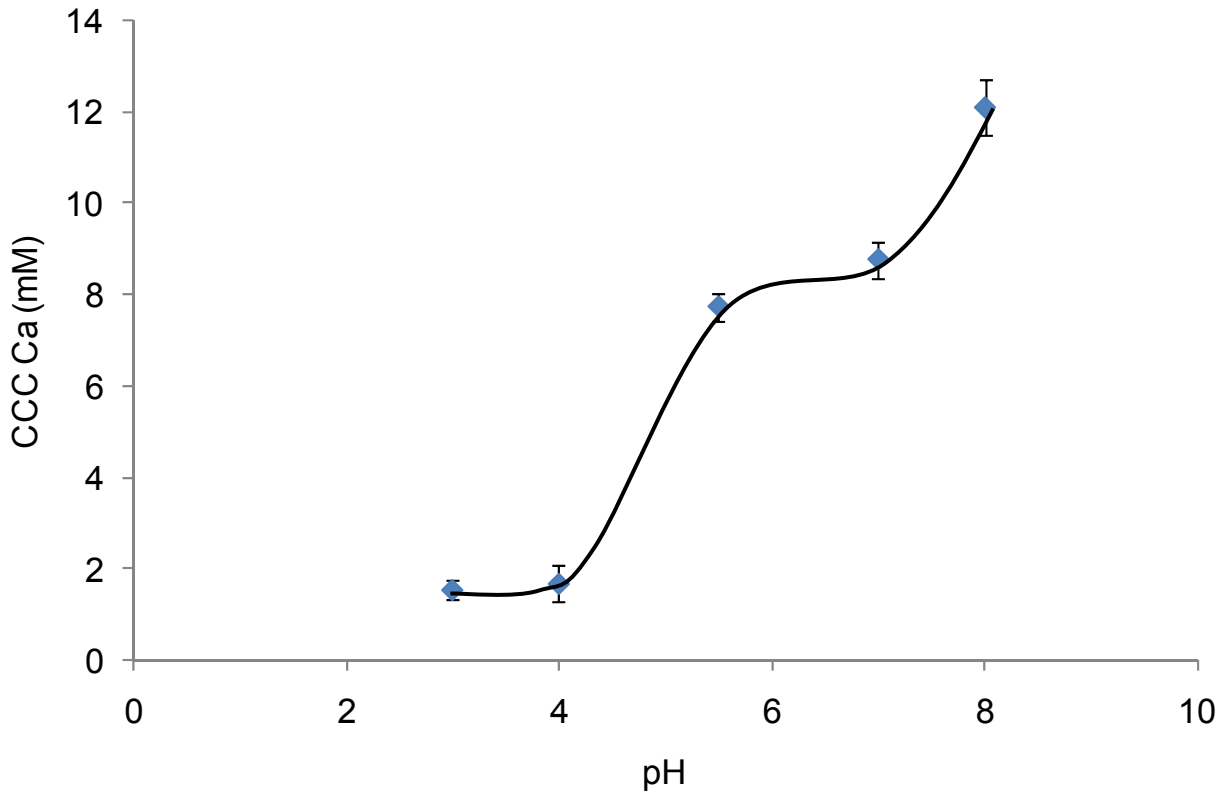

Figure 6.8: Critical coagulation concentration with respect to the pH of the supernatant solution.

The de-protonation of the colloidal surface between pH 6.5 and 8.5 requires a large amount of OH for very little change in the pH of the colloidal solutions, by comparison to the change in the pH for dialysis water, as shown in Figure 6.9. This indicates there should be large variation in the surface chemistry of the particle over this pH change.

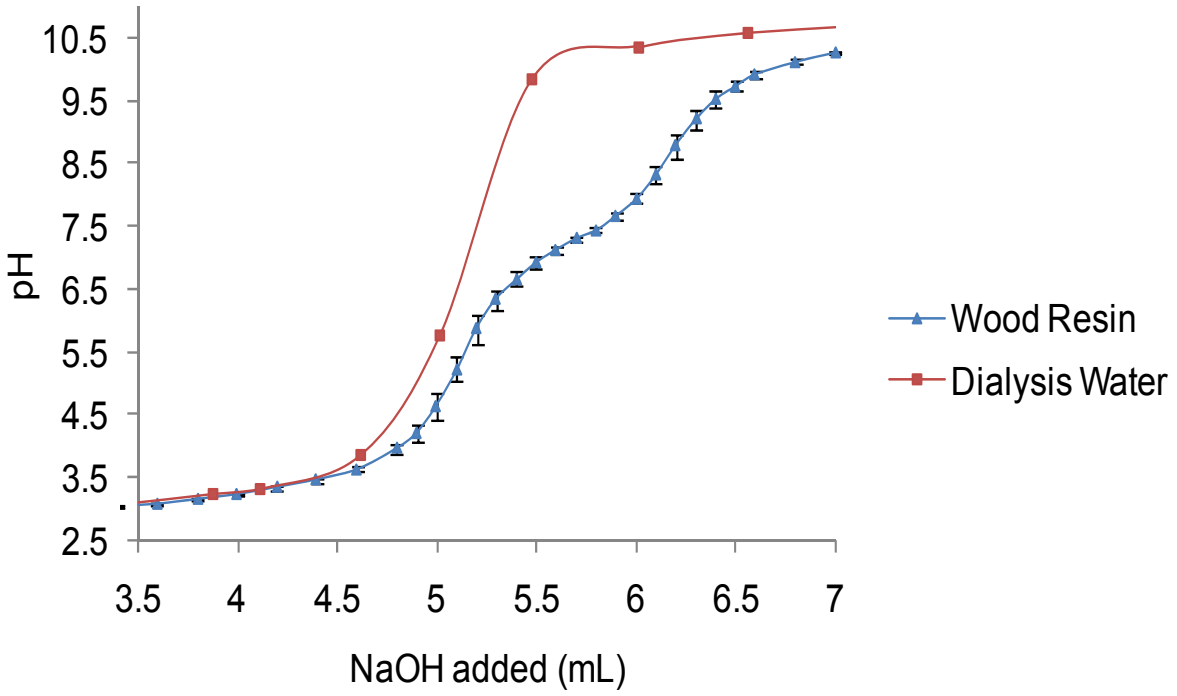

Figure 6.9: Variation in the pH with the addition of NaOH to dialysis wat3er and wood resin (100 mg/L) solutions.

6.2.5 SHEAR

Calculation of g values from rpm

Tam Doo et al. [203] experimentally found a relationship between shear and RPM within the Britt jar under similar conditions and stirrer, as shown in Figure 6.10A. The relationship is observed to be non-linear over this large RPM range. However, by looking at the low shear regime shown in Figure 6.10B, the result does appear to be linear. Given that this linear region is over the same shear rates as the current work, the linear regime is used to calculate the G values from the RPM. From Figure 6.10B, the relationship is G = 4 x RPM.

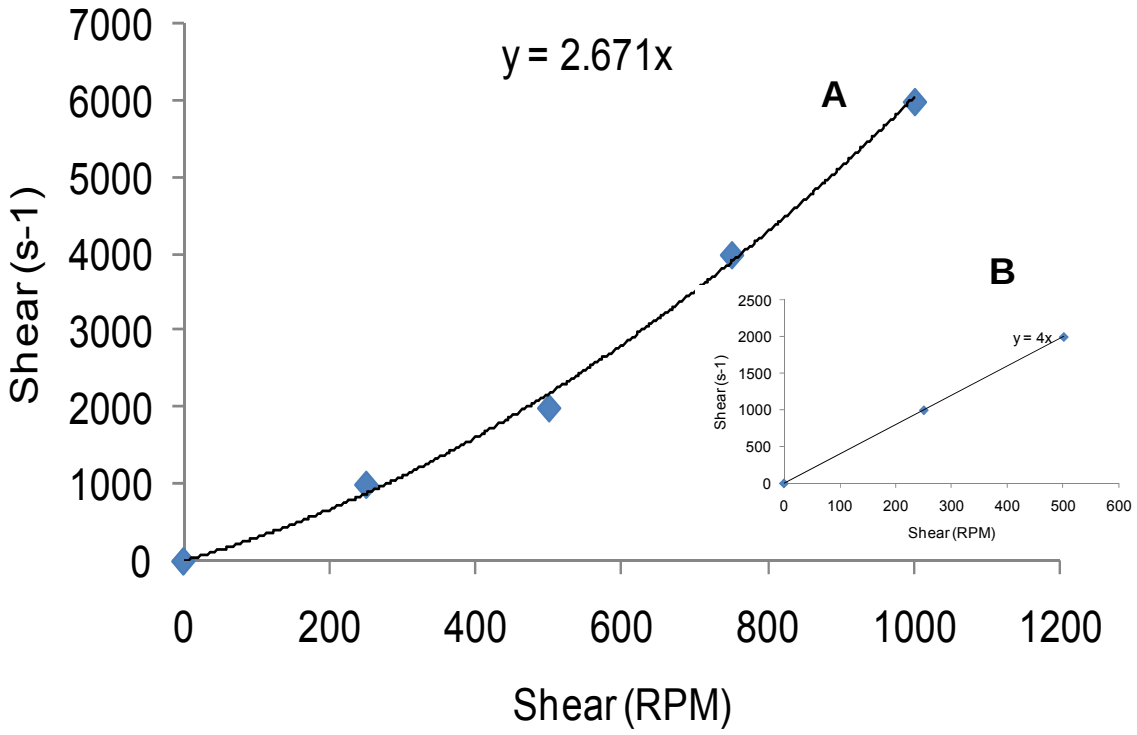

Figure 6.10: Relationship between G values and RPM within the Britt jar under similar conditions as shown by Tam Doo et al. *[203]. Relationship over:* ***A:*** *large shear range;* ***B:*** *low shear regime.*

The effect of the addition of various concentrations of $Al_2(SO_4)_3$ to the wood resins colloidal suspension at a G of 1000 s^{-1} is shown in Figure 6.11. As the concentration of added Al increases, the rate of coagulation increases. This increase in the rate of coagulation with increasing salt concentration was observed for all salts tested. The increase is an outcome of the reduction of the electrical double-layer associated with the particles [61].

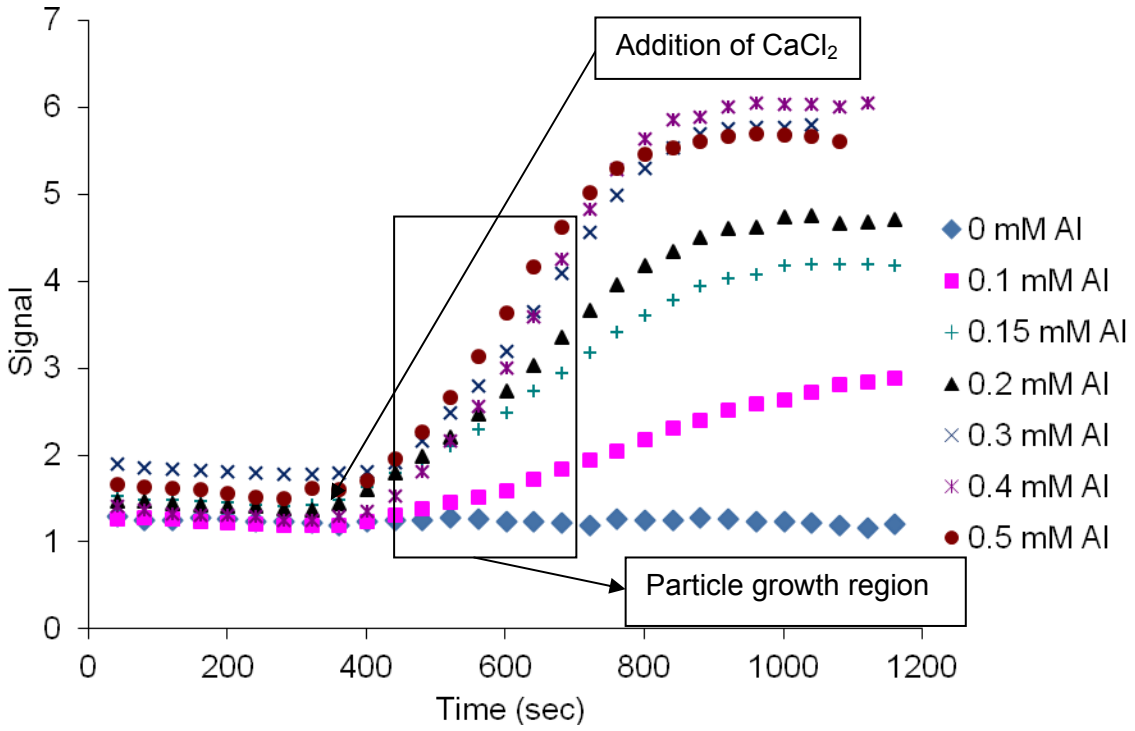

Figure 6.11: Effect of variation in the concentration of $Al_2(SO_4)_3$ addition to wood resin colloids, on the rate of coagulation at G = 1000 s^{-1}.

From Equation 6.2, it is expected that an increase in shear will result in an increased coagulation rate. Figures 6.12A and B illustrate the experimental outcomes for the change in coagulation rate due to an increase in the shear of the system. In Figure 6.12A, the shear increases from 1400 s^{-1} to 1600 s^{-1} for two concentrations of added $CaCl_2$ (7.5 mM and 10 mM). In Figure 6.12B, the shear increases from 1000 s^{-1} to 1400 s^{-1} with three concentrations of added $Al_2(SO_4)_3$ (0.1 mM, 0.2 mM and 0.4 mM).

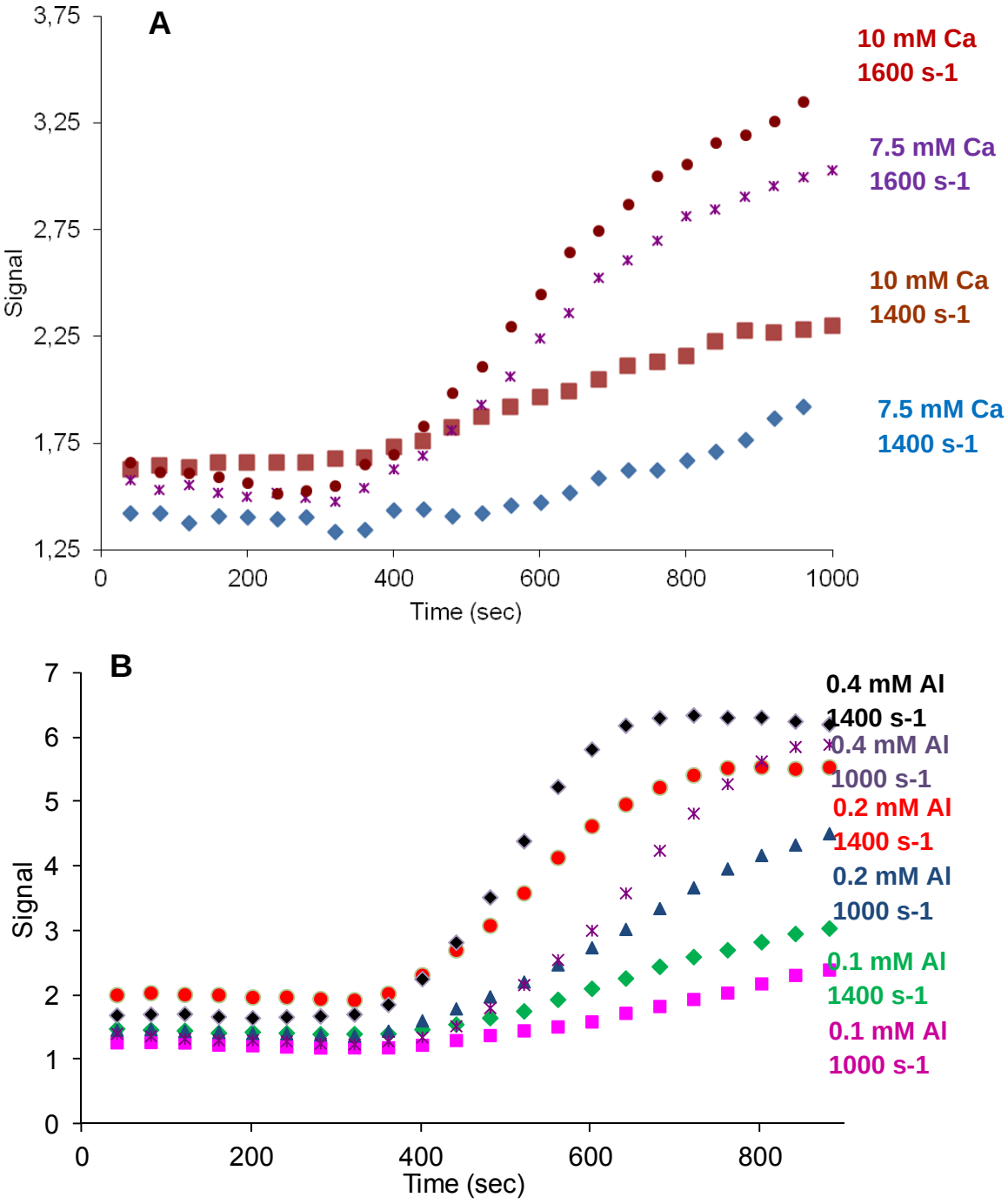

Figure 6.12: Effect of variation in the shear experienced by the colloids and its resulting effect on the rate of coagulation: ***A****: with changes in the concentration of* $CaCl_2$ *addition to wood resin colloids;* ***B****: with changes in the concentration of* $Al_2(SO_4)_3$ *addition to wood resin colloids.*

In Figure 6.12, from the increased slope in the transition region for the PDA curves at all concentrations for both salt types, it is clear that the rate of coagulation increases with increasing shear.

In Figure 6.13, the effect of variation of shear on the stability factor (W) is shown. The initial decline in the experimentally calculated W's with increasing G suggests that concentration of salts and shear both have an effect on the calculated W for the system, which results in a non-linear change. This implies that shear is not only acting on the rate of particle-particle interaction but is also influencing the efficiency of coagulation, as indicated by van der Ven and Mason [78]. It is possible that one of the ways in which this occurs is through the disruption of the electrical double-layer. However, the magnitude of the effect for shear on the stability ratio is much greater, which could be a result of the CCC or the metal ions present.

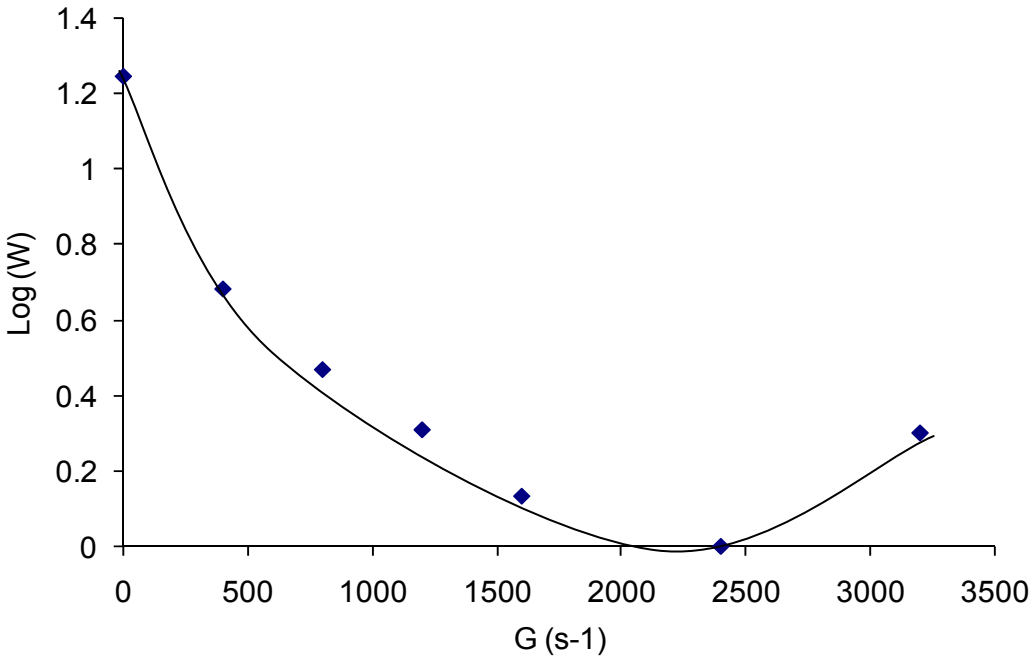

Figure 6.13: Effect of variation in the shear experienced by the colloids and its resulting effect on the stability factor (W) with the addition of 20 mM $CaCl_2$.

Restabilisation of the colloids was found to occur at high shear (Figure 6.13). The increase in stability of the colloids to coagulation is due to shear breakup at high shear (G) values, as detected by Hubbe et al. [93]. Breakup of the flocs results in an apparent decrease in

the rate of coagulation. The restabilisation of the colloids at high shear is not salt concentration-dependant. Wood resins are soft colloids that coalesce when two particles come together and form a permanent attachment [204]. The breakup or tearing of soft colloids will be dependent on the intra- not the inter-particle forces. On the other hand, hard spheres' [205] coagulation results in a point-to-point contact between particles, meaning the inter-particle forces determine the breaking point.

It is noted by van de Ven and Mason [78] that the coagulation efficiency under orthokinetic conditions varies with respect to the applied shear. The variation in efficiency was found to be proportional to $G^{0.82}$. Figure 6.14 shows the effect of the shear within the system on the efficiency of coagulation.

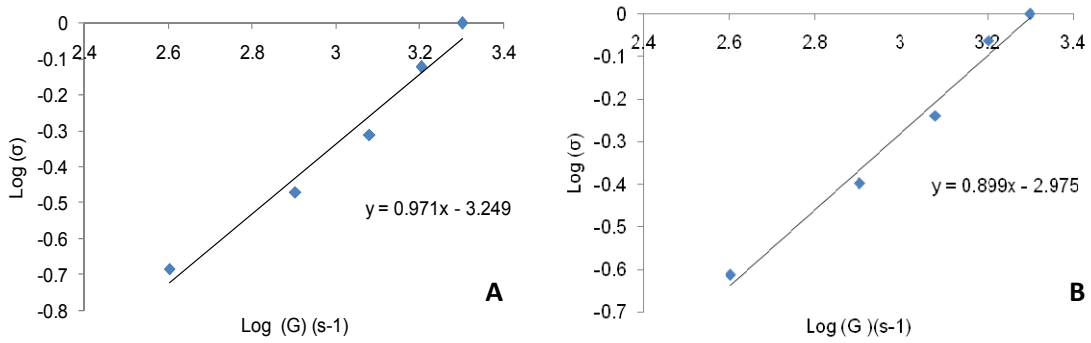

Figure 6.14: Effect of applied shear on the coagulation efficiency. ***A****: The effect of shear on the coagulation efficiency (σ) for the addition of $CaCl_2$ 20 mM,* ***B****: The effect of shear on the coagulation efficiency for the addition of $CaCl_2$ 5 mM.*

As shown in Figure 6.14, variation in the capture efficiency with respect to the applied shear is observed to fluctuate with the concentration of salt added. For example, shear influences the 20 mM additions of $CaCl_2$ to a greater extent than for the addition of 5 mM $CaCl_2$, as shown by the variation in the slopes for Figure 6.14**A** and Figure 6.14**B**. For both cases, however, the effect on the efficiency is noted to be in a similar region as that shown by van de Ven and Mason

[78]. The 20 mM additions' capture efficiency varies proportionally to $G^{0.97}$ and for the 5 mM $CaCl_2$ additions $G^{0.89}$.

Work by van de Ven and Mason [78] was a reinterpretation of a coagulation study performed by Curtis and Hocking[206]. The original work used neutral polystyrene latex spheres. The variation between the effect of shear on the efficiency of coagulation between this work and that shown by van de Ven and Mason may be the result of differences in the particle type, salt type or salt concentration dependence. It is assumed that the salt concentrations affect the coagulation of the wood resins as much or greater than the shear. As it is not purely deterministic, the coagulation of the wood resins results as a combination of both the deterministic regimes for shear-induced coagulation and Brownian motion.

For the addition of 20 mM of $CaCl_2$ to the wood resins, there is an apparent inflection in the curve at about log (G) 3.14, as shown in Figure 6.15.

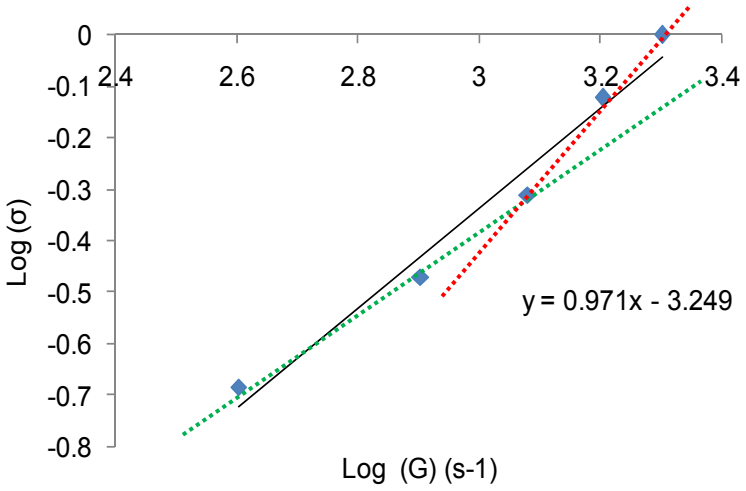

Figure 6.15: Effect of shear on the wood resin coagulation efficiency upon the addition of $CaCl_2$ 20 mM. (Green line – below inflection (m = 0.775), Red line – above inflection (m = 1.685)).

Comparison between this inflection and the work in the previous section (variation in the CCC with shear) indicate that the inflection may correlate to the critical shear level where 20 mM of $CaCl_2$ is the CCC. Above the possible inflection point shown in Figure 6.15, the effect of shear on the coagulation efficiency increases, which suggests that the effect of shear below the

CCC is reduced. Above the CCC, any particle-particle interaction should result in permanent attachment, signifying shear and van de Waals force are the only forces acting on the particles. As such, it is observed that greater shear is directly related to increased particle-particle interaction.

Variation in log (w) and CCC with shear

As the efficiency of coagulation is dependent on the shear, it follows that the CCC should also vary with shear. In Figure 6.16, the effect of variation in the rate of shear on the stability curves for wood resin on addition of $Al_2(SO_4)_3$ to solution is shown. The results indicate that as the shear the colloids are subjected to increases, the stability curves shift to the left (lower salt concentration) and vice versa.

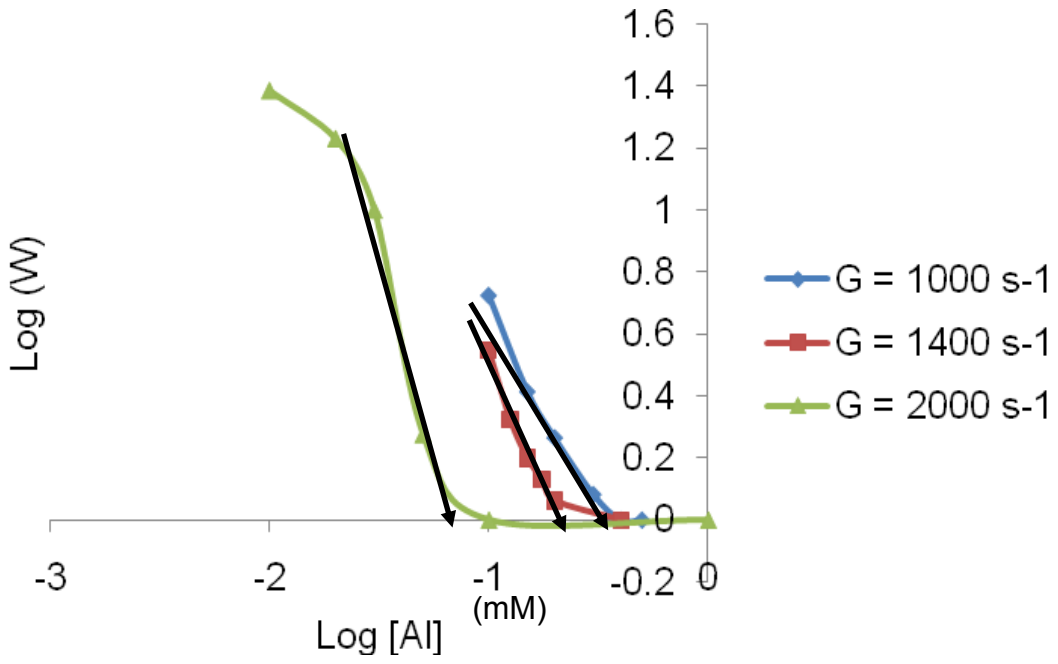

Figure 6.16: Effect of shear on stability curves for the addition of $Al_2(SO_4)_3$ to wood resin colloids.

The CCC is calculated in the same manner as previously shown via Equation 2.20. Where this linear relationship intersects with the x-axis corresponds to the concentration of salt required

to achieve constant destabilisation of the colloid through reduction of the V_R term and dominance of the attractive forces (V_A) of the DLVO theory [61]. Therefore, the shift to the left with the increase in the shear indicates a decrease in the critical coagulation concentration that is unaccounted for by conventional theory.

Figure 6.17 shows the variation in the CCC for wood resin colloids with changes to the shear the system is subjected to at various salts concentrations. It is noted that this phenomenon is not salt- or valency-specific, and occurs for all salts tested. However, the magnitude of the shear effect on the CCC varies with the counter ion charge. These changes in the CCC are observed in Figure 6.17, within valency +2 for both calcium and magnesium (where there is a change in the rate of variation with shear) and between valencies as shown for +1, +2 and +3. The shift in the CCC due to changes in shear is not accounted for by the Shultz-Hardy rule (Equation 2.10 and 2.11). The variations in CCC due to the changes in the shear that the colloids are subjected to during coagulation are noted to deviate from a direct proportionality for all salt types. The deviation in the CCC is apparently related to the valency and the salt type with differences in the curve observed for all salts tested. For sodium (Figure 6.17**A**), magnesium (Figure 6.17**B**) and aluminium (Figure 6.17**D**), the deviation follows the same trend with higher shear resulting in a decrease in CCC. The decrease in the result is valency-dependent, increasing with the charge on the counter ion. However, calcium (Figure 6.17**C**) is noted not to follow this trend. There is an apparent linear transition region from G value 1000 s^{-1} to 1600 s^{-1} and then a flattening in the curve at higher G.

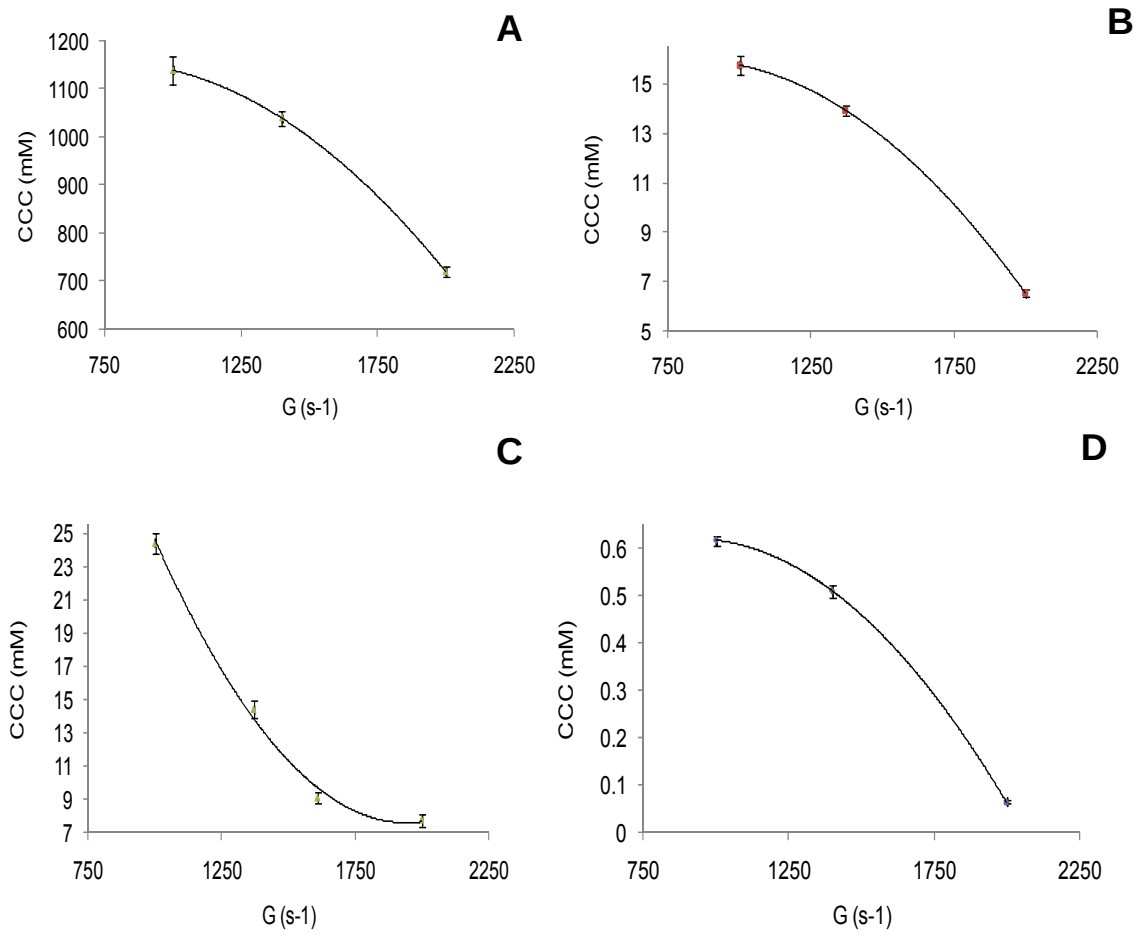

Figure 6.17: Effect of shear on the wood resin critical coagulation concentration (CCC): ***A*** *NaCl addition to wood resin colloids,* ***B*** *$MgCl_2$ addition,* ***C*** *$CaCl_2$ addition and* ***D*** *$Al_2(SO_4)_3$ addition. pH = 6 and T = 25℃.*

Both the shift in the CCC and the deviation from linear dependence may result from the deformation of the electrical double-layer under shear conditions, re-forming from a sphere to a "flame-like" conformation noted previously by Okubo T. et al. for silica spheres [74].

Variation in CCC with counter ion charge for different shears.

The effect of salt valency on colloidal wood resin CCC at different shear rates is better illustrated in Figure 6.18 using a logarithmic scale. Should the critical coagulation concentration

(CCC) of a colloid suspension be affected by shear? By defining the CCC as the electrolyte point at which, due to compression of the electrical double-layer, there is no energy barrier between two charged colloids (V=0) and there is an inflection point (dV/dH=0), Equation 2.10 is achieved by applying the DLVO theory. From a traditional DLVO theory perspective, the CCC is independent of shear. Another approach is the analysis of the stability ratio or the efficiency of coagulation defined by Equation 2.17. Both constant rates k_i and k*, defining W or σ, are shear-dependent, following Equation 2.18. Van de Ven and Mason showed the coagulation efficiency to scale up with shear as: $\sigma \alpha G^{-0.82}$. Since CCC is determined from extrapolation of the log W-C relationships at different shears, CCC should be a function of G from a hydrodynamic contribution. Furthermore, this result does not contradict the classical DLVO theory making abstraction of the hydrodynamic forces. As well, the relaxation effects linked to the shear driven deformation of the electrical double-layer have been neglected from this simple analysis [74].

As noted in Section 5.2.5, the ions of aluminium and iron can form polynuclear hydroxide species in solution. Figure 6.18 shows the correlation for the hydrolysis of the aluminium to a 4+ species with respect to the Shultz-Hardy rule.

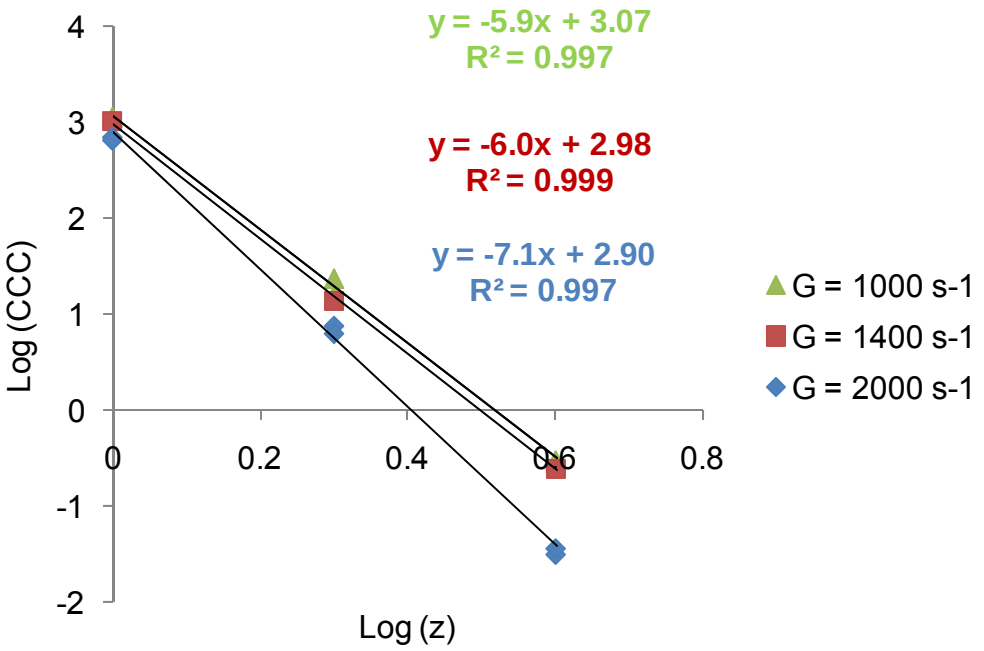

Figure 6.18: Variation of the CCC with respect to the valency of the destabilising ion (assuming Al^{4+} and Fe^{4+}) and shear.

Relatively linear relationships are observed with the slope increasing with shear. The result for the trivalent aluminium ions is a little surprising, since at the pH investigated, these ions should exist in a number of hydrated forms of varying charge and not strictly in a trivalent form [207, 208]. The slope (log CCC versus log z) follows the expectation of the Shultz-Hardy rule at low shear (CCC α z^{-6}) but deviates with further increases in shear (CCC α $z^{-7.1}$). This is unexpected from the work by van der Ven and Mason [199] (Equations 6.4 and 6.5), and their work indicates that the proportionality of CCC to z will remain unaffected and the G will vary in constant proportion to each z. This was not expected from the moderate charge of the wood resin colloids. This suggests that the critical coagulation has not only a component contribution from the cation valency but also one from shear:

$$CCC \alpha (\Omega z)^{-6\tau} \qquad \textbf{Equation 6.6}$$

$$\text{or } CCC \alpha z^{-6\tau} + \Omega^{-1} \qquad \textbf{Equation 6.7}$$

Where Ω and τ are non-equal functions of shear (f(G) and g(G)).

For the low shear rates, the experimental results seem to support the predictions of the Shultz-Hardy's rule with slopes of around –6.

For the values of CCC at high G, there is a notable deviation from this rule. It is probable that this deviation from the Shultz-Hardy rule is a result of the previously reported deformation of the electrical double-layer to a flame conformation [74], which will result in variation in the inter-particle forces. At high shear, the variation between sodium, magnesium and aluminium ionic radii will affect the degree to which the electrical double-layer is deformed due to shear.

6.3 CONCLUSIONS

The wood resin stability upon salt addition is a function of pH or wood resin charge, with higher stability achieved at higher charge (pH). This follows the predictions from the DLVO theory, with regard to the effect of changes to the surface charge of the colloids. Temperature also affected wood resin stability accordingly to expectations. However, the effect of temperature upon salt destabilisation was a strong function of the type of salt. This might suggest the occurrence of temperature-induced selective ion adsorption onto colloids, affecting zeta potential. Temperature and pH affect not only wood resin stability, but also wood resin solubilisation and probably the visco-elastic properties of the wood resin colloid and its surface composition [209].

All salts investigated, with the exception of $CaCl_2$, exhibited a wood resin CCC decreasing with shear at a faster rate as shear increases. At low shear, the wood resin critical coagulation concentration (CCC) scales with salt valency to the -6 power, following the Shultz-Hardy rule for highly charged colloids. This is surprising because of the moderate charge of colloidal wood resin. Deviations from the Shultz-Hardy rule become important as shear increases and a CCC α $z^{-7.1}$ relationship was measured at the highest shear. We suggest a relationship of the form: CCC α $(\Omega z)^{-6\tau}$ or CCC α $z^{-6\tau} + \Omega^{-1}$ where Ω=f(G) and τ = g(G). Hydrodynamic

forces are typically omitted from the DLVO equation; an additional term would be required for the systems under orthokinetic conditions usually found in industry.

The critical coagulation concentration is, therefore, not a thermodynamic property but rather a variable describing a particular colloidal system. Shear rate was a more important characteristic than expected to predict the stability of a colloidal suspension. Its effect should be considered into the DLVO theory to predict the behaviours of colloids under industrial conditions.

CHAPTER SEVEN

EXTRACTED WOOD POLYMERS AND COLLOIDAL WOOD RESIN STABILITY UNDER HIGH IONIC STRENGTH.

The stabilisation of colloidal materials in the process water can be accomplished in a number of ways. Interestingly, the natural wood polymer extracts released from the wood during the pulping process have been found to stabilise the wood resins and reduce wood resin deposition.

This chapter looks at the interaction of the water-soluble wood polymers and the colloidal wood resins with and without salt in solution. Characterisation of the wood polymers was conducted with the use of nuclear magnetic resonance (NMR) (C^{13}, H_1 and NOSY), size exclusion chromatography, the Ubbelohde viscometer and the results were compared to work with northern hemisphere wood extracts.

Under conditions typical of papermaking, wood resin colloid stability on addition of the water-soluble wood polymers was studied using the Photometric Dispersion Analyser (PDA 2000). The extracted wood polymers, which consist mostly of galactoglucomannans, were determined by NMR. A comparison of the polymer structures of *Pinus radiata* and *Pices abies*, was made. The effect of ionic strength on reorganisation of the wood polymers extracts was also investigated. The effect of the extracted wood polymers on colloidal wood resin stability was examined under varying ionic strength conditions.

7.1 INTRODUCTION

During the pulping process, there is not only the release of the hydrophobic wood resins but also dissolved hydrophilic compounds. These hydrophilic components that leach from the wood are often in the form of natural polymers. These polymers are a mixture of numerous different galactoglucomannans, a high molecular weight hemicellulose and have been shown to interact with the wood resin colloids and alter their stability in solution [70, 95, 105, 147, 210-213].

7.1.1 POLYMER AND HEMICELLULOSE INTERACTIONS WITH COLLOIDS

Traditionally, the interaction of polymers with colloids is classified into four main regions of stability: bridging flocculation, steric stabilisation, depletion flocculation and depletion stabilisation [88]. Polymer adsorption and surface conformation can occur in a number of different ways. The flocculation properties of the polymers are governed by the manner in which the polymers interact with the colloid both in terms of the conformation and way it is adsorbed. The surface adsorption is affected by numerous solution physiochemical factors such as the pH, ionic strength, polymer concentration, colloidal particle concentration, solvent and colloidal surface chemistry [200, 214-217]. The conformation of the polymers on the colloidal surface has been described in terms of trains, loops, tails, flat, coiled and stretching or dangling conformations amongst others [218]. The flocculation mechanism can be different for each of these conformations, e.g. it occurs by bridging if the polymer is in dangling form while it takes place by charge or patch neutralisation if the polymer adsorbs in the form of coils at the interface [218].

Studies into wood resin colloidal stability have focused largely on the effect of salt addition and stabilising polymers arising from synthetic polymers or from naturally-occurring polymers found in the dissolved colloidal material in the papermaking waste water [67-70]. Many studies have investigated the effect of dissolved organic extracts on wood resin deposition

with wood types such as *Picea abies* (Norway Spruce), *Populus tremula* or Aspen [98, 106, 147, 219]. However, little is understood about the stability of wood resin in the presence of extracted wood polymers under the high ionic strength conditions typical of system closure, originating from *Pinus radiata* [99, 100].

Johnsen [147], with the use of the QCM-D, quantified the adsorption of the hemicellulose onto wood resins. From this work, there is no apparent adsorption maxima for a 100 mg/L sample of water-soluble wood polymers onto any of the three surfaces tested (lignin, wood resins and cellulose) within the allowed time at low ionic strength. In 10 mM sodium chloride solution, 2.655 mg/m^2 of hemicellulose was found to adsorb to the wood resins surface and at 100 mM sodium chloride it increased to 5.015 mg/m^2. The addition of higher sodium ion concentration to solution resulted in high adsorption of wood polymers to the different surfaces. This was a result of screening of the repulsion forces between the hemicellulose and the surface. Additionally, the charged hemicellulose becomes more coiled at the high ionic strength [147]. Greater adsorption of wood polymers to the cellulose surface than for both the wood resin and lignin surfaces was noted. This was a result of the low electrostatic repulsion between the cellulose surfaces and wood polymers. The large anionic charge at the extractives surface increases the repulsion, decreasing adsorption of wood polymers [147].

7.1.2 CHARACTERISATION OF WOOD POLYMERS AND HEMICELLULOSE

Most studies investigating hemicellulose have been carried out on *Picea abies* (Norway Spruce) [96, 97], *Populus tremula* (aspen) and *Pinus sylverstris* (pine wood) [98]. Fengel and Wegener [101] summarised the polysaccharides in various woods including *Pices abies* and two pinus species (*Pinus strobes* and *Pinus sylverstris).* A typical structure of the hemicellulose (a major constituents in the water-soluble wood polymers) can be seen in Figure 7.1, with the relative abundances of the different sugars as found by Fengel and Wegener [101] shown in Table 7.1.

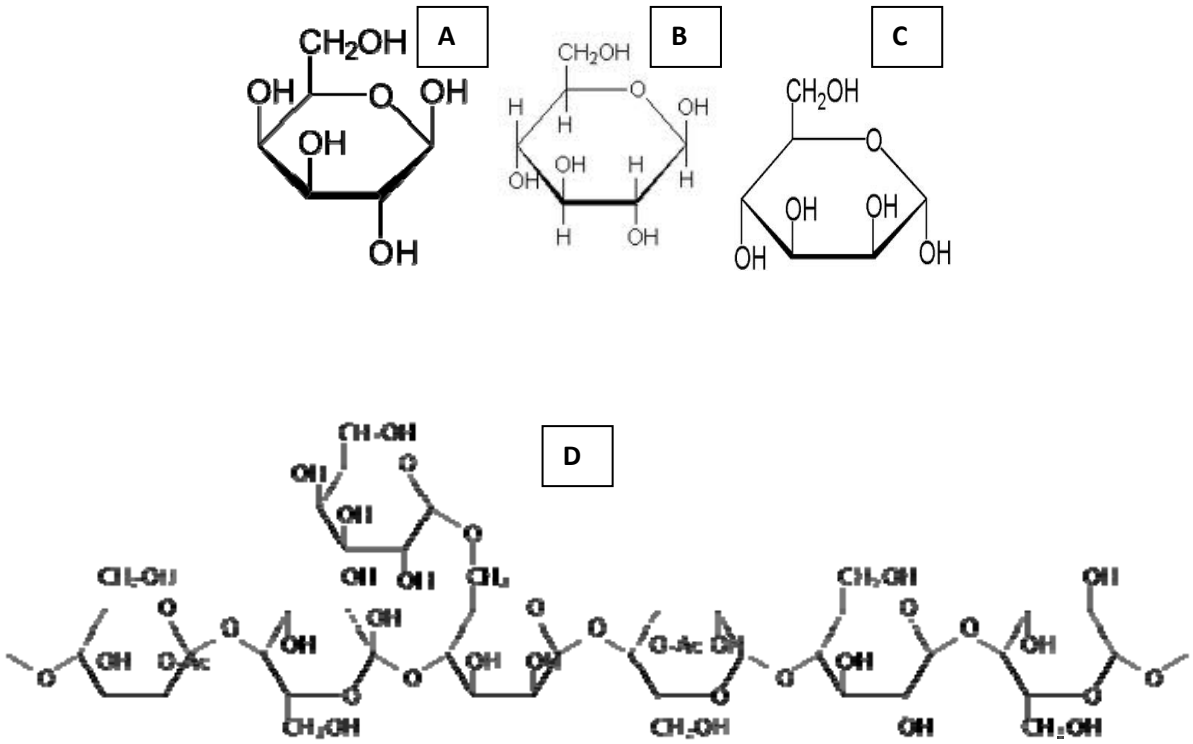

Figure 7.1: The major constituents of water-soluble wood polymers. Structure of ***A****: Galactose,* ***B****: Glucose,* ***C****: Mannose,* ***D****: Structure of a typical hemicellulose, in this case galactoglucomannin, a major constituent of northern hemisphere* spruce.

With the use of mass spectroscopy and NMR, McDonald et al. showed that the hemicellulose present in *Pinus radiata* is a complex, branched polymer sugar of galactomannan, xylan, arabinan and galactans. Furthermore, the galactomannan is acetylated with substitution occurring at the third carbon on the mannose residue as shown in Figure 7.1 [102, 103]. The o-acetyl group is split off during the alkaline peroxide bleaching process in the pulp and paper industry [147].

Analysis of the hemicellulose can be carried out by GC after digestion of the hemicellulose into its simple sugars. This digestion can be carried out by acid hydrolysis or acid methanolysis. Acid hydrolysis was used by earlier researchers, but more recently acid methanolysis has been used [97, 98, 147]. Acid methanolysis has been found to be more efficient, as it accounts for both the neutral and acidic sugars. Acid hydrolysis was found to

depolymerise cellulose into glucose, which results in an excess amount of glucose in the analysis process, relative to other sugars [97].

Table 7.1: Polyoses in various wood species – taken from Fengel and Wegener [101].

Species	% Mannose	% Xylan	% Galactose	% Arabanose	% Uronic acid	% Rhamnose	Degree of Acetylation %
Picea Abies	13.6	5.6	2.8	1.2	1.8	0.3	
Pinus Strobus	8.1	7.0	3.8	1.7	5.2		1.2
Pinus sylvestris	12.4	7.6	1.9	1.5	5.0		1.6

7.1.3 HEMICELLULOSE EXTRACTION

Since as early as 1946 [101], research groups from around the world have developed different methods of extraction of hemicellulose. Their extraction methods had many steps (as highlighted by Fengel and Wegener [101]), most of which involved soaking TMP in either neutral, acidic or alkaline solution. Many previous studies of hemicellulose also use similar methods for its extraction [147, 148, 220-223], with regards to the assessment of various sugar monamer concentrations in the wood polymer which was undertaken by Sundberg A. et al. [98].

7.2 RESULTS AND DISCUSSION

7.2.1 SOLUBLE WOOD POLYMER CHARACTERISATION

Characterisation of the extracted water-soluble wood polymers from *Pinus radiata* was undertaken with results given in Table 7.2. It was found that, as with northern hemisphere wood types, the main constituent of the extracted wood polymers at around 95%w/w, was carbohydrates. A small amount of lignin was detected in the extracted wood polymer samples. The total yield of sugar monomers was only 72%. This is similar to the sugar yield obtained by others using the acid methanolysis method [224]. The ratio of galactose: glucose: mannose was found to be 0.4:1:2.4 using gas chromatography. Using similar extraction methods and temperatures, the ratio for northern hemisphere spruce is slightly lower in mannose residues and much lower in its content of glucose. This is in comparison to the amount of galactose present in the wood polymer backbone with a ratio of 0.8:1:3.5 [225]. It was noted by Willfor et al. that the ratio of galactose to glucose can vary from 0.1 to 1.4 and mannose to galactose 3.4 to 5.4 in spruce [225], depending on the temperature and time of extraction.

Table 7.2: Composition of wood polymers extracted from P. radiata TMP pulp (as per Chapter 3, Section 3.4).

Average wood polymer concentration	873 mg/L
Carbohydrate	95 ± 2 %
Lignin	7.6 ± 0.2 %
Total sugars	72 ± 10 %
Cationic Demand mmol/g equiv charge [16]	0.42
galactose: glucose: mannose ratio	0.4: 1: 2.4

Figure 7.2 shows the ^{1}H NMR spectra for the extracted water-soluble wood polymers with the spectra normalised to the water peak at 4.78 for DHO at 25ºC. The spectra shows that the extracted wood polymers from *Pinus radiata* are similar in composition to other northern and southern hemisphere wood types [104]. The spectrum indicates that the most abundant sugars are galactose, glucose and mannose with lower concentrations of galacturonic acid, arabinose, xylose and glucuronic acid. Furthermore, the peak at 2.201 ppm indicates the presence of an acetyl group.

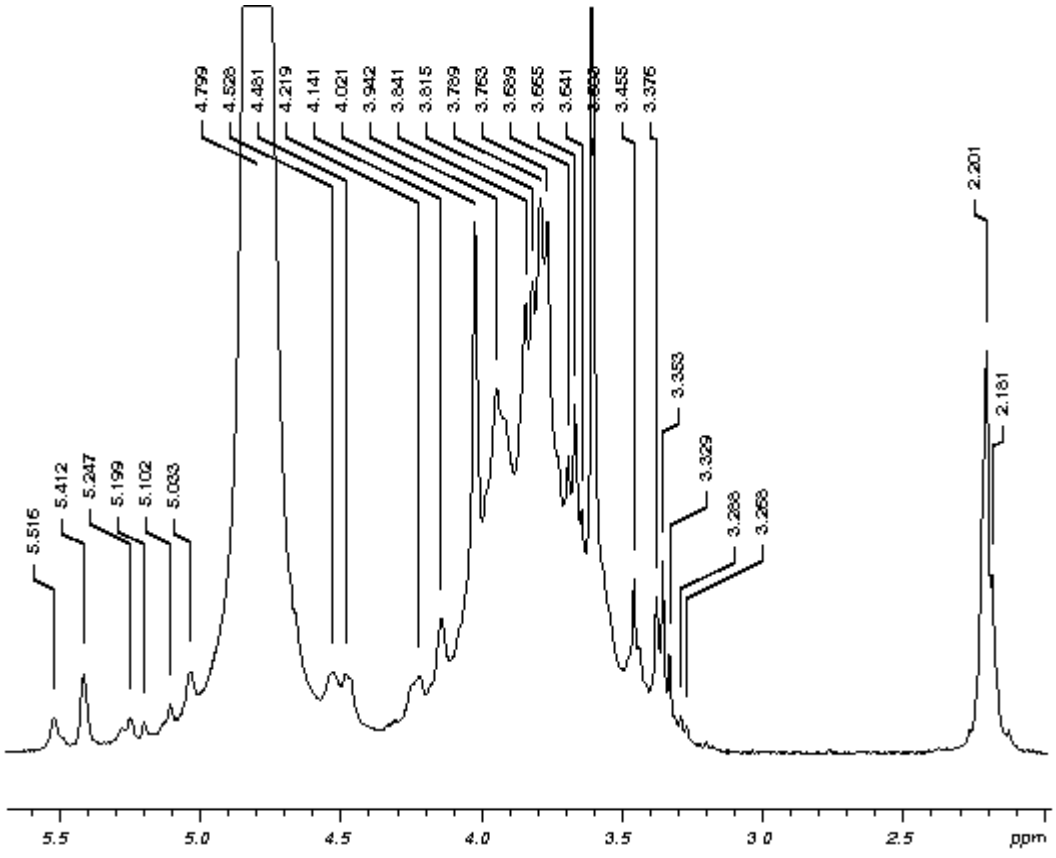

Figure 7.2: ^{1}H NMR for water-soluble wood polymers extracted from P. radiata TMP pulp (as per Chapter 3 Section 3.4).

Peak assignments to the water-soluble wood polymers from Figure 7.2 ^{1}H NMR are given in Appendix 4. These results show good correlation to peak assignments given for the northern hemisphere spruce [104].

Table 7.3 presents the chemical shifts for the sugars present in the water-soluble wood polymers, from experimental ^{13}C NMR. The ^{13}C NMR shifts correlate well with those found by Hannuksela et al. for northern hemisphere spruce extracts [104].

Table 7.3: NMR shift assignments for water-soluble wood polymers from P. radiata TMP (as per Chapter 3, Section 3.4), for ^{13}C NMR experiments, extracted from P. radiata TMP.

Residue	C-1 (PPM)	C-2 (PPM)	C-3 (PPM)	C-4 (PPM)	C-5 (PPM)	C-6 (PPM)
D-galactose	100.6	70.3	71.3	71.1	73	63
D-glucose	104.2	74.8	76.6	80.4	75.9	62.4
						68.6
D-mannose	101.9	71.8	73.3	78.3	76.9	62.5
	95.6			78.5		68.4

Figure 7.3 shows the 2D NOSY spectra for the water-soluble wood polymers referenced to the water peak at 4.78 ppm. The region between 3 ppm to 4.5 ppm corresponds to the wood polymer sugar backbone with a fingerprint region for the sugars at 4.9 ppm to 5.55 ppm. The correlations at 2.18 ppm and 5.52 ppm shown in Figure 7.3 correspond to the acetyl group's association to the wood polymer backbone. This correlation indicates that the acetyl group is attached to the polymer backbone at carbon C-2 of the mannose residue [104]. The attachment of the O-acetyl group on the mannose is also shown for northern hemisphere spruce by Hannuksela et al. [104]. They showed that for spruce galactoglucomannans, the substitution occurs at every tenth mannose in the backbone [104]. The attachment of the acetyl group becomes important as it has been shown that its removal results in changes in the solubility and interactions with colloidal species in solution [105].

It is interesting to note that although there is large variation between the growth conditions and wood types between the *P. radiata* from this study and the previous studies by

Hannuksela et al. [104], there is good correlation in the structure of the water-soluble wood polymers extracted from the wood pulps. This suggests that their interaction with the wood resins, and hence their effect on the stability of the colloidal particle in solution, will follow similar trends.

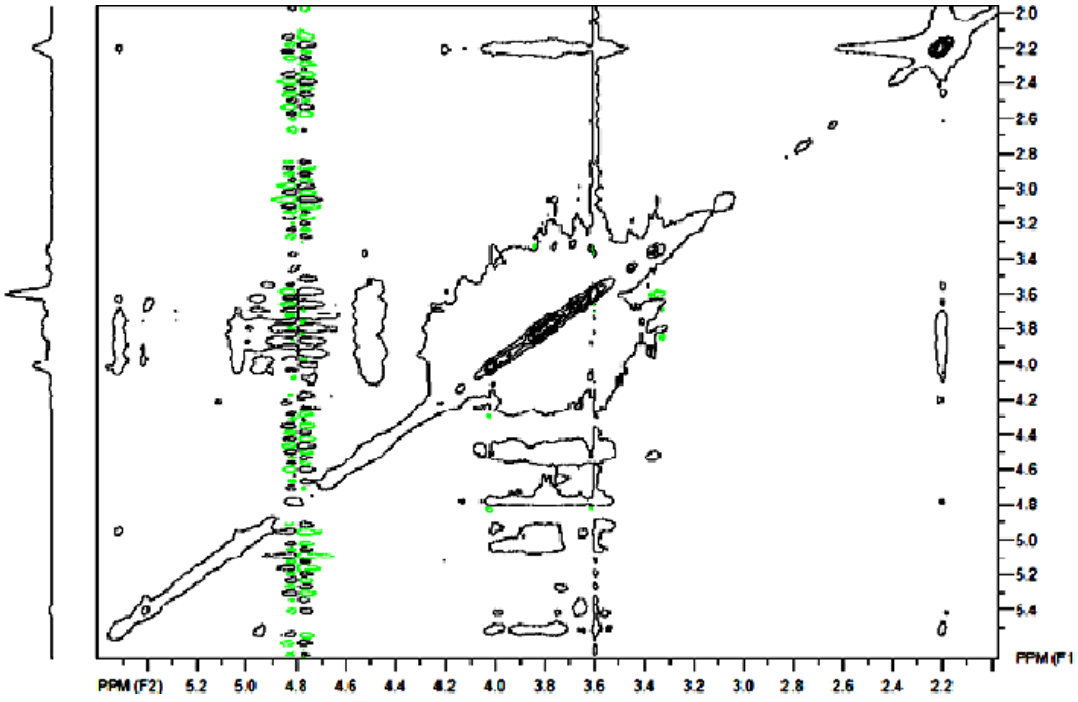

Figure 7.3: 2D NOSY NMR spectra for water-soluble wood polymers.

7.2.2 MOLECULAR MASS DISTRIBUTION OF WOOD POLYMERS.

Figure 7.4 shows the high performance size exclusion chromatography (HP – SEC) profile for crude extracted wood polymers and dextran standards. In Figure 7.5, the calibration curve for the retention times of the polysaccharides is shown. The upper and lower limits for the detection of the mass range are the points at which the curve bends.

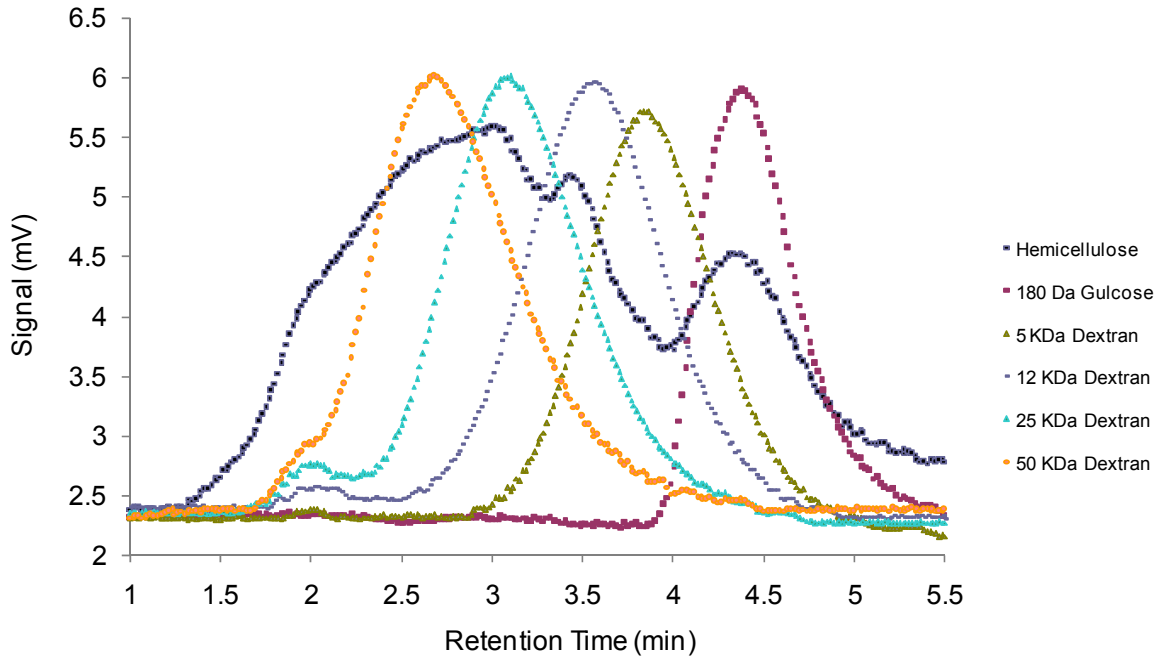

Figure 7.4: Size exclusion chromatography profile for a range of dextran standards and a water-soluble wood polymer extract in aqueous solution (signal obtained from HPLC-PDA detector).

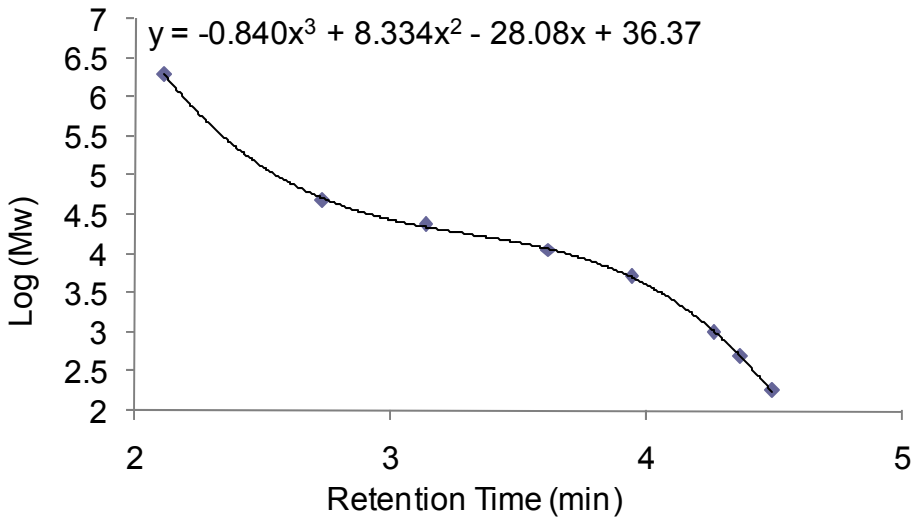

Figure 7.5: Calibration curve for standard retention times from size exclusion chromatography for polysaccharides standards.

The mass distribution for the hemicellulose in the extracted crude sample has a wide variation (Figure 7.6), from greater than 50,000 Da to 180 Da. The hemicellulose is separated into a number of different molar mass regions with a large percentage in the low molecular mass range and a number of different species at high molecular mass. The majority of the hemicellulose is between 5,000 Da and 50,000 Da. The average molar mass for the extracted wood polymers is calculated to be 16,300 Da. This equates to about 92 sugar units in the polysaccharide chain. The distribution of the wood polymers molecular mass from HPLC-SEC compares well with previous work on northern hemisphere spruce galactoglucomannans. The wood polymers extracted in this study have a larger average molecular mass than those determined by Lundqvist et al. in his study where he used a lower extraction temperature than that employed here (70°C) [226]. Lundqvist et al. [226] suggest that lower temperatures result in larger average molecular masses as the degradation of the wood polymers during extraction is reduced [226]. The work conducted by Lundqvist et al. was conducted at a range of temperatures between 170°C and 220°C for short periods of time (2 to 20 min), looking at the changes in the wood polymers as a result of the conditions [226].

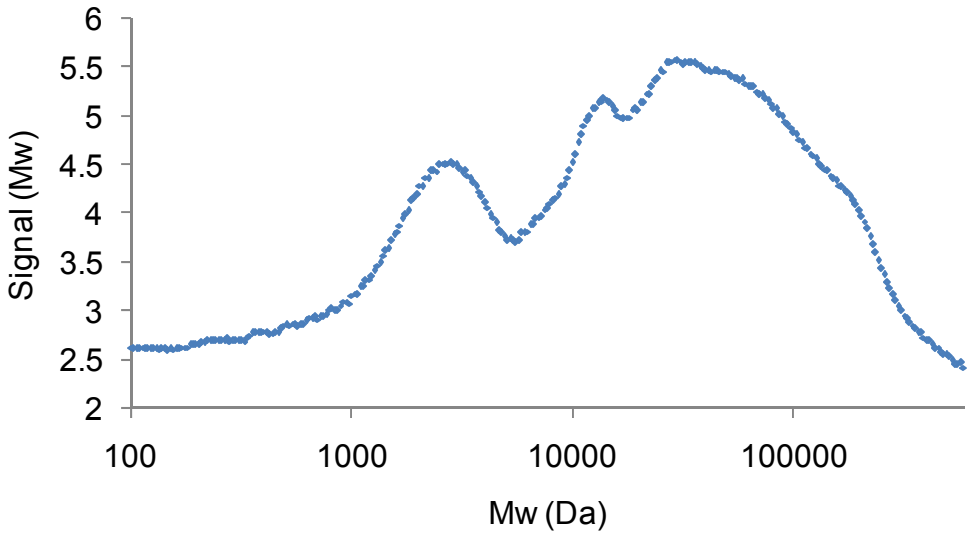

Figure 7.6: Molecular mass distribution of extracted wood polymers in solution from size exclusion chromatography (signal obtained fron HPLC –PDA detector).

The proportion of the water-soluble wood polymers at low molar mass is most likely made up of mono- and di- saccharides, pectic acids and lignan oligomers [225, 226], with the higher molar mass constituents comprising the bulk of the wood polymers resulting from the branched galactoglucomannans (hemicellulose). Similar molecular mass distributions have been reported for spruce hemicelluloses and polysaccharides, showing a range of molecular mass fractions [227].

7.2.3 EFFECT OF IONIC STRENGTH ON EXTRACTED WOOD POLYMERS

Using the PDA, the aggregation behaviour and colloidal properties of the extracted wood polymers were investigated at pH 5.5 and room temperature, as shown in Figure 7.7. The wood polymer solution contained only the water-soluble components from the *P. radiata*, extracted as per Section 3.4 without any colloidal components present in the sample. In the absence of $CaCl_2$, the PDA signal is relatively flat, indicating that no aggregation is occurring and that the extracted

wood polymers are stable under the shear conditions imposed. On addition of 10mM $CaCl_2$, a small increase in the PDA signal occurs. This response represents an aggregation or reorganisation of the wood polymers. The plateau in the signal following the aggregation of the wood polymers indicates that the aggregated polymers are stable to deposition, disintegration and further coagulation. The addition of 20mM $CaCl_2$ resulted in a significant increase in the PDA signal, reaching a maximum before decreasing. This shape in the PDA signal represents floc aggregation followed by floc breakup due to the flocs not being stable [113]. Several possibilities exist to explain the decrease in the PDA signal that was observed, including the breakup of the flocs or the collapse of the flocs due to collapse of the polymer chains. The breakup of the flocs following the aggregation is possibly due to the formation of weak bonding within the formed floc that is broken up by the shear forces. Alternatively, the flocs formed from the addition of 20 mM of $CaCl_2$ to solution are unstable and deposit in a short time span resulting in a decrease in the concentration in solution.

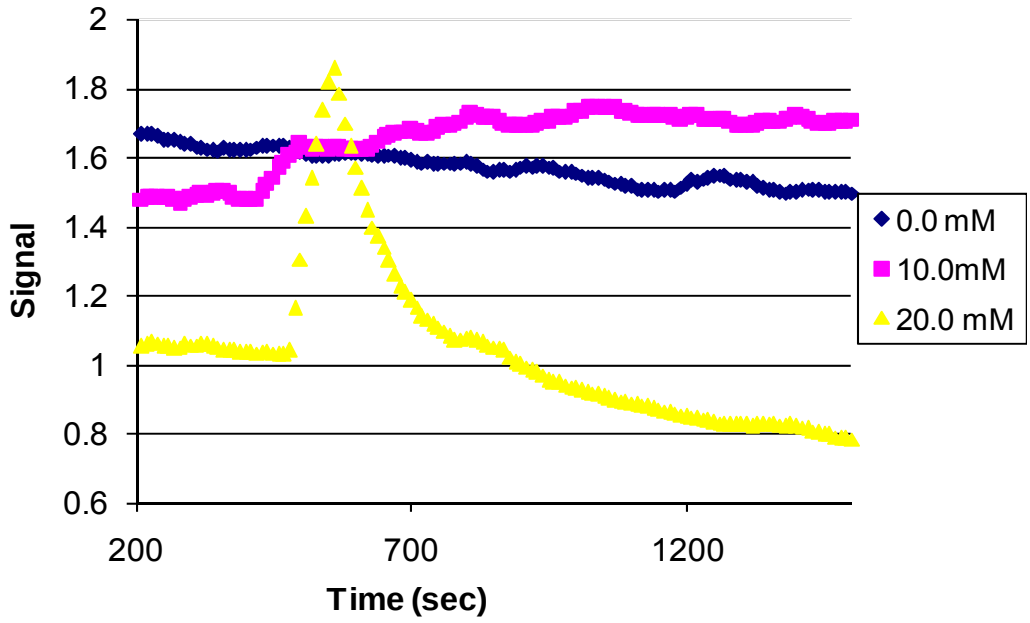

Figure 7.7: Effect of $CaCl_2$ on the dynamics of extracted wood polymers destabilisation and rearrangement (Extracted wood polymer concentration = 360 mg/L). The signal was obtained from a HPLC –PDA detector.

The effect of ionic strength on the extracted wood polymer was further studied using viscosity measurements. Viscosity measurements were taken on 5 g/L (higher concentrations were used to reduce variation in results) extracted wood polymer solutions using an Ubbelohde viscometer. The time for a wood polymer solution in relation to the time for distilled water to pass the top and bottom timing lines can be used to calculate the relative viscosity (η_r) of each solution.

$$\eta_r = \frac{T_{polymer}}{T_{water}} \qquad \textbf{Equation 7.1}$$

η_r is the relative viscosity, $T_{polymer}$ is the time required for wood polymer solutions to pass through the Ubbelohde viscometer and T_{water} is the time required for distilled water to pass through. Each measurement was done in triplicate and average values are reported.

Figure 7.8 shows a decrease in the wood polymer relative viscosity with increasing $CaCl_2$ addition. Changes in the viscosity are related to the radius of the particles via the Stokes-Einstein Equation [228-230]. A decrease in the viscosity indicates a decrease in the hydrodynamic radius arising from a collapse of the polymer chains even at low levels of $CaCl_2$ present in solution [229, 230]. This collapsing of polymer chains due to the addition of salt to solution has previously been reported for guar gum, (a substance very similar to the wood polymers) [230] and other polymer types [228, 231-233].

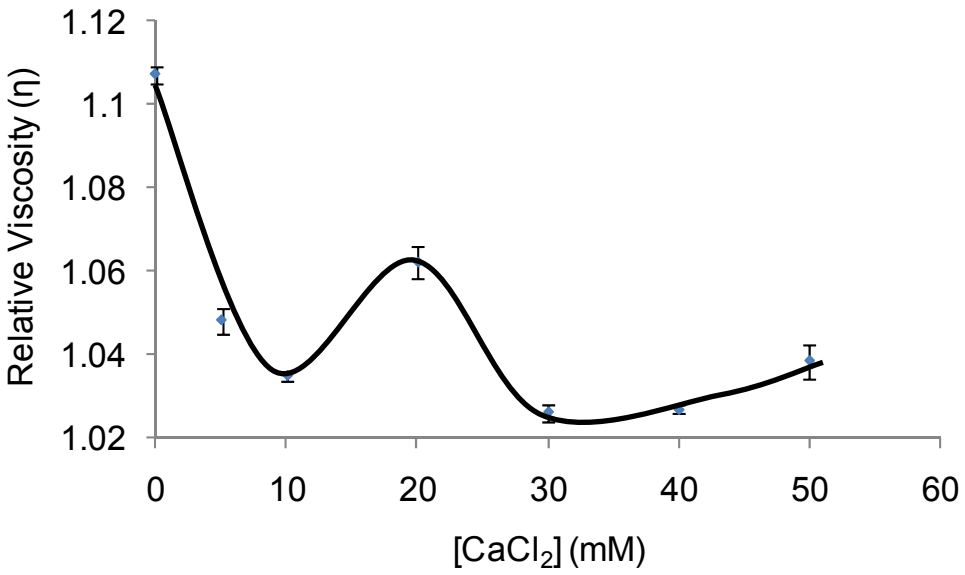

Figure 7.8: Effect of $CaCl_2$ concentration salt on the relative viscosity of wood polymers (Extracted wood polymer concentration = 360 mg/L).

Apart from the point at 20 mM $CaCl_2$, the data suggests a downward trend. The departure at 20 mM from the general downwards trend noted above is interesting. The coagulation kinetics of the wood polymers on addition of 20 mM $CaCl_2$ was observed to result in a significant increase in the PDA signal. This increase in the signal then reaches a maximum and begins to decrease. There is an apparent jump in the viscosity at 20 mM $CaCl_2$. It has been suggested that the variation in the hydrodynamic radius shown in Figure 7.8 may be due to a number of varying changes in intermolecular structure of the wood polymers with the initial decrease in viscosity being a result of a decrease in the radius of gyration. The spike at 20 mM of $CaCl_2$ addition may be a result of the formation of a network of coagulated material. The second minimum is possibly due to the breakup of the formed networks and the final increase a result of increasing ionic strength. Further work is needed to better define what effect 20 mM of $CaCl_2$ has on the wood polymers and how it differs from the other additions of salt to solution.

7.2.4 EFFECT OF WOOD POLYMERS ON WOOD EXTRACTIVE COLLOIDAL STABILITY

The effect of extracted wood polymer concentration on wood extractive colloidal stability and rate of aggregation of the wood extractive colloids is shown in Figure 7.9. An increase in the slope of the PDA signal occurs after the addition of extracted wood polymers at 450 sec. The stability factor, W, was determined from the slopes in Figure 7.9 for each wood polymer concentration and is plotted in Figure 7.10.

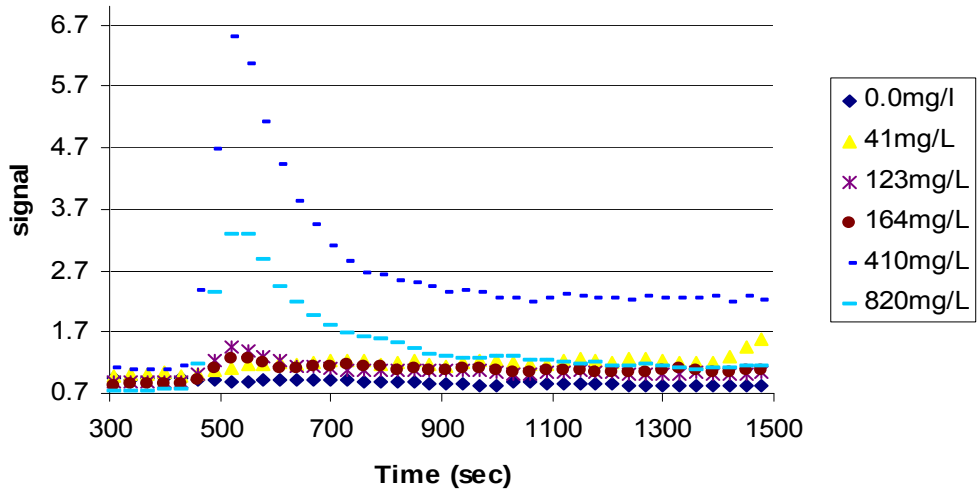

Figure 7.9: Effect of extracted wood polymers concentration on the dynamics of colloidal wood resin coagulation (Wood resin concentration is approximately 100 mg/L, pH 5.5, 25℃, 500 RPM and 1 mM KCl). The signal was obtained from a HPLC-PDA detector.

Figure 7.10 shows the effect of changing wood polymer concentration on the extractive colloids' stability. The dominant features are the regions of destabilisation at 10 mg/L and 400 mg/L extracted wood polymers. After the destabilisation of the colloids apparent at 10 mg/L of wood polymer, addition of higher concentrations of extracted wood polymers increased colloidal

stability, as evident by the increase in the slope of the curve until a maximum of around 50 mg/L. This behaviour is typical of low polymer additions to colloidal suspensions with destabilisation and aggregation of the colloids via bridging flocculation, followed by steric stabilisation with polymers anchored to the colloidal surface up to full polymer coverage of the surface [88]. Further additions result in the aforementioned instability. This second region of destabilisation is a result of depletion flocculation [88]. The observed destabilisation-stabilisation-destabilisation and restabilisation behaviour of the wood extractive colloids with the addition of wood polymers is typical of synthetic polymers [88]. It indicates that the previously reported [96-98] stabilisation of wood extractives by wood polymers is more complicated and very much dependent on the level of wood polymers present. It also indicates that increased accumulation of the wood polymers in papermaking process water may be detrimental to the stability of wood extractives at particular concentration ranges of 7.5–20 mg/L and 100-400 mg/L. The lower region of instability will be more of an issue if various process removal mechanisms are used to remove the wood resins as it will also remove the wood polymers from solution. It has been noted previously that for Norway spruce containing a concentration of 50 mg/L (wood resin) and about 250 mg/L (wood polymers), the dispersion is stable for weeks. It is important to note that by comparison with the current work, the ratio of mg (wood polymer): mg (wood resins) for the Norway spruce correlate to the initial part of the second stable region. From the current work, it is unknown how this will affect the surface deposition of the wood resins to different surfaces.

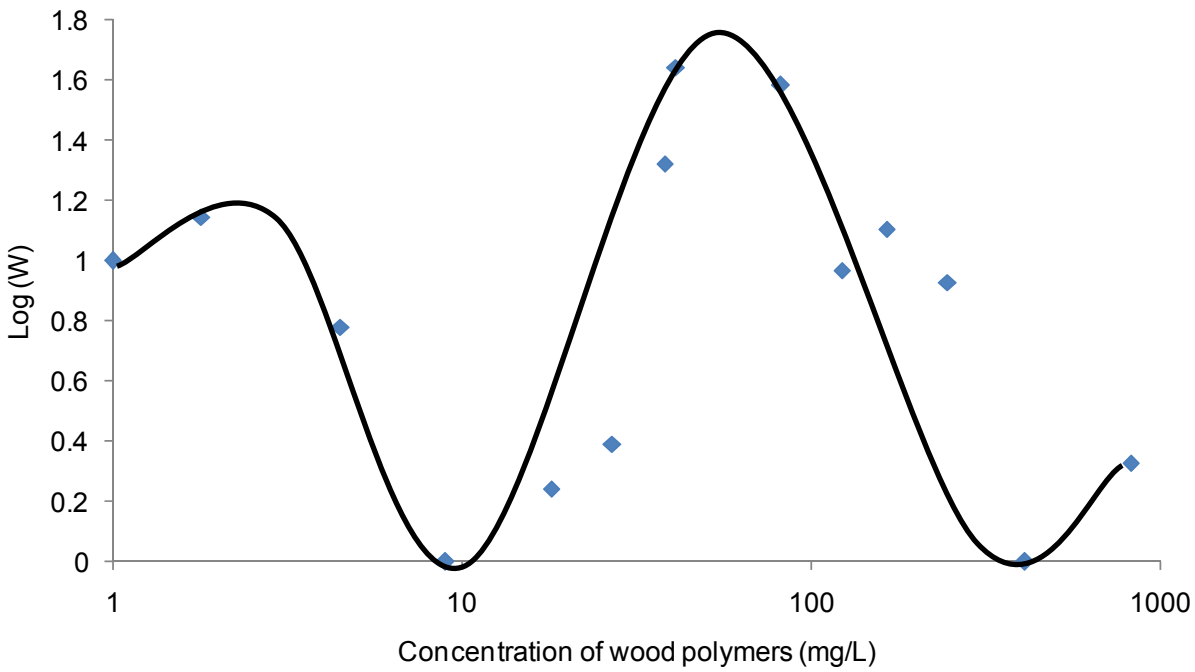

Figure 7.10: Effect of extracted wood polymers concentration on colloidal wood resin stability (100mg/L wood resin).

7.2.5 ADSORPTION OF HEMICELLULOSE TO WOOD RESINS

The Langmuir isotherm is used to describe adsorption on homogeneous surfaces. The linear form of Langmuir isotherm can be expressed as:

$$\frac{C}{Q} = \frac{1}{Q_m K_L} + \frac{1}{Q_m} C$$

Equation 7.2

where C is the concentration of water-soluble wood polymers at equilibrium (mg/L), Q is the amount of wood polymers adsorbed per unit mass of the wood resins (mg/g), Q_m is the maximum adsorption capacity (mg/g) and K_L is the Langmuir constant related to the affinity of the binding sites and the energy of adsorption (L/mg). The Langmuir isotherm makes the assumption of

monolayer adsorption on uniformly energetic adsorption sites with no interactions between adsorbate molecules [234]. Due to sample volumes and low concentration of wood polymers for the adsorption of the wood polymers to the wood resins experiments, the concentration in solution is determined by the Oricinol method.

From Figure 7.11 and 7.12, the adsorption of wood polymers to deposited wood resins is shown. For ease of interpretation, the results in Figure 7.11 were re-presented as a log-log plot in Figure 7.12. Figures 7.11 and 7.12 show a plateau effect in the adsorption of the water-soluble wood polymers to the wood resin surface. Following this, there is an apparent secondary adsorption of the polymers onto the surface. This suggests a multilayer adsorption of wood polymers to the wood resins.

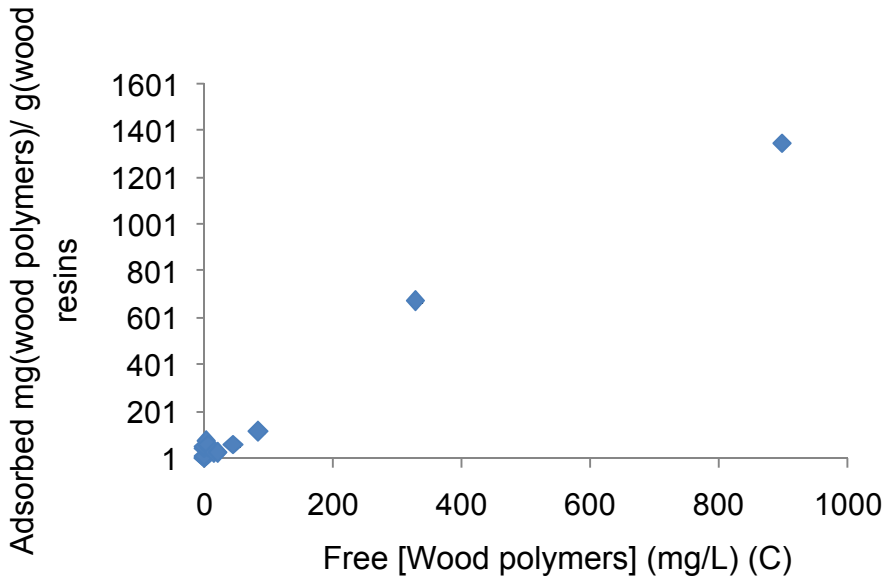

Figure 7.11: Adsorption of water-soluble wood polymers to wood resins (assuming complete wood resin coverage of microscope slide).

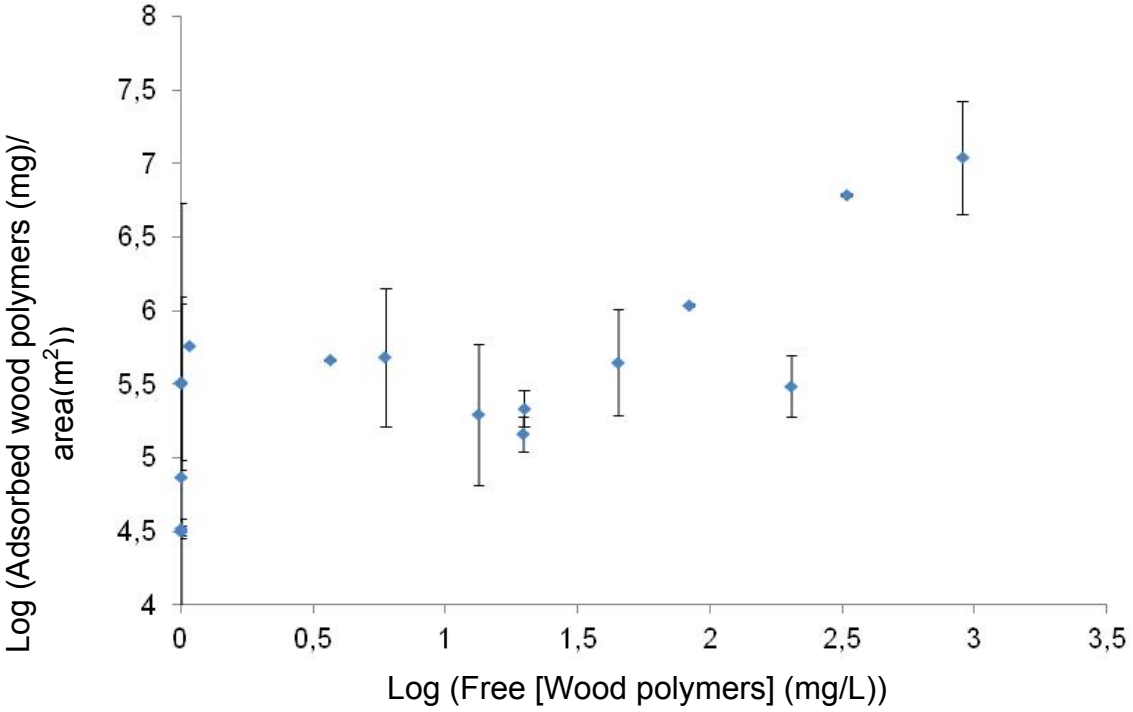

Figure 7.12: Adsorption isotherm for water-soluble wood polymers to wood resins (assuming complete wood resin coverage of microscope slide) (Log/Log Scale).

An interesting question arises as to what is the driving force for the interaction that occurs between the hydrophilic negatively-charged wood polymers and the hydrophobic negatively-charged wood extractives. There is no electrostatic attraction between them in solution due to the negative charge on both at pH 5.5 or any hydrophobic interactions. The most likely mechanism is through hydrogen bonding of the hydroxide functional groups present on both species.

On fitting the data to the Langmuir isotherm equation (Equation 7.2), shown in Figure 7.13 and 7.14, we see high affinity for the surface at low additions of the wood resins and the reduction of the apparent secondary adsorption region. It must be noted that the data shown in Figure 7.13 does not fit with the Langmuir isotherm for the adsorption of wood polymers to the

surface of the colloidal wood resin. For Figure 7.14, the data was fitted to a log – log scale to improve visibility of the changes to the adsorption.

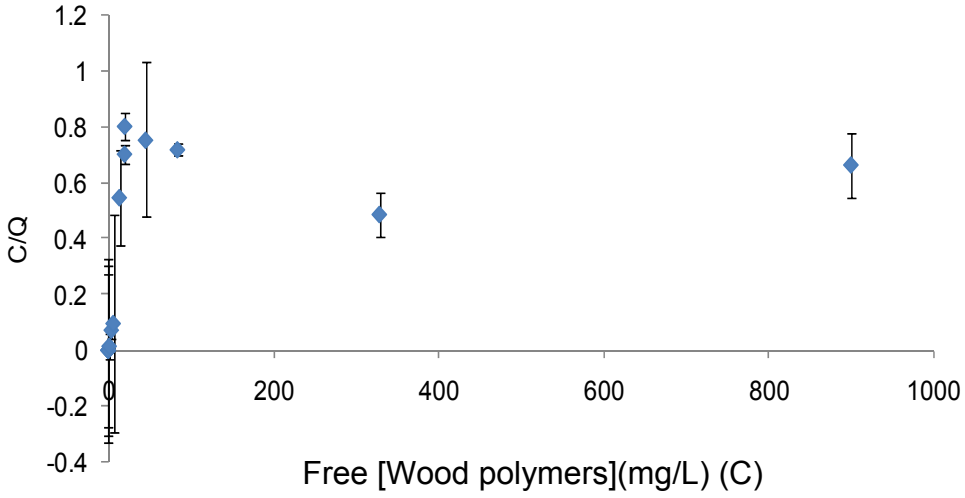

Figure 7.13: Adsorption isotherm for water-soluble wood polymers to wood resins (log – log scale).

Given the poor fit for the adsorption data shown in Figures 7.11 through 7.13 with the Langmuir isotherm theory, the data was fitted to the Freundlich isotherm model. Figure 7.14 shows the fit for this adsorption to the Freundlich isotherm. The fit for this is just as bad as was noted for the Langmuir isotherm.

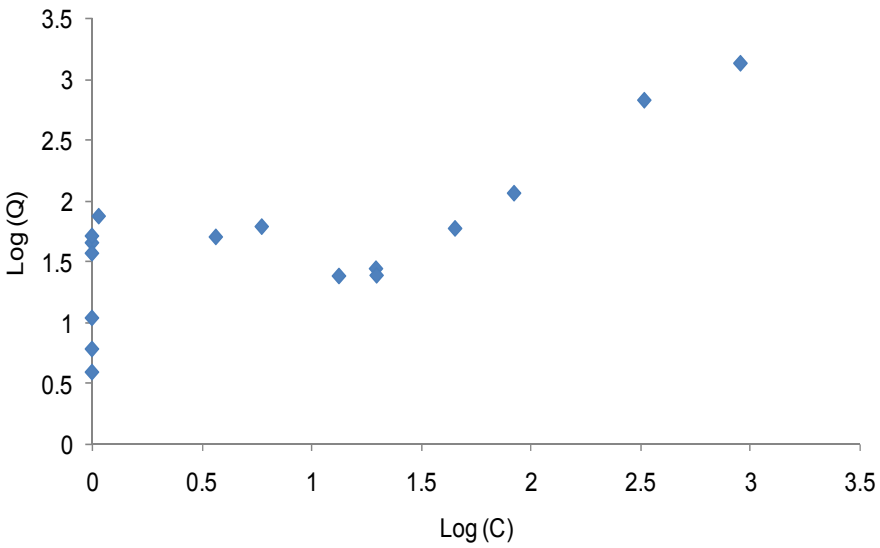

Figure 7.14: Freundlich *adsorption isotherm for water-soluble wood polymers to wood resins.*

It is possible that the adsorption of the wood polymers to the wood resins is occurring via an anomalous isotherm. Anomalous isotherms are characterised by Stepwise isotherms associated with the formation of a complete monolayer before each subsequent multilayer commences [235], similar stepwise isotherms have been noted for the adsorption Krypton at 90 K onto carbon graphitised at 3000 K [236]. From Figure 7.15, the isotherm shows two distinct steps corresponding to the complete formation of the first and second layers with an odd depression between the two formations. This anomalous isotherm formation may be a result of a number of different factors, including the formation of multiple layers or given that the wood polymers have been noted to self aggregate. It may be possible that this occurs as a result of the interaction of the wood polymers and the wood resins occurring by a mechanism similar to that seen for the interaction of two dissimilar colloids.

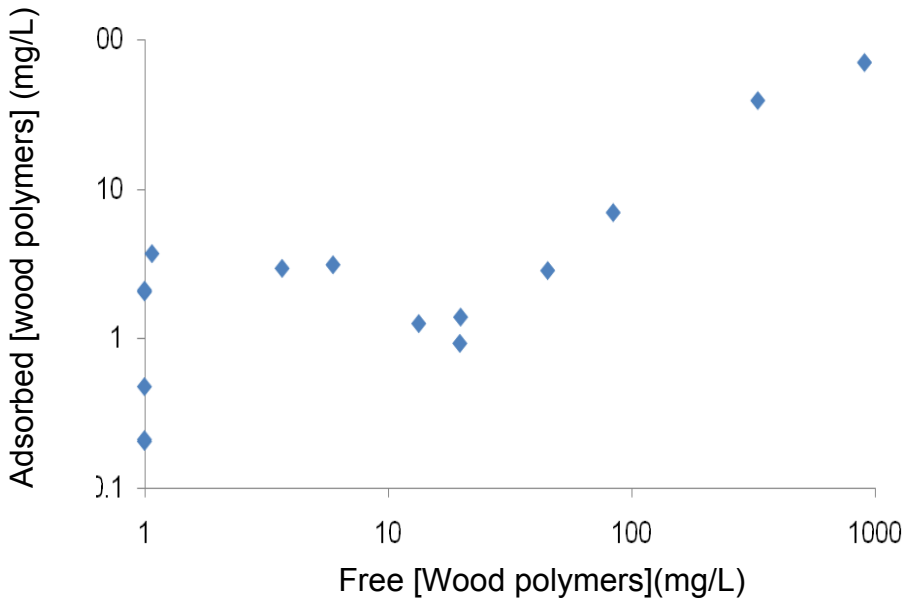

Figure 7.15: Adsorption of wood polymers to wood resin surface (log – log scale).

Figure 7.16 shows the adsorption of the water-soluble wood polymers to deposited wood resins. With comparison to the stability of the wood resins on addition of the wood polymers to solution, there is an apparent maximum in the adsorption of the wood polymers to the wood resins at the restabilisation region that could be assigned to steric stabilisation.

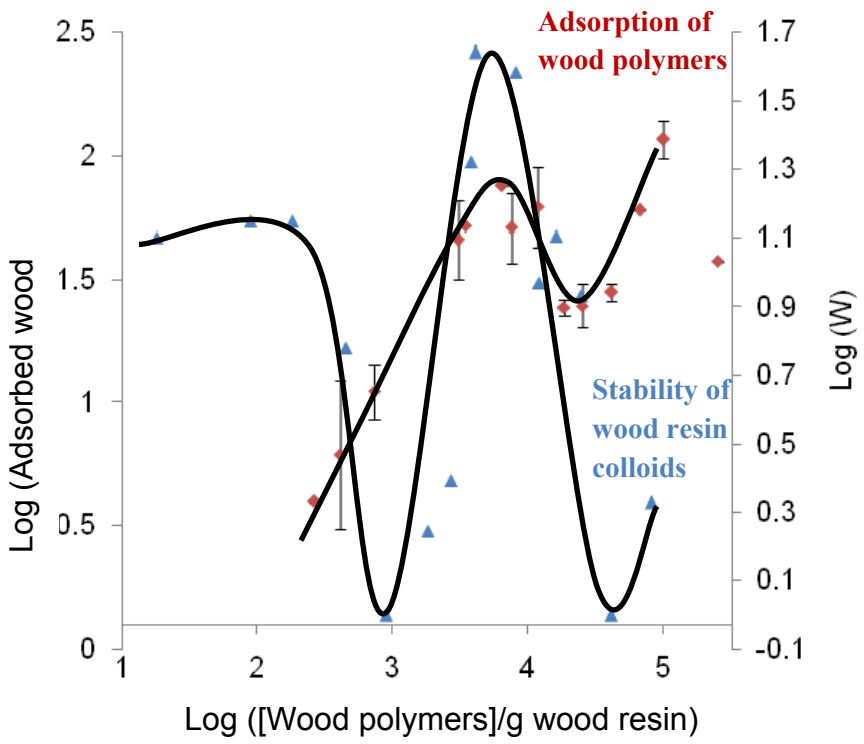

Figure 7.16: Comparison of adsorbed wood polymers to stability of the wood resins on addition of wood polymers to solution.

Bridging flocculation occurs when there are areas of polymer-free particle surfaces at low concentrations of polymer adsorption. 50-percent coverage may result in the best performances of polymer flocculation via bridging flocculation. Steric stabilisation occurs as a result of similar interaction, as noted for bridging flocculation. However, polymer-free particle surfaces are reduced as the concentration of polymer adsorption increases. The repulsion occurs when the polymer chains adsorbed to a particle interact with those on an adjacent particle resulting in this stability. The ideal particle surface coverage is 100-percent [216, 237, 238]. The results indicate that this point of stability with no salt present and polysaccharides of similar size is at about 1 g of hemicellulose per g of wood resin.

7.2.6 EFFECT OF SALT CONCENTRATION ON THE WOOD POLYMER RESIN COLLOIDAL STABILITY

The formation of colloids of the wood polymers and colloidal wood resins is dependent on a number of different variables, for example, the time allowed for the colloids to form and the manner in which they are formed (with or without shear). The formation of these mixed colloids will, in turn, influence the effect of adding salt to the colloidal suspension. Furthermore, the concentration of electrolyte added to solution will play a role in the stability of the colloids formed from this addition.

Figure 7.17 shows the effect of extracted wood polymer concentration on the dynamic stability of preformed colloidal wood resin and extracted wood polymer complexes upon addition of 10mM $CaCl_2$. The complexes were performed by adding the appropriate amount of wood polymers to an aqueous dispersion of wood extractives while stirring vigorously. The solution was dialysed for 24 hours to remove acetone from the wood extractive dispersion. The addition of 10mM $CaCl_2$ was found to cause aggregation in all the solutions. At the lower levels of wood polymers (41mg/L and 82mg/L), aggregation continues for quite a long period of time (5-30 minutes), while at the higher wood polymer levels, a stable floc size is reached after 1-3 minutes.

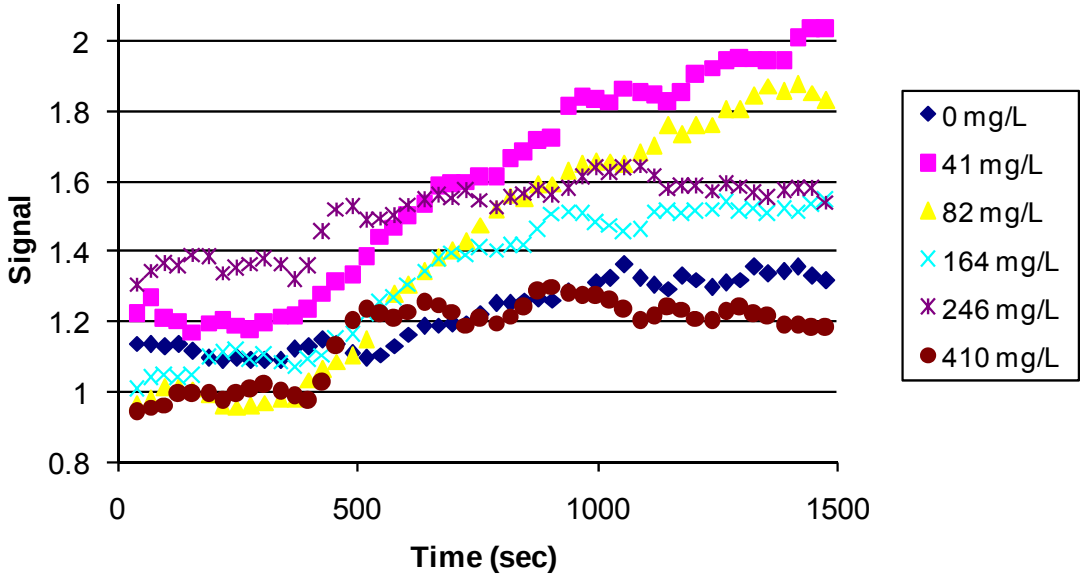

Figure 7.17: Effect on the PDA Signal on addition of extracted wood polymers concentration on the stability dynamics of preformed wood resin/extracted wood polymers complex upon addition of 10 mM $CaCl_2$ (100 mg/L wood resin solution).

Figure 7.18 represents the stability curve for the data in Figure 7.17. At low wood polymer concentrations, the colloidal complexes are destabilised upon addition of electrolyte, as shown by the decrease in log W to 0 at approximately 50mg/L. As the extracted wood polymers concentration is increased above 100 mg/L, the colloids restabilise. Unlike what is shown in Figure 7.10, the colloids continue to be stabilised at wood polymers additions as high as 400mg/L, in the presence of 10mM $CaCl_2$. 100mg/L of wood extracted polymer appears to be the critical concentration of wood polymer to stabilise the wood extractives in the presence of 10mM $CaCl_2$.

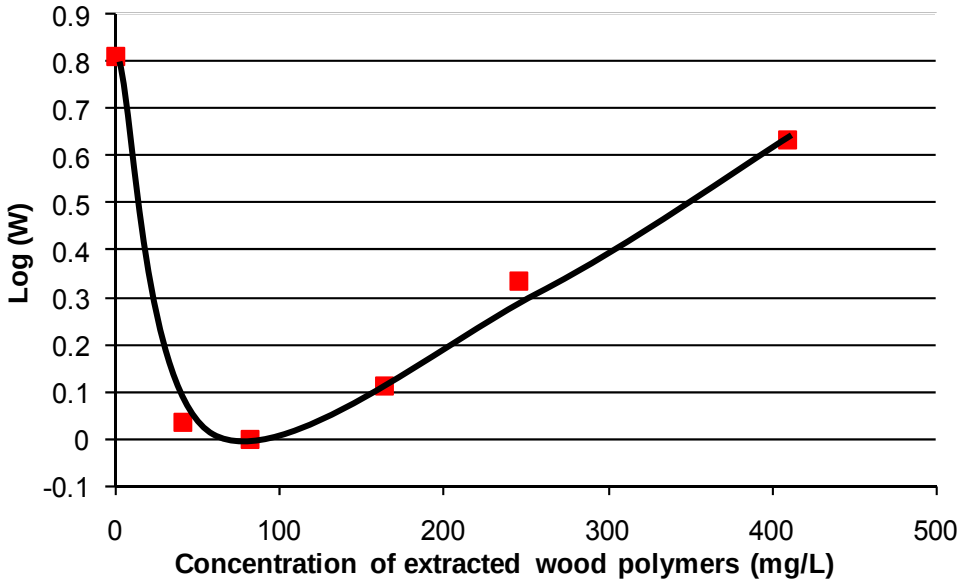

Figure 7.18: Effect of extracted wood polymers concentration on the stability of preformed colloidal wood resin/ extracted wood polymers complexes upon the addition of 10mM $CaCl_2$ (above wood resin CCC for the solution physiochemical conditions for 100 mg/L wood resin sample).

Figure 7.10 indicates that in the absence of $CaCl_2$, steric stabilisation occurs with the addition of 50 mg/L wood polymers to the colloidal wood resin solution. On the other hand with the addition of 10 mM $CaCl_2$ (Figure 7.18), destabilisation of the colloidal wood resins occurs at the same wood polymer addition. The water-soluble polymers are added as a concentrated solution to the wood resin colloids to give final concentrations of 0, 50, 80, 150, 250 and 450 mg/L wood polymers. The initial concentration of the wood polymer solution was calculated on the basis of a dry mass. As the concentration of wood polymers is increased in Figure 7.18 from 0 mg/L to about 80 mg/L, an increase in the rate of coagulation corresponding to a decrease in the stability of the colloid is observed in the presence of 10 mM $CaCl_2$. This occurs at the concentrations of wood polymers that previously induced depletion flocculation. At increased salt concentrations, higher concentrations of wood polymers are needed to stabilise the colloidal suspension. This could be a result of the reduced hydrodynamic radius of the polymers resulting

from addition of salt to solution as observed with the decrease in wood polymer viscosity in Figure 7.8. This decrease in the apparent geometric size of the polymer in solution results in a decrease in the surface coverage of the colloidal particles and the concentration of wood polymers required to stabilise the colloid is proportionally increased.

Very high salt concentrations are expected in modern papermaking under increased system closure. The stabilising effect of extracted wood polymers on wood resin stability was therefore also quantified upon addition of 50mM $CaCl_2$. This salt concentration is above the colloidal wood resin critical coagulation concentration (CCC) for $CaCl_2$ under these physiochemical conditions. Above the CCC, it is expected that the rate of coagulation will remain unaffected by changes to the concentration of added salt unless there is a change in the repulsive forces [62]. Figure 7.19 compares the effect of pre-forming the wood resin/wood polymer complex (complex colloids formed over 12 hr) and newly formed wood resin - wood polymer complex (complex colloids formed over 15 min) at 50mM $CaCl_2$.

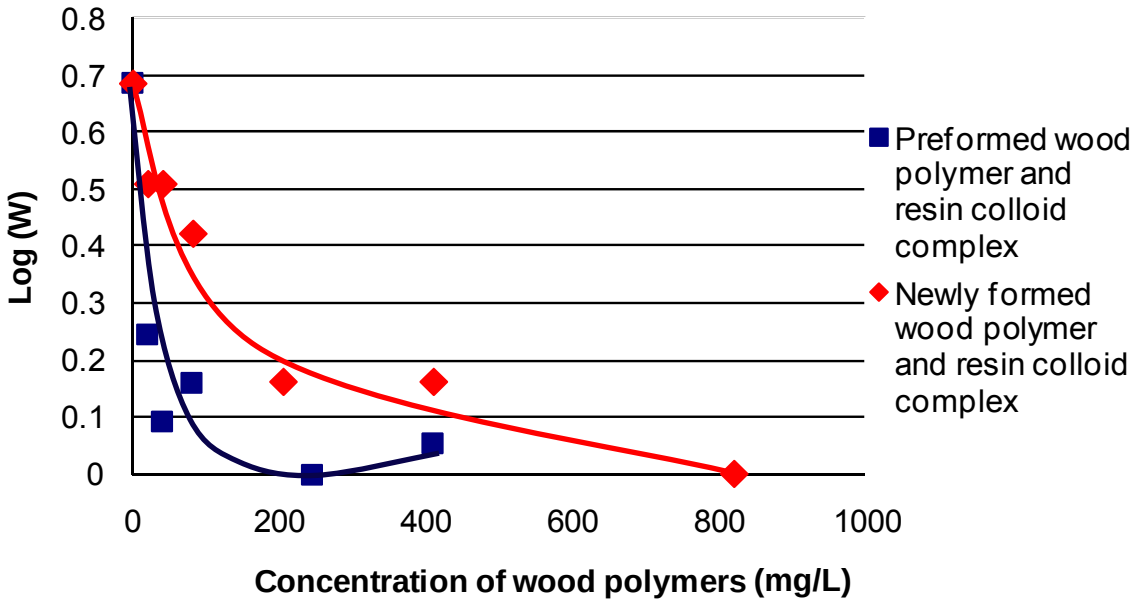

Figure 7.19: Effect of extracted wood polymers concentration on the stability of preformed and newly formed colloidal wood resin/ extracted wood polymers complexes upon 50mM $CaCl_2$ addition (above wood resin CCC for the solution physiochemical conditions, for 100 mg/L wood resin sample).

In the presence of 50 mM $CaCl_2$, the addition of wood polymer was found to cause only destabilisation of the colloids. The restabilisation of the colloid that was evident in the absence and presence of 10 mM $CaCl_2$ did not occur at 50 mM $CaCl_2$ addition. The manner in which the wood polymer and wood extractive colloids were formed and the length of time allowed for the colloids to reorganise is shown to affect the destabilisation of the colloids. Comparison of the newly formed wood resin - wood polymers complex colloids with the preformed wood resin - wood polymers, in which the wood polymers were allowed to reach their equilibrium conformation on the wood resin colloids, reveals that it takes four times more wood polymer to reach maximum flocculation with newly formed wood resin/ wood polymer complexes. At the very high electrolyte concentration, the adsorbed collapsed wood polymer chains seem to have lower surface coverage at a given concentration when newly formed than when the colloids are allowed to reorganise over a period of time.

7.2.7 SIGNAL VARIANCE

As noted previously, PDA output signal variance indicates the floc homogeneity and porosity [113]. The time-weighted variance in the raw ratio signal values for the addition of the wood polymers to the wood resins is shown in Figure 7.20.

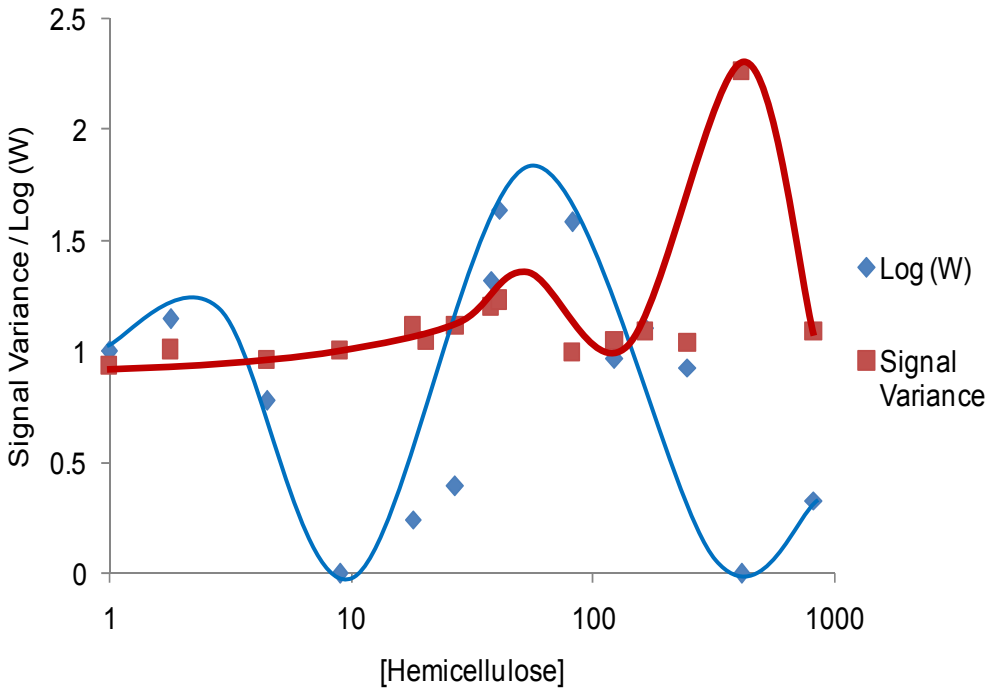

Figure 7.20: Comparison of signal variance and stability curves for the addition of the wood polymers to the wood resins.

The floc variation remains steady up to the two apparent peaks in the variance. The first of the peaks correlates well with the stability region attributed to steric stabilisation. The second peak in the variance values correlates to the region of destabilisation attributed to depletion flocculation. Both of these peaks result from the structure of the flocs formed in solution. As flocculation occurs due to the addition of polymers to solution, they will have a more open/porous structure resulting in the changes in the variance.

7.3 CONCLUSIONS

Dissolved wood polymers released from *Pinus radiata* TMP, consisting mostly of large oligomers of galactoglucomannans, coagulate or collapse their polymer chains upon addition of $CaCl_2$ in the same way that is noted for guar gum with the addition of sodium salts.

Stabilisation against electrolyte-induced aggregation of *Pinus radiata* wood extractives by wood polymers was found to occur. However, some other interesting results were observed, which have not been reported before.

Among these, the observation that in the absence of added electrolyte, low concentrations of wood polymers destabilise wood extractives; while at higher wood polymers concentration, the wood extractive colloids are completely stabilised. This is an indication of steric stabilisation through polymer adsorption. At even higher wood polymers concentration, the wood resin colloids coagulate again, very likely by depletion coagulation.

Wood polymers adsorption on colloidal wood resins is affected by both ionic strength and time. Wood polymers adsorb/reorganise into more compact coils at high ionic strength and lower rearrangement time. However, steric stabilisation was achieved at high wood polymer concentration only for salt concentrations of around 10mM. At very high salt concentrations (50mM $CaCl_2$), the wood polymers were unable to stabilise the wood extractive colloids.

The adsorption of the wood polymers follows an anomalous isotherm formation. This adsorption is thought to result from two main factors, the formation of multiple layers or the interaction of the wood polymers with the wood resins occurs by a mechanism similar to the interaction of two dissimilar colloids.

CHAPTER EIGHT

WOOD RESIN DEPOSITION AT THE SOLID-LIQUID INTERFACE.

A study of factors affecting the deposition of wood resins onto surfaces is essential in better understanding the mechanism behind the deposition. This chapter explores the factors, such as the surface hydrophilicity/hydrophobicity and how different salts of the same valency affect the deposition rate of wood resin particles at the solid-liquid interface.

8.1 INTRODUCTION

Multivalent cations, such as calcium or aluminium, react with the soluble resin acids to form sticky deposits of insoluble metal soaps, through reaction between the carboxylic acid head groups and the metal ion. The metal ions formed with magnesium and sodium do not seem to form the same sticky deposits [28, 29, 239-243].

Previous studies in literature investigated changes in wood resin concentration in solution as a function of salt concentration, valency and type [67-70]. In Chapter 5, the colloidal wood resin stability using the PDA has shown that the rate of particle aggregation is dependent on the concentration of salt present, valency and salt type. The wood resins were found to be a well-behaved colloid with reasonable correlation to DLVO theory (Chapter 5, Section 5.2.5).

Colloid deposition on a surface is not only affected by the particle-surface interactions at the liquid-solid interface, but also by the hydrodynamic conditions in the region of the surface and particle transport [139, 140]. Direct measurement of the deposition rate is possible with techniques such as impinging jet microscopy (IJM) combined with video imaging. IJM gives quantitative information of particles absorbed onto the surface with well-defined hydrodynamic and physical-chemical properties [244].

8.1.1 USE OF IMPINGING JET IN COLLOIDAL DEPOSITION.

The use of the impinging jet microscopy (IJM) and video imaging makes it possible to do direct quantitative measurements of the deposition rate [140]. IJM gives quantitative information of particles absorbed onto the surface under well-defined hydrodynamic and physical-chemical conditions [244]. The technique has been used to probe numerous deposition problems including the competitive deposition of PEI coated particles and the absorption of PEI to a surface [245]. The kinetics of adhesion for phosphatidylcholine liposomes to quartz surfaces [246] and the deposition of particles onto cellulose films [247] have also been studied using impinging jet apparatus.

Figure 8.1 shows the schematic view of the impinging jet consisting of two plates (collector plate and bottom confiner plate) where r is the radius of the jet and h is the distance between the plates. Within the impinging jet, the flow of particles forms a Newtonian flow [248-250], which enters through a circular hole impinging onto the collector plate. The flow/shear distribution is defined by the dimensionless ratio of h/r, as defined in Figure 8.1. The experimental rate of deposition (j) is defined as the number of particles on the surface (n_s) with time (t):

$$j = \frac{n_s}{t} \qquad \textbf{Equation 8.1}$$

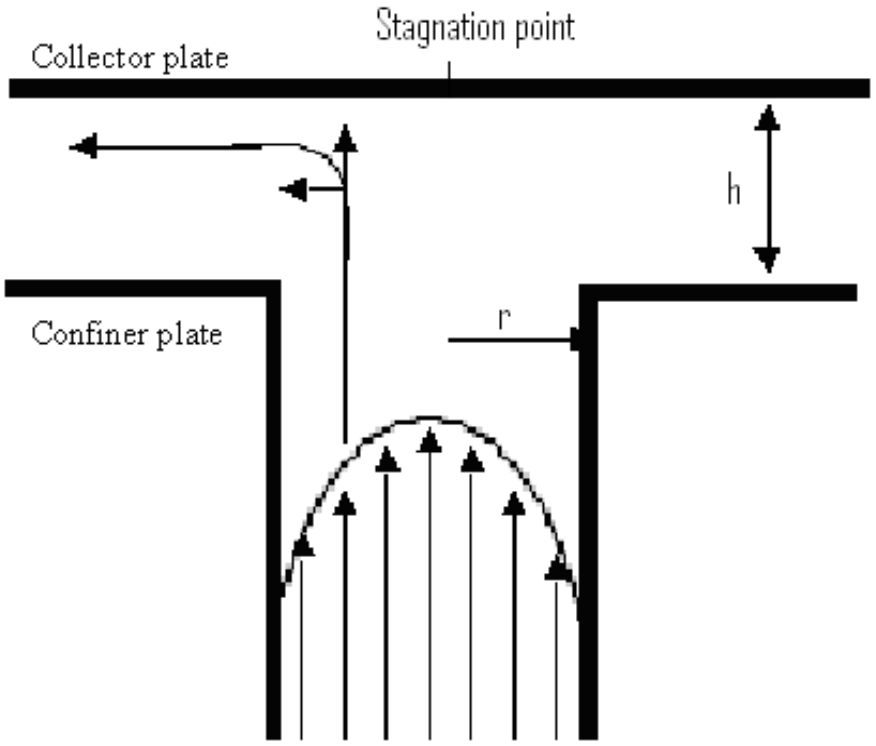

Figure 8.1: Schematic view of a radial impinging jet.

8.2 RESULTS

In Chapter 5, the stability of wood resin colloidal suspensions with various concentrations of electrolyte was studied via PDA. Slight differences in aggregation behaviour were observed between the two divalent salts investigated. The critical coagulation concentrations (CCC) were found to be 7 mM and 8 mM for $MgCl_2$ and $CaCl_2$, respectively.

Differences in the aggregated floc homogeneity were also observed between the two divalent salts [113]. A higher variance in flocs, following the addition of $CaCl_2$ compared to $MgCl_2$, occurred. This implies that the addition of the calcium to solution results in a more variable, looser floc formation.

8.2.1 HYDROPHOBISATION AND CHARACTERISATION OF MODEL DEPOSITION SURFACES

In order to study the deposition of wood resins dispersions onto different surfaces, two model surfaces were prepared: a hydrophilic glass surface and hydrophobic silanised glass surface.The hydrophobisation of the surface was conducted as per Chapter 3, Section 3.13. The contact angle of a water droplet on each surface was measured to confirm the hydrophobicity of each surface. A contact angle of 18^{o} in air was measured for the hydrophilic surface (Figure 8.2), while a contact angle of 118^{o} was measured for the trimethylchlorosilane treated surface (Figure 8.3). The hydrophobic model surface represents the many polymeric surfaces found on a paper machine including the wires, felts, doctor blades and rolls.

Figure 8.2: Contact angle of a water droplet with the model hydrophilic surface in air (18°).100 μL water droplet; the diameter of the needle is 50 μm.

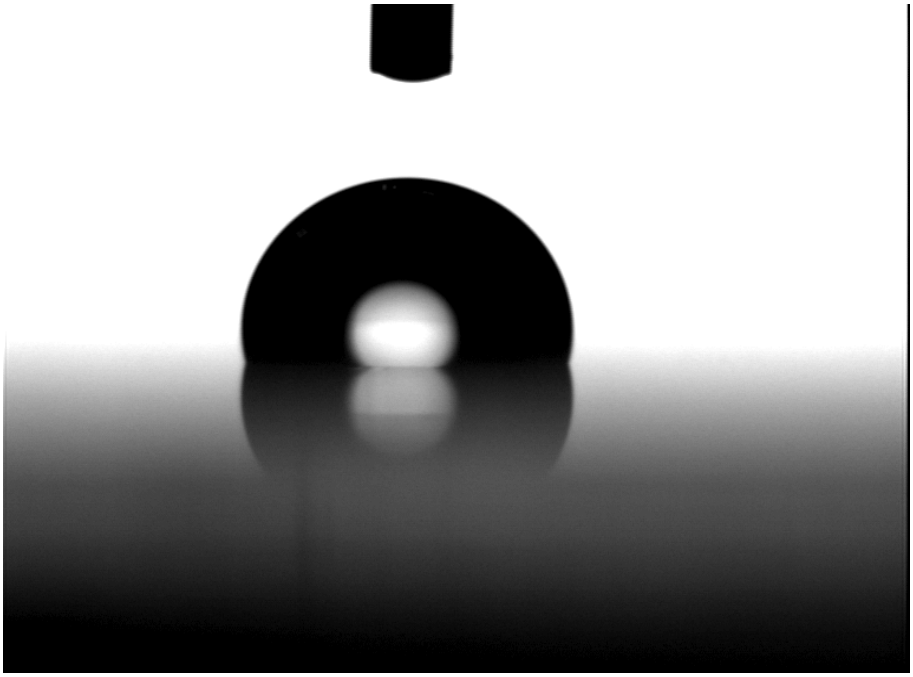

Figure 8.3: Contact angle of a water droplet in air with the model hydrophobic surface (118 °); the diameter of the needle is 50 μm.

8.2.2 EFFECT OF SURFACE HYDROPHOBICITY ON WOOD RESIN CONTACT ANGLE

Droplets of neat hexane extracted wood resin, placed onto the two model surfaces in air, formed a contact angle of 18° for both surfaces. Figure 8.4 shows the low contact angle for neat wood resins on the hydrophobic surface. It is apparent from the contact angle measurements in air that the surface has little or no effect on the contact angle of wood resin in the absence of water.

Figure 8.4: Contact angle of a neat wood resin droplet on a model hydrophobic surface in air (18°).

8.2.3 IMPINGING JET STUDIES INTO WOOD RESIN DEPOSITION

The deposition of colloidal wood resin suspensions onto the two model surfaces was studied using impinging jet microscopy (wood resin dispersions were prepared as per Chapter 3, Section 3.2 and 3.4 for the hexane extracted wood resins). The rate of deposition was assessed by counting the total number of particles on the surface at various times. The type of electrolyte in the colloidal wood resin suspension was varied. The typical deposition pattern of wood resin particles onto the glass surface (hydrophilic) from wood resin suspension, containing 20 mM of $MgCl_2$ and 20 mM $CaCl_2$ respectively, is shown in Figures 8.5A and 8.5B. For both salts, colloidal wood resin deposits as distinct droplets on the hydrophilic glass surface. These droplets may be distinguished from the background via the ring encircling the particles from the reflection of light and the difference in refractive indices between water and wood resin. The presence of these droplets indicates a high contact angle between the surface and the wood resin.

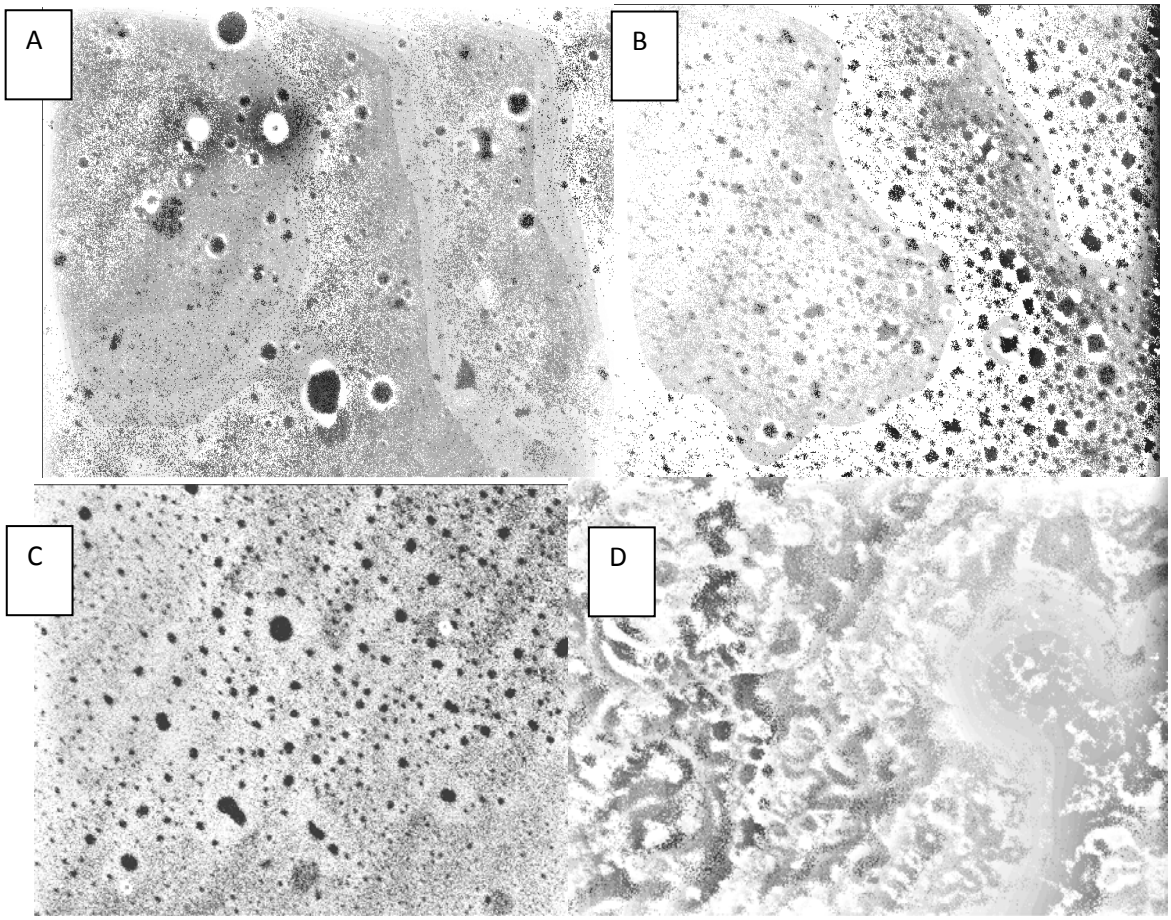

Figure 8.5: View of wood resin particle deposition through impinging jet. ***A:*** *Shows colloidal wood resin particles deposited with 20 mM $MgCl_2$ onto the model hydrophilic surface.* ***B:*** *Colloidal wood resin particles deposited with 20 mM $CaCl_2$ onto the model hydrophilic surface.* ***C:*** *Colloidal wood resin particles with 20 mM $CaCl_2$ deposited onto the model hydrophobic surface.* ***D:*** *Colloidal wood resin particles deposited with 20 mM $CaCl_2$ onto the model hydrophobic surface; after a period of time an oil layer appeared.*

The deposition of colloidal wood resin onto a hydrophobic surface is shown in Figure 8.5C and 8.5D. It can be seen from the absence of the "halo" around the particles that the droplets do not retain their shape but wet the hydrophobic surface and hence have a low contact angle.

Over a period of time, the deposited wood resins formed an oil film on the hydrophobic surface as seen in Figure 8.5D. This phenomenon was not observed with the model hydrophilic surface even for prolonged periods. The effect is known as film thinning. The oil film was found to obscure measurement of the rate of colloidal wood resin deposition. The surface was cleaned after each run to overcome this effect.

8.2.4 SIZE OF IMPINGING JET DEPOSITED COLLOIDS

Figure 8.6 presents the effect of salt on the average size of wood resin particles on the two model surfaces after 60 sec of deposition. Four observations are of interest. First, the particles on the hydrophilic surfaces are smaller than those on the hydrophobic surfaces. Second, there are little or no differences in particle size (colloidal wood resin with $MgCl_2$ or $CaCl_2$) observed for the model hydrophilic surface. Third, the large difference between the hydrophobic surfaces for the calcium and magnesium salts is related to the amount of film thinning or the effect of wetting. Last, more film thinning was observed for wood resins with the calcium salt. As a result, a larger average particle size was measured with a larger variation in the particle size as indicated by the error bars.

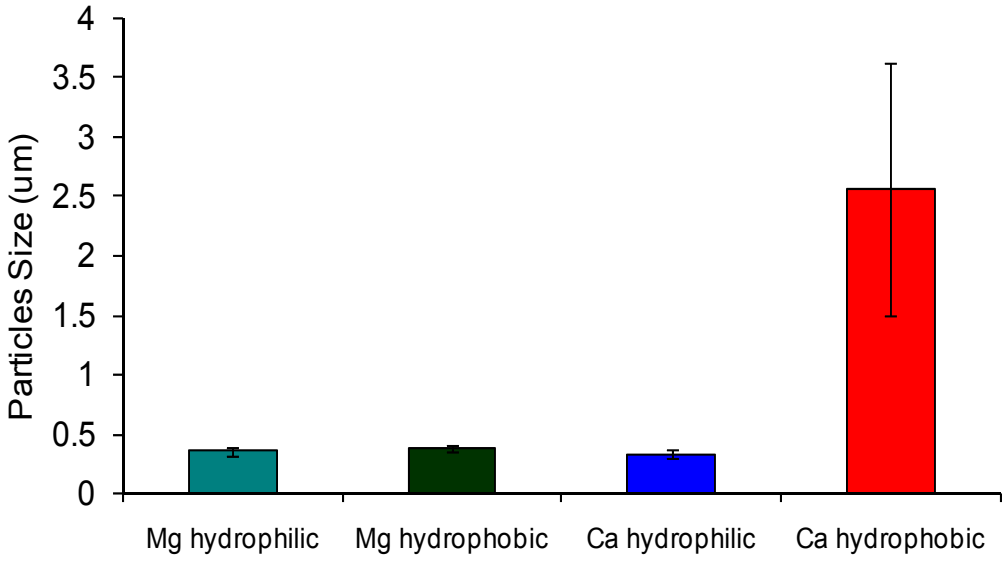

Figure 8.6: Comparison of average particle size for the deposited wood resins after 60 sec of deposition onto a hydrophilic and hydrophobic surface with calcium and magnesium salts.

There was a large difference in colloidal particle size observed on the hydrophobic surface between the wood resin particles with magnesium salts and those with calcium salts. Different behaviours of wood resin film thinning were also recorded onto the hydrophobic and hydrophilic surfaces. These observations indicate that the wood resin particles are interacting with the surface in different ways. The film thinning observed on the hydrophobic surface enables the wood resin particles to conform easily to the surface, gradually forming a complete oil film. In time, this phenomenon obscured the measurement of the particles deposition onto the model surface.

8.2.5 RATE OF COLLOIDAL DEPOSITION THROUGH IMPINGING JET STUDIES

Particles were found to deposit faster onto the hydrophobic surface compared to the hydrophilic surface (Figure 8.7). The rate of wood resin deposition corresponds to the ratio of particles/time and was measured as the slope of the best fit lines in Figure 8.7. On the hydrophilic surface, the wood resin deposition rate in the presence of magnesium salt (Mg) was 41 counts/sec, and this increased to 103 counts/sec with changing to a hydrophobic surface. This represented a 2.5 times increase in particle-surface interaction. On both model surfaces, the wood resin deposition was faster in the presence of calcium salt (Ca). The rate of deposition was 62 counts/sec for the hydrophilic surface, and 115 counts/sec for the hydrophobic surface, representing a 1.8 fold increase.

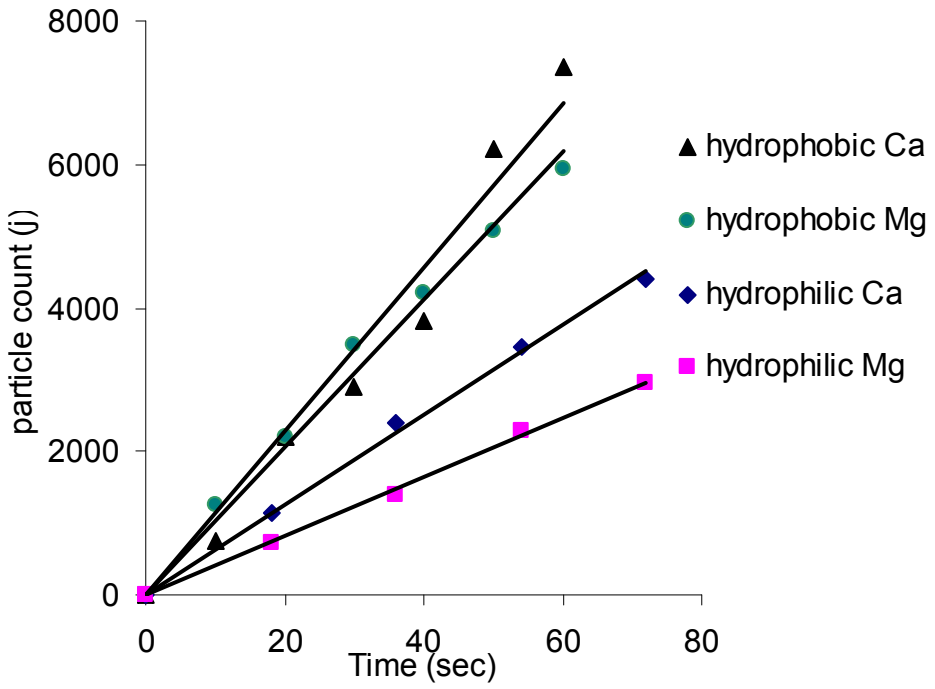

Figure 8.7: Flux of particles to the surface with different salt types ($CaCl_2$ and $MgCl_2$) and surface conditions (hydrophobic and hydrophilic).

Deposition occurred on both hydrophobic and hydrophilic surfaces (Figures 8.5). However, the rate of deposition was linked to the surface polarity/hydrophobicity; the wood resins having higher affinity for the hydrophobic surface. According to Audry et al. [251], hydrophobisation of the glass surface results in reduction of the surface potential. As a result, the electrical field of the double-layer associated with the surface is reduced, and thus the repulsive forces are also reduced – allowing for greater particle-surface interaction [251] which is governed by van der Waals forces. In the case of a hydrophilic surface, electrostatic repulsion and a small energy barrier between the wood resin particle and the hydrophilic surface reduces the interaction between the wood resin and surface. The difference that was found between the rate of deposition for the calcium and magnesium salts suggests that this energy barrier is slightly different for the different soap structures on the wood resin surface.

The high calcium concentration (800 mg/L) investigated in this study corresponds to the salt levels expected in the process water of a modern pulp and paper mill under a strategy of increased water recycling. Soluble calcium concentrations of 80-150 mg/L are typical of the levels in many mills' process waters. Our results indicated that the hydrophobic surfaces of the paper machine form oil films at a higher deposition rate (2.5X) than hydrophilic surfaces do. This wood resin oil film then adheres to the fibres and minerals of paper, resulting in tacky deposits. However, for the current process, unless magnesium or calcium alkali and process chemicals are selected instead of the current sodium, the concentrations of magnesium in the process water are below the critical threshold to create deposit issues. Overall, the choice of the cation has little effect on wood resin deposition on hydrophilic surfaces but a major impact for hydrophobic surfaces with regard to the formation of wood resin films.

8.2.6 WOOD RESIN SURFACE REORGANISATION

The wood resin dispersions deposited on the surfaces were measured at a pH of 5.5, which is below the pK_a's of the resin acid (7.1-7.3), the saturated fatty acid (7.1-10.2), and the unsaturated fatty acids (6.8-8.3) [10]. Nylund et al. [252] showed the degree of dissociation of charges on colloidal particles at pH 5.5 resulting in a surface charge on the colloidal particles.

The molecules forming the wood resin colloids contain a small hydrophilic head group (carboxylic acid) and a long hydrophobic tail (Figure 2.1 and 2.2). The low contact angle observed for neat wood resins on both the hydrophilic and hydrophobic surfaces in air (Figure 8.4) suggests that wood resin molecules have some ability to reorientate within the colloid in order to be able to strongly interact with both types of surfaces. The molecules can reorientate themselves so that the polar group interacts with a hydrophilic surface or the non-polar groups can orientate toward the hydrophobic surface.

From the observations with the impinging jet experiments, different behaviour occurs in water compared to the air environment as the shape of the droplets were quite different for the two different surfaces. The wood resins have a lower affinity for the hydrophilic surface in water compared to in air. This suggests that the orientation of the constituent molecules of wood resin in a water environment is restricted by the water-wood resin interactions. Similar results were obtained by Kallio et al. who measured the spreading and adhesion of lipophilic extractives onto different surfaces [253]. They also noted that the interfacial tension of wood resin with aqueous solutions was affected by the presence of calcium in solution [254]. Figure 8.8 shows a pictorial representation of the behaviour of the wood resin droplets under varying conditions.

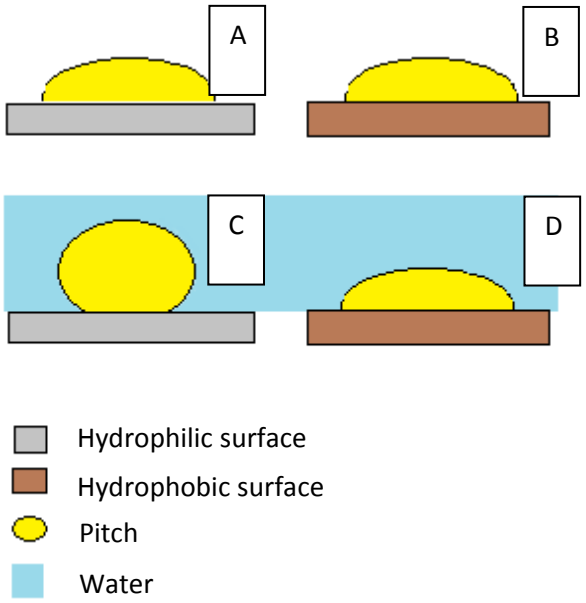

Figure 8.8: Schematic representation of the wood resin droplet shape under various conditions. A: neat wood resin on hydrophilic surface in air. B: neat wood resin on hydrophobic surface in air. C: wood resin deposited onto the hydrophilic surface in aqueous environment through impinging jet microscopy. D: wood resin deposited onto the hydrophilic surface in aqueous environment through impinging jet microscopy.

It is proposed that the more hydrophobic components of wood resins preferentially migrate toward the solid hydrophobic surface while the more hydrophilic wood resin molecules reorient toward the water interface. This reorientation/migration phenomenon driven by reduction of the hydrophobic-hydrophilic interface area to minimise the system free energy was previously observed by Kallio et al. and Koberstein [254-256]. Combined with this, the small fraction of ionised resin components is able to react with the calcium ions present in solution forming non-polar metal soaps. Because of the hydrophobicity of the colloid core combined with the wood resin molecular mobility, the non-polar metal resinates may migrate toward the core of the particles. This re-conformation would result in an increased concentration of non-polar components in the particle and the consumption of the resins acids resulting in a more hydrophobic colloid.

8.3 CONCLUSION

From contact angle measurements of wood resin droplets onto hydrophilic and hydrophobised glass slides, it can be concluded that in an air environment, the hydrophobicity of the surface does not affect the affinity for wood resin. The deposition behaviour of wood resins from an aqueous environment in the presence of divalent salts was found to differ depending on the surface hydrophobicity and salt type.

Wood resin deposition was slightly faster for a calcium salt (at 800 mg/L concentration of salt) than magnesium salt at the same concentration onto both a hydrophilic and a hydrophobic surface using impinging jet microscopy. The rate of deposition onto the hydrophobic surface was up to 2.5 times greater than the hydrophilic surface for both salts. Variations in the wood resin shape and size occurred on the different surfaces. On a hydrophobic surface, the wood resin particle size for both salts was 0.33 -0.35 μm while for the hydrophobic surface the particle size was five times higher for calcium than magnesium salts. Film thinning or wetting of the wood resin colloid occurred on a hydrophobic surface with calcium salt and to a lesser extent with magnesium salt.

It is proposed that the deposition behaviour of wood resin colloids, in different environments, is governed by its ability to undergo molecular reorganisation. Being a soft colloid, wood resin is able to phase separate and molecularly reorientate to decrease its free energy upon interaction with its environment. At an air interface, reorientation of the polar and non-polar ends of the fatty acids and resin acid components in the wood resin colloids can occur with the groups reorienting themselves in opposite directions depending on the surface hydrophobicity. In an aqueous environment, reorientation of the polar and non-polar ends is restricted by the strong interaction between the polar groups and the water environment. Under these conditions, surface hydrophocity is found to play a significant role in the rate of deposition. Metal resinates that form between divalent cations, such as magnesium and calcium, and the fatty acids and resin acid components also affect the deposition behaviour and the molecular rearrangement within the colloid in different ways. Non-polar, insoluble calcium resinates that form are believed to migrate to the hydrophobic core of the wood resin colloid decreasing the amount of polar groups at the colloid surface and promoting a higher affinity for hydrophobic

surfaces and film thinning compared to magnesium resinates which are more soluble and thus slightly more polar.

CHAPTER NINE

CONCLUDING REMARKS

From EPR spectra obtained from model wood resin colloids, it is proposed that the colloidal structure models stipulated for both the northern hemisphere spruce and *Pinus radiata* wood resins should be altered with respect to the outer shell composition. As previously proposed, the core of the colloid will predominantly be the hydrophobic components of triglycerides and sterols. However, in regard to the colloidal shell, the fatty acids form a mobile phase apparently separate from the resin acid shell that can undergo lateral phase separation. The amount of interaction of the fatty acids with the solution outside the colloid is dependent on the concentration of both the fatty acids and non-polar components present within the colloid. The formation of a lateral phase separation between the resin and fatty acids accounts for the variation in the colloidal stability on changes to the concentration of non-polar components in the core of the colloid.

Furthermore, the EPR spectra are noted to change on the addition of electrolytes to solution only for those components at the core of the wood resin colloids, little or no changes in the mobility of the fatty acids is noted for this addition. This is a result of movement of metal resinate complexes to the colloid's centre, affecting the viscosity of the microscopic environment within the core of the colloid.

The surface charge of the wood resin colloids was found to increase with the pH of the solution. Comparison between the zeta potentials found with the use of the qNano system, shows a large reduction by comparison to the zeta potentials calculated from mobility data for the northern hemisphere wood resins. This variation may be a result of the differences in composition. However, given the higher percentage of resin acids in the *Pinus radiata,* a greater charge than the spruce wood extracts would be expected. The surface charges determined from potentiometric titrations show good correlation in their magnitude to the surface charges found

on the wood fibres of both northern hemisphere spruce and *Pinus radiata*. The average particle size for the wood resins from *Pinus radiata* was found to be 0.45 μm.

Wood resins in solution form a colloidal suspension that follows the basic concepts of the DLVO and coagulation kinetics theory. Colloidal wood resins are stabilised through the de-protonation of the carboxylic groups of its resin and fatty acids constituents, resulting in increased surface charge on the particles.

In Chapters 5 and 6, a detailed study in the coagulation kinetics of wood resins derived from *Pinus radiata* with variation in a number of key physiochemical factors and salt types is given. The critical coagulation concentrations for a number of different salts (NaCl, KCl, $CaCl_2$, $MgCl_2$, $FeCl_3$ and $Al_2(SO_4)_3$) were determined from the coagulation rate data. The effect of colloidal suspension pH, temperature and the rate of shear on the coagulation dynamics and thus the CCC for the wood resins were determined. On comparison with the literature values found for the spruce extracts (Table 2.3), it can be seen that for the addition of the monovalent and trivalent ions to solution, there is a large increase in the stability of the colloid to coagulation at all shears tested. For the addition of the divalent ions to solution, variation with the reported values is dependent on the shear and increases with increasing shear, with very large differences noted at $G = 200\ s^{-1}$.

Multivalent ions of both Al and Fe, readily form various hydroxide species which influence their interaction with the surface and also affect the electrical-double layer. It is proposed that the multivalent salts adsorb on to the potential-determining ions (various associated and disassociated hydroxide species as discussed in Chapter 2 and 4) at the surface of the colloidal wood resins and destabilise the wood resin colloids through surface adsorption and reduction of the surface charge.

The wood resin colloidal stability upon salt addition is a function of pH or wood resin charge, with higher stability achieved at higher charge (pH). This follows the predictions from the DLVO theory. Temperature also affected wood resin stability accordingly to expectations from DLVO theory. However, the effect of temperature upon salt destabilisation was a strong function of the type of salt. This might suggest the occurrence of temperature induced selective

ion adsorption onto colloids, affecting zeta potential. Temperature and pH affect not only colloidal wood resin stability, but also wood resin solubilisation and likely the visco-elastic properties of the wood resin colloid and its surface composition [209].

As the efficiency of coagulation (σ) is dependent on shear (G), it follows that the critical coagulation concentration (CCC) should also vary with shear. All salts investigated, with the exception of $CaCl_2$, exhibited a colloidal wood resin CCC decreasing with shear at a faster rate as shear increases. At low shear, the wood resin critical coagulation concentration (CCC) scales with salt valency to the -6 power, following the Shultz-Hardy rule for highly charged colloids. This is surprising because of the moderate charge of wood resin. Deviations from the Shultz-Hardy rule become important as shear increases and a CCC α $z^{-7.1}$ relationship was measured at the highest shear. Hydrodynamic forces are typically omitted from the DLVO equation. It is apparent that there is a dependency on shear. An additional term in the CCC expression would be required for the systems under orthokinetic conditions usually found in industry. The results also indicate that the critical coagulation concentration is not a thermodynamic property but rather a variable describing a particular colloidal system. We suggest a relationship of the form: CCC α $(\Omega z)^{-6\tau}$ or CCC α $z^{-6\tau} + \Omega^{-1}$ where Ω=f(G) and τ = g(G). CCC α $z^{-6\Omega}$ with Ω=f(G).

Given that mill process water is a complex mixture containing more than one salt, the effect of multiple salts on the system was assessed. A reduction in the critical coagulation concentration for a given multivalent ion was found to occur. The change in the CCC was not a simple addition of the salts, i.e. if there is half the Na CCC added to solution and Ca is varied, the new CCC was not equal to half the original CCC for Ca. This was shown for the addition of Ca^{+2} in the presence of Na^{+} and for Al^{3+} with Na^{+}.

On addition of salt concentrations greater than the CCC for the multivalent ion in the presence of sodium ions, there is a notable restabilisation of the colloid in solution that is unreported previously for the wood resins. This effect is not seen for the addition of a single salt to the colloidal suspensions.

Both the deviation from the expected simple additive behaviour and the restabilisation of the wood resins on the addition of multiple salts to solution could result from either solvent

effects or ion adsorption to the surface. The restabilisation of the colloids may result from solubilisation of the multivalent ion resinate complexes in the presence of the sodium ions in solution. Polymeric ions such as Keggin ions have been found to be stable over large changes in supernatant pH (pH 3 to 7). However, it may be that the mechanism of coagulation is changing as the sodium ion concentration increases and the charge naturalisation for the colloids occurs at lower concentrations, and the restabilisation occurs through charge reversal.

The water-soluble wood polymers released during the pulping process have previously been reported to stabilise the wood resin in solution. However, in Section 7.2.3, Figures 7.7 and 7.8, the dissolved wood polymers released from *Pinus radiata* TMP were found to coagulate or undergo polymer chain collapse on addition of $CaCl_2$ to solution, in a manner that has been noted for guar with the addition of sodium salts. As can be seen in Figures 7.10, 7.18 and 7.19 the stability of the wood resins to the addition of wood polymers to solution is greatly dependant on both the wood polymer concentration and the concentration of salt in solution.

Stabilisation against electrolyte-induced aggregation of *Pinus radiata* wood extractives by wood polymers was found to occur. However, some other interesting results were observed, which have not been reported before. The concentration of the wood polymers in solution was found to affect the stability of the wood resins in solution; the kinetic studies show that the interaction between the wood resins colloids and the water-soluble wood polymers have all four regions of a classical colloid-polymer interaction expected for synthetic polymers under ideal conditions. In the absence of added electrolyte, low concentrations of wood polymer destabilise the colloidal wood resin, while at higher wood polymer concentration, the wood resin colloids are completely stabilised. This is an indication of steric stabilisation through polymer adsorption. At even higher wood polymer concentration, the wood resin colloids coagulate again, very likely by depletion coagulation.

Wood polymer adsorption on wood resin is affected by both ionic strength and time. Wood polymers adsorb/reorganise into more compact coils at high ionic strength and lower rearrangement time. However, steric stabilisation was achieved at high wood polymer concentration only for salt concentrations of 10mM. At very high salt concentrations (50mM

$CaCl_2$), the wood polymers were unable to stabilise the wood extractive colloids and result in less stable complex colloids.

From contact angle measurements of wood resin droplets onto hydrophilic and hydrophobised glass slides, it can be concluded that, in an air environment, the hydrophobicity of the surface does not affect the affinity for wood resins. The deposition behaviour of wood resins from an aqueous environment in the presence of divalent salts was found to differ depending on the surface hydrophobicity and salt type.

Wood resin colloidal deposition was slightly faster for a calcium salt (at 800 mg/L concentration of salt) than magnesium salt at the same concentration onto both a hydrophilic and a hydrophobic surface using impinging jet microscopy. The rate of deposition onto the hydrophobic surface was up to 2.5 times greater than the hydrophilic surface for both salts. Variations in the colloidal wood resin shape and size occurred on the different surfaces. On a hydrophobic surface the wood resin particle size for both salts was 0.33 -0.35 μm while for the hydrophobic surface the particle size was five times larger for calcium than magnesium salts. Film thinning or wetting of the wood resin colloid occurred on a hydrophobic surface with calcium salt and to a lesser extent with magnesium salt.

It is proposed that the deposition behaviour of wood resin colloids, in different environments, is governed by its ability to undergo molecular reorganisation. Being a soft colloid, wood resin is able to phase separate and molecularly reorientate to decrease its free energy upon interaction with its environment. At an air interface, reorientation of the polar and non-polar ends of the fatty acids and resin acid components in the wood resin colloid can occur with the groups reorienting themselves in opposite directions depending on the surface hydrophobicity. In an aqueous environment, reorientation of the polar and non-polar ends is restricted by the strong interaction between the polar groups and the water environment. Under these conditions, surface hydrophocity is found to play a significant role in the rate of deposition. Metal resinates that form between divalent cations, such as magnesium and calcium, and the fatty acids and resin acid components also affect the deposition behaviour and the molecular rearrangement within the colloid in different ways. Non-polar, insoluble calcium resinates that form are believed to migrate to the hydrophobic core of the wood resin colloid decreasing the

amount of polar groups at the colloid surface and promoting a higher affinity for hydrophobic surfaces and film thinning compared to magnesium resinates which are more soluble and hence slightly more polar.

9.1 INDUSTRIAL RELEVANCE

Within the mill, there is large variation in the extractives and their makeup over the course of the year. The variation in the wood resins in solution relates to the seasonal variation in tree growth. In Figure 9.1, the variations in the different components in the mill are shown over a number of years. It can be seen that there is a decrease in the glycerides in the summer months (November through March) and an increase in the resin and fatty acids during this time.

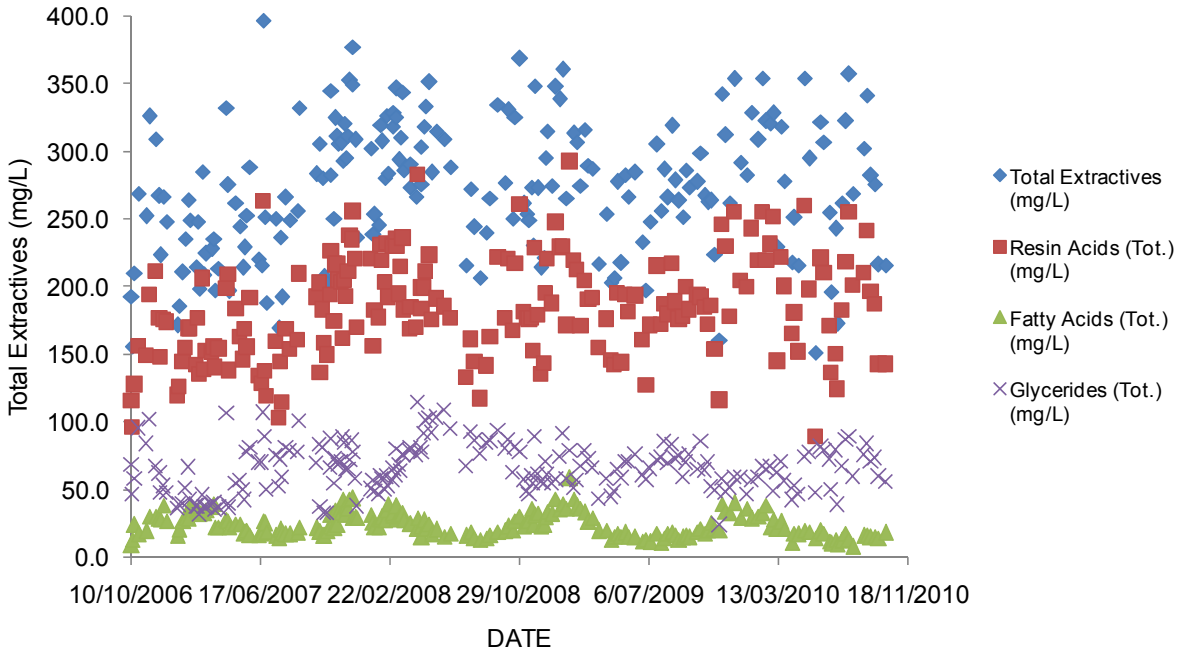

Figure 9.1: Variation in various wood resin components with time (extracted from mill records).

The variation in the breaks in the dry end paper sheet, are noted to be related to variation in the composition of the wood resins in solution. From Figure 9.2, the number of dry end

breaks increase as the concentration of the glycerides and/or the fatty acids increase, suggesting that the stability of the wood resins changes with the composition.

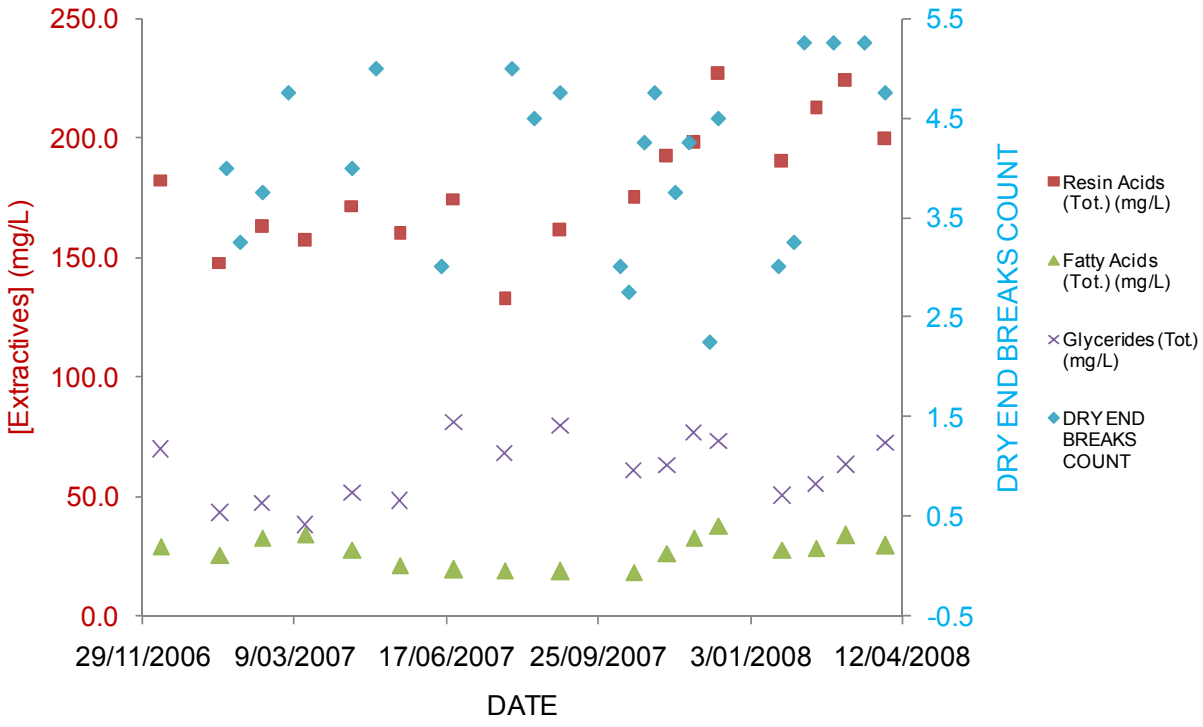

Figure 9.2: Variations in various wood resin components with time and the associated wet end breaks in the fibre mat (extracted from mill records).

The new model proposed from the work with the EPR (Chapter 4) explains the variation in the wood resin deposit problems or "pitch season" as it relates to the changes in the makeup of the colloidal wood resins (Figure 9.2) and how the variation in the amount of glycerides can affect the apparent interactions in solution and with the different surfaces. The previous model of the colloidal wood resins did not explain the change in the stability with variation in the components in the colloid, as noted in Chapter 4.

Within the mill, there is particular relevance for this work. In regions of high shear/turbulence, high levels of salt will result in coagulation and/or deposition of the wood resins. This is not an issue for sodium, as the current mill concentrations are well below the CCC even at the very high shear tested in Chapters 5 and 6 (CCC_{Na} = 720 mM CCC_K = 670 mM). However, for the different multivalent ions, especially calcium and aluminium, which are known to be in relatively high abundance, the CCC levels were determined to be 8mM (300mg/L) and 0.065mM (2mg/L), respectively. The current concentrations of these metal ions are in the transition regions for the stability curves, shocks in shear, pH and temperature can be highly detrimental to the stability of the wood resin colloids.

The operating team at the mill needs to identify regions where these shocks in pH, temperature and shear are likely to occur. These regions will be the most problematic in deposition of the wood resins. The mill needs to adopt strategies to eliminate the shocks. In Figure 9.3, the changes in the concentration of calcium in the mill solutions are shown, along with the number of dry end paper web breaks. At the current levels of calcium in solution, there is no apparent correlation seen in Figure 9.3 for the number of web breaks in the paper sheet to the concentration of the calcium ions in solution. However, it is in the transition region of the stability curves suggesting that it can induce instability with slight changes in solution.

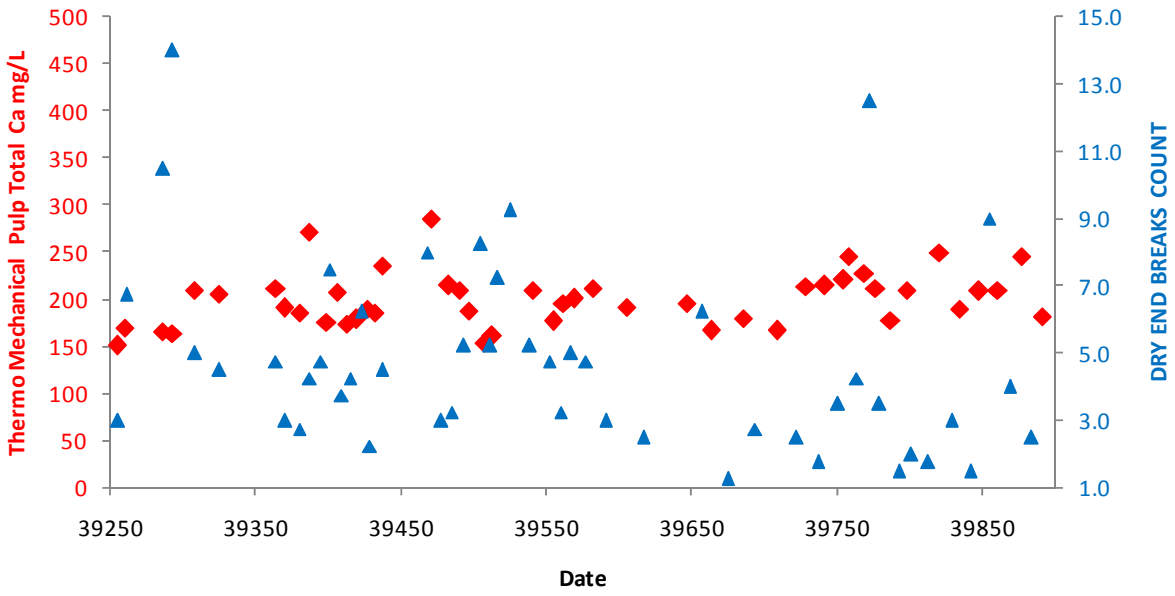

Figure 9.3: Changes in the calcium concentration and its effect on the dry end paper web breaks (extracted from mill records)

The interaction between the wood resin colloids and the salts is more difficult than is generally apparent. The interaction of the calcium with the wood resins is not occurring by its self and the other salts present in solution will affect the stability. The concentrations of the salts and their interaction with each other and the surface of the colloids and multiple salts results in reduced stability of the colloids in solution (Chapter 5).

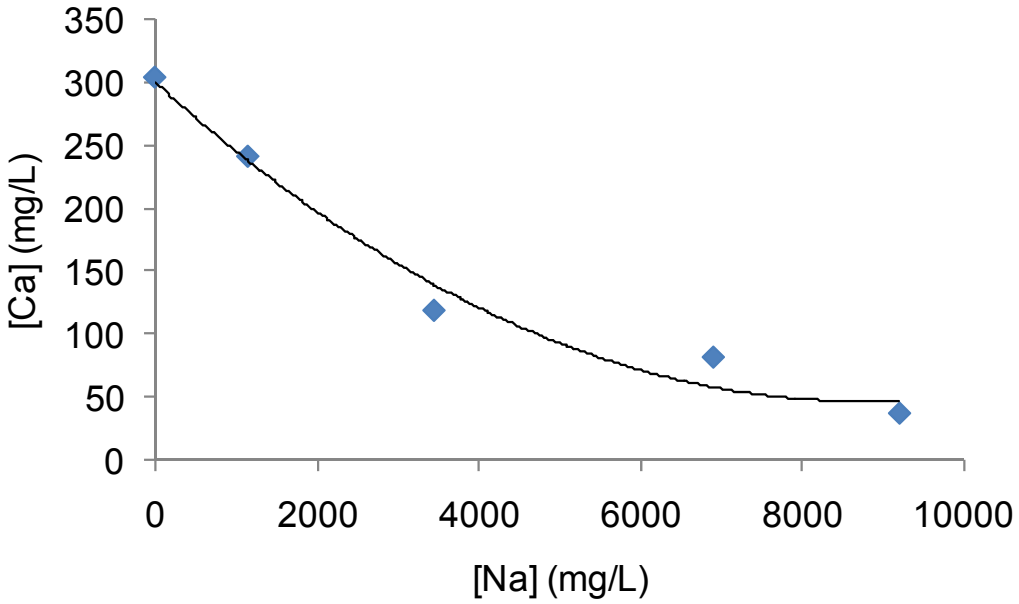

Figure 9.4: Effect of sodium concentration on the critical coagulation concentration for the addition of calcium to the wood resins Chapter 5.

From Figure 9.4, it is noted that at the average calcium concentrations in the mill solutions (150 mg/L), the concentration of sodium required to induce coagulation is in the order of 3000 mg/L. From Figure 9.5, it is noted that even at very high sodium concentrations the mill solutions are well below this threshold. In Figure 9.5, some correlation between the sodium concentrations and the dry end breaks can be seen. However, it shows less dependence on the concentration of the calcium (unexpected as calcium is a multivalent ion and should affect the colloid to a greater extent).

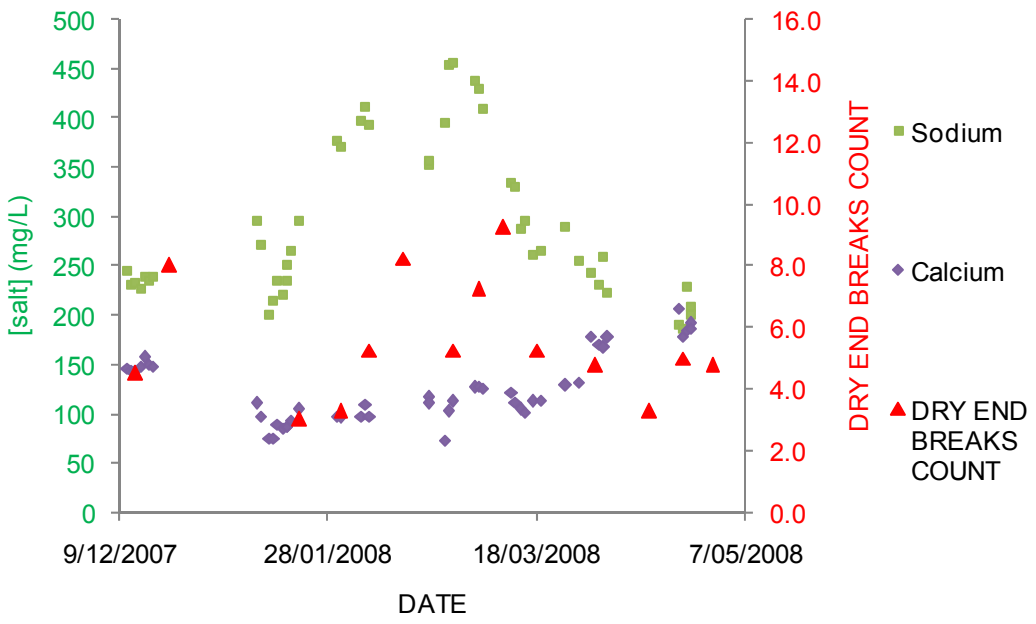

Figure 9.5: Variation in the calcium and sodium concentrations and its effect on the dry end paper breaks (extracted from mill records).

From Chapter, 5 increased salt may result in restabilisation of the colloids in solution; however, further work is needed to understand the mechanism behind this stabilisation. Further work is also needed to understand how the presence of the three main destabilising salts will interact together and the surface and the stability resulting from this. Unfortunately, the mill records do not include the monitoring of the aluminium concentrations.

At present, the Norske Skog Mills do not test the concentration of wood polymers (DOM) in solution on a regular basis. The presence of the wood polymers is shown to stabilise the colloids in solution at the current mill concentrations (≈100 mg/L). However, their interaction with the metal ions in solution results in a reduction of this stability (Chapter 7). As the metal ion concentration in solution increases, the wood polymers (DOM) will destabilise the wood resins, resulting in greater deposition and coagulation. It will become more important to monitor the concentration of the wood polymers in solution as the mill recycles more water. Further work

will also be required to determine the changing stability of the wood resin/polymer complex colloids with the changes in the concentrations of polymer and salt.

As noted previously, there are currently a number of different mechanisms used to facilitate removal of the wood resins from solution in different mills worldwide. One example of this includes the fixing of the wood resin colloids to the wood fibres with the wood resins being accumulated onto the paper sheet. Fixation is achieved through the addition of synthetic polymers and other filler additives to the solution. However, it is important to note that the addition of such substances can and will affect the various balances in the system, Further experimentation is required to better understand how the addition of each of the different polymeric species will affect and be affected by the presence of hemicelluloses and various metal ions. The use of talcs and other such filler particles can result in improved system reliablity. However, the processes involved and their long term effects need to be better understood as the amount of water recycling is increased within the mills. It is also important to note how the addition will affect the downtime on the paper machines as a result of deposit fouling and paper breaks caused by wood resins within the system. Further work is also needed to better understand the processes by which the resins have been found to de-adsorb to other surfaces over time.

CHAPTER TEN

REFERENCES

[1] http://www.bom.gov.au/climate/drought/livedrought.shtml, Living with Drought, in: A.G.-B.o. Meteorology (Ed.), Australian Government - Bureau of Meteorology, http://www.bom.gov.au/climate/drought/livedrought.shtml, 2011.

[2] I.P.P.a.C.I. European commission, Best Available Techniques in the Pulp and Paper Industry, in: I.P.P.a.C. (Ed.), IPPC, 2001.

[3] J. Uprichard, Chapter 1, in Pulp and Paper from Radiata Pine, Appita and Forest Research, Carlton, 2002, 2-3.

[4] M. Qin, T. Hannuksela, B. Holmbom, Physico-chemical characterisation of TMP resin and related model mixtures, Colloids and Surfaces A: Physiochemical and Engineering Aspects 221 (2003) 243-254.

[5] J. Nylund, K. Sundberg, Q. Shen, J. Rosenholm, Determination of surface energy and wettability of wood resins, Colloids and Surfaces A: Physiochemical and Engineering Aspects 133 (1998) 261-268.

[6] D. Vercoe, K. Stack, A. Blackman, B. Yates, D. Richardson, An innovative approach characterising the interactions leading to pitch deposition, Journal of Wood Chemistry and Technology 24 (2004) 115-137.

[7] I. McDonald, L. Porter, Resin and fatty acid composition of *Pinus radiata* whole wood, and its relation to the yield and composition of New Zealand tall oil, New Zealand Journal of Science 12 (1969) 352-362.

[8] D. McLean, K. Stack, D. Richardson, The effect of wood extractives composition, pH and temperature on pitch deposition, Appita Journal 58 (2005) 52-55, 76.

[9] D. McLean, D. Vercoe, K. Stack, D. Richardson, The colloidal pK_a of lipophilic extractives commonly found in *Pinus radiata*, Appita Journal 58 (2005) 362-366.

[10] D. McLean, D. Vercoe, K. Stack, D. Richardson, The pK_a of lipophilic extractives commonly found in *Pinus radiata*, 58th Appita Annual General Conference Proceedings, Canberra, Australia, 2004, 73-77.

[11] J. Kanicky, D. Shah, Effect of degree, type, and position of unsaturation on the pK(a) of long-chain fatty acids, Journal of Colloid and Interface Science 256 (2002) 201-207.

[12] J. Kanicky, D. Shah, Effect of premicellar aggregation on pK_a of fatty acid soap solutions, Langmuir 19 (2003) 2034-2038.

[13] E. Sjostrom, Wood Chemistry Fundamentals and applications, second ed., Academic Press, 1993.

[14] G. Uçar, D. Fengel, Variation in composition of extractives from wood of *Pinus nigra* varieties, Phytochemistry 38 (1995) 877-880.

[15] H. Hafizoglu, B. Holmbom, Chemical composition of extractives from *Abies nordmanniana*, Holz als Roh- und Werkstoff 53 (1995) 273-275.

[16] J. Zhang, Effect of dissolved salt, dissolved organic material and wood resin concentration on paper properties, M.Sc. Thesis, School of Chemistry Univeristy of Tasmania, Hobart, 2010.

[17] D. McLean, The effect of wood extractive composition on pitch deposition, M.Sc. Thesis, School of Chemistry, University of Tasmania, Hobart, 2003, 106.

[18] M. Blazey, S. Grimsley, G. Chen, Indicators for forecasting "pitch season", Tappi Journal 1 (2002) 28-30.

[19] A. Gutiérrez, J. del Río, F. González-Vila, J. Romero, Variation in the composition of wood extractives from Eucalyptus globulus during seasoning, Journal of Wood Chemistry and Technology 18 (1998) 439-446.

[20] E. Back, Chapter 6 - Resin in suspension and mechanisms of it's deposition, in: E.L. Back, L.H. Allen (Eds.), Pitch Control, Wood Resin and Deresination, TAPPI Press, Atlanta, 2000, 151-183.

[21] K. Stack, B. Yates, The use of molecular modelling in studying pitch deposition, Appita Journal 61 (2008) 203-208.

[22] V. Saarimaa, A. Sundberg, A. Pranovich, B. Holmbom, M. Svedman, F. Orsa,, Influence of pectic acids on aggregation and deposition of colloidal pitch., Nordic Pulp and Paper Research Journal 21 (2006) 613-619.

[23] D. McLean, K. Stack, D. Richardson, Wood pitch deposition versus composition, WPP 2003 Chemical Technology of Wood, Pulp and Paper International Conference, Bratislava, Slovak Republic, 2003, 115-120.

[24] L. Hlivka, K. Wai, Pitch control composition and process for inhibiting pitch deposition, in: A. Inc (Ed.), United States Patent, Ashland Inc, 1997.

[25] D. McLean, K. Stack, D. Richardson, Wood pitch deposition versus composition, 57th Appita Annual General Conference Proceedings, Melbourne, Australia, 2003, 203-210.

[26] A. Sundberg, A. Strand, L. Vahasalo, B. Holmbom, Phase distribution of resin and fatty acids in colloidal wood pitch emulsions at different pH-levels, Journal of Dispersion Science and Technology 30 (2009) 912-919.

[27] D. MacNeil, A. Sundberg, L. Vahasalo, B. Holmbom, Effect of calcium on the phase distribution of resin and fatty acids in pitch emulsions, Journal of Dispersion Science And Technology 32 (2011) 269-276.

[28] L. Ödberg, S. Forsberg, G. McBride, M. Persson, P. Stenius, G. Ström, Surfactant behavior of wood resin components. Part 2. Solubilization in micelles of rosin and fatty acids, Svensk Papperstidning 88 (1985) 118-125.

[29] H. Palonen, P. Stenius, G. Ström, Surfactant behavior of wood resin components. The solubility of rosin and fatty acid soaps in water and in salt solutions, Svensk Papperstidning 85 (1982) 93-99.

[30] D. Vercoe, K. Stack, A. Blackman, D. Richardson, A multi-component insight into the interactions leading to wood pitch deposition, 58th Appita Annual General Conference Proceedings, Canberra, Australia, 2004, 65-71.

[31] D. Vercoe, K. Stack, A. Blackman, D. Richardson, A study of the interactions leading to wood pitch deposition, 59th Appita Annual General Conference Proceedings, Appita, Auckland, New Zealand, 2005, 123-130.

[32] K. Stack, D. Vercoe, L. Maher, B. Yates, The use of molecular modelling to study pitch deposition and interactions with fixatives, First Applied Pulp and Paper Molecular Modelling Symposium (FAPPMMS), Montreal, Canada, 2005.

[33] M. Qin, T. Hannuksela, B. Holmbom, Deposition tendency of TMP resin and related model mixtures, Journal of Pulp and Paper Science 30 (2004) 279-283.

[34] M. Qin, B. Holmbom, Effect of hydrophilic substances in spruce TMP resin on its physio-chemical characterization and deposition tendency, Colloids and Surfaces A: Physiochemical and Engineering Aspects 312 (2008) 226-230.

[35] F. CamettiMariette, Investigations of food colloids by NMR and MRI, Current Opinion in Colloid and Interface Science 14 (2009) 203-211.

[36] M. Nydena, K. Holmberg, NMR for studying structure and dynamics in colloidal systems, Current Opinion in Colloid and Interface Science 14 (2009) 169-170.

[37] J. Kalus, U. Schmelzer, Small angle neutron (SANS) and x-ray (SAXS) scattering on micellar systems, Physica Scripta T49B (1993) 629-635.

[38] M. Ballauff, SAXS and SANS studies of polymer colloids, Current Opinion in Colloid and Interface Science 6 (2001) 132-139.

[39] S. Gandini, R. Itra, D. Neto, M. Tabak, Porphyrin effects on zwitterionic HPS micelles as investigated by small angle X-ray scattering (SAXS) and electron paramagnetic resonance (EPR), Journal of Physical Chemistry 109 (2005) 22264-22272.

[40] M. Ottaviani, N. Turro, S. Jockusch, D. Tomalia, Characterization of starburst dendrimers by EPR. 3. Aggregational processes of a positively charged nitroxide surfactant., Journal of Physical Chemistry 100 (1996) 13675-13686.

[41] S. Weber, T. Wolff, G. von Bunau, Molecular mobility in liquid and in frozen micellar solution: EPR spectroscopy of nitroxide free radicals, Journal of Colloid and Interface Science 184 (1996) 163-169.

[42] E. Gelamo, R. Itra, A. Alonsa, D. Silva. J, M. Tabak, Small- angle X-ray scattering and electron paramagnetic resonance study of the interaction of bovine serum albumin with ionic surfactants, Journal of Colloid and Interface Science 277 (2004) 471-482.

[43] P. Santiago, D. Neto, L. Barbosa, R. Itra, M. Tabak, Interaction of meso-tetrakis (4-sulfnatophenyl) porphyrin with cationic CTAC micelles investigated by small angle X-ray scattering (SAXS) and electron paramagnetic resonance (EPR), Journal of Colloid and Interface Science 316 (2007) 730-740.

[44] P. Marzola, C. Forte, C. Pinzino, C. Veracin, Activity and conformational changes of a-chymotrypsin in reverse micelles studies by spin labelling, Federation of European Biochemical Societies Letters 289 (1991) 29-32.

[45] B. Dejanovic, K. Mirosavljevic, V. Noethig-Laslo, S. Pecar, M. Sentjurc, P. Walde, An ESR characterisation of micelles and vesicles formed in aqueous decanoic acid/sodium

decanoate systems using different spin labels, Chemistry and Physics of Lipids 156 (2008) 17-25.

[46] V. Livshits, D. Marsh, Spin relaxation measurements using first-harmonic out-of-phase adsorption EPR signals: rotational motion effects, Journal of Magnetic Resonance 145 (2000) 84-94.

[47] T. Wines, P. Somasundaran, N. Turro, S. Jockusch, F. Ottaviani, Investigation of the mobility of amphiphilic polymer- AOT reverse microemulsion systems using electron spin resonance, Journal of Colloid and Interface Science 285 (2005) 318-325.

[48] K. Zielinska, K. Wilk, A. Jezierski, T. Jesionowski, Microstructure and structural transition in microemulsions stabilised by aldonamide-type surfactants, Journal of Colloid and Interface Science 321 (2008) 408-417.

[49] B. Bales, C. Stenland, The spin probe-sensed polarity of sodium dodecyl sulfate micelles is proportional to the one-fourth power of the surfactant concentration, Chemical Physics Letters 200 (1992) 475-482.

[50] K. Earle, D. Budil, J. Freed, Millimeter wave electron spin resonance using quasi-optical techniques, Advances in Magnetic and Optical Resonance.19 (1996) 253-323.

[51] H. Fukuda, A. Goto, H. Toshioka, R. Goto, K. Morigaki, P. Walde, Electron spin resonance study of the pH induced transformation of micelles to vesicles in an aqueous oleic acid/oleate system, Langmuir 17 (2001) 4223-4231.

[52] V. Livshits, T. Pali, D. Marsh, Relaxation time determinations by progressive saturation EPR: effects of molecular motion and Zeeman modulation for spin labels, Journal of Magnetic Resonance 133 (1998) 79-91.

[53] B. Robinson, C. Mailer, A. Reese, Linewidth analysis of spin labels in liquids, Journal of Magnetic Resonance 138 (1999) 199-201.

[54] R. Subramanian, Y. Huang, S. Zhu, A. Hrymak, R. Pelton, Electron spin resonance study and reactive extrusion of polyacrylamide and polydiallyldimethylammmonium chloride, Journal of Applied Polymer Science 77 (2000) 1154-1164.

[55] G. White, L. Ottignon, T. Georgiou, C. Kleanthous, G. Moore, A. Thomson, V. Oganesyan, Analysis of nitroxide spin label motion in a protein-protein complex using multiple frequency EPR spectroscopy, journal of Magnetic Resonance 185 (2007) 191-203.

[56] G. Arizaga, A. Mangrich, J. Gardolinski, F. Wypych, Chemical modification of zinc hydroxide nitrate and Zn-Al0 layered double hydroxide with dicarboxylic acids, Journal of Colloid and Interface Science 320 (2008) 168-176.

[57] J. Weil, J. Bolton, J. Wertz, Electron paramagnetic resonance : elementary theory and practical applications A Wiley-Interscience publication, New York 1994.

[58] F. Cotton, G. Wilkinson, P. Gaus, Basic inorganic chemistry. Wiley, New York 1995.

[59] N. Atherton, Principles of electron spin resonance, Simon & Schuster, Chichester, 1993.

[60] S. Sigurdsson, Nitroxides and nucleic acids: Chemistry and electron paramagnetic resonance (EPR) spectroscopy, Pure and Applied Chemistry. 83 (2011) 677-686.

[61] D. Shaw, Introduction to colloid and surface chemistry, 4th ed., Butterworth-Heinemann, Oxford, 1992.

[62] H. Reerink, J. Overbeek, The rate of coagulation as a measure of the stability of silver iodide sols, Discussions of Faraday Society (1954) 74-84.

[63] J. Gregory, Particles in water- properties and processes, Taylor and Francis, 2006.

[64] S. Behrens, D. Christl, R. Emmerzael, P. Schurtenberger, M. Borkovec, Charging and aggregation properties of carboxyl latex particles: experiments versus DLVO theory, Langmuir 16 (2000) 2566-2575.

[65] T. Missana, A. Adell, On the applicability of DLVO theory to the prediction of clay colloids stability, Journal of Colloid and Interface Science 230 (2000) 150-156.

[66] C. van Oss, R. Giesse, P. Costanzo, DLVO and non-DLVO interactions in Hectorite, Clays and Clay Minerals 38 (1990) 151-159.

[67] J. Mosbye, J. Laine, S. Moe, The effect of dissolved substances on the adsorption of colloidal extractives to fines in mechanical pulp, Nordic Pulp and Paper Research Journal 18 (2003) 63-68.

[68] A. Sihvonen, K. Sundberg, A. Sundberg, B. Holmbom, Stability and deposition tendency of colloidal wood resin, Nordic Pulp and Paper Research Journal 13 (1998) 64-67.

[69] K. Sundberg, C. Pettersson, C. Eckerman, B. Holmbom, Preparation and properties of a model dispersion of colloidal wood resin from Norway spruce, Journal of Pulp and Paper Science 22 (1996) 248-252.

[70] I. Johnsen, M. Lenes, L. Magnusson, Stabilisation of colloidal wood resin by dissolved material from TMP and DIP, Nordic Pulp and paper Research Journal 19 (2004) 22-28.

[71] P. Spicer, S. Pratsinis, M. Trennepohl, Coagulation and fragmentation: the variation of shear rate and the time lag for attainment of steady state, Industrial and Engineering Chemistry Research 35 (1996) 3074-3080.

[72] K. Kusters, J. Wijers, D. Thoenes, Aggregation kinetics of small particles in agitated vessels, Chemical Engineering Science 52 (1997) 107--121.

[73] L. Ehrl, M. Soos, M. Morbidelli, M.. Bäbler, Dependence of initial cluster aggregation kinetics on shear rate for particles of different sizes under turbulence, AIChE Journal 55 (2009) 3076-3087.

[74] T. Okubo, H. Kimura, T. Hatta, T. Kawai, Rheo-optical study of colloidal crystals, Physical Chemistry Chemical Physics 4 (2002) 2260-2263.

[75] S. Garcia-Garcia, M. Jonsson, S. Wold, Temperature effect on the stability of bentonite colloids in water, Journal Colloid and Interface Science 298 (2006) 694-705.

[76] D. Gardner, D. Gunnells, M. Wolcott, Temperature dependence of wood surface energy, Wood and Fibre Science 26 (1994) 447-455.

[77] L. Kang, J. Cleasby, Temperature effects on flocculation kinetics using Fe(III) Coagulant, Journal of Environmental Engineering 121 (1995) 893-901.

[78] T. Van de Ven, S. Mason, The microrheology of colloidal dispersions VII. Orthokinetic doublet formation of spheres, Colloid and Polymer Science 255 (1977) 468-479.

[79] M. Bäbler, A collision efficiency model for flow-induced coagulation of fractal aggregates, AIChE Journal 54 (2008) 1748.

[80] A. Olsen, G. Franks, S. Biggs, G. Jameson, An improved collision efficiency model for particle aggregation, Journal of Chemical Physics 125 (2006) 184906

[81] L. Claudotte, N. Rimbert, P. Gardin, M. Simonnet, J. Lehmann, B. Oesterlé, A multi-QMOM framework to describe multi-component agglomerates in liquid steel, AIChE Journal 56 (2010) 2347-2355.

[82] B. Balakin, A. Hoffmann, P. Kosinski, Population balance model for nucleation, growth, aggregation, and breakage of hydrate particles in turbulent flow, AIChE Journal 56 (2010) 2052-2062.

[83] L. Ehrl, M. Soos, H. Wu, M. Morbidelli, Effect of flow field heterogeneity in coagulators on aggregate size and structure, AIChE Journal 56 (2010) 2573-2587.

[84] D. Sato, M. Kobayashi, Y. Adachi, Capture efficiency and coagulation rate of polystyrene latex particles in a laminar shear flow: Effects of ionic strength and shear rate, Colloids and Surfaces A-Physicochemical and Engineering aspects 266 (2005) 150-154.

[85] J. Peula, R. Santos, J. Forcada, R. Hidalgo-Alvares, F. Nieves, Study on the colloidal stability Mechanisms of acetal-functionalized latexes, Langmuir 14 (1998) 6377-6384.

[86] E. Logtenberg, H. Stein, Coagulation in a shear field generated by stirring in a cylindrical vessel, Journal of Colloid and Interface Science 104 (1985) 258-268.

[87] M. Dishon, O. Zohar, U. Sivan, From Repulsion to attraction and back to repulsion: The effect of NaCl, KCl and CsCl on the Force between silica surfaces in aqueous solution, Langmuir 25 (2009).

[88] R. Hunter, Introduction to modern colloid science, 1st ed., Oxford University Press, Oxford, 1993.

[89] M. Bostrom, D. Williams, B. Ninham, Specific ion effects: Why DLVO theory fails for biology and colloids systems, Physical Review Letters 97 (2001).

[90] T. Zemb, L. Belloni, M. Dubbois, A. Aroti, E. Leontidis, Can we use area per surfantant as a quantitative test model of specific ion effects?, Current Opinion in Colloid and Interface Science 9 (2004) 74-80.

[91] J. Gregory, Chapter 4- Colloid interactions and colloid stability, in: C. Press (Ed.), Particles in Water- Properties and processes Taylor and Francis, 2006, pp. 63-92.

[92] E. Back, The mechanism of pulp resin accumulation at solid surfaces, Svensk Papperstidning 63 (1960) 556-564.

[93] M. Hubbe, O. Rojas, R. Venditti, Control of tacky deposits on paper machines- a review, Nordic Pulp and Paper Research Journal 21 (2006) 154-171.

[94] J. Kekkonen, A. Laukkanen, P. Stenius, H. Tenhu, Adsorption of polymeric additives and their effect on the deposition of wood materials in paper production, Colloids and Surfaces a-Physicochemical and Engineering Aspects 190 (2001) 305-318.

[95] K. Sundberg, J. Thornton, B. Holmbom, R. Ekman, Effects of wood polysaccharides on the stability of colloidal wood resin, Journal of Pulp and Paper Science 22 (1996) J226-J230.

[96] M. Palm, G. Zacchi, Extraction of hemicellulosic oligosaccharides from spruce using microwave oven or steam treatment, Biomacromolecules 4 (2003) 617-623.

[97] P. Bevington, Chapter Eleven. Least-squares fit to an arbitrary function, Data reduction and error analysis for the physical sciences, McGraw-Hill Book Company, New York, 1969, 204-246.

[98] A. Sundberg, K. Sundberg, C. Lillandt, B. Holmbom, Determination of hemicelluloses and pectins in wood and pulp fibres by acid methanolysis and gas chromatography, Nordic Pulp and Paper Research Journal 11 (1996) 216-220.

[99] D. Brasch, The chemistry of *pinus radiata* VI. The water-soluble galactoglucomannan, Australian Journal of Chemistry 36 (1983) 947-954.

[100] D. Brasch, A. Wilkins, Applications of 13C nuclear magnetic resonance spectroscopy to the structure of wood-derived polysaccharides, Appita Journal 38 (1985) 353-358.

[101] D. Fengel, G. Wegener, Wood: Chemistry, ultrastructure, reactions, Walter de Gruyter & Co., Berlin, 1984.

[102] A. McDonald, A. Clare, Chemical characterisation of the neutral water soluble components from radiata pine high temperature TMP fibre, Proceedings of 53rd APPITA Annual General Conference, Roturua NZ, 1999, 641-647.

[103] A. McDonald, J. Gifford, P. Dare, D. Steward, Characterisation of the condensate generated from vacuum-drying of radiata pine wood, Holz Als Roh-Und Werkstoff 57 (1999) 251-258.

[104] T. Hannuksela, C. Herve du Penhoat, NMR structural determination of dissolved O-acetylated galactoglucomannan isolated from spruce thermomechanical pulp, Carbohydrate Research 339 (2003) 301-312.

[105] D. Otero, K. Sundberg, A. Blanco, C. Negro, J. Tijero, B. Holmbom, Effects of wood polysaccharides on pitch deposition, Nordic Pulp and Paper Research Journal 15 (2000) 607-613.

[106] T. Hannuksela, B. Holmbom, Stabilization of wood-resin emulsions by dissolved galactoglucomannans and galactomannans, Journal of Pulp and Paper Science 30 (2004) 159-164.

[107] A. Pranovich, K. Sundberg, B. Holmbom, Chemical changes in thermomechanical pulp at alkaline conditions, Journal of Wood Chemistry and Technology 23 (2003) 87-110.

[108] J. Thornton, R. Ekman, B. Holmbom, C. Pettersson, Effects of alkaline treatment on dissolved carbohydrates in suspensions of Norway spruce thermomechanical pulp, Journal of Wood Chemistry and Technology 14 (1994) 177-194.

[109] J. Thornton, C. Eckerman, R. Ekman, Effects of peroxide bleaching of spruce TMP on dissolved and colloidal organic substances, 6th International Symposium of. Wood Pulping Chemistry 1991, 571-577.

[110] A. Zouboulis, G. Traskas, Comparable evaluation of various commercially available aluminium-based coagulants for the treatment of surface water and for the post-treatment of urban wastewater, Journal of Chemical Technology and Biotechnology 80 (2005) 1136-1147.

[111] M. Burgess, J. Curley, N. Wiseman, H. Xiao, On-line optical determination of floc size. Part 1: Principles and Techniques, Journal Pulp and Paper Science 28 (2002) 63-65.

[112] H. Xiao, N. Cezar, Organo-modified cationic silica nanoparticles/anionic polymer as flocculants, Journal of Colloid and Interface Science 267 (2003) 343-351.

[113] C. Hopkins, J. Ducoste, Characterising flocculation under heterogeneous turbulence, Journal of Colloid and Interface Science 264 (2003) 184-194.

[114] H. Ching, T. Tanaka, M. Elimelech, Dynamics of coagulation of kaolin particles with ferric chloride, Water Resource 28 (1994) 559-569.

[115] A. Poraj-Kozminski, R. Hill, T. Van de Ven, Flocculation of starch-coated solidified emulsion droplets and calcium carbonate particles, Journal of Colloid and Interface Science 309 (2007) 99-105.

[116] R. Fernandes, G. Gonzalez, E. Lucas, Evaluation of polymeric flocculants for oily water systems using a Photometric dispersion analyser, Colloid and Polymer Science 283 (2004) 219-224.

[117] M. Burgess, J. Curley, N. Wiseman, H. Xiao, On-line optical determination of floc size. Part 2: The effect of shear on floc size, Journal of Pulp and Paper Science 28 (2002) 323-326.

[118] F. Mietta, C. Chassagne, J. Winterwerp, Shear-induced flocculation of a suspension of kaolinite as function of pH and salt concentration, Journal of Colloid and Interface Science 336 (2009) 134-141.

[119] J. Tripathy, D. Misha, K. Behari, Graft copolymerisation of N-vinylformamide onto sodium carboxymethylcellulose and study of its swelling, metal ion sorption and flocculation behaviour, Carbohydrate Polymers 75 (2009) 604-611.

[120] D. Lehner, G. Kellner, H. Schnablegger, O. Glatter, Static light scattering on dense colloidal systems: New instrumentation and experimental results, Journal of Colloid and Interface Science 201 (1998) 34-47.

[121] S. Clarke, R. Ottewill, A. Renniw, Light scattering studies of dispersions under shear, Advances in Colloid and Interface Science 60 (1995) 95-118.

[122] D. Vleeschauwer, P. Van der Meeren, A dynamic light scattering study of the influence of the phospholipid concentration in a model perfluorocarbon emulsion, Colloids and Surfaces B: Biointerfaces 11 (1998) 321-329.

[123] F. Muller, Measurement of electrokinetic and size characteristics of estuarine colloids by dynamic light scattering spectroscopy, Analytica Chimica Acta 331 (1996) 1-15.

[124] J. Poznanski, J. Szymanski, T. Basinska, S. Slomkowski, W. Zielenkiewicz, Aggregation of aqueous lysozyme solutions followed by dynamic light scattering and 1H NMR spectroscopy, Journal of Molecular Liquids 121 (2005) 21-26.

[125] E. Sutherland, S. Mercer, M. Everist, D. Leaist, Diffusion in solutions of micelles. What does dynamic light scattering measure?, J.Chem. Eng.Data 54 (2009) 272-278.

[126] N. Tanaka, K. Nakagawa, H. Nagayama, K. Hosoya, T. Ikegami, A. Itaya, M. Shibayama, Effects of electrokinetic chromatography conditions on the structure and properties of polyallylamine-supported pseudo-stationary phase. A study by dynamic light scattering, Journal of Chromatography A 836 (1999) 295-303.

[127] J. Alfano, P. Carter, J. Whitten, Use of scanning laser microscopy to investigate microparticle flocculation performance, Journal of Pulp and Paper Science 25 (1999) 189-195.

[128] J. Alfano, P. Carter, A. Gerli, Characterisation of the flocculation dynamics in a papermaking system by non-imaging reflectance scanning microscopy (SLM), Nordic Pulp and Paper Research Journal 13 (1998) 159-165.

[129] C. Lumpe, L. Joore, K. Homburg, E. Verstraeten, Focused beam reflectance measurement (FBRM) a promising tool for wet-end optimisation and web break prediction, Paper technology (2001) 39-44.

[130] L. Wagberg, A device for measuring the kinetics of flocculation following polymer addition in turbulent flow suspensions., Sven. Papperstidn. 88 (1985) 48-56.

[131] B. Miller, R. Lines, Recent advances in particle size measurements: a critical review, CRC Critical Reviews in Analytical Chemistry 20 (1988) 75-116.

[132] M. Grubb, H. Wray, D. Richardson, The use of flow cytometry for managing extractives associated with pitch deposits, 63rd Appita Annual General Conference, Melbourne, 2009, 347-352.

[133] L. Vahasalo, R. Degerth, B. Holmbom, The use of flow cytometry in wet end research, Paper Technology 44 (2003) 45-49.

[134] R. Mathews, A. Donald, Conditions for imaging emulsions in the environmental scanning electron microscope, Scanning 24 (2002) 75-85.

[135] T. Sakai, K. Kamogawa, F. Harusawa, N. Momozawa, H. Sakai, M. Abe, Direct observation of flocculation/coalescence of metastable oil droplets in surfactant-free oil/water emulsion by freeze-fracture electron microscopy, Langmuir 17 (2001) 255-259.

[136] D. Wedlock, I. Fabris, J. Grimsey, Sedimentation in polydisperse particulate suspensions. Colloids and Surfaces A: Physicochemical and Engineering Aspects 43 (1990) 67-81.

[137] L. Allen, P. Sennett, C. Lapointe, R. Truitt, B. Sithole, Pitch deposition in newsprint mills using certain kaolin pigments, TAPPI Journal 81 (1998) 137-138.

[138] L. Allen, B. Sitholé, C. Lapointe, R. Truitt, Press Roll pitch deposition problems associated with the use of certain clay products in newsprint manufacture, 82nd Annual Meeting, Technical Section, Canadian Pulp and Paper Association, 1996, 135-138.

[139] Z. Adamczyk, B. Siwek, L. Szyk, M. Zembala, Adsorption of colloid particles affected by hydrodynamic-forces, Bulletin of the Polish Academy of Sciences-Chemistry 41 (1993) 41.

[140] T. van de Ven, The capture of colloidal particles on surfaces and in porous material: basic principles, Colloids and surfaces. A, Physicochemical and engineering aspects 138 (1998) 207.

[141] D. McLean, K. Stack, D. Richardson, Evaluation of cationic polymers to control pitch deposition, Appita Journal 63 (2010) 199-205.

[142] D. Vercoe, K. Stack, A. Blackman, D. Richardson, A multicomponent insight into the interactions leading to wood pitch deposition, Appita Journal 58 (2005) 208-213.

[143] L. Maher, K. Stack, D. McLean, D. Richardson, Adsorption behaviour of cationic fixatives and their effect on pitch deposition, Appita Journal 60 (2007) 112-119, 128.

[144] L. Vähäsalo, B. Holmbom, Factors affecting white pitch deposition, Nordic Pulp and Paper Research Journal 20 (2005) 164168.

[145] Z. Dai, Y. Ni, Thermal stability of metal-pitch deposits from a spruce thermomechanical pulp by use of a differential scanning calorimeter, Bioresources 5 (2010) 1923-1035.

[146] K. Stack, E. Stevens, D. Richardson, T. Parsons, S. Jenkins, Factors affecting the deposition of pitch in process waters and model dispersions, 52nd Appita Annual General Conference Proceedings, Brisbane, Australia, 1998, 59-66.

[147] I. Johnsen, The impact of dissolved hemicellulose on adsorption of wood resin to TMP fines, PhD Thesis, Department of Chemical Engineering, Norwegian University of Science and Technology, Trondheim, 2007, 53.

[148] F. Bertaud, A. Sundberg, B. Holmbom, Evaluation of acid methanolysis for analysis of wood hemicelluloses and pectins, Carbohydrate Polymers 48 (2002) 319-324.

[149] Measurement of soluble carbohydrates- Orcinol method, in: N. Skog (Ed.), Norske Skog Research, 2005.

[150] A. Gerli, B. Keiser, M. Strand, The use of a flocculation sensor as a predictive tool for paper machine retention program performance, Tappi Journal (2000).

[151] B. Bales, C. Stenland, The spin probe-sensed polarity of sodium dodecyl sulfate micelles is proportional to the one-fourth power of the surfactant concentration Chemical Physics Letters 200 (1992) 475-482

[152] S. Futamura, Z. Zong, Photobromination of side-chain methyl groups on arenes with N-bromosuccinimide –Convenient and selective syntheses of bis(bromomethyl)- and (bromomethyl)methylarenes–, Bulletin of the Chemical Society of Japan 65 (1992) 345-348.

[153] J. Barluenga, L. Alonso-Cires, G. Asensio, Mercury(II) oxide/tetrafluoroboric acid - A new reagent in organic synthesis; A convenient diamination of olefins synthesis 1979 (1979) 962-964.

[154] J. Barluenga, F. Ortiz, F. Palacios, V. Gotor, Reactions of ketimines and ethyl phenylpropiolate. Synthesis of 4-oxodihydropyridines, Synthetic Communications 13 (1983) 411 - 417.

[155] K. Earle, D. Budil, J. Freed, Millimeter wave electron spin resonance using quasioptical techniques Advances in Magnetic and Optical Resonance 19 (1996) 253-323.

[156] D. Young, Chapter 35 Mesoscale Methods, Computational chemistry: a practical guide for applying techniques to real world problems, John Wiley & Sons, Inc., New York, 2001, 273-276.

[157] B. Doiron, Chapter 8 Retention Aid Systems, in: J. Gess (Ed.), Retention of fines and fillers during papermaking, TAPPI Press, Atlanta, 1998, 159-176.

[158] M. Blomquist, Fast and convenient methods for characterization of pitch deposits and pitch deposition tendency, PhD Thesis, Åbo Akademi University, 2003, 1-13.

[159] M. Pregetter, R. Prassel, B. Schuster, M. Kriechbaum, F. Nigon, J. Chapman, P. Laggner, Microphase separation in low density lipoproteins, Journal of Biological Chemistry 274 (1999) 1334-1341.

[160] J. Chen, N. Jayaraj, S. Jockusch, F. Ottaviani, V. Ramamurthy, N. Turro, An EPR and NMR study of supramolecular effects on paramagnetic interaction between a nitroxide incarcerated within a nanocapsule with a nitroxide in bulk aqueous media, Journal of the American Chemical Society 130 (2008) 7206-7207.

[161] A. Fan, N. Turro, P. Somasundaran, A study of dual polymer flocculation, Colloids and Surfaces A: Physiochemical and Engineering aspects 162 (2000) 141-148.

[162] V. Livshits, B. Dzikovski, D. Marsh, Anisotropic motion effects in CW non-linear EPR spectra: relaxation enhancement of lipid spin labels, Journal of Magnetic Resonance 162 (2003) 429-442.

[163] M. Ottaviani, E. Cossu, N. Turro and D. Tomalia, Characterization of starburst dendrimers by EPR. 2. positively charged nitroxide radicals of variable chain length used as spin probes, Journal of American Chemical society 117 (1995), 4387–4398.

[164] A. Swerin, L. Ödberg, L. Wågberg, Preparation and some properties of the colloidal pitch fraction from a thermomechanical pulp, Nordic Pulp and Paper Research Journal 3 (1993) 298-301, 337.

[165] J. Weil, J. Bolton, J. Wertz, Electron paramagnetic resonance: elementary theory and practical applications Wiley-Interscience, NewYork, 1994.

[166] M. Ottaviani, N. Turro, S. Jockusch, D. Tomalia, Characterization of starburst dendrimers by EPR. 3. Aggregational processes of a positively charged nitroxide surfactant, Journal of Physical Chemistry 100 (1996) 13675-13686.

[167] M. Porel, M. Ottaviani, S. Jockusch, N. Jayaraj, N. Turro, V. Ramamurthy, Suppression of spin–spin coupling in nitroxyl biradicals by supramolecular host–guest interactions, Chemical Communications 46 (2010) 7736-7738.

[168] T. Ahn, C. Yun, Phase separation in phosphatidylcholine/anionic phospholipid membranes in the liquid-crystalline state revealed with fluorescent probes, Journal of Biochemistry 124 (1998) 622-627.

[169] G. Longo, M. Schick, I. Szleifer, Stability and liquid-liquid phase separation in mixed saturated lipid bilayers, Biophysics Journal 96 (2009) 3977-3986.

[170] E. Shimshick, H. McConnell, Lateral phase separation in phospholipid membranes, Biochemistry 12 (1973) 2351-2360.

[171] T. Zhu, K. Kuys, I. Parker, N. Vanderhoek, Studies on the surface charge of eucalypt pulps by potentiometric titration, 8th International. Symposium in Wood and Pulping Chemistry, 1995, 243-248.

[172] K. Kuys, Surface chemistry of high yield pulps from *Eucalyptus* species and *Pinus radiata*, 6th International Symposia in Wood and Pulping Chemistry, Melbourne, Australia, 1991, 85-91.

[173] T. Herrington, B. Midmore, Adsorption of ions at the cellulose/aquiouse electrolyte interface. Part 3 - Calculation of the potential at the surface of cellulose fibres, Journal of the Chemical Society, Faraday Transactions 80 (1983) 1553-1566.

[174] D. Gantenbein, J. Schoelkopf, P. Gane, P. Matthews, Influence of pH on the adsorption of dissolved and colloidal substances in a thermo-mechanical pulp filtrate onto talc, Nordic Pulp and Paper Research Journal 25 (2010) 288.

[175] M. Bostrom, V. Deniz, G. Franks, B. Ninham, Extended DLVO theory: Electrostatic and non-electrostatic force in oxide suspensions, Advances in Colloids and Interface Science 123-126 (2006) 5-15.

[176] L. Hanus, R. Hartzler, N. Wagner, Electrolyte-induced aggregation of acrylic latex. 1. Dilute particle concentrations, Langmuir 17 (2001) 3136-3147.

[177] Rank Brothers Ltd, Photometric Dispersion Analyser PDA2000 Operating Manual, 2002.

[178] B. Pacewska, M. Keshr, O. Kluk1, Influence of aluminium precursor on physico-chemical properties of aluminium hydroxides and oxides Part I. $AlCl_3 \times 6H_2O$, Journal of Thermal Analysis and Calorimetry 86 (2006) 351-359.

[179] B. Pacewska, O. Kluk-Płoskońska, D. Szychowski, Influence of aluminium precursor on physico-chemical properties of aluminium hydroxides and oxides Part II. $Al(ClO_4)_3 \cdot 9H_2O$ Journal of Thermal Analysis and Calorimetry 86 (2006) 751-760.

[180] W. Stumm, J. Morgan, Aquatic Chemistry, 3rd Ed ed., Wiley Interscience, 1996.

[181] S. Manahan, Environmental Chemistry, 6th Ed ed., Lewis Publishers 1994.

[182] E. Matijevic, K. Mathai, R. Ottewill, M. Kerker, Detection of metal ion hydrolysis by coagulation. III. Aluminum, Journal of Physical Chemistry 65 (1961) 826-830.

[183] J. Gregory, Particles in water- properties and processes, Taylor and Francis, 2006.

[184] G. Gavelin, The effect of mill water on pitch troubles in paper mills, Pulp and Paper Magazine of Canada (1949) 59-64.

[185] J. Molina-Bolívar, J. Ortega-Vinuesa, How proteins stabilize colloidal particles by means of hydration forces, Langmuir 15 (1999) 2644-2653.

[186] R. Corkery, Artificial biomineralisation and metallic soaps, Applied Mathematics Department, PhD Thesis,Australian National University, Canberra, 1998, 401.

[187] Y. Liu, J. Shang, G. Xue, H. Hu, F. Fu, J. Wang, A Dimeric Fe(III)-substituted a-keggin tungstogermanate: $\{[a\text{-}GeFe_2W_{10}O_{38}(OH)]_2\}_{14}$), Journal of Cluster Science 18 (2007) 205.

[188] I. Johnsen, P. Stenius, Effects of selective wood resin adsorption on paper properties, Nordic Pulp and Paper Research Journal 22 (2007) 452-461.

[189] F. Klingstedt, The chemical causes of resin difficulties, Canadian Pulp and Paper Association 8 (1938) 7-9.

[190] A. Korpela, Removal of resin from mechanical pulps by selective flotation: mechanisms of resin flotation and yield loss of fibres, Journal of Wood Chemistry and Technology 26 (2006) 175-186.

[191] J. Lloyd, N. Deacon, C. Horne, The influence of pulping and washing conditions on the resin content of radiata pine mechanical pulps, Appita Journal 43 (1990) 429-434.

[192] W. Mohn, V. Martin, Z. Yu, Biochemistry and ecology of resin acid biodegradation in pulp and paper mill effluent treatment systems, Water Science and Technology 40 (1999) 273-280.

[193] J. Mosbye, Colloidal wood resin: analyses and interactions, PhD Thesis, Department of Chemical Engineering, NTNU Trondheim Norwegian University of Science and Technology, Trondheim, 2003, 65.

[194] M. Hubbe, O. Rojas, Colloidal stability and aggregation of lignocellulosic materials in aqueous suspension: a review, Bioresources 3 (2008) 1419-1491.

[195] J. Nylund, O. Lagus, C. Eckerman, Character and stability of colloidal substances in a mechanical pulp suspension, Colloids and Surfaces a-Physicochemical and Engineering Aspects 85 (1994) 81-87.

[196] H. Yotsumoto, R. Yoon, Application of extended DLVO Theory 1. Stability of rutile suspensions, Journal of Colloid and Interface Science 157 (1993) 426-433.

[197] H. Yotsumoto, R. Yoon, Application of extended DLVO Theory II. Stability of silica Suspensions, Journal of Colloid and Interface Science 157 (1993) 434-441.

[198] F. Xiao, J. Ma, P. Yi, J. Huang, Effects of low temperature on coagulation of kaolinite suspensions, Water Research 42 (2008) 2983-2992.

[199] T. Van de Ven, S. Mason, The microrheology of colloidal dispersions IV. Pairs of interacting spheres in shear flow Journal of Colloid and Interface Science 57 (1976) 505-516.

[200] S. Agarwal, Efficiency of shear-induced agglomeration of particulate suspensions subjected to bridging flocculation, M.Sc. Thesis, Department of Chemical Engineering, West Virginia University, Morgantown, 2002, 150.

[201] D. Kumar, The effect of pressure and temperature on aluminium hydrolysis: Implications to trace metal scavenging in natural waters, Indian Journal of Marine Sciences 28 (1999) 1-4.

[202] D. Macdonald, P. Butler, D. Owen, Hydrothermal hydrolysis of AI3+ and the precipitation of boehmite from aqueouse solution, The Journal of Physical Chemistry 77 (1973) 2474-2479.

[203] P. Tam Doo, R. Kerekes, R. Pelton, Estimates of maximum hydrodynamic shear stresses on fibre surfaces in papermaking, Journal of Pulp and Paper Science 10 (1984) J80-J88.

[204] X. Jia, J. McLaughlin, K. Kontomaris, Lattice Boltzmann simulations of drop coalescence and chemical mixing, Physica A 362 (2006) 62-67.

[205] P. Li, J. Xu, Q. Wang, C. Wu, Surface functionalization of polymer latex particles: 4. Tailor-making of aldehyde-functional poly(methylstyrene) latexes in an emulsifier-free system, Langmuir 16 (2000) 4141-4147.

[206] A. Curtis, L. Hocking, Collision efficiency of equal spherical particles in a shear flow. The influence of London-van der Waals forces, Transactions of the Faraday Society 66 (1970) 1381-1390.

[207] B. Pacewska, M. Keshr, O. Klukl, Influence of aluminium precursor on physico-chemical properties of aluminium hydroxides and oxides Part 1. $AlCl_3.6H_20$, J. Thermal Analysis and Calorimetry 86 (2006) 351-359.

[208] B. Pacewska, O. Kluk-Ploskonska, D. Szychowski, Influence of alumnium precursor on physico-chemical properties of aluminium hydroxides and oxides Part II. $Al(ClO_4)_3$, $9H_20$, Journal of Thermal Analysis and Calorimetry 86 (2006) 751-760.

[209] R. Lee, K. Stack, T. Lewis, G. Garnier, D. Richardson, T. Van de Van, Measurement of pitch deposition by impinging jet microscopy: Effect of divalent salts, in: 64th Appita Annual General Conference, Appita, Melbourne, 2010, 273-279.

[210] P. Capek, J. Alfoldi, D. Liskova, An acetylated galactoglucomannan from Picea abies L. Karst, Carbohydrate Research 337 (2002) 1033-1037.

[211] T. Hannuksela, P. Fardim, B. Holmbom, Sorption of spruce O-acetylated galactoglucomannans onto different pulp fibres, Cellulose 10 (2003) 317-324.

[212] T. Hannusksela, B. Holmbom, G. Mortha, D. Lachenal, Effect of sorbed galactoglucomannans and galactomannans on pulp and paper handsheet properties, especially strength properties, Nordic Pulp and Paper Research Journal 19 (2004) 237-244.

[213] S. Willför, P. Rehn, A. Sundberg, K. Sundberg, B. Holmbom, Recovery of water-soluble acetylgalactoglucomannans from mechanical pulp of spruce, Tappi Journal 2 (2003) 27-32.

[214] E. Pelssers, M. Stuart, G. Fleer, Kinetic aspects of polymer bridging: Equilibrium flocculation and nonequilibrium flocculation, Colloids and Surfaces A-Physiochemical and Engineering Aspects 38 (1989) 15-25.

[215] T. Tripattharanan, M. Hubbe, J. Heitmann, R. Venditti, Effect of idealised flow conditions on retention aid performance. Part 2: polymer bridging, charged patches, and charge neutralisation, Appita Journal 57 (2004) 448-454.

[216] J. Thwala, J. Goodwin, P. Mills, Dispersion properties of silica particles in nonaqueous media with a non-ionic surfactant, dodecyl hexaethylene glycol monoether, $C_{12}E_6$ Colloids and Surfaces A-Physiochemical and Engineering Aspects 331 (2008) 162-174.

[217] T. Smith-Palmer, R. Pelton, Flocculation of particles, Encyclopedia of Surface and Colloid Science 1 (2006) 2584-2599.

[218] P. Somasundaran, V. Runkana, P.C. Kapur, Flocculation and dispersion of colloidal suspensions by polymers and surfactants: Experimental and modeling studies, in: Stechemesser, Dobias (Eds.), Coagulation and flocculation Taylor & Francis Group, 2005, 767-803.

[219] T. Tammelin, I. Johnsen, M. Osterberg, P. Stenius, J. Laine, Adsorption of colloidal extractives and dissolved hemicelluloses on thermomechanical pulp fiber components studied by QCM-D, Nordic Pulp and Paper Research Journal 22 (2007) 93-101.

[220] F. Örså, B. Holmbom, A convenient method for the determination of wood extractives in papermaking process waters and effluents, Journal of Pulp & Paper Science 20 (1994) 361-365.

[221] J. Thornton, R. Ekman, B. Holmbom, F. Örså, Polysaccharides dissolved from Norway spruce in thermomechanical pulping and peroxide bleaching, Journal of Wood Chemistry and Technology 14 (1994) 159-175.

[222] F. Örså, B. Holmbom, J. Thornton, Dissolution and dispersion of Spruce wood components into hot water, 8th International Symposium on Wood and Pulping Chemistry, Helsinki Finland, 1995, 613-620.

[223] F. Orså, B. Holmbom, J. Thornton, Dissolution and dispersion of spruce wood components into hot water, Wood Science and Technology 31 (1997) 279-290.

[224] B. Thiele, J. Kopp, Charge balances of paper machine systems - a method of process optimisation, 12th PTS Symposium Chemische Technologie der Papierherstellung, Munich, 1996, 19.

[225] S. Willfor, R. Sjoholm, C. Laine, M. Roslund, J. Hemming, B. Holmbom, Characterisation of water-soluble galactoglucomannans from Norway spruce wood and thermomechanical pulp, Carbohydrate Polymers 52 (2003) 175-187.

[226] J. Lundqvist, A. Teleman, L. Junel, G. Zacchi, O. Dahlman, F. Tjerneld, H. Stalbrand, Isolation and characterisation of galactoglucomannan from spruce (*picea abies*), Carbohydrate Polymers 48 (2002) 29-30.

[227] A. Teleman, M. Tenkanen, A. Jacobs, O. Dahlman, Characterisation of O-acetyl-(4-o-methylglucurono)xylan isolated from birch and beech, Carbohydrate Research 337 (2002) 373-377.

[228] W. Banks, C. Greenwood, Hydrodynamic properties and dimensions of linear potato amylose molecules in dilute aqueous salt solution Die Makromolekulare Chemie 67 (2003) 49 - 63.

[229] D. Lavalette, C. Tétreau, M. Tourbez, Y. Blouquit, Microscopic viscosity and rotational diffusion of proteins in a macromolecular environment., Biophysics Journal 76 (1999) 2744-2751.

[230] M. Gittings, L. Cipelletti, V. Trappe, D. Weitz, M. In, J. Lal, The effect of solvent and ions on the structure and rheological properties of guar solutions, Journal of Physical Chemistry 105 (2001) 9310-9315.

[231] R. Sartori, L. Sepulveda, F. Quina, E. Lissi, E. Abuin, Binding of electrolytes to poly(ethylene oxide) in aqueous solutions, Macromolecules 23 17 (1990) 3878-3881.

[232] M. Nagasawa, A. Holtzer, The helix-coil transition in solutions of polyglutamic acid, Journal of the American Chemical Society 86 (1964) 538-543.

[233] A. Güner, Properties of aqueous salt solutions of polyvinylpyrrolidone. I. Viscosity characteristics, Journal of Applied Polymer Science 62 (1998) 785 - 788.

[234] Y. Qi, A. Hoadley, A. Chaffee, G. Garnier, Characterisation of lignite as an industrial adsorbent, Fuel 90 (2011) 1567-1574.

[235] G. Halsey, Physical adsorption on non-uniform surfaces, Journal of Chemical Physics 16 (1948) 931-937.

[236] W. Kratschmer J. Rathousky A. Zukal, Adsorption of krypton at 77K on fullerene C60, graphitized carbon black and diamond, Carbon 37 (1999) 301-305.

[237] M. Einarson, J. Berg, Electrosteric stabilsation of colloidal Latex dispersions, Journal of Colloid and Interface Science 155 (1993) 165-172.

[238] M. Polverari, T. Van de Ven, Electrostatic and steric interactions in particle deposition studied by evanescent wave light scattering, Journal of Colloid and Interface Science 173 (1995) 343-353.

[239] B. Sitholé, T. Thu Ngoc, L. Allen, Quantitative determination of aluminum soaps in pitch deposits, Nordic Pulp and Paper Research Journal 11 (1996) 64-69.

[240] L. Allen, The importance of pH in controlling metal-soap deposition, Tappi Journal 71 (1988) 61-64.

[241] D. Beneventi, B. Carre, A. Gandini, Precipitation and solubility of calcium soaps in basic aqueous media, Journal of Colloid and Interface Science 237 (2001) 142-144.

[242] M. Rutland, R. Pugh, Calcium soaps in flotation deinking; fundamental studies using surface force and coagulation techniques, Colloids and Surfaces A: Physiochemical and Engineering aspects 125 (1997) 33-46.

[243] M. Douek, L. Allen, A laboratory test for measuring calcium soap deposition from solutions of tall oil, Tappi Journal (1983) 105-106.

[244] P. Harwot, T. Van de Ven, Effects of sodium oleate and calcium chloride on the deposition of latex particles on an air/water interface, Colloids and Surfaces A: Physiochemical and Engineering aspects 121 (1997) 229-237.

[245] T. Van de Ven, S. Kelemena, Characterizing polymers with an impinging jet, Journal of Colloid and Interface Science 181 (1996) 118-123.

[246] Z. Xia , T. Van de Ven, Adhesion kinetics of phosphatidylcholine liposomes by evanescent wave light scattering, Langmuir 8 (1992) 2938-2946.

[247] M. Kamiti, T. Van de Ven, Kinetics of deposition of calcium carbonate particles onto pulp fibres, Journal Pulp and Paper Science 20 (1994) 199-205.

[248] T. Van de Ven, S. Kelemena, Characterizing polymers with an impinging jet, Journal of Colloid and Interface Science 181 (1996) 118-123.

[249] Z. Xia, Adhesion kinetics of phosphatidylcholine liposomes by evanescent wave light scattering, Langmuir 8 (1992) 2938-2946.

[250] C. Yang, A visualizing method for study of micron bubble attachment onto a solid surface under varying physicochemical conditions, Industrial and Engineering Chemistry Research 39 (2000) 4949.

[251] M. Audry, A. Piednoir, P. Joseph, E. Charlaix, Amplification of electro-osmotic flows by wall slippage: direct measurements on OTS-surfaces, Faraday Discussions 146 (2010) 113-124.

[252] J. Nylund, A. Sundberg, K. Sundberg Dissolved and colloidal substances from a mechanical pulp suspension—Interactions influencing the sterical stability, Colloids and Surfaces A: Physicochemical and Engineering Aspects**, 301 (**2007) 335–340.

[253] T. Kallio, J. Lindfors, J. Laine, P. Stenius, Spreading and adhesion of lipophilic extractives on surfaces in paper machines, Nordic Pulp and Paper Research Journal 23 (2008) 108-119.

[254] T. Kallio,Interfacial interactions and fouling in paper machines, PhD Thesis, Laboratory of Forest Products Chemistry, Helsinki University of Technology, Helsinki, 2007.

[255] T. Kallio, J. Kekkonen, Fouling in the paper machine wet end, Tappi Journal 4 (2005) 20-24.

[256] J. Koberstein, Molecular design of functional polymer surfaces, Journal of Polymer Science: Part B: Polymer Physics 42 (2004) 2942-2956.

APPENDIX 1

Symbols relevant to equations.

Symbol	Meaning	Equation
V	interaction potential	1, 6
V_A	van der Waals attractive forces	1, 2, 6, 7
V_R	electrostatic repulsion	1, 3, 6, 7, 18
C_R	contribution of electric double-layer repulsion	21, 22
C_A	van der Waals attraction	21, 23
A	Hamaker constant	2, 6, 8, 9, 10, 23
z	Charge of the counter-ion	3, 4, 5, 6, 8, 9, 10, 11, 12
T	Temperature in Kelvin	3, 4, 5, 6, 8, 9, 10, 15, 18, 24
a	radius of the colloidal spheres	2, 3, 6, 8, 14, 19, 20, 22, 23, 24
d	diameter of the particle,	18.5
ε	permeability of the dispersion medium	3, 5, 6, 8, 9, 10, 22
k_B	Boltzmann constant	3, 4, 5, 6, 8, 9, 10, 15, 18, 24
e	charge on an electron	3, 4, 5, 6, 8, 9, 10
H	shortest distance between the Stern layer of two particles	2, 3, 6, 7, 22
γ	$\gamma = \frac{\exp[ze\Psi_d / 2k_BT] - 1}{\exp[ze\Psi_d / 2k_BT] + 1}$	3, 4, 6, 8, 9, 10
κ	$\kappa = \left(\frac{2e^2 N_A c z^2}{\varepsilon k_B T} \right)^{1/2}$	3, 5, 6, 7, 8, 22, 24
c	electrolyte concentration	5, 25
N_A	Avogadro's number	5, 10

Ψ_d	Stern potential	4, 12
Ψ_o	surface potential	22
k_2 and k_1	second order kinetic constant	13
k*	rate of fastest coagulation	15, 17
k_i	coagulation rate of interest	17
x_i and x_3	rate constant	25
m	coagulation rate	20
n_o	initial number of colloids	14
n	number of colloids	13, 14, 20
D	Combining Einstein's diffusivity equation ($D = kT/6\pi\eta a$)	14
W	Colloid stability ratio	16, 17, 24, 25
σ	efficiency of coagulation	17, 18, 19, 20, 21
u	dimensionless separation distance (u=2h/d)	18
h	separation distance	18.5
R_c	capture cross-section	19
G	Shear	20, 22, 23
k_{ij}	rate of coagulation of the particles	20
E_C	dielectric constant	22
CCC	critical coagulation concentration	10, 11, 12
t	Time	13, 14
ɳ	viscosity of the solution	15, 22, 23
$\kappa_{(coagulation)}$	capa value at the CCC	19
x	constant determined from experimentally obtained values	21
V_{max}	Maximum interaction in the potential curve	24

APPENDIX 2

Experimentally determined CCCs and relevant system settings.

CCC (mM)	Error (mM)	Salt	z	Shear (G) (s^{-1})	pH	temp. (C)
720	36	**NaCl**	1	2000	5.5	20
1600	50	**NaCl**	1	2000	5.5	50
1140	40	**NaCl**	1	1000	5.5	20
1040	20	**NaCl**	1	1400	5.5	20
670	33	**KCl**	1	2000	5.5	20
7.8	0.3	**$CaCl_2$**	2	2000	5.5	20
1.6	0.2	**$CaCl_2$**	2	2000	3	20
1.7	0.4	**$CaCl_2$**	2	2000	4	20
8.8	0.4	**$CaCl_2$**	2	2000	7	20
12	0.6	**$CaCl_2$**	2	2000	8	20
24	1	**$CaCl_2$**	2	2000	5.5	50
24	0.4	**$CaCl_2$**	2	1000	5.5	20
14	0.4	**$CaCl_2$**	2	1400	5.5	20
9	0.5	**$CaCl_2$**	2	1600	5.5	20
6.5	0.4	**$MgCl_2$**	2	2000	5.5	20
16	0.3	**$MgCl_2$**	2	1000	5.5	20
14	0.2	**$MgCl_2$**	2	1400	5.5	20
0.065	0.003	**$Al_2(SO_4)_3$**	3	2000	5.5	20
0.09	0.004	**$Al_2(SO_4)_3$**	3	2000	5.5	50
0.617	0.01	**$Al_2(SO_4)_3$**	3	1000	5.5	20
0.51	0.01	**$Al_2(SO_4)_3$**	3	1400	5.5	20
0.075	0.005	**$FeCl_3$**	3	2000	5.5	20

APPENDIX 3

Experimentally determined multiple salt CCCs and relevant system settings.

[Na] mM	CCC (mM)	Error (mM)	Second Salt	z	Shear (G) (s^{-1})	pH	temp. (C)
50	6	0.2	**$CaCl_2$**	2	2000	5.5	20
150	3	0.2	**$CaCl_2$**	2	2000	5.5	20
300	2	0.1	**$CaCl_2$**	2	2000	5.5	20
400	0.9	0.04	**$CaCl_2$**	2	2000	5.5	20
50	0.06	0.005	**$Al_2(SO_4)_3$**	3	2000	5.5	20
150	0.02	0.002	**$Al_2(SO_4)_3$**	3	2000	5.5	20
400	0.01	0.0007	**$Al_2(SO_4)_3$**	3	2000	5.5	20

APPENDIX 4

^{1}H chemical shifts for the sugars present in the water-soluble wood polymers.

chemical shift	Sugar	chemical shift	sugar
5.516	Man(2-O-Ac) H2	3.689	Glucose (1-min) H4 Man (2-O-ac maj) H6
5.412	Gly/man	3.665	Man (1) H3 Glucose (1-min) H3
5.247	Man?	3.580	Man (3-O-ac-min) H5 Man (3-O-ac-w) H5
5.199	Man H1		
5.102	Man(3-O-ac) H3	3.455	Man (1) H5 Man(1-min-1) H5
5.033	Man H3	3.376	Glucose (1-maj) H2
4.799	Water	3.353	Gluycose (1-min) H2
4.528	Glucose H1 major	3.329	
4.481	Glucose H1	3.288	
4.219	Man (3-O-ac maj) H2	3.268	
4.141	Man (1-maj) H2	2.19	Acetyl
4.021	Man (maj) H2	2.17	Acetyl
3.942	Man (maj) H3/ galactose H5		
3.841	Man (2-O-ac-min) H4		
3.815	Man (1-maj) H3 Man (1-min-1) H4		

	Glucose (1-maj) H5		
3.789	Man (1-min-2) H4		
	Man (1-min-1) H3		
3.763	Glactose (1-) H6		

APPENDIX 5

Journal papers

R. Lee, K. Stack, T. Lewis, D. Richardson, G. Garnier, Study of pitch colloidal stability using a photometric dispersion analyser., Appita Journal, 63 (2010) 387-391. (See appendix 7)

R. Lee, K. Stack, T. Lewis, D. Richardson, G. Garnier, Pitch deposition at the solid-liquid interface: effect of surface hydrophobicity/ hydrophilicity and cation specificity., Journal of Colloid and Surfaces A, 388 (2011) 84- 90. (See appendix 7)

R. Lee, K. Stack, T. Lewis, D. Richardson, G. Garnier, Effect of shear, temperature and ph on the dynamics of salt-induced pitch coagulation., Journal of Colloid and Surfaces A, 396, (2012) 106–114. (See appendix 7)

R. Lee, K. Stack, T. Lewis, D. Richardson, G. Garnier, The effect of extracted wood polymers on the colloidal stability of *pinus radiata* wood resin., Journal of Colloid and Interface Science, (2011).

R. Lee, K. Stack, T. Lewis, D. Richardson, G. Garnier, The effect of salt addition on the stability of colloidal *pinus radiata* wood resins, Journal of Colloid and Interface Science, (2011).

R. Lee, K. Stack, T. Lewis, D. Richardson, G. Garnier, Structure of wood extract colloids and effect of $CaCl_2$ on the molecular mobility, Nordic Pulp and Paper Research Journal, accepted for publication, (2012).

R. Lee, K. Stack, T. Lewis, D. Richardson, G. Garnier, Aggregation studies of *pinus radiata* wood extractives under increased system closure., Appita Journal, (2011).

APPENDIX 6

Conference papers

R. Lee, K. Stack, D. Richardson, T. Lewis, G. Garnier, Photometric Dispersion Analyser (PDA) to quantify pitch coagulation kinetics, in: APPITA (Ed.) 63rd Appita Annual General Conference, Melbourne, 2009, pp. 259-265. (See appendix 7)

R. Lee, K. Stack, T. Lewis, G. Garnier, D. Richardson, T. Van de Van, Measurement of pitch deposition by impinging jet microscopy: Effect of divalent salts, in: Appita (Ed.) 64th Appita Annual General Conference, Appita, Melbourne, 2010, pp. 273-279. (See appendix 7)

R. Lee, K.S.D. Richardson, T. Lewis, G. Garnier, Aggregation studies of *pinus radiata* wood extractives under increased system closure., in: appita (Ed.) 65th Appita Conference & Exhibition, APPITA, Rotorua, New Zealand, 2011. (See appendix 7)

R. Lee, K. Stack, D. Richardson, T. Lewis, G. Garnier, Coagulation kinetics of pitch based wood extractive colloids in the presence of Hemicellulose, in: 7th International Paper and Coating Chemistry Symposium, Hamilton, Canada, 2009, pp. 187-190. *(See appendix 7)*

APPENDIX 7

Study of pitch colloidal stability using a Photometric Dispersion Analyser

ROLAND LEE[1], KAREN STACK[2], DES RICHARDSON[3], TREVOR LEWIS[4], GIL GARNIER[5]

SUMMARY

This paper describes the use of a photometric dispersion analyser (PDA) to study and quantify the effect of wood resin preparation and salt on the colloidal stability of wood resin dispersions. The PDA technique has two major benefits over other techniques in that it can quantify the aggregation kinetics under dynamic shear conditions and at low concentrations of colloidal material. It is very sensitive to small changes in the solution and provides information about the floc structure and homogeneity.

To ensure reproducible results when analysing colloidal wood resin dispersions, conditioning of the tubing and a constant flow rate and stirring rate were required. The PDA signal response with time for the wood resin dispersions shows three distinct regions: a growth region, a peak region, and a decay region. The slope of the initial growth region was used to measure the kinetics of coagulation and to determine the stability ratio, W. The critical coagulation concentration of different salts was also determined. The time-weighted variance of the PDA output showed that potassium salts resulted in more homogeneous aggregates than those formed with the addition of magnesium salts.

KEY WORDS

Photometric dispersion analyser, PDA, wood extractives, pitch, salt, kinetics, colloid, aggregation.

INTRODUCTION

As many paper mills worldwide reduce water consumption and close the water loop, they are faced with the need to develop strategies that reduce the accumulation of substances that cause deposits and other paper machine problems. One of the biggest problems is pitch deposition, and as salt levels increase with process water closure the problem could potentially become worse. In order to develop suitable strategies to reduce pitch deposition, a greater understanding of the effect of system closure with increasing salt levels and other components on colloidal stability and aggregation kinetics is needed.

Pitch deposits arise from the agglomeration of colloidal particles formed from the lipophilic components in the wood (*1-5*). Many factors have been found to affect the formation of deposits (*6-9*) and the behaviour of colloidal particles (*10-13*). Several studies have been undertaken investigating the effect of salt on the colloidal stability of wood extractives and have shown that salts destabilize the colloids and increase deposition tendency (*14,15*). The presence of dissolved organic material originating from the pulp has been found to stabilize the pitch colloids and reduce the effect of the salt (*5,16-18*). Work has also been undertaken to investigate the effect of synthetic polymers on pitch deposition, colloidal stability and aggregation of the wood resin colloids (*19-22*).

A number of techniques have been used to study coagulation and aggregation of colloidal particles and particle size. These include laser diffraction (*23,24*), photometric dispersion analysis (25-27), focused beam reflectance measurement (*28-31*), flow cytometry (*20,23,32,33*) and image analysis (*34-37*). Most of the techniques are based on light scattering, where the intensity of light scattered is proportional to the sixth power of the diameter for small particles.

The photometric dispersion analyser (PDA) has been found to be a useful research tool to study colloidal aggregation (*25-27*) . The PDA measures the turbidity variations of a moving colloidal suspension. The instrument measures the direct current (DC) voltage (V_{DC}), which corresponds to the average transmitted light intensity, and the root mean square (RMS) value of the fluctuations in intensity of light transmitted (V_{rms}), which indicates aggregation of the suspension. The ratio (R) of V_{rms} / V_{DC} has been shown to be a function of the particle concentration and particle size (*38*) and has been used to measure the degree of aggregation of colloidal particles. More importantly, it has been found to be unaffected by contamination of the optical surfaces or drift in the electronic components (*39*).

In this paper, a PDA has been used to study the coagulation of colloidal pitch dispersions prepared from extracted wood resins and model compounds. The effects of pitch composition and preparation along with the addition of salt on the colloidal stability and coagulation of wood resin colloidal dispersions were studied.

EXPERIMENTAL

Pulp

Thermomechanical pulp (TMP) studied was *Pinus radiata* collected from the primary refiners at Norske Skog's Boyer mill in Tasmania. The pulp was freeze dried and stored at -24°C.

Wood Resin Colloidal Dispersions

Wood resin colloidal dispersions were prepared in two ways using methods developed by both Sundberg *et al*. (*5*) and Stack *et al*. (*9*). The first, which is denoted "extracted pitch", was prepared by hexane extraction of freeze-dried TMP fibres using a soxhlet apparatus for a period of 8 hours. The hexane was removed by rotary evaporation and the resulting wood resin ("extracted pitch") was stored at -24°C until required. Prior to preparation of the aqueous pitch dispersion the extracted pitch was dissolved in acetone (99.5% purity).

The second procedure was to prepare wood resins from model compounds of abietic acid (technical grade, 70% purity, Aldrich), oleic acid (technical grade, 90% purity, Aldrich) and triolein (technical grade, 65% purity, Aldrich). Acetone

[1]PhD student, [2]Research Fellow and corresponding author (K.R.Stack@utas.edu.au), [4]Senior Lecturer
University of Tasmania
[3]Senior Specialist, Process Chemistry
Norske-Skog Paper Mills (Australia) Ltd
[5]Professor
Australian Pulp and Paper Institute
Monash University

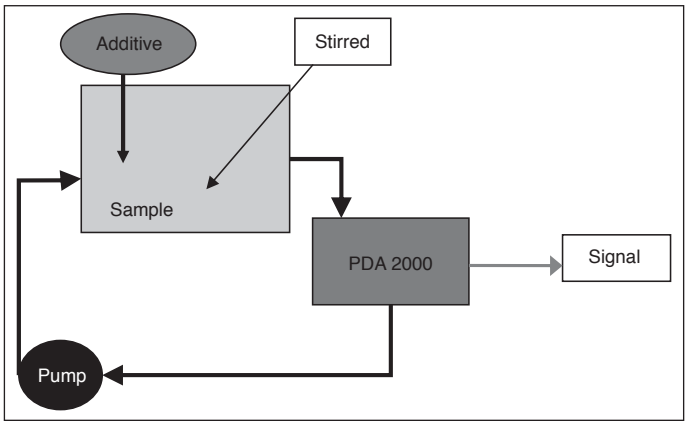

Fig. 1 Photometric dispersion analyser (PDA) experimental setup.

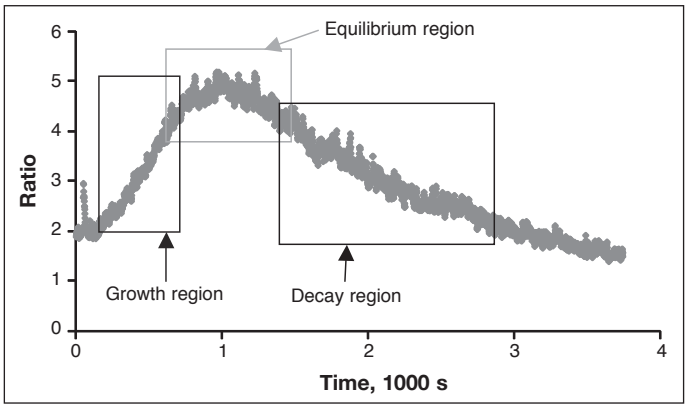

Fig. 2 PDA output (V_{rms} / V_{DC}) for undialysed hexane extracted pitch with 625 mM KCl.

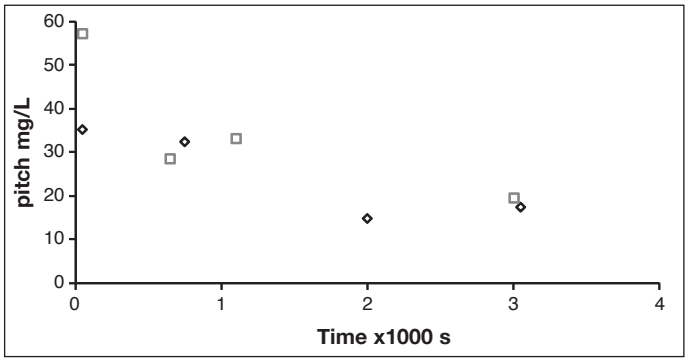

Fig. 3 Change in pitch concentration during duplicate PDA measurements of hexane extracted wood resin with 625 mM KCl.

solutions of each component were prepared as required and they were then mixed in the ratio of resin acid to fatty acid to triglycerides of 2:1:2.3. The pitch solution prepared from these model compounds was denoted "designer pitch".

Aqueous pitch dispersions were prepared by adding either acetone solutions of extracted pitch or designer pitch to a volume of distilled water with a concentration of 1 mM KNO_3, and pH adjusted to 5.5. The dispersions were dialysed for 24 hours to remove the acetone. Dialysis was conducted using a cellulose membrane tubing (Sigma D-9402, 76mm wide, >12,000 MW).

Pitch Analysis

The pitch colloids were extracted from the aqueous colloidal dispersions using tertiary-butylmethylether (*t*-BME). They were then silylated and analysed by gas chromatography (GC) as described previously (*8*).

PDA Pitch Colloid Aggregate Analysis

The PDA used in this study was a PDA 2000, from Rank Brothers, Cambridge, UK. A Cole Palmer Masterflex L/S peristaltic pump and 3 mm tubing were used to circulate the suspension. The instrument was initially calibrated with distilled water and the DC gain control was adjusted to give a DC value of 10 V as suggested in the operating manual (*31*) and also by Hopkins *et al*. (*40*). The output from the PDA is a ratio of the RMS signal to the DC voltage. A schematic of the instrument is shown in Figure 1

RESULTS AND DISCUSSION

The rate of aggregation of a colloid is dependant on a number of variables, such as concentration of colloid and electrolyte, shear, particle size, particle charge and temperature, amongst other physiochemical properties.

The addition of 625 mM KCl (at t = 0) to a colloidal dispersion prepared from extracted pitch was found to result in a change in the PDA output with time, as shown in Figure 2. The curve obtained is typical of other colloidal systems (*40*) and shows three distinct regions: an initial region with a positive slope, rising to a peak, and then tailing off. The slope of the initial growth region indicates the rate at which flocs develop/aggregate. The peak represents the steady state between aggregation and disruption of the aggregates. Most reported studies find that the ratio output maintains a constant value after the peak while some indicate that a lower steady state is reached representing the balance between floc formation and floc breakup induced by shear (*40*). In Figure 2, the graph continues to decrease to a level lower than the starting value. This could reflect a change in particle concentration or a disruption of aggregates as the weak salt induced flocs are broken down by shear to a lower equilibrium size. The time-weighted variance in the output provides an indication of the variations in the homogeneity of the colloidal flocs and can be used to measure the floc structural differences and the effect of changes in solution on the floc variation. Small variations in output signal indicate a tighter floc size distribution and a more homogeneous, dense and less porous floc structure.

During the PDA measurements shown in Figure 2, the sample concentration was also monitored by taking samples at regular time intervals. Figure 3 shows the changes in pitch concentration with time. It is noted from Figure 3 that the concentration of pitch colloids in solution was decreasing throughout the PDA experiment. This decrease in concentration is most likely due to deposition of pitch onto the tubing and/or sample vessel of the PDA apparatus.

During the initial stages of experimentation the signal response was found to increase with repeated measurements of the same solution through the apparatus. It was found that conditioning of the tubing was required prior to measurement to ensure reproducible and reliable results. It appeared that the hydrophobic tubing material and sample vessels were absorbing pitch prior to the PDA detector and a

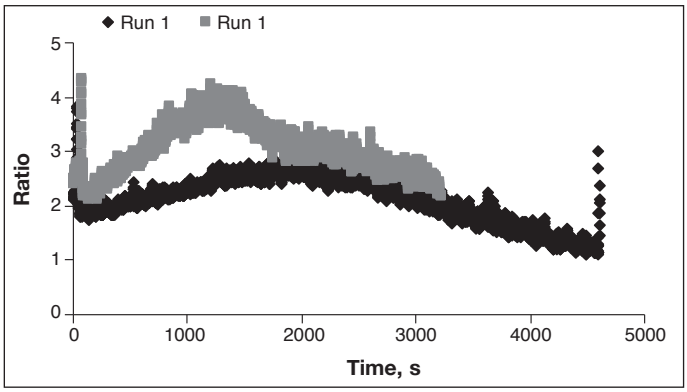

Fig. 4 Effect of conditioning of tubing on PDA output (V_{rms} / V_{DC}) for addition of 625 mM KCl to 100 mg/L extracted pitch.

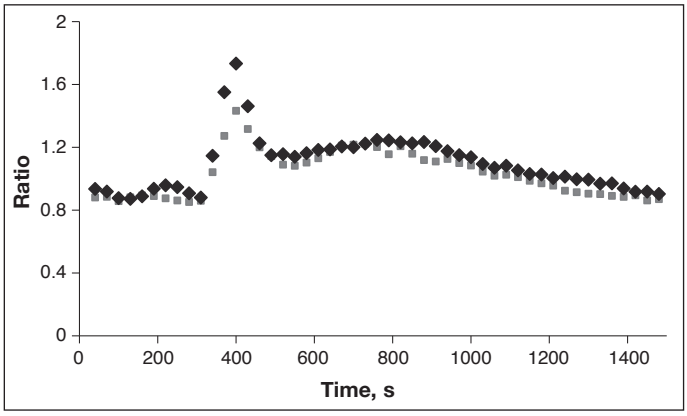

Fig. 6 PDA output (V_{rms} / V_{DC}) for duplicate measurements of dialyzed hexane extracted pitch with 600 mM KCl added.

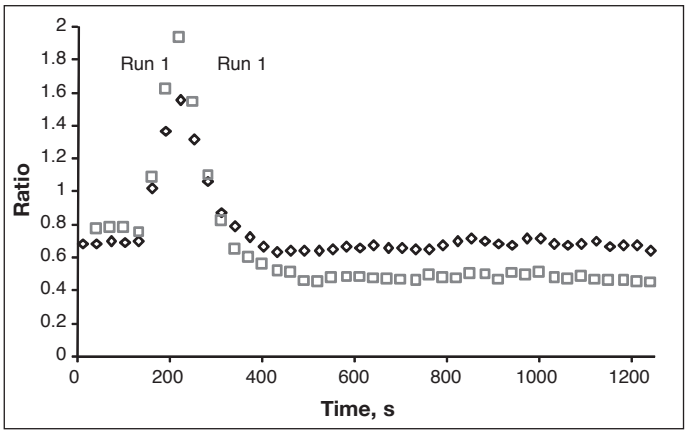

Fig. 5 PDA output (V_{rms} / V_{DC}) for duplicate measurements of deionised water after the addition of 600mM KCl.

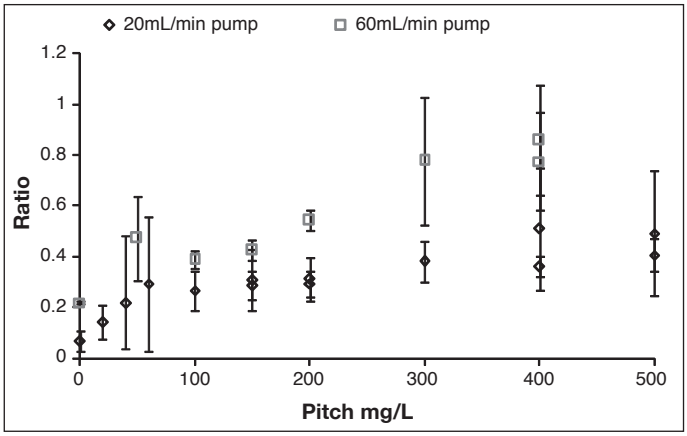

Fig. 7 Effect of pitch concentration on PDA output (V_{rms} / V_{DC}) at 20 mL/min and 60 mL/min flow rate. (Error bars are 1 standard deviation).

period of time was needed to condition these surfaces. To condition the apparatus a pitch sample was allowed to pass through the tubing for a period of 12 hours until the signal response became more reproducible. No further conditioning was required during experimentation unless changes in tubing or other components were made. Reducing the tubing length was also found to increase reproducibility and reduce the conditioning time required. Figure 4 shows the variation in the signal due to conditioning after six consecutive runs of one sample.

The PDA was found to be very sensitive to aggregation of species in solution, even at very low concentrations. The aggregation of contaminants in a deionised water sample was observed in Figure 5 on addition of 625 mM KCl to the water. The rapid return of the signal to the value of the initial baseline indicates that either only weak flocs are formed that are easily broken by shear or the particles formed reorientate and form a tighter floc structure.

It was found that the coagulation of two different colloidal materials could be followed using the PDA. Figure 6 shows the coagulation of water born contaminants and colloidal pitch. The faster coagulating material (peak at about 400 seconds) was identified as the contaminant observed in the deionised water (Fig. 5) while the slower coagulating material (broad peak at about 800 seconds) is the coagulation of colloidal extracted pitch. The difference in the peak height for the contaminant found in deionised water compared to the pitch is a result of the variation in the mobility, concentration, distribution and size of the final aggregate formed from the different coagulating substances. This capability to distinguish between different colloids is very significant. It enables the separation of coagulation of any background contaminants from the coagulation of the sample, as seen in Figure 6. Furthermore, this capacity to differentiate the coagulations of substances also makes it possible to assess if added components are being incorporated into the initial colloid or are themselves forming new colloidal material.

The reproducibility of the system is shown in both Figures 5 and 6. The signals have been smoothed with the use of a moving average over 40 points. It can be seen that there is a small variation between the replicates; however, the trends and slope for the growth region are reproducible for both samples.

During the experiments, several other factors were found to affect the behaviour of the colloid in solution and thus the PDA signal. These included the concentration, flow rate and stirring of the pitch sample. Figure 7 shows the effect of pitch concentration and flow rate (controlled by the pump speed) on the signal ouput and variance in the output. It is noted that as the concentration of pitch colloids in solution is increased, the PDA output (V_{rms} / V_{DC}) also increased. Furthermore, the increase in flow rate from 20 mL/min to 60 mL/min increased the signal output. This is thought to be the result of changes to the shear experienced by the colloid.

Within the system, it is noted that there are two sources of shear: the first is the result of pump flow rate and the second is

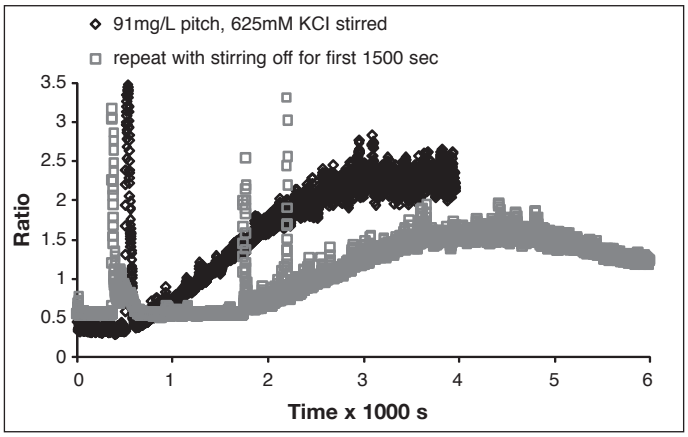

Fig. 8 Effect of stirring on PDA output (V_{rms} / V_{DC}).

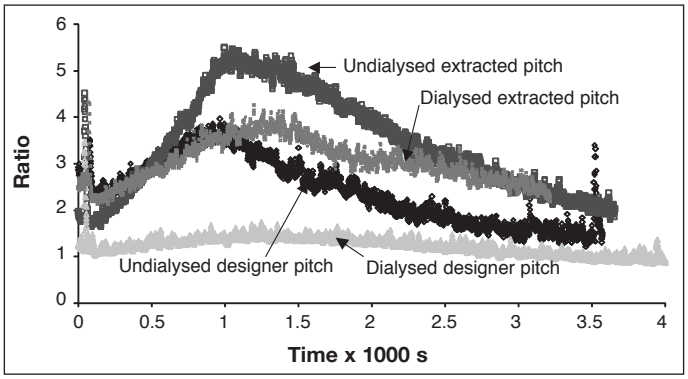

Fig. 9 Comparison of aggregation behaviour of pitch dispersions (625 mM KCl at t = 0 sec).

the result of stirring within the sample vessel. Figure 8 shows the output signal for both a stirred and an unstirred pitch sample at the same concentration of both pitch and electrolyte (625 mM KCl at t = 500 sec). The initial slope for the growth of colloids on addition of salt was greater with continuous stirring. The plot also indicates that under continuous shear conditions, the flocs reach a maximum size and then stabilise at this size, as indicated by the plateau region in Figure 8. When the experiment was repeated without stirring, the output from the PDA was unaffected.

As a result of the variability of the PDA output due to these physiochemical conditions, it was noted that the pitch concentration, sample stirring and pump flow rate are variables that must be controlled for all experiments if comparison between samples and quantification of coagulation rates are to be carried out.

The rate of aggregation for different pitch preparations of dialysed and undialysed extracted pitch and designer pitch dispersions were compared (Fig. 9). The composition of the different pitch dispersions is shown in Table 1. The results in Figure 9 show that the undialysed extracted pitch has a greater slope, and hence faster aggregation, than the dialysed extracted pitch dispersion. The same trend with dialysis was observed for designer pitch. The change in aggregation rate arising from dialysis of the sample is possibly due to the removal of acetone from solution which affects the particle size and distribution.

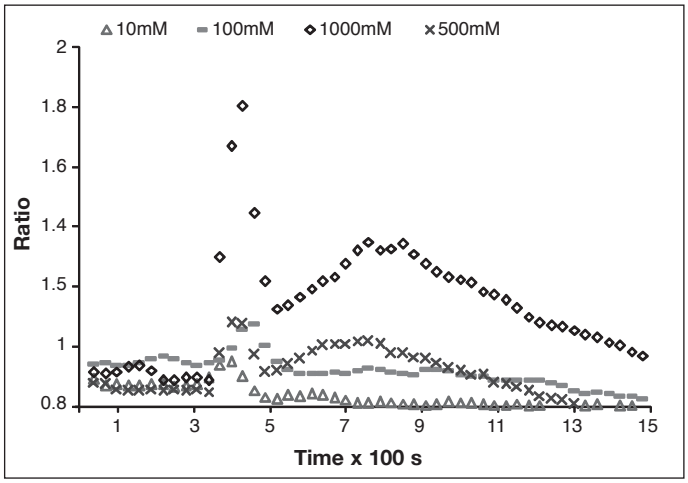

Fig. 10 Effect of KCl concentration on PDA output (V_{rms} / V_{DC}) (salt added at t=300 s).

The effects of electrolyte concentration and valency on pitch stability were quantified with the PDA to better understand the coagulation behaviour of pitch colloids within the paper mill. The effect of KCl concentration on pitch stability is illustrated in Figure 10. The initial slope, the maximum ratio level and the decay time to break up flocs were all found to increase as a function of salt concentration. The output for the PDA has been smoothed with the use of a moving average over 40 points.

The rate of pitch coagulation at the different electrolyte concentrations was quantified by the stability ratio (W) which was determined from the slopes of the curves in Figure 10 using the following equation (41):

$$W = \frac{K_1}{K^*} \qquad [1]$$

where K_1 is the fastest coagulation slope and K^* slope of coagulation due to addition of electrolyte of interest.

A plot of log W against salt concentration (Fig. 11) defines the colloidal stability of the system. At low salt additions, the system has a high value for log W and is said to be stable. As salt is added and aggregation of the colloids occurs, the system becomes unstable. The point at which log W intercepts the x-axis defines the critical coagulation concentration (CCC) for that particular salt.

The effect of salt valency on pitch stability was studied using $MgCl_2$ and KCl and the stability curves for the two salts are shown in Figure 11. The critical coagulation concentration at pH 5.5 for each salt was estimated from the curves to be CCC_{Mg2+} = 5.9 mM and CCC_{K+} = 625

Table 1
Composition of pitch dispersions

	%Fatty Acid	%Resin Acid	%Triglyceride
Extracted pitch undialysed (3% acetone)	11	48	41
Extracted pitch dialysed	11	41	48
Designer pitch undialysed (3% acetone)	19	36	45
Designer pitch dialysed	22	44	33

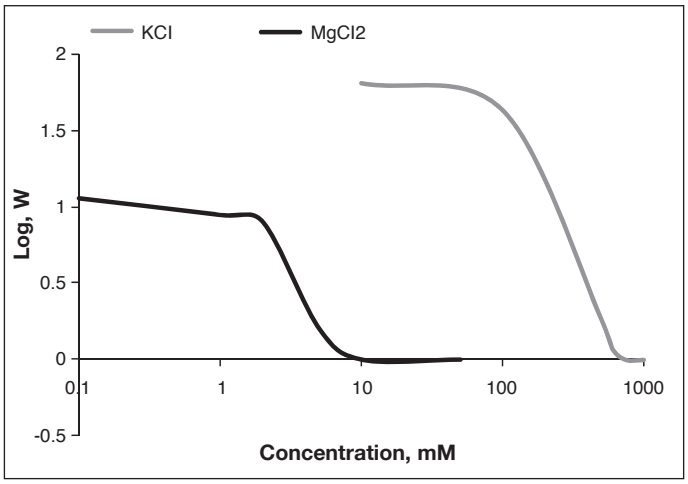

Fig. 11 Stability curves of mono and divalent salts.

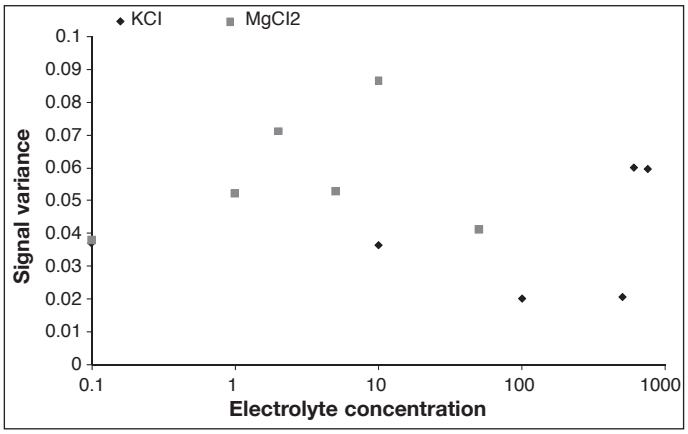

Fig. 12 Comparison of PDA output (V_{rms} / V_{DC}) variance for KCl and $MgCl_2$.

mM. These results are similar to values reported for other monovalent (Na) and divalent (Ca) salts (*5,16,17*). Swerin (42) noted that if colloidal pitch was stabilized only by electrostatic means then coagulation should occur at 100 mM NaCl and 1-2 mM $CaCl_2$. Since higher salt concentrations are needed to stabilize the pitch suspensions, it was proposed that other mechanisms (steric stabilization) might be occurring to stabilize the pitch dispersions.

Pitch colloids can be considered as "soft colloids" capable of molecular reorganization with changes to the environment. The variance in the PDA output signal is an indication of the floc homogeneity in solution as they pass the detector, with larger variance indicating increased variation in the floc size distribution The time-weighted variance in the raw ratio signal values is shown in Figure 12. It is noted that there is a higher variance in flocs following the addition of $MgCl_2$ compared to KCl. Decreases in signal variance indicate that the flocs formed when KCl is present are more uniform and tighter in structure. Above the CCC for KCl, the floc structure does appear to become less homogenous, and a greater variation in the signal is observed. The changes in variance could have two explanations: the first being that the aggregate size distribution becomes narrower, and the second explanation being that molecular reorganization and deformation of the colloids occurs.

CONCLUSIONS

Unlike other methods of investigating coagulation, the PDA is able to quantify pitch coagulation under the dynamic conditions relevant to papermaking at low concentrations. The stability ratio was determined to quantify the rate of coagulation and the critical coagulation concentrations (CCC) were found to be 5.9 mM for $MgCl_2$ and 625 mM for KCl, at 23°C and pH5.5. From the signal variation it is noted that flocs formed on addition of potassium to pitch are more homogeneous than those formed from the addition of magnesium to pitch.

Due to the sensitivity of PDA to aggregation of solution components, the technique was able to differentiate between different species that were aggregating, allowing determination as to whether or not components were aggregating as a unit or as separate entities in the solution.

In order to ensure good reproducibility when analysing pitch colloids, up to 12 hours conditioning of the tubing and sample vessel were required along with a constant flow rate through the instrument and a constant stirring rate within the sample reservoir.

ACKNOWLEDGEMENTS

Financial support for this project was provided by Norske-Skog Paper and an ARC Linkage grant.

REFERENCES

(*1*) Dreisbach, D. and Michalopoulos, D. – Understanding the behavior of pitch in pulp and paper mills, *Tappi J*. **72**(6):129 (1989).

(*2*) McLean, D., Stack, K. and Richardson, D. – Wood pitch deposition versus composition, *Proc. 57th Appita Ann. Gen. Conf.*, Melbourne, p.203 (2003).

(*3*) Vercoe, D., Stack, K., Blackman, A., Yates, B., and Richardson, D. – An Innovative Approach Characterising the Interactions Leading to Pitch Deposition, *J. Wood Chemistry and Technol*. **24**(2):115 (2004).

(*4*) Qin, M., Hannuksela, T. and Holmbom, B. – Physico-chemical characterisation of TMP resin and related model mixtures, *Colloids and Surfaces A: Physiochem. and Eng. Aspects*. **221**(1-3):243 (2003).

(*5*) Sundberg, K., Pettersson, C., Eckerman, C., and Holmbom, B. – Preparation and properties of a model dispersion of colloidal wood resin from Norway spruce, *J. Pulp Pap. Sci*. **22**(7):248 (1996).

(*6*) McLean, D., Stack, K. and Richardson, D. – Wood pitch deposition versus composition, *WPP 2003 Chem. Technology of Wood, Pulp and Paper Intl. Conf.*, Bratislava, p.115 (2003).

(*7*) Vercoe, D., Stack, K., Blackman, A. and Richardson, D. – A multi-component insight into the interactions leading to wood pitch deposition, *Proc. 58th Appita Ann. Gen. Conf.*, Melbourne, p.65 (2004).

(*8*) McLean, D., Stack, K. and Richardson, D. – The effect of wood extractives composition, pH and temperature on pitch deposition, *Appita J*. **58**(1):52 (2005).

(*9*) Stack, K., Stevens, E., Richardson, D., Parsons, T. and Jenkins, S. – Factors affecting the deposition of pitch in process waters and model dispersions, *Proc. 52nd Appita Ann. Gen. Conf.*, Melbourne, p.59 (1998).

(*10*) Harwot, P. and Van de Ven, T. – Effects of sodium oleate and calcium chloride on the deposition of latex particles on an air/water interface, *Colloids and Surfaces A: Physiochem. and Eng. aspects*. **121**:229 (1997).

(*11*) Polverari, M. and van de Ven, T. – Electrostatic and steric interactions in particle deposition studied by evanescent wave light scattering, *J. Colloid and Interface Sci*. **173**:343 (1995).

(*12*) Dabros, T. and van de Ven, T. – A direct method for studying particle deposition onto solid surfaces, *Colloid Polym Sci*. **261**:694 (1983).

(*13*) Bauer, D., Killmann, E. and Jaeger, W. – Flocculation and stabilization of colloidal silica by the adsorption of poly-diallyl-dimethyl-ammoniumchloride (PDADMAC) and of copolymers of DADMAC with N-methyl-N-vinyl acetamide (NMVA), *Colloid Polym Sci*. **276**(8):698 (1998).

(*14*) Beneventi, D., Carre, B. and Gandini, A. – Precipitation and solubility of calcium soaps in basic aqueous media, *J. of Colloid and Interface Sci*. **237**(2):142 (2001).

(*15*) Edge, S. – The Laboratory Investigation of Pitch Problems, *The Technical Section of the Paper Makers Association*. **15**(2):283 (1935).

(*16*) Mosbye, J., Laine, J. and Moe, S. – The effect of dissolved substances on the adsorption of colloidal extractives to fines in mechanical

Continued on page 406

35:1827 (2000)
(*15*) Maldague, X.P.V. – **Theory and Practice of Infrared Technology for Nondestructive Testing**, John Wiley & Sons, Inc. New York (2001)
(*16*) Maillet, D. et al. – Non-destructive thermal evaluation of delaminations in a laminate: Part 1 – Identification by measurement of thermal contrast, *Composite Sci. and Tech.* **47**:137 (1993)
(*17*) Cielo, P., Maldague, X., Deom, A.A. and Lewak, R. – Thermographic nondestructive evaluation of industrial materials and structures, *Materials Evaluation* **45**(6):452 (1987)
(*18*) e.g. National Astronomical Observatory edit. – **Chronological Scientific Table 2006**, Maruzen Co., Ltd., Japan, p.400 and p.486 (2005)
(*19*) Sato, J. and Hutchings I.M. – Non-destructive testing of paper products by infra-red thermography, *Proc. Progress in Paper Physics*, Espoo, B1, p.267 (2008)
(*20*) Vavilov, V.P. and Taylor, R. – Theoretical and practical aspects of the thermal nondestructive testing of bonded structures, In R.S.Sharpe (ed.) **Research Techniques in Non-Destructing Testing, 5**, Academic Press, London, p.239(1982)
(*21*) Wallbrink,C., Wade,S.A. and Jones, R. – The effect of size on the quantitative estimation of defect depth in steel structures using lock-in thermography, *J. Appl. Phys.* **101**:104907 (2007)
(*22*) Bama, G.K., Devi, P.I., and Ramachandran, K. – Structural and thermal properties of PVDF/PVA blends, *J. Mater. Sci.* **44**:1302 (2009)
(*23*) Balageas, D.L., Deom, A.A., and Boscher, D.M. – Characterization and nondestructive testing of carbon-epoxy composites by a pulsed photothermal method, *Materials Evaluation* **45**(4):466 (1987)

Original manuscript received 20 January 2009, revision accepted 27 April 2010

Continued from page 391

pulp, *Nord. Pulp Pap. Res. J.* **18**(1):63 (2003).
(*17*) Sihvonen, A., Sundberg, K., Sundberg, A. and Holmbom, B. – Stability and Deposition Tendency of Colloidal Wood Resin, *Nord. Pulp Pap. Res. J.* **13**(1):64 (1998).
(*18*) Johnsen, I., Lenes, M. and Magnusson, L. – Stabilisation of colloidal wood resin by dissolved material from TMP and DIP, *Nord. Pulp Pap. Res. J.* **19**(1):22 (2004).
(*19*) Hassler, T. – Pitch deposition in papermaking and the function of pitch-control agents, *Tappi J.* **71**(6):195 (1988).
(*20*) Belouadi, C., Blum, R. and Esser, A. – A Novel Approach to Avoiding White Pitch Deposition, *Pulp and Paper Canada*. **101**(9):254 (2000).
(*21*). Yu, L., Allen, L. and Esser, A. – Evaluation of polymer efficiency in pitch control with a laser–optical resin particle counter, *J. Pulp Pap. Sci.. 29*(8):260 (2003).
(*22*) Nguyen, D. – Prevention of pitch and stickies deposition on paper-forming wires via adsorption of a cationic polymer associated with anionic species, *Tappi J.* **81**(6):143 (1998).
(*23*) Vahasalo, L., Degerth, R. and Holmbom, B. – The use of flow cytometry in wet end research, *Pap. Technol.* **44**(1):45 (2003).
(*24*) McLean, D., Stack, K., Richardson, D. and Haddad. P. – Wood pitch fixative selection by laser particle size analysis. *Proc. 60thAppita Ann. Gen. Conf.,* Melbourne, p.413 (2006).
(*25*) Porubská, J., Alince, B. and van de Ven, T. – Homo- and heteroflocculation of papermaking fines and fillers, *Colloids and Surfaces a-Physicochem. and Eng. Aspects*. **210**(2-3):223 (2002).
(*26*) Wu, M., Paris, J. And van de Ven, T. – Polyethylene oxide induced fines flocculation and retention: from bench top experiments to paper machine performance, *Nord. Pulp Pap. Res. J.* **21**(5):646 (2006).
(*27*) Poraj-Kozminski, A., Hill, R. and Van de Ven, T. – Flocculation of starch-coated solidified emulsion droplets and calcium carbonate particles, J. *of Colloid and Interface Sci.*. **309**:99 (2007).
(*28*) Blanco, A., Fuente, E., Monte, M. and Tijero, J. – Focused beam reflectant measurement as a tool to measure flocculation, *Tappi J.* **1**(10):14 (2002).
(*29*) Blanco, A., Negro, C., Hooimeijer, A. and Tijero, J. – Polymer optimisation in paper mills by means of a particle size analyser: an alternative to zeta potential measurements, *Appita J.* **49**(2):113 (1996).
(*30*) Dunham, A., Sherman, L. and Alfano, J. – Effect of dissolved and colloidal substances on drainage properties of mechanical pulp suspensions, *J. of Pulp Pap. Sci.*. **28**(9):298 (2002).
(*31*) Gerli, A., Keiser, B. and Strand, M. – The use of a flocculation sensor as a predictive tool for paper machine retention program performance. *Tappi J.* **83**(10):59 (2000)
(*32*) Kröhl, T., Lorencak, P., Gierulski, A., Eipel, H. and Horn, D. – A new laser-optical method for counting colloidally dispersed pitch. *Nord. Pulp Pap. Res. J.* **9**(1):26 (1994).
(*33*) Saarimaa, V., Vahasalo, L., Sundberg, A., Pranovich, A., Holmbom, B., Svedman, M. and Orsa, F. – Influence of pectic acids on aggregation and deposition of colloidal pitch, *Nord. Pulp Pap. Res. J.* **21**(5):613 (2006).
(*34*) Wågberg, L. and Lindström, T. – Flocculation of cellulosic fibres by cationic polyacrylamides with different charge densities, *Nord. Pulp Pap. Res. J.* **4**:152 (1987).
(*35*) Solberg, D. and Wågberg, L. – On the mechanism of cationic-polyacrylamide-induced flocculation and re-dispersion of a pulp fiber dispersion. *Nord. Pulp Pap. Res. J.* **18**(1):55 (2003).
(*36*) Solberg, D. – Adsorption kinetics of cationic polyacrylamides on cellulose fibres and its influence on fibre flocculation, in *Fibre and Polymer Technology, Royal Institute of Technology: Stockholm*. p. 41 (2003).
(*37*) Chang, Y., Lui, Q. and Zhang, J. – Flocculation control study based on fractal theory, *J. of Zhejiang University SCI. B*. **6**(10):1038 (2005).
(*38*) Gregory, J. – Turbidity Fluctuations in Flowing Suspensions, *J. of Colloid and Interface Sci.*. **105**(2):357 (1985).
(*39*) Photometric Dispersion Analyser PDA 2000 Operating Manual, *Rank Bros Ltd*. (2002)
(*40*) Hopkins, C. and Ducoste, J. – Characterising flocculation under heterogeneous turbulence, *J. of Colloid and Interface Sci.*. **264**:184 (2003).
(*41*) Shaw, D., – Introduction to Colloid and Surface Chemistry, Butterworth-Heinerman, 4th edition (1992).
(*42*) Swerin, A., Ödberg, L. and Wågberg, L. – Preparation and some properties of the colloidal pitch fraction from a thermomechanical pulp, *Nord. Pulp Pap. Res. J.* **8**(3):298 (1993).

Original manuscript received 25 December 2009, revision accepted 10 April 2010

Pitch deposition at the solid-liquid interface: Effect of surface hydrophobicity/ hydrophilicity and cation specificity

ROLAND LEE[1], GIL GARNIER[2*], TREVOR LEWIS[1], DESMOND RICHARDSON[3], THEO G.M. VAN DE VEN[4] and KAREN STACK[1**]

[1] School of Chemistry, University of Tasmania

[2] Department of Engineering, Professor, Monash University*

[3] Process Chemistry, Norske Skog Paper Mills (Australia) Ltd

[4] Department of Chemistry, McGill University

*Email: gil.garnier@monash.edu, Fax: +61 3 9905 3413, Phone: +61 3 9905 3456

**Email: K.R.Stack@utas.edu.au, Fax: +61 3 6226 2858, Phone: +61 3 6226 2169

Abstract

The deposition rate of colloidal pitch onto hydrophobic and hydrophilic model surfaces was measured at the solid-liquid interface by impinging jet microscopy (IJM) and the effect of cation specificity in solution on deposition was quantified. On both model surfaces, the pitch deposition was slightly faster with calcium ions than with magnesium at the same concentration (800 mg/L). This concentration is around twice the critical coagulation concentration.

The rate of colloidal pitch deposition on hydrophobic surfaces was far greater (up to a 2.5 times) than on hydrophilic surfaces for both salts. Contact angle measurements inferred that in the air-surface environment, the hydrophobicity of the surface does not affect its affinity for pitch suggesting molecular mobility within the pitch colloid. IJM shows variation in the pitch shape on the model surfaces. On hydrophilic surfaces, the pitch particle size for both salts ranges from 0.33 to 0.35 μm while for hydrophobic surfaces the particle size is 5 times higher for calcium salt than for magnesium salt. Film thinning or spreading of the pitch particles occurred on the hydrophobic surfaces with calcium and to a lesser extent with magnesium salt.

Key words

Pitch; impinging jet; liquid solid interface; hydrophilic; hydrophobic; deposition; soft colloid; surface; cation

Introduction

Pitch has plagued papermaking by creating deposits linked to sheet breaks ever since its beginning. The French expression: “Quelle poix!”- what a pitch!- describing literally and figuratively a sticky situation illustrates how the severity of the issue has become a linguistic allegory. The pitch released from the wood during pulping can deposit onto most surfaces of the papermaking equipment in what has been a chaotic fashion [1-3]. There is a need to better understand the mechanism by which pitch deposits at the liquid-solid interface and the controlling variables; these are the objectives of this study.

Pitch, also known as wood resins, is a complex blend made of fatty acids, resin acids and triglycerides from the extractives of resinous trees. In water, it forms a stable colloid suspension. There is evidence suggesting a core-sheath structure for the pitch colloid with the triglycerides preferentially located inside while the fatty acids and resin acids are concentrated in the shell of the particle (Figure 1) [4-6]. Pitch is an interesting colloid to investigate for its industrial impact and as a model colloid able to interact with its environment. We raise the hypothesis that a pitch suspension is, at room temperature, a soft colloid with enough molecular mobility to allow reorganization or phase separation; it is able to form metallic soaps through interaction of its carboxylic groups with multivalent cations present in water. Specific inorganic ions, such as calcium or aluminum, react with the soluble resin acids to form sticky deposits of metal soaps that are not seen upon the addition of other ions such as magnesium and sodium [7-13].

Previous studies investigated changes in extractive concentrations as a function of salt concentration, valency and type [14-17]. Recent work on colloidal pitch stability using a photometric dispersion analyzer (PDA) has shown that the rate of particle aggregation is dependent on the concentration of salt present and its valency; pitch is probably a electro-sterically stabilized colloid [18].

Colloid deposition on a surface is not only affected by the particle-surface interactions at the liquid-solid interface, but also by the hydrodynamic conditions in the region of the surface and particle transport [19, 20]. Direct measurement of the deposition rate is possible with techniques such as impinging jet microscopy (IJM) combined with video imaging. IJM gives quantitative information of particles absorbed onto the surface with well-defined hydrodynamic and physical-chemical properties [21].

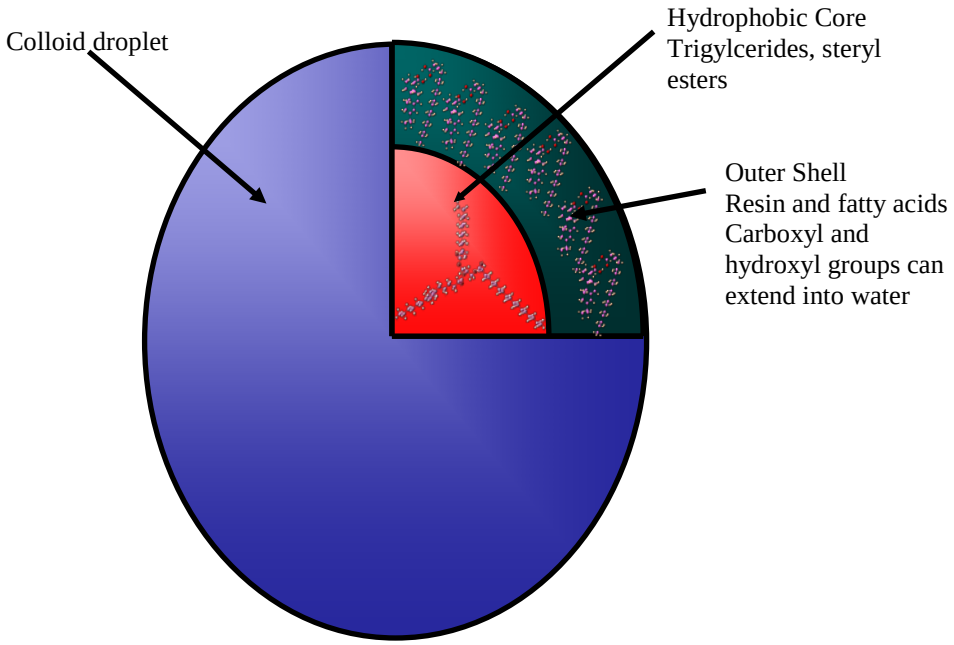

Figure 1: Schematic representation of the core-sheath pitch model with the triglycerides in the core and the fatty acids and resin acids in the sheath [5].

Impinging jet microscopy allows the observation of only those particles that are absorbed to the surface [20]. The technique has been used to probe numerous deposition problems including the competitive deposition of PEI coated particles and the absorption of PEI to a surface [22]. Using the impinging jet technique to quantify pitch deposition was pioneered by Pelton et.al. [23] for the deposition of synthetic pitch onto transparent plastic films. Without specific chemical additives or surface treatment, very

high surface depositions were recorded. Chemical additives and surface treatment proved to be efficient in decreasing pitch deposition rate, but without ever preventing full deposition. The kinetics of adhesion for phosphatidylcholine liposomes to quartz surfaces [24] and the deposition of particles onto cellulose films [25] have also been studied using impinging jet apparatus.

The surface and chemical composition of the colloid interacting with the surface are important. Qin et al. [4, 26] showed that the contact angle formed by a droplet of water on smooth surfaces coated with the various pitch components (in air) was dependent on its chemical composition. Pulping wood also releases hemicelluloses into the process water which can interact with the pitch colloids and modify their stability [17, 27-33]. However, the mechanism of pitch deposition by itself is poorly understood and already a complex phenomena. The role of hemicellulose on pitch stability deserves a study by itself and was addressed elsewhere [34]. Furthermore, the analysis of many pitch deposits reveals the triglycerides, acid and fatty acids of pitch, but no polysaccharides. For all these reasons, this study focused on the pitch deposition without the stabilizing effect of hemicelluloses.

This study aims at quantifying the effect of surface hydrophilicity/hydrophobicity and the effect of the type of divalent salt on the deposition rate of pitch particles at the solid-liquid interface. In the first part of the study, the effect of two divalent salts, $MgCl_2$ and $CaCl_2$, on the pitch suspension stability is quantified using a photometric dispersion analyzer (PDA). In the second, the rate of pitch deposition is measured by impinging jet microscopy combined with image analysis using two model surfaces. Finally, the results are analyzed in the context of papermaking and more generally in terms of soft colloids able to reconform and react with their environment.

Experimental

Materials

A thermomechanical pulp (TMP) made from *Pinus radiata* was collected from the primary refiners at Norske Skog, Boyer, Tasmania, Australia. The pulp was air-dried

and soxhlet extracted for 8 hours with hexane. The wood resins were recovered from the hexane and stored at -4°C until needed.

All electrolytes used were dissolved in distilled water as stock solutions. Constant volumes were added to the impinging jet sample solution, such that the final volume had the required concentration of salt. $CaCl_2$ and KNO_3 were purchased from BDH (99.8 purity %). $MgCl_2$ (99.8% purity) was obtained from Merck.

Methods

Pitch Preparation

Aqueous wood resin dispersions of 100 mg/L concentration were prepared by the addition of dissolved extracted wood resin in acetone (99.5% purity, Sigma-Aldrich) to a 1 mM KNO_3 solution in distilled water with a pH of 5.5. Dialysis of the dispersion was performed using cellulose membrane tubing with a molecular mass cut off of 12,000 amu (Sigma-Aldrich D9402-100FT), to remove acetone. The wash water used was 1 mM KNO_3, with pH adjusted to 5.5. This was changed every hour for the first 5 h and then at 24 h. The pitch extracted forms a viscous yellowish liquid at room temperature. The composition of the wood resins was analysed using gas chromatography and the results shown in Table I. The method used has been reported previously by McLean [35].

Table I: Composition of wood extractives from pinus radiata

Fatty Acid	Resin Acid	Triglycerides
2 mg/g_{pulp}	9.2 mg/g_{pulp}	8.8 mg/g_{pulp}

PDA Wood Resin Coagulation Analysis

A Photometric Dispersion Analyzer (PDA 2000, Rank Brothers, Cambridge, UK) was used to monitor the changes in aggregation of the wood resin colloidal dispersions. A Cole Palmer Masterflex L/S peristaltic pump and 3 mm tubing were used to circulate the suspension. The technique has been described elsewhere [36, 37]. The instrument was initially calibrated with distilled water and the DC gain control was adjusted to give a DC

value of 10V [38, 39]. The PDA measures turbidity fluctuations of a flowing suspension under controlled shear conditions. The PDA signal is the ratio of the root mean square (rms) measured as the AC voltage, to the DC voltage; this is plotted as a function of time. Three replicates are measured for each condition. The PDA signal was smoothed using a 40 point moving average.

Peristaltic pump flow rate was set at 70mL/min and stirring was also induced with a variable rotor at 500 rpm using a flat impeller (d = 4 cm). The PDA system was connected with 2 mm tubing to the cell tubing of 1 mm. Total sample added was constant at 200 mL

Hydrophobic conversion of glass slides

Microscope glass slides (CANEMCO & MARIVAC frosted end microscope slides 75 x 25 mm) were immersed in a 50/50 solution of trimethylchlorosilane and pyridine (≥99% Sigma- Aldrich) at 60°C for 12 h, removed and cleaned with hexane (99.8% Sigma-Aldrich) and air dried.

Contact angle measurements

The contact angle measurements were conducted with the use of a Data Physics OCA 20. A 100 µL drop of water was placed on the surface and the contact angle assessed with SCA20 software. This procedure was the same for the contact angle of pitch with the model surfaces. A 100 µL drop of pure extracted pitch, prior to formation of the pitch colloids, was introduced to the model surfaces and the contact angle of the pitch on the surface was determined.

Impinging jet

Figure 2 represents the schematic view of the impinging jet consisting of two plates (collector plate and bottom confiner plate) where r is the radius of the jet, and h is the distance between the plates. The flowing particles suspension forms a Newtonian fluid within the impinging jet [22, 24, 40-42]. The pitch suspension enters through a circular hole impinging onto the particle collector plate and counts were collected at the

stagnation point. The rate of deposition and flow distribution is defined by the dimensionless ratio of h/r. The experimental rate of deposition (j) is defined as the number of particles on the surface (n_s) with time (t):

$j = n_s / t$

The dialysed pitch colloidal dispersion was made up to a salt concentration of 20 mM with the desired salt and stirred for 10 min to allow particles to aggregate. The h/r ratio (Figure 2) within the jet was kept at 1.7 for all experiments, with a constant flow rate of 70 mL/min through the impinging jet. Magnification with a 10X objective was achieved with an Autoplan microscope. Images were captured with an IMI tech Han series digital camera. Time zero was taken as the time at which the pitch suspension first contacted the surface.

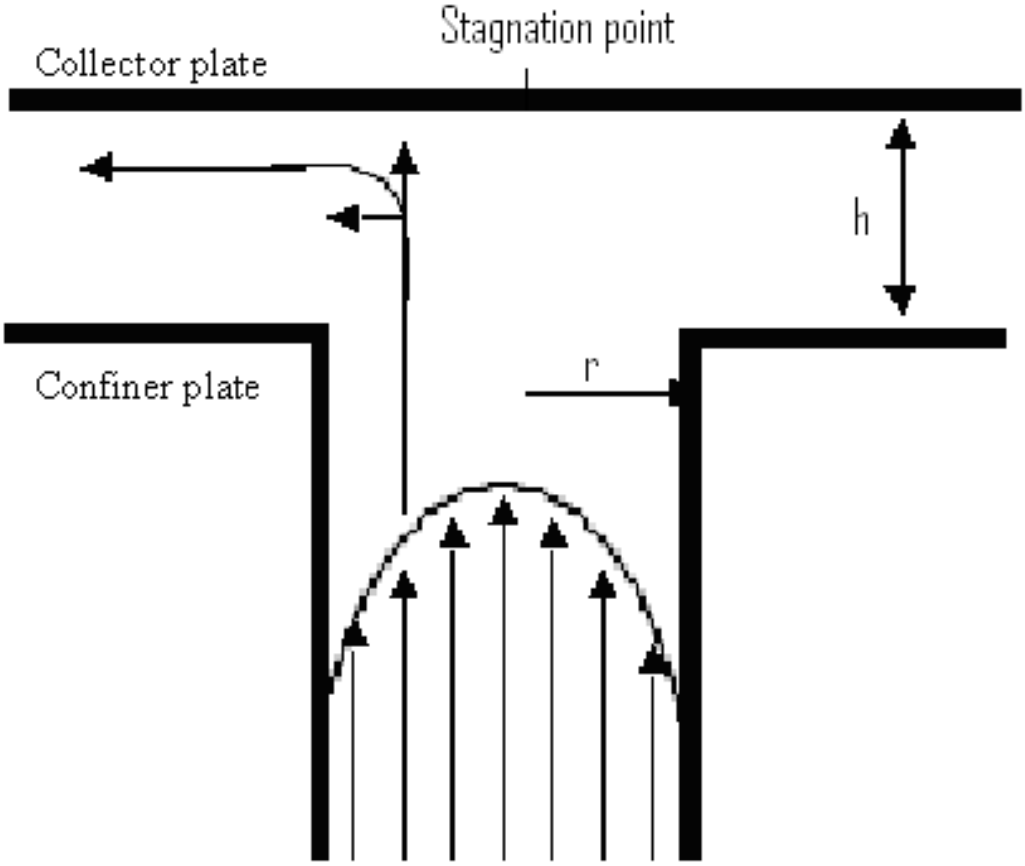

Figure 2: Schematic view of a radial impinging jet.

Results

The stability of pitch suspensions with various concentrations of electrolyte was studied under shear by PDA. Slight differences in aggregation behaviour were observed between the two divalent salts being investigated. The results of the stability curves are shown on Figure 3 for $MgCl_2$ and $CaCl_2$. From the curves and extrapolation of the linear decreasing section of the graph to the x axis, the critical coagulation concentrations (CCC) can be determined. These were found to be 6.5 mM and 7.8 mM for $MgCl_2$ and $CaCl_2$, respectively.

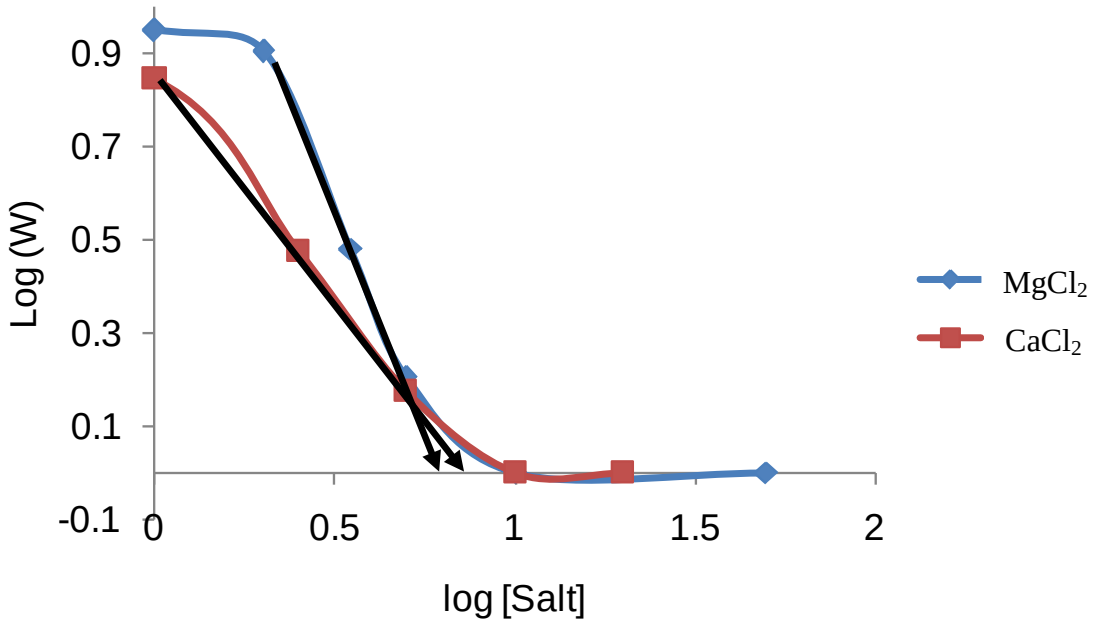

Figure 3: Effect of salt concentration and type of divalent cation on the stability of a pitch suspension. (Arrows indicate CCC).

Differences in the aggregated floc homogeneity were also observed between the two divalent salts. The results in Figure 4, show the time-weighted variance in the PDA output signal which is an indication of the floc homogeneity in solution [39]. There was a higher variance in flocs following the addition of $CaCl_2$, compared to $MgCl_2$.

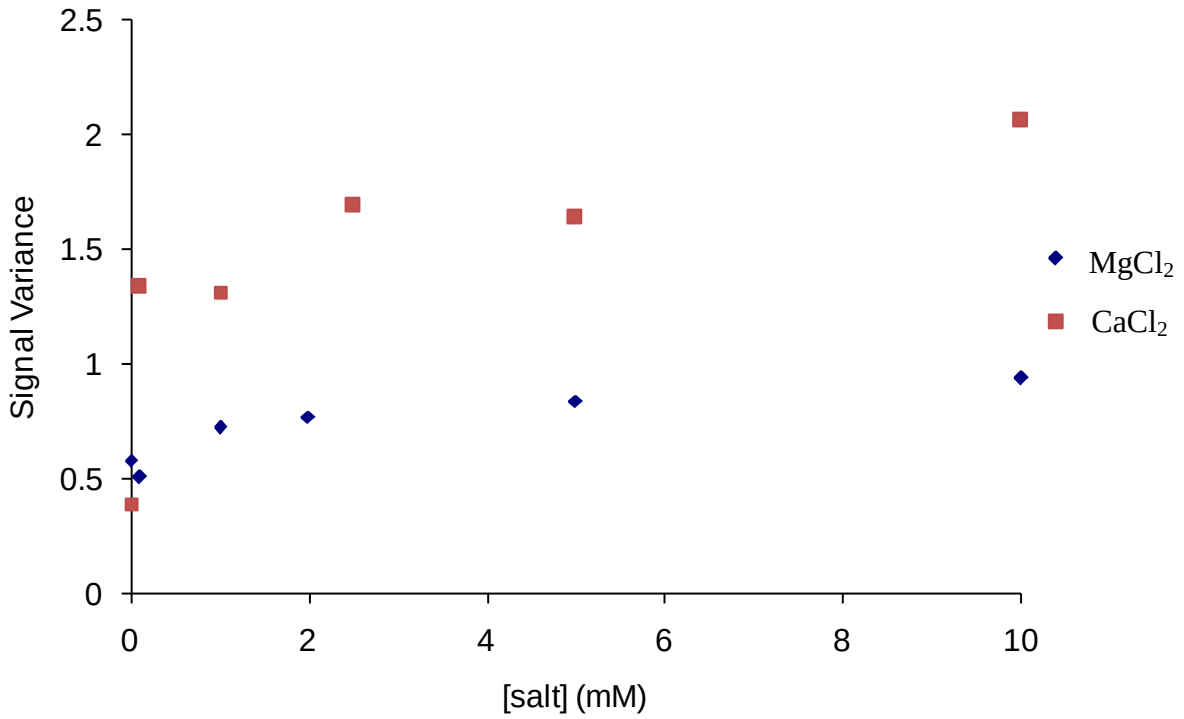

Figure 4: Comparison of the variance in floc homogeneity as determined by the degree of variance in the PDA output signal (plateau value) for $MgCl_2$ and $CaCl_2$ addition to pitch dispersions.

In order to study the deposition of pitch dispersions onto different surfaces, two model surfaces were prepared: a hydrophilic glass surface and hydrophobic silanised glass surface. The contact angle of a water droplet on each surface was measured to confirm the hydrophobicity of each surface. A contact angle of 18^o, in air, was measured for the hydrophilic surface while a contact angle of 118^o was measured for the trimethylchlorosilane treated surface. The hydrophobic model surface represents the many polymeric surfaces found on a paper machine including the wires, felts, doctor blades and rolls. Droplets of neat pitch placed onto the two model surfaces in air formed a contact angle of 18° for both surfaces (Figure 5). It is apparent from the contact angle measurements in air that the surface has little or no effect on the contact angle of pitch in the absence of water.

Figure 5: Contact angle of a neat pitch droplet on a model hydrophobic surface in air (18°). The pitch extractive is liquid at room temperature.

The deposition of aqueous pitch colloidal suspensions onto the two model surfaces was studied using impinging jet microscopy. The rate of deposition was assessed by counting the total number of particles on the surface at various times. The type of electrolyte in the pitch suspension was varied. The typical deposition pattern of pitch particles onto the glass surface (hydrophilic) from pitch suspension containing 20 mM of $MgCl_2$ and 20 mM $CaCl_2$, respectively, is shown in Figures 6A and 6B. For both salts, pitch deposits as distinct droplets on the hydrophilic glass surface. These droplets may be distinguished from the background via the ring encircling the particles from the reflection of light and the difference in refractive indices between water and pitch. The presence of these droplets indicates a high contact angle between the surface and the pitch.

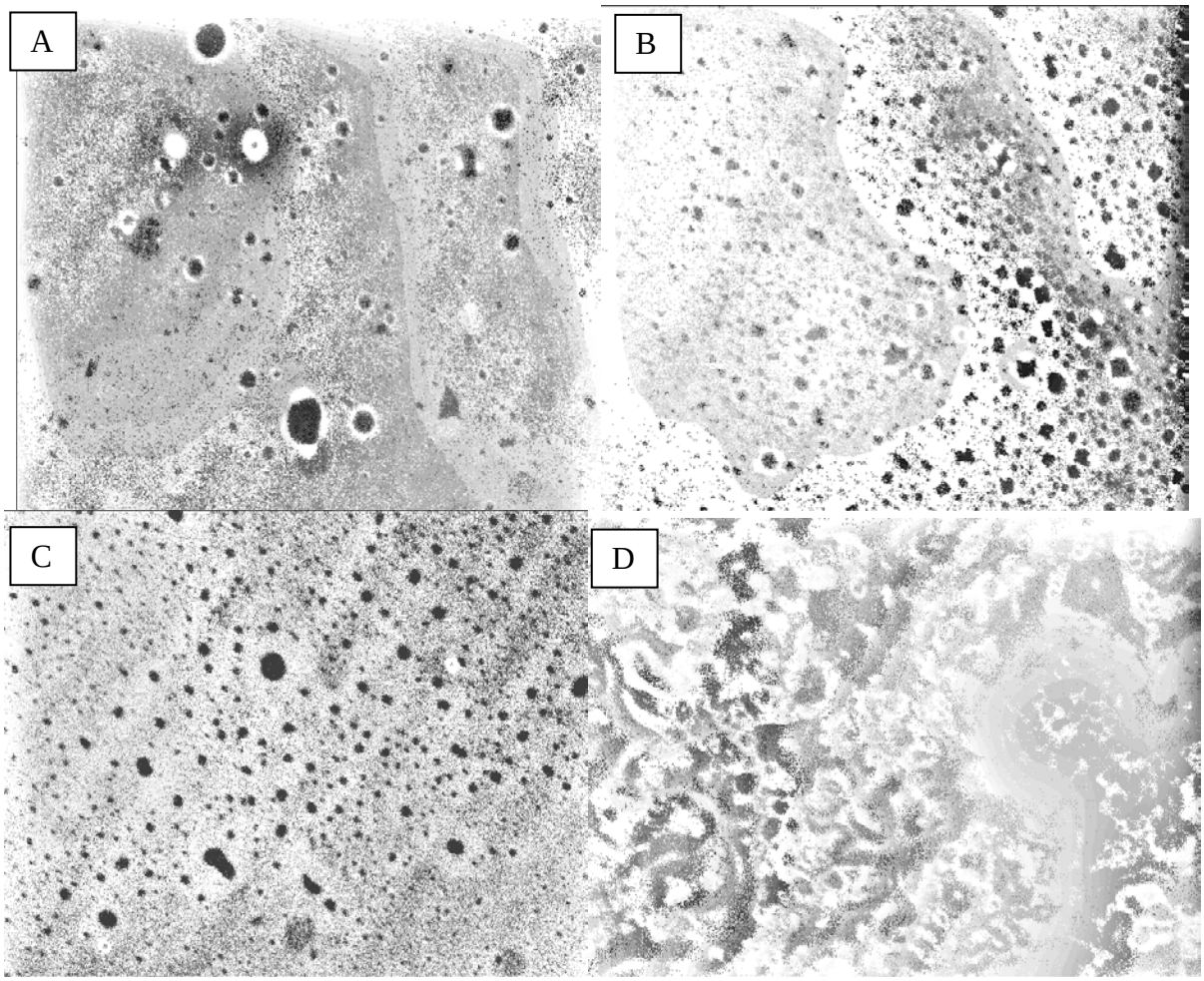

Figure 6: View of pitch particle deposition through impinging jet. (A) Shows pitch particles deposited with 20 mM $MgCl_2$ onto the model hydrophilic surface. (B) Pitch particles deposited with 20 mM $CaCl_2$ onto the model hydrophilic surface. (C) Pitch particles with 20 mM $CaCl_2$ deposited onto the model hydrophobic surface. (D) Pitch particles deposited with 20 mM $CaCl_2$ onto the model hydrophobic surface showing an oil layer that appeared after a period of time.

The deposition of pitch onto a hydrophobic surface is shown in Figure 6C and 6D. It can be seen from the absence of the “halo” around the particles that the droplets do not retain their shape but wet the hydrophobic surface and hence have a low contact angle. Over a period of time the deposited pitch formed an oil film on the hydrophobic surface as seen in Figure 6D. This phenomenon was not observed with the model hydrophilic

surface even for prolonged periods. The effect is known as film thinning. The oil film was found to obscure measurement of the rate of pitch deposition. The surface was cleaned after each run to overcome this effect.

Figure 7 presents the effect of salt on the average size of pitch particles on the two model surfaces after 60 sec of deposition. Four observations are of interest. First, the particles on the hydrophilic surfaces are smaller than those on the hydrophobic surfaces. Second, there are little or no differences in particle size (pitch with $MgCl_2$ or $CaCl_2$) observed for the model hydrophilic surface. Third, the large difference between the hydrophobic surfaces for the calcium and magnesium salts is related to the amount of film thinning or the effect of wetting. Last, more film thinning was observed for pitch with the calcium salt; as a result, a larger average particle size was measured with a larger variation in the particle size as indicated by the error bars.

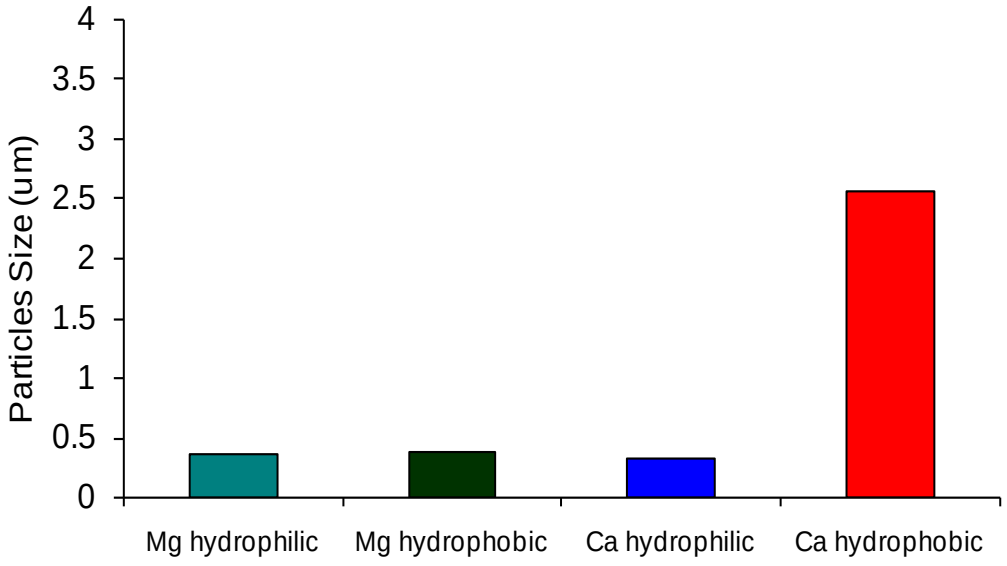

Figure 7: Comparison of average particle size for the deposited pitch after 60 sec of deposition onto a hydrophilic and hydrophobic surface with calcium and magnesium salts.

Particles were found to deposit faster onto the hydrophobic surface compared to the hydrophilic surface (Figure 8). The rate of pitch deposition corresponds to the ratio of particles /time and was measured as the slope of the best fit lines in Figure 8. On the hydrophilic surface, the pitch deposition rate in the presence of magnesium (Mg) was 41 counts/sec and this increased to 103 counts/sec with changing to a hydrophobic surface. This represented a 2.5 times increase in particle-surface interaction. On both model surfaces the pitch deposition was faster in the presence of calcium salt (Ca). The rate of deposition was 62 counts/sec, for the hydrophilic surface, and 115 counts/sec, for the hydrophobic surface, representing a 1.8 fold increase.

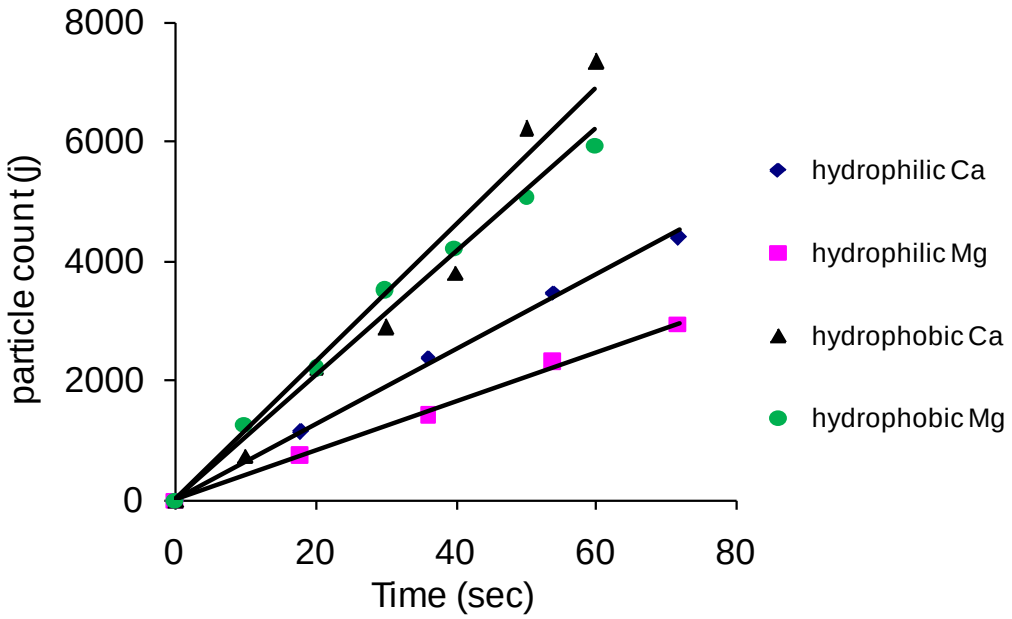

Figure 8: Flux of particles to the surface with different salt types ($CaCl_2$ and $MgCl_2$) and surface conditions (hydrophobic and hydrophilic).

Discussion

The wood resin dispersions deposited on the surfaces were measured at pH of 5.5, which is below the pKa's of the resin acid (7.1-7.3), the saturated fatty acid (7.1-10.2), and the unsaturated fatty acids (6.8-8.3) [43]. At this pH, pitch is mostly un-ionised possessing a minimum negative charge [44]. The molecules forming the pitch colloids contain a small hydrophilic head group (carboxylic acid) and a long hydrophobic tail. The low contact angle observed for neat pitch on both the hydrophilic and hydrophobic surfaces in air (Figure 5) suggests that pitch molecules have some ability to reorientate within the colloid in order to be able to strongly interact with both types of surfaces. The molecules can reorientate themselves so that the polar group interacts with a hydrophilic surface or the non-polar groups can orientate toward the hydrophobic surface.

From the observations with the impinging jet experiments, different behaviour occurs in water compared to the air environment as the shape of the droplets were quite different for the two different surfaces. The wood resins have a lower affinity for the hydrophilic surface in water compared to in air. This suggests that the orientation of the constituent molecules of pitch in a water environment is restricted by the water-pitch interactions. Similar results were obtained by Kallio et.al. who measured the spreading and adhesion of lipophilic extractives onto different surfaces [45]. They also noted that the interfacial tension of pitch with aqueous solutions was affected by the presence of calcium in solution [46]. Figure 9 shows a pictorial representation of the behaviour of the pitch droplets under varying conditions.

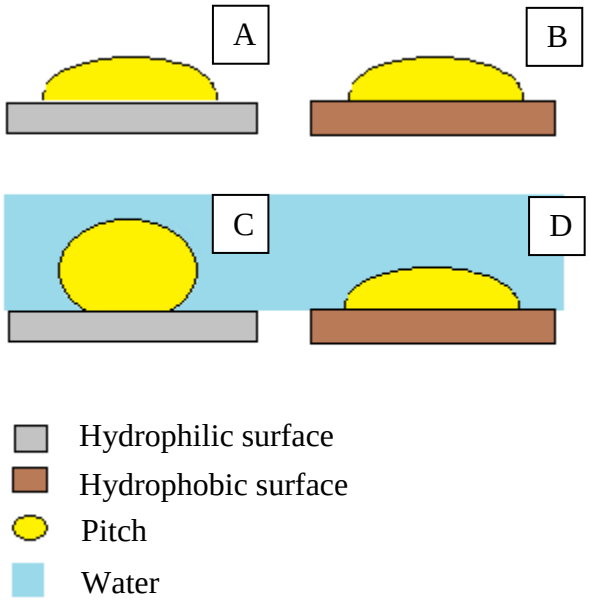

Figure 9: Schematic representation of the pitch droplet shape under various conditions. A: neat pitch on hydrophilic surface in air. B: neat pitch on hydrophobic surface in air. C: pitch deposited onto the hydrophilic surface in aqueous environment through impinging jet microscopy. D: pitch deposited onto the hydrophobic surface in aqueous environment through impinging jet microscopy.

A large difference in colloidal particle size was observed on the hydrophobic surface between the pitch particles with magnesium salts and those with calcium salts. Different behaviours of pitch film thinning were also recorded onto the hydrophobic and hydrophilic surfaces. These observations indicate that the pitch particles are interacting with the surface in different ways. The film thinning observed on the hydrophobic surface enables the pitch particles to conform easily to the surface, gradually forming a complete oil film. In time, this phenomenon obscured the measurement of the particles deposition onto the model surface.

It is proposed that the more hydrophobic components of pitch preferentially migrate toward the solid hydrophobic surface while the more hydrophilic pitch molecules reorient toward the water interface. This reorientation/migration phenomena driven by reduction of the hydrophobic-hydrophilic interface area to minimize the system free energy was

previously observed by Kallio et.al. and Koberstein [46-48]. Combined with this, the small fraction of ionized resin components is able to react with the calcium ions present in solution forming non-polar metal soaps. Because of the hydrophobicity of the colloid core combined with the pitch molecular mobility, the non-polar metal resinates may migrate toward the core of the particles. This reconformation would result in an increased concentration of non-polar components in the particle and the consumption of the resins acids resulting in a more hydrophobic colloid.

As all experiments were conducted above the critical coagulation concentration, the deposition of pitch readily occurred through compression of the electrical double layer promoting aggregation and destabilization of the particles. Deposition occurred on both hydrophobic and hydrophilic surfaces. However, the rate of deposition was linked to the surface polarity/hydrophobicity; the wood resins having higher affinity for the hydrophobic surface. According to Audry et.al. [49], hydrophobization of the glass surface results in reduction of the surface potential. As a result, the electrical field of the double layer associated with the surface is reduced, and hence the repulsive forces is also reduced allowing for greater particle-surface interaction [49] with the interaction being governed by van der Waals forces. In the case of a hydrophilic surface, electrostatic repulsion and a small energy barrier between the pitch particle and the hydrophilic surface reduces the interaction between the pitch and surface. The difference that was found between the rate of deposition for the calcium and magnesium salts suggests that this energy barrier is slightly different for the different soap structures on the pitch surface.

The high salt concentration (800 mg/L) investigated in this study corresponds to the salt levels expected in the process water of a modern pulp and paper mill under a strategy of advanced water recycling. Soluble calcium concentrations of 80-150 mg/L are typical of the levels in many mills' process waters. Our results indicated that the hydrophobic surfaces of the paper machine form oil films at a higher deposition rate (2.5X) than hydrophilic surfaces do. This pitch oil film then adheres to the fibres and minerals of paper, resulting in tacky deposits. However, for the current process, unless magnesium

or calcium alkali and process chemicals are selected instead of the current sodium, the concentrations of magnesium in the process water are below the critical threshold to create deposit issues. The choice of the cation has little effect on pitch deposition on hydrophobic surfaces, but a major impact for hydrophilic surfaces.

Conclusion

The aggregation behaviour of a colloidal wood resin suspension, measured by PDA under dynamic conditions, was similar for calcium and magnesium salts though differences in the homogeneity of the flocs formed were observed. Slight differences in the critical coagulation concentrations were also found with the CCC for calcium and magnesium being 7.8 mM and 6.5 mM respectively.

From contact angle measurements of wood resin droplets onto hydrophilic and hydrophobized glass slides it can be concluded that, in an air environment, the hydrophobicity of the surface does not affect the affinity for pitch. The deposition behaviour of wood resins from an aqueous environment in the presence of divalent salts was found to differ depending on the surface hydrophobicity and salt type.

Pitch deposition was slightly faster for a calcium salt (at 800 mg/L concentration of salt) than magnesium salt at the same concentration onto both a hydrophilic and a hydrophobic surface using impinging jet microscopy. The rate of deposition onto the hydrophobic surface was up to 2.5 times greater than the hydrophilic surface for both salts. Variations in the pitch shape and size occurred on the different surfaces. On a hydrophobic surface the pitch particle size for both salts was 0.33 -0.35 µm while for the hydrophobic surface the particle size was 5 times higher for calcium than magnesium salts. Film thinning or wetting of the pitch colloid occurred on a hydrophobic surface with calcium salt and to a lesser extent with magnesium salt.

It is proposed that the deposition behaviour of wood resin pitch colloids, in different environments, is governed by its ability to undergo molecular reorganisation. Pitch being a soft colloid is able to phase separate and molecularly reorientate to decrease its

free energy upon interaction with its environment. At an air interface, reorientation of the polar and non-polar ends of the fatty acids and resin acid components in the pitch colloid can occur with the groups reorienting themselves in opposite directions depending on the surface hydrophobicity. In an aqueous environment, reorientation of the polar and non polar ends is restricted by the strong interaction between the polar groups and the water environment. Under these conditions surface hydrophobicity is found to play a significant role in the rate of deposition. Metal-resinates that form between divalent cations, such as magnesium and calcium, and the fatty acids and resin acid components also affect the deposition behaviour and the molecular rearrangement within the colloid in different ways. Non polar, insoluble calcium resinates that form are believed to migrate to the hydrophobic core of the pitch colloid decreasing the amount of polar groups at the colloid surface and promoting a higher affinity for hydrophobic surfaces and film thinning compared to magnesium resinates.

Acknowledgments

Financial support for this project was provided by Norske-Skog Paper and an Australian Research Council Linkage grant LP882355. Many thanks to Jean-Phillipe Guay and Alfred Kluck, McGill University Chemistry Department, for technical support.

References

[1] L.H. Allen, P.S. Sennett, C.L. Lapointe, R.E. Truitt, B.B. Sithole, Pitch deposition in newsprint mills using certain kaolin pigments, Tappi Journal 81 (1998) 137.

[2] L.H. Allen, B.B. Sitholé, C.L. Lapointe, R. Truitt, Press roll pitch deposition problems associated with the use of certain clay products in newsprint manufacture, 82nd Annual Meeting, Technical Section, CPPA, 1996, 135.

[3] M.A. Blazey, S.A. Grimsley, G.C. Chen, Indicators for forecasting "pitch season", Tappi Journal 1 (2002) 28.

[4] M. Qin, T. Hannuksela, B. Holmbom, Physico-chemical characterisation of TMP resin and related model mixtures, Colloids and Surfaces A: Physiochemical and Engineering Aspects 221 (2003) 243.

[5] D. Vercoe, K. Stack, A. Blackman, B. Yates, D. Richardson, An innovative approach characterising the interactions leading to pitch deposition, Journal of Wood Chemistry and Technology 24 (2004) 115.

[6] J. Nylund, K. Sundberg, Q. Shen, J.B. Rosenholm, Determionation of surface eneregy and wettability of wood resins, Colloids and Surfaces A: Physiochemical and Engineering Aspects 133 (1998) 261.

[7] B.B. Sitholé, T. Thu Ngoc, L.H. Allen, Quantitative determination of aluminum soaps in pitch deposits, Nordic Pulp and Paper Research Journal 11 (1996) 64.

[8] L.H. Allen, The importance of pH in controlling metal-soap deposition, Tappi Journal 71 (1988) 61.

[9] H. Palonen, P. Stenius, G. Ström, Surfactant behavior of wood resin components. The solubility of rosin and fatty acid soaps in water and in salt solutions, Svensk Papperstidning 85 (1982) 93.

[10] L. Ödberg, S. Forsberg, G. McBride, M. Persson, P. Stenius, G. Ström, Surfactant behavior of wood resin components. part 2. solubilization in micelles of rosin and fatty acids, Svensk Papperstidning 88 (1985) 118.

[11] D. Beneventi, B. Carre, A. Gandini, Precipitation and solubility of calcium soaps in basic aqueous media, Journal of Colloid and Interface Science 237 (2001) 142.

[12] M. Rutland, R. Pugh, Calcium soaps in flotation deinking; fundamental studies using surface force and coagulation techniques, Colloids and Surfaces A: Physiochemical and Engineering aspects 125 (1997) 33.

[13] M. Douek, L.H. Allen, A laboratory test for measuring calcium soap deposition from solutions of tall oil, Tappi Journal (1983) 105.

[14] J. Mosbye, J. Laine, S. Moe, The effect of dissolved substances on the adsorption of colloidal extractives to fines in mechanical pulp, Nordic Pulp and Paper Research Journal 18 (2003) 63.

[15] A.L. Sihvonen, K. Sundberg, A. Sundberg, B. Holmbom, Stability and deposition tendency of colloidal wood resin, Nordic Pulp and Paper Research Journal 13 (1998) 64.

[16] K. Sundberg, C. Pettersson, C. Eckerman, B. Holmbom, Preparation and properties of a model dispersion of colloidal wood resin from Norway spruce, Journal of Pulp and Paper Science 22 (1996) 248.

[17] I. Johnsen, M. Lenes, L. Magnusson, Stabilisation of colloidal wood resin by dissolved material from TMP and DIP, Nordic Pulp and Paper Research Journal 19 (2004) 22.

[18] R. Lee, K.S.D. Richardson, T. Lewis, G. Garnier, AGgregation studies of pinus radiata wood extractives under increased system closure, 65th Appita Conference and Exhibition, Appita, Rotorua, New Zealand, 2011.
[19] Z. Adamczyk, B. Siwek, L. Szyk, M. Zembala, Adsorption of colloid particles affected by hydrodynamic-forces, Bulletin of the Polish Academy of Sciences-Chemistry 41 (1993) 41.
[20] T. van de Ven, The capture of colloidal particles on surfaces and in porous material: basic principles, Colloids and Surfaces. A, Physicochemical and Engineering Aspects 138 (1998) 207.
[21] P. Harwot, T. Van de Ven, Effects of sodium oleate and calcium chloride on the deposition of latex particles on an air/water interface, Colloids and Surfaces A: Physiochemical and Engineering aspects 121 (1997) 229.
[22] T. Van de Ven, S.J. Kelemena, Characterizing polymers with an impinging jet, Journal of Colloid and Interface Science 181 (1996) 118.
[23] R. Pelton, D. Lawrence, A new laboratory approach for evaluating kraft mill pitch deposit control additives, Journal of Pulp and Paper Science 17 (1991) 80.
[24] Xia Z., T. Van de Ven, Adhesion kinetics of phosphatidylcholine liposomes by evanescent wave light scattering, Langmuir 8 (1992) 2938.
[25] M. Kamiti, T. van de Ven, Kinetics of deposition of calcium carbonate particles onto pulp fibres, Journal Pulp and Paper Science 20 (1994) 199.
[26] M. Qin, T. Hannuksela, B. Holmbom, Deposition tendency of TMP resin and related model mixtures, Journal of Pulp and Paper Science 30 (2004) 279.
[27] P. Capek, J. Alfoldi, D. Liskova, An acetylated galactoglucomannan from Picea abies L. Karst, Carbohydrate Research 337 (2002) 1033.
[28] T. Hannuksela, P. Fardim, B. Holmbom, Sorption of spruce O-acetylated galactoglucomannans onto different pulp fibres, Cellulose 10 (2003) 317.
[29] T. Hannusksela, B. Holmbom, G. Mortha, D. Lachenal, Effect of sorbed galactoglucomannans and galactomannans on pulp and paper handsheet properties, especially strength properties, Nordic Pulp and Paper Research Journal 19 (2004) 237.
[30] S. Willför, P. Rehn, A. Sundberg, K. Sundberg, B. Holmbom, Recovery of water-soluble acetylgalactoglucomannans from mechanical pulp of spruce, Tappi Journal 2 (2003) 27.
[31] I. Johnsen, The impact of dissolved hemicellulose on adsorption of wood resin to TMP fines, Department of Chemical Engineering, Norwegian University of Science and Technology, Trondheim, 2007, 53.
[32] K. Sundberg, J. Thornton, B. Holmbom, R. Ekman, Effects of wood polysaccharides on the stability of colloidal wood resin, Journal of Pulp and Paper Science 22 (1996) 226.
[33] D. Otero, K. Sundberg, A. Blanco, C. Negro, J. Tijero, B. Holmbom, Effects of wood polysaccharides on pitch deposition, Nordic Pulp and Paper Research Journal 15 (2000) 607.
[34] R. Lee, K. Stack, D. Richardson, T. Lewis, G. Garnier, Coagulation kinetics of pitch based wood extractive colloids in the presence of Hemicellulose, 7th International Paper and Coating Chemistry Symposium, Hamilton, Canada, 2009, 187.
[35] D.S. McLean, K.R. Stack, D.E. Richardson, The effect of wood extractives composition, pH and temperature on pitch deposition, Appita Journal 58 (2005) 52.
[36] R. Lee, K. Stack, D. Richardson, T. Lewis, G. Garnier, Photometric dispersion analyser (PDA) to quantify pitch coagulation kinetics, 63rd Appita Annual General Conference, Melbourne, 2009, 259.
[37] R. Lee, K. Stack, D. Richardson, T. Lewis, G. Garnier, Study of pitch colloidal stability using a photometric dispersion analyser, Appita Journal 63 (2010) 387.

[38] A. Gerli, B. Keiser, M. Strand, The use of a flocculation sensor as a predictive tool for paper machine retention program performance, Tappi Journal 83 (2000).
[39] C. Hopkins, J. Ducoste, Characterising flocculation under heterogeneous turbulence, Journal of Colloid and Interface Science 264 (2003) 184.
[40] C. Yang, T. Dabros, D. Li, J. Czarnecki, J.H. Masliyah, A visualizing method for study of micron bubble attachment onto a solid surface under varying physicochemical conditions, Industrial and Engineering Chemistry Research 39 (2000) 4949.
[41] T. Dabro, T. Van de Ven, A direct method for studying particle deposition onto solid surfaces Colloid and Polymer Science 261 (1983) 694.
[42] T. Vandeven, S.J. Kelemena, Characterizing polymers with an impinging jet, Journal of Colloid and Interface Science 181 (1996) 118.
[43] D.S. McLean, D. Vercoe, K.R. Stack, D. Richardson, The pK_a of lipophilic extractives commonly found in *Pinus radiata*, 58th Appita Annual General Conference Proceedings, Canberra, Australia, 2004, 73.
[44] A. Swerin, L. Ödberg, L. Wågberg, Preparation and some properties of the colloidal pitch fraction from a thermomechanical pulp, Nordic Pulp and Paper Research Journal 8 (1993) 298.
[45] T. Kallio, J. Lindfors, J. Laine, P. Stenius, Spreading and adhesion of lipophilic extractives on surfaces in paper machines, Nordic Pulp and Paper Research Journal 23 (2008) 108.
[46] T. Kallio, Interfacial interactions and fouling in paper machines, Laboratory of Forest Products Chemistry, Helsinki University of Technology, Helsinki, 2007.
[47] T. Kallio, J. Kekkonen, Fouling in the paper machine wet end, Tappi Journal 4 (2005) 20.
[48] J.T. Koberstein, Molecular design of functional polymer surfaces, Journal of Polymer Science: Part B: Polymer Physics 42 (2004) 2942.
[49] M.-C. Audry, A. Piednoir, P. Joseph, E. Charlaix, Amplification of electro-osmotic flows by wall slippage: direct measurements on OTS-surfaces, Faraday Discussions 146 (2010) 113.

This article has been removed for copyright or proprietary reasons.

Lee, R., Stack, K., Richardson, D., Lewis, T., G Garnier, G., 2012. Effect of shear, temperature and ph on the dynamics of salt-induced pitch coagulation of wood resin colloids, Colloids and surfaces A: physicochemical and engineering aspects, 396, 106–114.

AGGREGATION STUDIES OF *PINUS RADIATA* WOOD EXTRACTIVES UNDER INCREASED SYSTEM CLOSURE.

Roland Lee[1], Karen Stack[1], Des Richardson[2], Trevor Lewis[1] and Gil Garnier[3]
[1]School of Chemistry, University of Tasmania, Hobart, Tasmania
[2]Norske Skog, Paper Mill, Boyer, Tasmania
[3]Department of Chemical Engineering, Monash University, Victoria

SUMMARY

Within the pulp and paper industry, the recycling of process water to reduce water consumption leads to accumulation of colloidal Material in this water and greater risk of deposition. A major factor in the colloidal stability of these substances, which arise from the wood extractives, is the presence of natural polymers originating from the wood as well as salts that accumulate in the process water as a result of increased system closure. This work explores the factors that affect the stability of wood extractive colloids under varying conditions of ionic strength, ionic valency, shear, pH, mixtures of cations and wood polymers released from *pinus radiata* thermomechanical pulp.

Coagulation of a colloidal wood extractive solution by a single salt was found to follow the Schultz-Hardy rule, with the critical salt coagulation concentration (CCC) strongly influenced by salt valency (z). Changes to both pH and shear experienced by the colloid, were observed to affect the concentration of salt required to destabilise the colloid. However, on addition of a second salt to the solution, the CCC decreased for calcium + sodium in comparison to when only a single salt was present.

Addition of wood polymers to an aqueous dispersion of wood extractives caused two stages of destabilization of the wood extractive colloids, which were separated by an apparently stable region. The behaviour was typical of aggregation by polymers in which polymer bridging at low polymer additions caused firstly colloid destabilization, followed by steric stabilisation of the colloids at medium concentration of the polymer, then depletion flocculation followed finally by depletion stabilization at higher polymer concentrations.

KEYWORDS

wood extractives, pitch, aggregation, photometric dispersion analyzer, critical coagulation concentration, polysaccarides, shear

INTRODUCTION

White water in the pulp and paper process is a complex mixture of naturally occurring substances leached from the wood, additives used to stabilize these substances, inorganic chemicals arising from brightening the pulp and fillers added to the paper. The lipophilic wood extractives that are released from the wood during pulping form soft colloidal substances which are known to deposit throughout the paper mill. To control these naturally occurring substances, it is essential to develop an understanding of the effect that the other components have on the colloids.

The stability of colloidal wood extractives is very dependent on the attractive and repulsive forces that exist between the colloidal particles. Stability is achieved when the repulsive forces are greater than the attractive forces while destabilization and aggregation of the colloids occurs when the repulsive forces are reduced sufficiently for the attractive forces to dominate. The repulsive forces arise from the negative charge on the particles and the resulting redistribution of the ions in solution that form an electrical double layer. The charge on wood extractive colloids comes about from the presence of carboxylic acid groups which will deprotonate and so ionize the colloid as pH is increased *(1)*.

There are several factors that affect the colloidal stability of the wood extractive particles and their aggregation. One of the main factors is the presence of electrolytes. Electrolytes in solution influence the electrical double layer and in some cases, the surface charge. At high electrolyte concentration, the thickness of the electrical double layer is compressed *(2)*. A critical electrolyte concentration, know as the critical coagulation concentration (CCC), exists at which the colloid is completely destabilized. Numerous studies have been undertaken to determine the CCC for a range of salts for wood extractive colloids *(3-5)*. Although there are some differences between the reported values, generally the CCC is highly dependent on the valency of the destabilizing electrolyte *(2, 6)*. An understanding of the effect of increasing salt levels on wood extractive colloidal stability is essential, particularly when most mills are undertaking increased recycling of process water in order to reduce water usage.

Another important factor found to influence the colloidal stability of wood extractives is the presence of dissolved polysaccharides originating from the wood. These polysaccharides have been shown to interact with the wood extractives and significantly affect colloidal stability by stablizing them in solution *(7-11)*. Other factors that influence aggregation and colloidal stability include shear, presence of other additives such as

polymers and the chemical composition of the material in the colloids.

Aggregation of wood extractive colloids has been studied in a number of different ways, including direct deposition measurements *(12-16)*, and counting of pitch particles *(15, 17)*. The kinetics of aggregation of colloidal particles such as wood extractives, under dynamic shear conditions, has also been investigated using a Photometric Dispersion Analyzer (PDA) *(18-25)*. Use of a PDA makes it possible to look at both the growth and distribution of colloid sizes *(22)*.

This paper explores the factors that affect the aggregation of wood extractive colloids from *pinus radiata*. The effect of various salts, shear, pH and polysaccharides are investigated using a PDA to study the aggregation kinetics, stability factor and the CCC of different electrolytes. The effect of multiple salts is also investigated in order to better understand the effect of mixtures of cations that are present in a typical mill situation along with polysaccharides and other substances, all competing and interacting with each other and the wood extractives. A basic understanding of the interactions between all the factors is needed in order to allow the mill to develop strategies to deal with increased wood extractives and other substances that affect their stability with reduced water usage and increased system closure.

EXPERIMENTAL

Materials

All electrolytes used were dissolved in distilled water as stock solutions. Constant volumes were added to the PDA solution with desired concentration of stock solutions, such that the final volume (300 mL) had the required concentration of salt. Salts of $CaCl_2$ and KNO_3 were purchased from BDH at 99.8% purity. NaCl and $Al_2(SO_4)_3$ (99.8%), were obtained from Merck.

A thermomechanical pulp (TMP) from *pinus radiata* was collected from the primary refiners at Norske Skog, Boyer, Tasmania.

Preparation of wood extractives

TMP was freeze dried and soxhlet extracted with hexane. The hexane was removed by rotary evaporation to obtain the neat wood extractives (stored at -4ºC until needed). The composition of the wood extractives is shown in Table 1.

Table 1: Composition of wood extractives from *pinus radiata* (mg/g of dry pulp)

Fatty Acid	Resin Acid	Triglycerides
1.44	6.17	5.89

Aqueous wood extractive dispersions were prepared by dissolving 500 mg of wood extractives in 50 mL acetone (99.5% purity, Chem.- Supply) and adding this to 1500 mL distilled water containing 1 mM KNO_3 with pH adjusted to 5.5 (with 0.5 M HNO_3, BDH). The dispersion was dialysed for 24 hours using cellulose membrane tubing with a molecular mass cut off of 12,000 amu (Sigma-Aldrich D9402-100FT) to remove acetone. The wash water, containing 1 mM KNO_3 adjusted to pH 5.5, was changed every hour for the first 5 hours. Due to sample loss during dialysis final concentration of extractives is in the region of 100 mg/L.

Preparation of extracted wood polymers

Extracted wood polymers were obtained by soxhlet extraction of *pinus radiata* TMP following the procedure of Johnsen *(26)*. The pulp was disintegrated in water at 2% consistency at 60°C for 3 hours, repeating this process up to 5 times after filtering the wet wood fibre. The solution was then concentrated through air drying. This dispersion was dialysed for 24 hours in 1 mM KNO_3 with pH adjusted to 5.5 to remove unwanted material. Dialysis was conducted using a cellulose membrane tubing (Sigma D-9402, 76mm wide, >12,000 MW).

The chemical composition of the wood polymers is shown in Table 2.

Table 2: Chemical Analysis of wood polymers

Carbohydrate	14.3 ± 0.3 mg/g dry pulp
Lignin	1.14 ± 0.03 mg/g dry pulp
total sugars	10.8 ± 1.5 mg/g dry pulp
Cationic Demand mmol/g equiv charge	0.42
galactose: glucose: mannose	0.4: 1: 2.4

Methods

PDA Wood Extractive Aggregation

A Photometric Dispersion Analyzer (PDA 2000, Rank Brothers, Cambridge, UK) was used to monitor the changes in aggregation of the wood extractive colloidal dispersions. The 200 mL solutions were stirred at 500 RPM in a Britt Jar fitted with a 4 cm diameter flat impeller rotor. A

peristaltic pump was used to recirculate the dispersions through the PDA at a flow rate of 70 mL/min.

The instrument was initially calibrated with distilled water and the DC gain control was adjusted to give a DC value of 10 V *(22, 27)*. The turbidity fluctuations of a flowing suspension under controlled shear conditions were recorded by the PDA. The ratio of the root mean square (RMS) of the AC voltage to the DC voltage was monitored as a function of time. Three replicates were measured for each condition. The PDA signal was smoothed using a 40-point moving average.

RESULTS AND DISCUSSION

Critical Coagulation Concentration

The effect of salt concentration and the salt itself (NaCl, $CaCl_2$ and $Al_2(SO_4)_3$) on the aggregation of wood extractive dispersions was studied using a PDA. At the on-set of aggregation with salt addition, there is a linear increase in the PDA output as shown in Figure 1 before the signal stabilizes. This initial PDA slope of aggregation is related to the coagulation constant or stability ratio (W) *(28)*. The stability ratio (W) is determined from the experimental results of the aggregation kinetics by the relationship,

$$W = \frac{k_{fast}}{k_i} \qquad \text{(Eq. 1)}$$

where k_i is the slope orf a particular salt and k_{fast} is the fastest response to the addition of a salt.

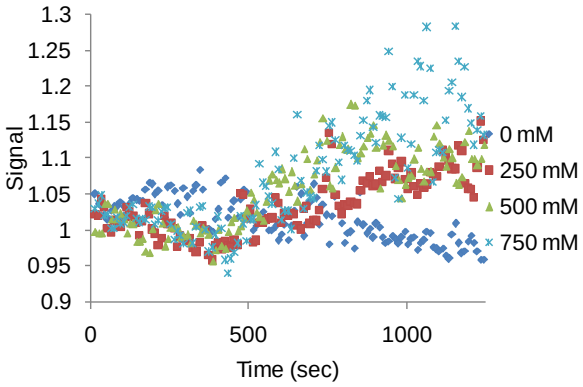

Figure 1: The response of wood extractives to the addition of various concentrations of NaCl.

Figure 2 shows the stability curves for the three salts studied. These are obtained by plotting log W as a function of salt concentration (logarithmic scale). Sigmoidal curves with three distinct regions are observed:

1. an initial flat region at low salt concentration (a stability zone),
2. a region in which Log W decreases rapidly (a transition zone of colloidal instability); and
3. a region in which Log W is 0 at higher salt concentration (complete aggregation of the colloid).

The critical salt concentrations, (CCC), for each salt, determined by extrapolating the slope of the linear transition to the x-axis, are summarized in Table 3.

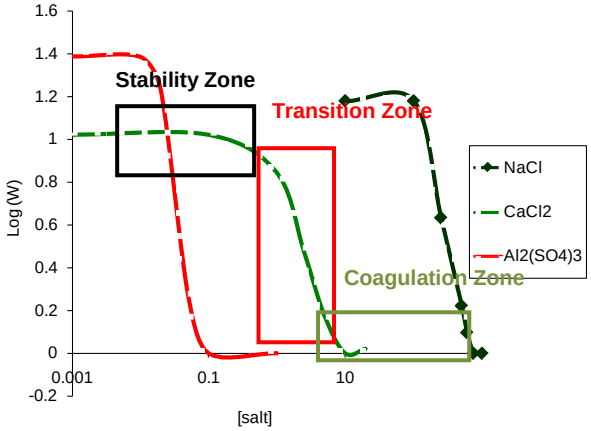

Figure 2: Wood extractive stability curves under dynamic conditions for various electrolytes (pH 5.5, 23°C).

Table 3: Wood extractive Critical Coagulation Concentration (CCC) under dynamic conditions for different electrolytes at pH 5.5.

Salt	CCC (mM)
Na^{+1}	720
Ca^{+2}	7.8
Al^{+3}	0.065

The results in Figure 2 and Table 3 show a strong dependence on the salt valency. The transition in the curves and the CCC values for the monovalent electrolytes occurs at a concentration around two orders of magnitude higher than that of divalent salts and similarly for the trivalent ions compared to divalent ions. A linear relationship between the CCC and cation valency was obtained as shown in Figure 3. The Shultz-Hardy rule predicts the critical coagulation concentration (CCC) to vary inversely with the sixth power of the cation valency (z) *(2)*. The slope for the line of best fit shown in Figure 3 is -8.3. It is debatable whether or not the slope of the relationship in Figure 3 fully supports the Shultz-Hardy's rule that predicts a slope of –6. However, given that the effect of metal ions can be influenced by other side reactions within the solvent not accounted for by the Shultz-Hardy rule, the resulting CCCs appear

to fit reasonably with this theory. Further it can be argued that the discrepancy falls well within experimental error due to the complexity of a non-ideal industrial suspension that is heterogeneous in size, composition and contaminants. The result for the trivalent aluminium ions is a little surprising, given that at the pH investigated, these ions should exist in a number of hydrated forms of varying charge and not strictly in a trivalent form *(29, 30)*.

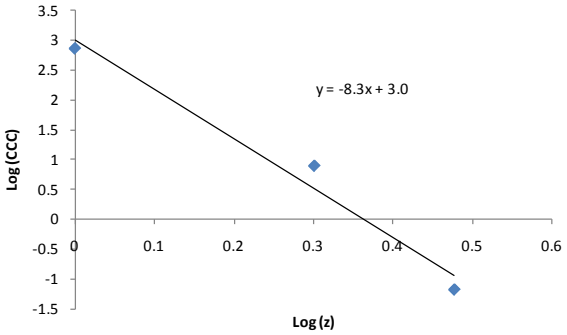

Figure 3: Effect of salt valency on the wood extractives critical coagulation concentration (CCC); pH 5.5 at 23^{o}C and 500 RPM.

It is important for a paper mill to understand where its system is on the stability salt curves. Are they in a region of stability, in a transition region or in a region of complete instability? This information is needed in order to understand how process changes, particularly related to salt concentration, will affect the colloidal stability of the wood extractives. at the Norske Skog Albury mill where water consumption is about 10m^3 per tonne of product cations in white water streams can be around 13 mM for Na^+, and 3 mM for Ca^{2+},. Al^{3+} concentrations, at the Tasman mill (where water consumption is > 20 m^3/tonne of product) can be around 0.06 mM. Although the level of sodium ions is well below its CCC, levels for the divalent and trivalent metal ions are within the transition region of the stability curves shown in Figure 2. This means that the paper mills are operating in critical regions for salt induced coagulation of the wood extractive colloids. Any changes to shear, pH and/or the temperature could induce coagulation and lead to wood extractive deposition.

Factors affecting the CCC

The CCC values obtained in Table 3 appear to be higher for sodium salts than that reported by Sundberg *(4)*, Sihvonen *(3)* and Mosbye *(5)*, while the calcium value appears to be slightly lower than values reported in the literature and summarized in Table 4. It is noted that the experimental conditions and procedures used in the work reported here are different to those in the cited references and that other factors such as pH and shear may also affect the CCC values. The surface charge and composition of wood extractives may also affect the CCC values for different salts. *Pinus radiata* wood extractives are higher in resin acids than Spruce wood extractives. Sihvonen *(3)* found that adding dehydroabietic acid to a model Spruce wood extractive dispersion to increase the amount of resin acids present resulted in an increase in surface charge of the wood extractives and increased the stability of the wood extractive colloids.

Table 4: Summary of wood extractive Critical Coagulation Concentrations (CCC) reported for various electrolytes and pH.

pH	NaCl (mM)	$CaCl_2$ (mM)	$Al_2(SO_4)_3$ (mM)	Reference
5	150	25		*(3)*
	200	10	0.02	*(4)*
5.5	100			*(5)*
6.4	600			*(5)*
8	500	25		*(3)*

To investigate the effect of shear on the CCC, a series of experiments were undertaken in which the salt- induced aggregation kinetics was measured for wood extractive colloids stirred at two different shear rates. Figure 4 shows the effect of increasing the shear rate of the stirred colloidal dispersion from 350 RPM to 500 RPM and the resulting stability curves and CCC values for NaCl. The CCC decreased from 1040 mM at 350 RPM to 720 mM at 500 RPM. The 500 RPM shear condition used in the Britt Jar to agitate the wood extractive dispersions can be equated to a shear force of 2 x 10^3 s^{-1} *(31)* which is equivalent to the shear forces experienced in the pressure screens and wet end of a modern paper machine.

The effect of shear on the CCC, as observed in Figure 4, may explain the differences in CCC for sodium salts reported by Sundberg *et al (4)* and Sihvonen *et al (3)* as different sample agitation methods were reported. When the samples underwent agitation for a short period of time before concentration determination, the CCC for sodium was found to be 200 mM. By contrast, the CCC for wood extractive colloids subjected to continued agitation was found to be 150 mM for sodium.

Coagulation requires two conditions:

1) collision among colloids, and

2) high probability of aggregation upon collision.

Increasing shear will increase the rate of collision and so increase the number of collisions occurring in a set time. This will cause an increase in aggregation rate and higher probability of

aggregation at lower salt concentrations as the shear is increased.

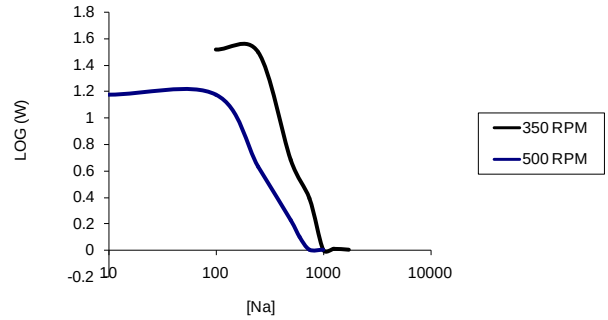

Figure 4: Wood extractive stability curves for various shear rates of sodium (pH 5.5, 23°C).

The effect of pH on colloidal stability at a constant shear was studied using $CaCl_2$ as the destabilizing salt. The results in Figure 5 show that as the pH is increased, the stability curve for the wood extractives shifts to the right, indicating greater stability in solution. In turn the critical coagulation concentration for $CaCl_2$ increases, from 1.7 mM at pH 3, to 7.8 mM at pH 5.5 and then to 12.1 mM at pH 8. These results indicate that at higher pH's more salt can be present in the process water before complete destabilization of the wood extractive colloids occurs. Part of the reason for the behaviour is that as the pH increases the solubility and charge of the colloidal components also increase and this in turn increases the colloidal stability.

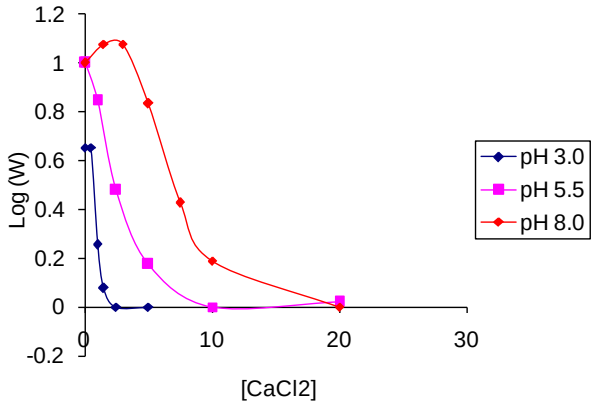

Figure 5: The effect of pH on the stability curve for the effect of $CaCl_2$.

Effect of multiple salts present in solution

A number of different salts exist in mill white water, all of which will affect the stability of the colloid. Although the monovalent salts may dominate, the presence of a small amount of divalent and trivalent salts will have a large impact on the colloidal stability as these salts have much lower CCC values as shown in Figure 2 and Table 3. Most studies are based on investigating the effect of a single salt. The effect of a second salt (sodium) on the CCC of a calcium salt was investigated and the results are shown in Figure 6. Several points can be observed from the results. The first is that as the concentration of the second salt (sodium) is increased the minimum in Log W, representing the CCC decreases. The second observation is that the colloids undergo re-stabilization as the concentrations of both salts increase, indicating that the colloid stability behaviour with multiple salts is complex. The effect of the second salt (sodium) on the CCC of calcium is presented in Table 4.

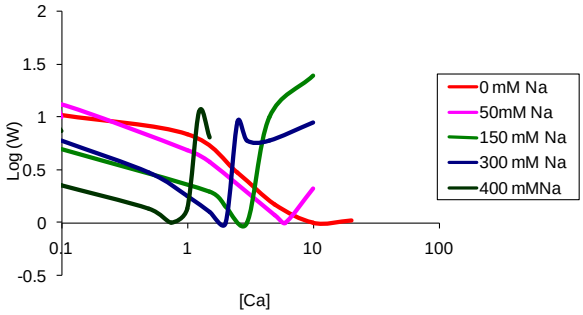

Figure 6: Wood extractive stability curves under dynamic conditions for various concentrations of second electrolyte added to calcium (pH 5.5, 23oC and 500 RPM).

Table 4: Calcium critical coagulation concentrations at different sodium concentrations for wood extractive colloids.

[Na] mM	CCC [Ca] (mM)	Ionic Strength (mM)
0	7.8	22.8
50	6.03	68.1
150	2.96	159
300	2.03	306
400	0.92	403
722	0	722

The results indicate that for a paper mill, in which a number of different salts are present in the white water, the critical salt levels at which the colloids will coagulate exhibit a complex relationship and are not strictly additive for the individual salts or based simply on ionic strength. The non linear effect on the CCC due to the second salt is shown in Figure 7.

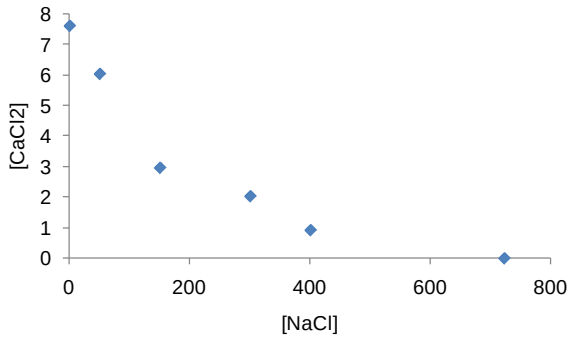

Figure 7: Calcium critical coagulation concentrations in a wood extractive solution with different sodium concentrations.

Effect of other stabilizing substances in solution

Literature indicates that the addition of naturally occurring wood polymers to solution stabilizes the wood extractive colloids *(7-11)*. The effect of dissolved wood polymers from *pinus radiata* TMP on the colloidal stability of *pinus radiata* wood extractives colloids was studied.

Figure 8 shows that at low wood polymer addition (1-10mg/L), destabilization of the colloids occurred. At additions of 10-80mg/L wood polymers, stabilization of the colloids was observed. This behaviour is typical of low polymer additions to solution with destabilization and aggregation of the colloids via bridging flocculation, followed by steric stabilization with polymers anchored to the colloidal surface and at full polymer coverage of the surface *(1)*. At wood polymer additions of 100-400mg/L further destabilization of the colloids occurred followed by a re-stabilization at additions above 400mg/L. Again this behaviour is typical of depletion flocculation and depletion stabilization of synthetic polymers *(1)*. The results indicate that the previously reported *(7-11)* stabilization of wood extractives by wood polymers is more complicated and very much dependent on the level of wood polymers present. It also indicates that increased accumulation of the wood polymers in papermaking process water may be detrimental to the stability of wood extractives at a particular concentration range of 100-400mg/L.

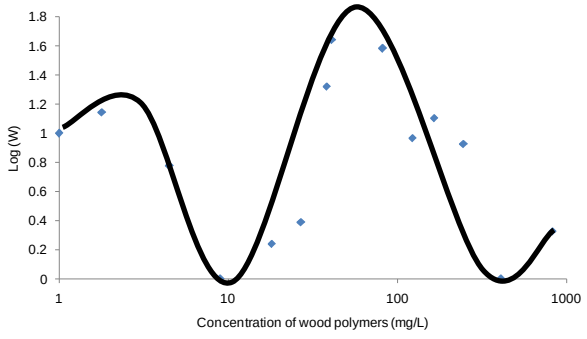

Figure 8: Effect of extracted wood polymers concentration on colloidal wood extractive stability.

CONCLUSIONS

Colloidal stability of wood extractives is affected by many variables in the paper making process. The critical coagulation concentration (CCC) for wood extractives from *pinus radiata* was found to be slightly higher for sodium salts (612mM) and lower for calcium salts (6.6mM) and aluminium salts (0.1mM) than reported in the literature for Spruce extractives.

Both shear and pH were shown to affect the CCC value. Increasing the amount of shear lowered the CCC due to the effect of shear on increasing the rate of collision and aggregation kinetics. Increasing the pH increased the CCC due to increased solubility and surface charge of the colloids increasing colloidal stability.

The presence of a second salt was found to have a greater effect on lowering the CCC and showed that the relationship was not a simple additive one but more complex. The results highlight the importance for papermakers to have a detailed knowledge of all the salt concentrations in the process water and the combined effect on colloidal stability. An important finding of the results in relation to increased water closure and build up of salts in solution, was the re-stabilization of the wood colloids at high salt levels.

The effect of wood polymers on colloidal stability of the wood extractives was dependent on the concentration of the wood polymers. The wood polymers were found to act like synthetic polymers in regards to their ability to both stabilize and destabilize the wood extractive colloids.

For paper mills planning to increase system closure a detailed understanding on the potential increase in levels of dissolved salts and wood polymers and the complex effect they have on wood extractives colloidal stability is essential in order to develop strategies to reduce increased deposition problems.

REFERENCES

1. Hunter, R.J., *Chapter 2 Microscopic Colloidal Behaviour*, in *Introduction to Modern Colloid Science*. 1993, Oxford University Press: Oxford. p. 32-56.
2. Shaw, D.J., *Chapter 8 Colloid stability*, in *Introduction to colloid and surface chemistry*. 1992, Butterworth-Heinemann: Oxford. p. 211-243.
3. Sihvonen, A.L., Sundberg, K., Sundberg, A., and Holmbom, B., Stability and Deposition Tendency of Colloidal Wood Resin. *Nordic Pulp and Paper Research Journal*. **13**(1): 64-67 (1998).
4. Sundberg, K., Pettersson, C., Eckerman, C., and Holmbom, B., Preparation and properties of a model dispersion of colloidal wood resin from

Norway spruce. *Journal of Pulp & Paper Science*. **22**(7): J 248-J 252 (1996).
5. Mosbye, J., Laine, J., and Moe, S., The effect of dissolved substances on the adsorption of colloidal extractives to fines in mechanical pulp. *Nordic Pulp and Paper Research Journal*. **18**(1): 63-68 (2003).
6. Reerink, H. and Overbeek, J.T.G., The rate of coagulation as a measure of the stability of silver iodide sols. *Discussions of Faraday Society*: 74-84 (1954).
7. Otero, D., Sundberg, K., Blanco, A., Negro, C., Tijero, J., and Holmbom, B., Effects of wood polysaccharides on pitch deposition. *Nordic Pulp and Paper Research Journal*. **15**(5): 607-613 (2000).
8. Sundberg, K., Thornton, J., Ekman, R., and Holmbom, B., Interactions between simple electrolytes and dissolved and colloidal substances in mechanical pulp. *Nordic Pulp and Paper Research Journal*. **9**(2): 125-8 (1994).
9. Sundberg, K., Thornton, J., Pettersson, C., Holmbom, B., and Ekman, R., Calcium-Induced Aggregation of Dissolved and Colloidal Substances in Mechanical Pulp Suspensions. *Journal of Pulp and Paper Science*. **20**(11): J317-J322 (1994).
10. Johnsen, I., Lenes, M., and Magnusson, L., Stabilisation of colloidal wood resin by dissolved material from TMP and DIP. *Nordic Pulp and paper Research Journal*. **19**(1): 22-28 (2004).
11. Welkener, U., Hassler, T., and McDermott, M., The effect of furnish components on depositability of pitch and stickies. *Nordic Pulp and Paper Research Journal*. **8**(1): 223-225 & 232 (1993).
12. Vincent, D.L., Studies on Pitch Deposition. *Pulp and Paper Magazine of Canada*: 150-156 (1957).
13. Dykstra, G.M., Hoekstra, P.M., and Suzuki, T. A new method for measuring depositable pitch and stickies and evaluating control agents. *Proc. Proceedings Tappi Papermakers Conference*. Chicago: 1988.
14. Negro, C., Blanco, A., Monte, M., Otero, D., and Tijero, J., Deposibility character of disturbing substances. *Paper Technology*: 29-34 (1999).
15. Allen, L.H., Mechanisms and control of pitch deposition in newsprint mills. *TAPPI Journal*. **63**(2): 81-87 (1980).
16. Stack, K.R., Stevens, E.A., Richardson, D.E., Parsons, T., and Jenkins, S. Factors affecting the deposition of pitch in process waters and model dispersions. *Proc. 52nd Appita Annual General Conference Proceedings*. Brisbane, Australia: 1998.
17. Dubeski, C.V., Branion, R.M.R., and Lo, K.V., Biological treatment of pulp mill wastewater using sequencing batch reactors. *Journal of Environmental Science & Health Part A-Toxic/Hazardous Substances & Environmental Engineering*. **36**(7): 1245-1255 (2001).
18. Zouboulis, A. and Traskas, G., Comparable evaluation of various commercially available aluminium-based coagulants for the treatment of surface water and for the post-treatment of urban wastewater. *J. Chem. Technol. Biotechnol.* **80**: 1136-1147 (2005).
19. Burgess, M., Curley, J., Wiseman, N., and Xiao, H., On-line optical determination of floc size. Part 1: Principles and Techniques. *Journal Pulp and Paper Science*. **28**(2): 63-65 (2002).
20. Kang, L. and Cleasby, J., Temperature effects on flocculation kinetics using Fe(III) Coagulant. *J. Env. Eng*. **121**(12): 893-901 (1995).
21. Xiao, H. and Cezar, N., Organo-modified cationic silica nanoparticles/anionic polymer as flocculants. *Journal of Colloid and Interface Science*. **267**: 343-351 (2003).
22. Hopkins, C. and Ducoste, J., Characterising flocculation under heterogeneous turbulence. *Journal of Colloid and Interface Science*. **264**: 184-194 (2003).
23. Ching, H.-W., Tanaka, T., and Elimelech, M., Dynamics of Coagulation of Kaolin Particles with Ferric Chloride. *Water Resource*. **28**(3): 559-569 (1994).
24. Poraj-Kozminski, A., Hill, R.J., and Van de Ven, T.G.M., Flocculation of starch-coated solidified emulsion droplets and calcium carbonate particles. *Journal of Colloid and Interface Science*. **309**: 99-105 (2007).
25. Fernandes, R., Gonzalez, G., and Lucas, E., Evaluation of polymeric flocculants for oily water systems using a Photometric dispersion analyser. *Colloid Polym. Sci.* **283**: 219-224 (2004).
26. Gerli, A., Keiser, B., and Strand, M., The use of a flocculation sensor as a predictive tool for paper machine retention program performance. *Tappi J.*, (2000).
27. Johnsen, I., *The impact of dissolved hemicellulose on adsorption of wood resin to TMP fines*, in *Department of Chemical Engineering*. 2007, Norwegian University of Science and Technology: Trondheim. p. 53.
28. Gregory, J., Turbidity Fluctuations in Flowing Suspensions. *Journal of colloid and interface science*. **105**(2): 357-371 (1985).
29. Pacewska, B., Keshr, M., and Klukl, O., Influence of aluminium precursor on physico-chemical properties of aluminium hydroxides and oxides Part 1. AlCl3.6H20, . *J. Thermal analysis and calorimetry*. **86**: 351-359 (2006).
30. Pacewska, B., Kluk-Ploskonska, O., and Szychowski, D., Influence of alumnium precursor on physico-chemical properties of aluminium hydroxides and oxides Part II. Al(ClO4)3, 9H20. *J.Thermal Analysis and Calorimetry*. **86**: 751-760 (2006).
31. Tam Doo, P.A., Kerekes, R.J., and Pelton, R.H., Estimates of maximum hydrodynamic shear

stresses on fibre surfaces in papermaking. *Journal Pulp Paper Science*. **10**: J80-J88 (1984).

This article has been removed for copyright or proprietary reasons.

Lee, R., Stack, K., Lewis, T., Garnier, G., Richardson, D., Van de Van, T. Measurement of pitch deposition by impinging jet microscopy: Effect of divalent salts, in: Appita (Ed.) 64th Appita Annual General Conference, Appita, Melbourne, 2010, pp. 273-279.

This article has been removed for copyright or proprietary reasons.

Lee, R., Stack,K., Richardson, D., Lewis, T., Garnier, G., Extracted wood polymers and colloidal pitch stability under high ionic strength. In: 7th International Paper and Coating Chemistry Symposium, Hamilton, Canada, 2009, pp. 187-190 (referred to as"Coagulation kinetics of pitch based wood extractive colloids in the presence of Hemicellulose" in Appendix 6)

AGGREGATION STUDIES OF *PINUS RADIATA* WOOD EXTRACTIVES UNDER INCREASED SYSTEM CLOSURE.

Roland Lee[1], Karen Stack[1], Des Richardson[2], Trevor Lewis[1] and Gil Garnier[3]
[1]School of Chemistry, University of Tasmania, Hobart, Tasmania
[2]Norske Skog, Paper Mill, Boyer, Tasmania
[3]Department of Chemical Engineering, Monash University, Victoria

SUMMARY

Within the pulp and paper industry, the recycling of process water to reduce water consumption leads to accumulation of colloidal Material in this water and greater risk of deposition. A major factor in the colloidal stability of these substances, which arise from the wood extractives, is the presence of natural polymers originating from the wood as well as salts that accumulate in the process water as a result of increased system closure. This work explores the factors that affect the stability of wood extractive colloids under varying conditions of ionic strength, ionic valency, shear, pH, mixtures of cations and wood polymers released from *pinus radiata* thermomechanical pulp.

Coagulation of a colloidal wood extractive solution by a single salt was found to follow the Schultz-Hardy rule, with the critical salt coagulation concentration (CCC) strongly influenced by salt valency (z). Changes to both pH and shear experienced by the colloid, were observed to affect the concentration of salt required to destabilise the colloid. However, on addition of a second salt to the solution, the CCC decreased for calcium + sodium in comparison to when only a single salt was present.

Addition of wood polymers to an aqueous dispersion of wood extractives caused two stages of destabilization of the wood extractive colloids, which were separated by an apparently stable region. The behaviour was typical of aggregation by polymers in which polymer bridging at low polymer additions caused firstly colloid destabilization, followed by steric stabilisation of the colloids at medium concentration of the polymer, then depletion flocculation followed finally by depletion stabilization at higher polymer concentrations.

KEYWORDS

wood extractives, pitch, aggregation, photometric dispersion analyzer, critical coagulation concentration, polysaccarides, shear

INTRODUCTION

White water in the pulp and paper process is a complex mixture of naturally occurring substances leached from the wood, additives used to stabilize these substances, inorganic chemicals arising from brightening the pulp and fillers added to the paper. The lipophilic wood extractives that are released from the wood during pulping form soft colloidal substances which are known to deposit throughout the paper mill. To control these naturally occurring substances, it is essential to develop an understanding of the effect that the other components have on the colloids.

The stability of colloidal wood extractives is very dependent on the attractive and repulsive forces that exist between the colloidal particles. Stability is achieved when the repulsive forces are greater than the attractive forces while destabilization and aggregation of the colloids occurs when the repulsive forces are reduced sufficiently for the attractive forces to dominate. The repulsive forces arise from the negative charge on the particles and the resulting redistribution of the ions in solution that form an electrical double layer. The charge on wood extractive colloids comes about from the presence of carboxylic acid groups which will deprotonate and so ionize the colloid as pH is increased *(1)*.

There are several factors that affect the colloidal stability of the wood extractive particles and their aggregation. One of the main factors is the presence of electrolytes. Electrolytes in solution influence the electrical double layer and in some cases, the surface charge. At high electrolyte concentration, the thickness of the electrical double layer is compressed *(2)*. A critical electrolyte concentration, know as the critical coagulation concentration (CCC), exists at which the colloid is completely destabilized. Numerous studies have been undertaken to determine the CCC for a range of salts for wood extractive colloids *(3-5)*. Although there are some differences between the reported values, generally the CCC is highly dependent on the valency of the destabilizing electrolyte *(2, 6)*. An understanding of the effect of increasing salt levels on wood extractive colloidal stability is essential, particularly when most mills are undertaking increased recycling of process water in order to reduce water usage.

Another important factor found to influence the colloidal stability of wood extractives is the presence of dissolved polysaccharides originating from the wood. These polysaccharides have been shown to interact with the wood extractives and significantly affect colloidal stability by stablizing them in solution *(7-11)*. Other factors that influence aggregation and colloidal stability include shear, presence of other additives such as

polymers and the chemical composition of the material in the colloids.

Aggregation of wood extractive colloids has been studied in a number of different ways, including direct deposition measurements *(12-16)*, and counting of pitch particles *(15, 17)*. The kinetics of aggregation of colloidal particles such as wood extractives, under dynamic shear conditions, has also been investigated using a Photometric Dispersion Analyzer (PDA) *(18-25)*. Use of a PDA makes it possible to look at both the growth and distribution of colloid sizes *(22)*.

This paper explores the factors that affect the aggregation of wood extractive colloids from *pinus radiata*. The effect of various salts, shear, pH and polysaccharides are investigated using a PDA to study the aggregation kinetics, stability factor and the CCC of different electrolytes. The effect of multiple salts is also investigated in order to better understand the effect of mixtures of cations that are present in a typical mill situation along with polysaccharides and other substances, all competing and interacting with each other and the wood extractives. A basic understanding of the interactions between all the factors is needed in order to allow the mill to develop strategies to deal with increased wood extractives and other substances that affect their stability with reduced water usage and increased system closure.

EXPERIMENTAL

Materials

All electrolytes used were dissolved in distilled water as stock solutions. Constant volumes were added to the PDA solution with desired concentration of stock solutions, such that the final volume (300 mL) had the required concentration of salt. Salts of $CaCl_2$ and KNO_3 were purchased from BDH at 99.8% purity. NaCl and $Al_2(SO_4)_3$ (99.8%), were obtained from Merck.

A thermomechanical pulp (TMP) from *pinus radiata* was collected from the primary refiners at Norske Skog, Boyer, Tasmania.

Preparation of wood extractives

TMP was freeze dried and soxhlet extracted with hexane. The hexane was removed by rotary evaporation to obtain the neat wood extractives (stored at -4ºC until needed). The composition of the wood extractives is shown in Table 1.

Table 1: Composition of wood extractives from *pinus radiata* (mg/g of dry pulp)

Fatty Acid	Resin Acid	Triglycerides
1.44	6.17	5.89

Aqueous wood extractive dispersions were prepared by dissolving 500 mg of wood extractives in 50 mL acetone (99.5% purity, Chem.- Supply) and adding this to 1500 mL distilled water containing 1 mM KNO_3 with pH adjusted to 5.5 (with 0.5 M HNO_3, BDH). The dispersion was dialysed for 24 hours using cellulose membrane tubing with a molecular mass cut off of 12,000 amu (Sigma-Aldrich D9402-100FT) to remove acetone. The wash water, containing 1 mM KNO_3 adjusted to pH 5.5, was changed every hour for the first 5 hours. Due to sample loss during dialysis final concentration of extractives is in the region of 100 mg/L.

Preparation of extracted wood polymers

Extracted wood polymers were obtained by soxhlet extraction of *pinus radiata* TMP following the procedure of Johnsen *(26)*. The pulp was disintegrated in water at 2% consistency at 60°C for 3 hours, repeating this process up to 5 times after filtering the wet wood fibre. The solution was then concentrated through air drying. This dispersion was dialysed for 24 hours in 1 mM KNO_3 with pH adjusted to 5.5 to remove unwanted material. Dialysis was conducted using a cellulose membrane tubing (Sigma D-9402, 76mm wide, >12,000 MW).

The chemical composition of the wood polymers is shown in Table 2.

Table 2: Chemical Analysis of wood polymers

Carbohydrate	14.3 ± 0.3 mg/g dry pulp
Lignin	1.14 ± 0.03 mg/g dry pulp
total sugars	10.8 ± 1.5 mg/g dry pulp
Cationic Demand mmol/g equiv charge	0.42
galactose: glucose: mannose	0.4: 1: 2.4

Methods

PDA Wood Extractive Aggregation

A Photometric Dispersion Analyzer (PDA 2000, Rank Brothers, Cambridge, UK) was used to monitor the changes in aggregation of the wood extractive colloidal dispersions. The 200 mL solutions were stirred at 500 RPM in a Britt Jar fitted with a 4 cm diameter flat impeller rotor. A

peristaltic pump was used to recirculate the dispersions through the PDA at a flow rate of 70 mL/min.

The instrument was initially calibrated with distilled water and the DC gain control was adjusted to give a DC value of 10 V *(22, 27)*. The turbidity fluctuations of a flowing suspension under controlled shear conditions were recorded by the PDA. The ratio of the root mean square (RMS) of the AC voltage to the DC voltage was monitored as a function of time. Three replicates were measured for each condition. The PDA signal was smoothed using a 40-point moving average.

RESULTS AND DISCUSSION

Critical Coagulation Concentration

The effect of salt concentration and the salt itself (NaCl, $CaCl_2$ and $Al_2(SO_4)_3$) on the aggregation of wood extractive dispersions was studied using a PDA. At the on-set of aggregation with salt addition, there is a linear increase in the PDA output as shown in Figure 1 before the signal stabilizes. This initial PDA slope of aggregation is related to the coagulation constant or stability ratio (W) *(28)*. The stability ratio (W) is determined from the experimental results of the aggregation kinetics by the relationship,

$$W = \frac{k_{fast}}{k_i} \qquad \text{(Eq. 1)}$$

where k_i is the slope orf a particular salt and k_{fast} is the fastest response to the addition of a salt.

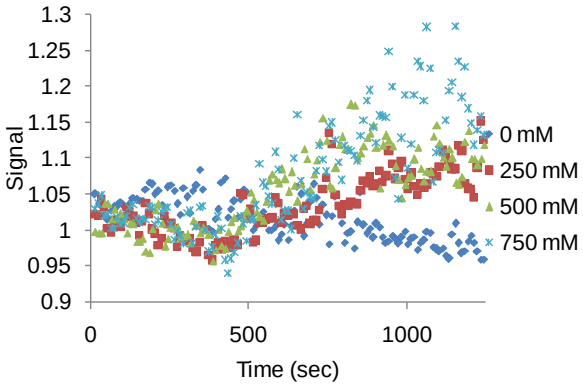

Figure 1: The response of wood extractives to the addition of various concentrations of NaCl.

Figure 2 shows the stability curves for the three salts studied. These are obtained by plotting log W as a function of salt concentration (logarithmic scale). Sigmoidal curves with three distinct regions are observed:

1. an initial flat region at low salt concentration (a stability zone),
2. a region in which Log W decreases rapidly (a transition zone of colloidal instability); and
3. a region in which Log W is 0 at higher salt concentration (complete aggregation of the colloid).

The critical salt concentrations, (CCC), for each salt, determined by extrapolating the slope of the linear transition to the x-axis, are summarized in Table 3.

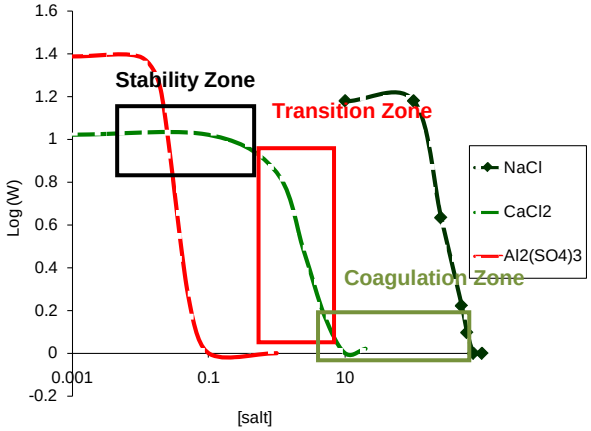

Figure 2: Wood extractive stability curves under dynamic conditions for various electrolytes (pH 5.5, 23°C).

Table 3: Wood extractive Critical Coagulation Concentration (CCC) under dynamic conditions for different electrolytes at pH 5.5.

Salt	CCC (mM)
Na^{+1}	720
Ca^{+2}	7.8
Al^{+3}	0.065

The results in Figure 2 and Table 3 show a strong dependence on the salt valency. The transition in the curves and the CCC values for the monovalent electrolytes occurs at a concentration around two orders of magnitude higher than that of divalent salts and similarly for the trivalent ions compared to divalent ions. A linear relationship between the CCC and cation valency was obtained as shown in Figure 3. The Shultz-Hardy rule predicts the critical coagulation concentration (CCC) to vary inversely with the sixth power of the cation valency (z) *(2)*. The slope for the line of best fit shown in Figure 3 is -8.3. It is debatable whether or not the slope of the relationship in Figure 3 fully supports the Shultz-Hardy's rule that predicts a slope of –6. However, given that the effect of metal ions can be influenced by other side reactions within the solvent not accounted for by the Shultz-Hardy rule, the resulting CCCs appear

to fit reasonably with this theory. Further it can be argued that the discrepancy falls well within experimental error due to the complexity of a non-ideal industrial suspension that is heterogeneous in size, composition and contaminants. The result for the trivalent aluminium ions is a little surprising, given that at the pH investigated, these ions should exist in a number of hydrated forms of varying charge and not strictly in a trivalent form *(29, 30)*.

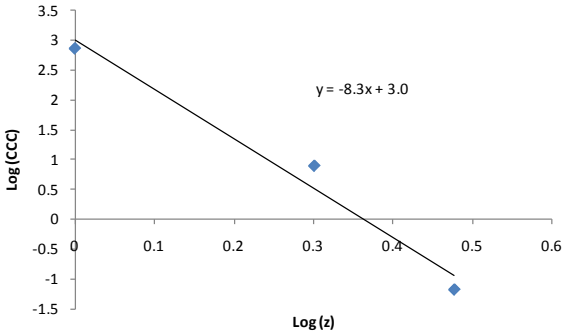

Figure 3: Effect of salt valency on the wood extractives critical coagulation concentration (CCC); pH 5.5 at 23^{o}C and 500 RPM.

It is important for a paper mill to understand where its system is on the stability salt curves. Are they in a region of stability, in a transition region or in a region of complete instability? This information is needed in order to understand how process changes, particularly related to salt concentration, will affect the colloidal stability of the wood extractives. at the Norske Skog Albury mill where water consumption is about 10m^3 per tonne of product cations in white water streams can be around 13 mM for Na^+, and 3 mM for Ca^{2+},. Al^{3+} concentrations, at the Tasman mill (where water consumption is > 20 m^3/tonne of product) can be around 0.06 mM. Although the level of sodium ions is well below its CCC, levels for the divalent and trivalent metal ions are within the transition region of the stability curves shown in Figure 2. This means that the paper mills are operating in critical regions for salt induced coagulation of the wood extractive colloids. Any changes to shear, pH and/or the temperature could induce coagulation and lead to wood extractive deposition.

Factors affecting the CCC

The CCC values obtained in Table 3 appear to be higher for sodium salts than that reported by Sundberg *(4)*, Sihvonen *(3)* and Mosbye *(5)*, while the calcium value appears to be slightly lower than values reported in the literature and summarized in Table 4. It is noted that the experimental conditions and procedures used in the work reported here are different to those in the cited references and that other factors such as pH and shear may also affect the CCC values. The surface charge and composition of wood extractives may also affect the CCC values for different salts. *Pinus radiata* wood extractives are higher in resin acids than Spruce wood extractives. Sihvonen *(3)* found that adding dehydroabietic acid to a model Spruce wood extractive dispersion to increase the amount of resin acids present resulted in an increase in surface charge of the wood extractives and increased the stability of the wood extractive colloids.

Table 4: Summary of wood extractive Critical Coagulation Concentrations (CCC) reported for various electrolytes and pH.

pH	NaCl (mM)	$CaCl_2$ (mM)	$Al_2(SO_4)_3$ (mM)	Reference
5	150	25		*(3)*
	200	10	0.02	*(4)*
5.5	100			*(5)*
6.4	600			*(5)*
8	500	25		*(3)*

To investigate the effect of shear on the CCC, a series of experiments were undertaken in which the salt- induced aggregation kinetics was measured for wood extractive colloids stirred at two different shear rates. Figure 4 shows the effect of increasing the shear rate of the stirred colloidal dispersion from 350 RPM to 500 RPM and the resulting stability curves and CCC values for NaCl. The CCC decreased from 1040 mM at 350 RPM to 720 mM at 500 RPM. The 500 RPM shear condition used in the Britt Jar to agitate the wood extractive dispersions can be equated to a shear force of 2 x 10^3 s^{-1} *(31)* which is equivalent to the shear forces experienced in the pressure screens and wet end of a modern paper machine.

The effect of shear on the CCC, as observed in Figure 4, may explain the differences in CCC for sodium salts reported by Sundberg *et al (4)* and Sihvonen *et al (3)* as different sample agitation methods were reported. When the samples underwent agitation for a short period of time before concentration determination, the CCC for sodium was found to be 200 mM. By contrast, the CCC for wood extractive colloids subjected to continued agitation was found to be 150 mM for sodium.

Coagulation requires two conditions:

1) collision among colloids, and

2) high probability of aggregation upon collision.

Increasing shear will increase the rate of collision and so increase the number of collisions occurring in a set time. This will cause an increase in aggregation rate and higher probability of

aggregation at lower salt concentrations as the shear is increased.

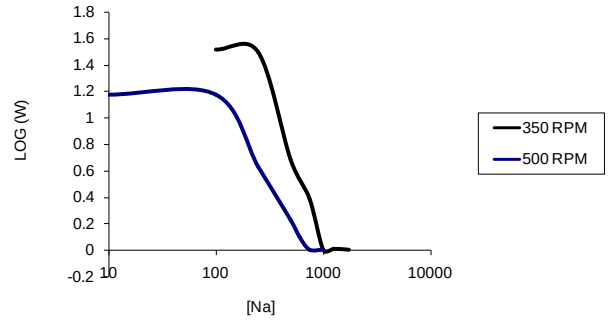

Figure 4: Wood extractive stability curves for various shear rates of sodium (pH 5.5, 23°C).

The effect of pH on colloidal stability at a constant shear was studied using $CaCl_2$ as the destabilizing salt. The results in Figure 5 show that as the pH is increased, the stability curve for the wood extractives shifts to the right, indicating greater stability in solution. In turn the critical coagulation concentration for $CaCl_2$ increases, from 1.7 mM at pH 3, to 7.8 mM at pH 5.5 and then to 12.1 mM at pH 8. These results indicate that at higher pH's more salt can be present in the process water before complete destabilization of the wood extractive colloids occurs. Part of the reason for the behaviour is that as the pH increases the solubility and charge of the colloidal components also increase and this in turn increases the colloidal stability.

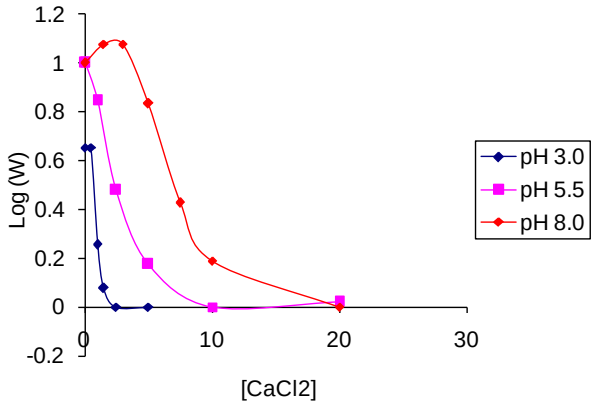

Figure 5: The effect of pH on the stability curve for the effect of $CaCl_2$.

Effect of multiple salts present in solution

A number of different salts exist in mill white water, all of which will affect the stability of the colloid. Although the monovalent salts may dominate, the presence of a small amount of divalent and trivalent salts will have a large impact on the colloidal stability as these salts have much lower CCC values as shown in Figure 2 and Table 3. Most studies are based on investigating the effect of a single salt. The effect of a second salt (sodium) on the CCC of a calcium salt was investigated and the results are shown in Figure 6. Several points can be observed from the results. The first is that as the concentration of the second salt (sodium) is increased the minimum in Log W, representing the CCC decreases. The second observation is that the colloids undergo re-stabilization as the concentrations of both salts increase, indicating that the colloid stability behaviour with multiple salts is complex. The effect of the second salt (sodium) on the CCC of calcium is presented in Table 4.

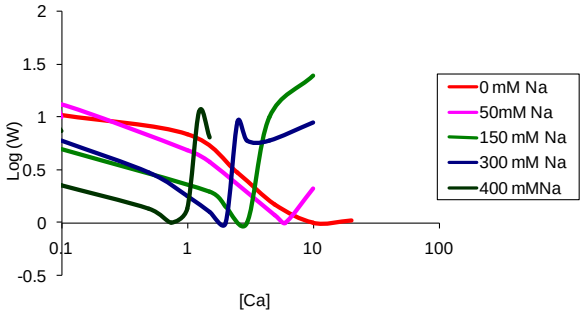

Figure 6: Wood extractive stability curves under dynamic conditions for various concentrations of second electrolyte added to calcium (pH 5.5, 23oC and 500 RPM).

Table 4: Calcium critical coagulation concentrations at different sodium concentrations for wood extractive colloids.

[Na] mM	CCC [Ca] (mM)	Ionic Strength (mM)
0	7.8	22.8
50	6.03	68.1
150	2.96	159
300	2.03	306
400	0.92	403
722	0	722

The results indicate that for a paper mill, in which a number of different salts are present in the white water, the critical salt levels at which the colloids will coagulate exhibit a complex relationship and are not strictly additive for the individual salts or based simply on ionic strength. The non linear effect on the CCC due to the second salt is shown in Figure 7.

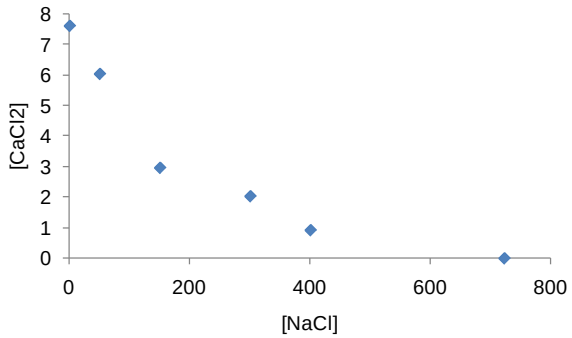

Figure 7: Calcium critical coagulation concentrations in a wood extractive solution with different sodium concentrations.

Effect of other stabilizing substances in solution

Literature indicates that the addition of naturally occurring wood polymers to solution stabilizes the wood extractive colloids *(7-11)*. The effect of dissolved wood polymers from *pinus radiata* TMP on the colloidal stability of *pinus radiata* wood extractives colloids was studied.

Figure 8 shows that at low wood polymer addition (1-10mg/L), destabilization of the colloids occurred. At additions of 10-80mg/L wood polymers, stabilization of the colloids was observed. This behaviour is typical of low polymer additions to solution with destabilization and aggregation of the colloids via bridging flocculation, followed by steric stabilization with polymers anchored to the colloidal surface and at full polymer coverage of the surface *(1)*. At wood polymer additions of 100-400mg/L further destabilization of the colloids occurred followed by a re-stabilization at additions above 400mg/L. Again this behaviour is typical of depletion flocculation and depletion stabilization of synthetic polymers *(1)*. The results indicate that the previously reported *(7-11)* stabilization of wood extractives by wood polymers is more complicated and very much dependent on the level of wood polymers present. It also indicates that increased accumulation of the wood polymers in papermaking process water may be detrimental to the stability of wood extractives at a particular concentration range of 100-400mg/L.

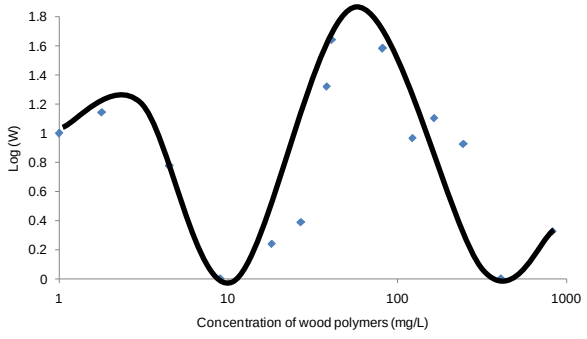

Figure 8: Effect of extracted wood polymers concentration on colloidal wood extractive stability.

CONCLUSIONS

Colloidal stability of wood extractives is affected by many variables in the paper making process. The critical coagulation concentration (CCC) for wood extractives from *pinus radiata* was found to be slightly higher for sodium salts (612mM) and lower for calcium salts (6.6mM) and aluminium salts (0.1mM) than reported in the literature for Spruce extractives.

Both shear and pH were shown to affect the CCC value. Increasing the amount of shear lowered the CCC due to the effect of shear on increasing the rate of collision and aggregation kinetics. Increasing the pH increased the CCC due to increased solubility and surface charge of the colloids increasing colloidal stability.

The presence of a second salt was found to have a greater effect on lowering the CCC and showed that the relationship was not a simple additive one but more complex. The results highlight the importance for papermakers to have a detailed knowledge of all the salt concentrations in the process water and the combined effect on colloidal stability. An important finding of the results in relation to increased water closure and build up of salts in solution, was the re-stabilization of the wood colloids at high salt levels.

The effect of wood polymers on colloidal stability of the wood extractives was dependent on the concentration of the wood polymers. The wood polymers were found to act like synthetic polymers in regards to their ability to both stabilize and destabilize the wood extractive colloids.

For paper mills planning to increase system closure a detailed understanding on the potential increase in levels of dissolved salts and wood polymers and the complex effect they have on wood extractives colloidal stability is essential in order to develop strategies to reduce increased deposition problems.

REFERENCES

1. Hunter, R.J., *Chapter 2 Microscopic Colloidal Behaviour*, in *Introduction to Modern Colloid Science*. 1993, Oxford University Press: Oxford. p. 32-56.
2. Shaw, D.J., *Chapter 8 Colloid stability*, in *Introduction to colloid and surface chemistry*. 1992, Butterworth-Heinemann: Oxford. p. 211-243.
3. Sihvonen, A.L., Sundberg, K., Sundberg, A., and Holmbom, B., Stability and Deposition Tendency of Colloidal Wood Resin. *Nordic Pulp and Paper Research Journal*. **13**(1): 64-67 (1998).
4. Sundberg, K., Pettersson, C., Eckerman, C., and Holmbom, B., Preparation and properties of a model dispersion of colloidal wood resin from

Norway spruce. *Journal of Pulp & Paper Science*. **22**(7): J 248-J 252 (1996).
5. Mosbye, J., Laine, J., and Moe, S., The effect of dissolved substances on the adsorption of colloidal extractives to fines in mechanical pulp. *Nordic Pulp and Paper Research Journal*. **18**(1): 63-68 (2003).
6. Reerink, H. and Overbeek, J.T.G., The rate of coagulation as a measure of the stability of silver iodide sols. *Discussions of Faraday Society*: 74-84 (1954).
7. Otero, D., Sundberg, K., Blanco, A., Negro, C., Tijero, J., and Holmbom, B., Effects of wood polysaccharides on pitch deposition. *Nordic Pulp and Paper Research Journal*. **15**(5): 607-613 (2000).
8. Sundberg, K., Thornton, J., Ekman, R., and Holmbom, B., Interactions between simple electrolytes and dissolved and colloidal substances in mechanical pulp. *Nordic Pulp and Paper Research Journal*. **9**(2): 125-8 (1994).
9. Sundberg, K., Thornton, J., Pettersson, C., Holmbom, B., and Ekman, R., Calcium-Induced Aggregation of Dissolved and Colloidal Substances in Mechanical Pulp Suspensions. *Journal of Pulp and Paper Science*. **20**(11): J317-J322 (1994).
10. Johnsen, I., Lenes, M., and Magnusson, L., Stabilisation of colloidal wood resin by dissolved material from TMP and DIP. *Nordic Pulp and paper Research Journal*. **19**(1): 22-28 (2004).
11. Welkener, U., Hassler, T., and McDermott, M., The effect of furnish components on depositability of pitch and stickies. *Nordic Pulp and Paper Research Journal*. **8**(1): 223-225 & 232 (1993).
12. Vincent, D.L., Studies on Pitch Deposition. *Pulp and Paper Magazine of Canada*: 150-156 (1957).
13. Dykstra, G.M., Hoekstra, P.M., and Suzuki, T. A new method for measuring depositable pitch and stickies and evaluating control agents. *Proc. Proceedings Tappi Papermakers Conference*. Chicago: 1988.
14. Negro, C., Blanco, A., Monte, M., Otero, D., and Tijero, J., Deposibility character of disturbing substances. *Paper Technology*: 29-34 (1999).
15. Allen, L.H., Mechanisms and control of pitch deposition in newsprint mills. *TAPPI Journal*. **63**(2): 81-87 (1980).
16. Stack, K.R., Stevens, E.A., Richardson, D.E., Parsons, T., and Jenkins, S. Factors affecting the deposition of pitch in process waters and model dispersions. *Proc. 52nd Appita Annual General Conference Proceedings*. Brisbane, Australia: 1998.
17. Dubeski, C.V., Branion, R.M.R., and Lo, K.V., Biological treatment of pulp mill wastewater using sequencing batch reactors. *Journal of Environmental Science & Health Part A-Toxic/Hazardous Substances & Environmental Engineering*. **36**(7): 1245-1255 (2001).
18. Zouboulis, A. and Traskas, G., Comparable evaluation of various commercially available aluminium-based coagulants for the treatment of surface water and for the post-treatment of urban wastewater. *J. Chem. Technol. Biotechnol.* **80**: 1136-1147 (2005).
19. Burgess, M., Curley, J., Wiseman, N., and Xiao, H., On-line optical determination of floc size. Part 1: Principles and Techniques. *Journal Pulp and Paper Science*. **28**(2): 63-65 (2002).
20. Kang, L. and Cleasby, J., Temperature effects on flocculation kinetics using Fe(III) Coagulant. *J. Env. Eng*. **121**(12): 893-901 (1995).
21. Xiao, H. and Cezar, N., Organo-modified cationic silica nanoparticles/anionic polymer as flocculants. *Journal of Colloid and Interface Science*. **267**: 343-351 (2003).
22. Hopkins, C. and Ducoste, J., Characterising flocculation under heterogeneous turbulence. *Journal of Colloid and Interface Science*. **264**: 184-194 (2003).
23. Ching, H.-W., Tanaka, T., and Elimelech, M., Dynamics of Coagulation of Kaolin Particles with Ferric Chloride. *Water Resource*. **28**(3): 559-569 (1994).
24. Poraj-Kozminski, A., Hill, R.J., and Van de Ven, T.G.M., Flocculation of starch-coated solidified emulsion droplets and calcium carbonate particles. *Journal of Colloid and Interface Science*. **309**: 99-105 (2007).
25. Fernandes, R., Gonzalez, G., and Lucas, E., Evaluation of polymeric flocculants for oily water systems using a Photometric dispersion analyser. *Colloid Polym. Sci.* **283**: 219-224 (2004).
26. Gerli, A., Keiser, B., and Strand, M., The use of a flocculation sensor as a predictive tool for paper machine retention program performance. *Tappi J.*, (2000).
27. Johnsen, I., *The impact of dissolved hemicellulose on adsorption of wood resin to TMP fines*, in *Department of Chemical Engineering*. 2007, Norwegian University of Science and Technology: Trondheim. p. 53.
28. Gregory, J., Turbidity Fluctuations in Flowing Suspensions. *Journal of colloid and interface science*. **105**(2): 357-371 (1985).
29. Pacewska, B., Keshr, M., and Klukl, O., Influence of aluminium precursor on physico-chemical properties of aluminium hydroxides and oxides Part 1. AlCl3.6H20, . *J. Thermal analysis and calorimetry*. **86**: 351-359 (2006).
30. Pacewska, B., Kluk-Ploskonska, O., and Szychowski, D., Influence of alumnium precursor on physico-chemical properties of aluminium hydroxides and oxides Part II. Al(ClO4)3, 9H20. *J.Thermal Analysis and Calorimetry*. **86**: 751-760 (2006).
31. Tam Doo, P.A., Kerekes, R.J., and Pelton, R.H., Estimates of maximum hydrodynamic shear

stresses on fibre surfaces in papermaking. *Journal Pulp Paper Science*. **10**: J80-J88 (1984).

Structure of wood extract colloids and effect of $CaCl_2$ on the molecular mobility

Roland Lee, Karen Stack, Trevor Lewis, Gil Garnier Desmond Richardson, M. Francesca Ottaviani, Steffen Jockusch, Nicholas J. Turro

KEYWORDS: Wood resin, pitch, colloid structure, electron paramagnetic resonance spectroscopy, EPR

SUMMARY: Electron paramagnetic resonance (EPR) was used to study the colloidal structure of model wood extractive colloids composed of a resin acid (abietic acid), a fatty acid (oleic acid) and a triglyceride (triolein). Two nitroxides were chosen as EPR probes to gain a greater understanding of the different regions of the colloid in order to assess the current proposed models of the structure of the wood extractive colloid. A non-polar nitroxide probed non-polar regions of the colloid, such as triglycerides, while a surfactant-type nitroxide probed regions occupied by fatty acids. The effect of varying the amounts of each of the model colloid components on the structure of the colloid and its interaction with the probe was investigated. Results of the EPR study confirm the existence of a hydrophobic core. However, surface tension and EPR results suggest that the outer layer of the colloid is composed of mostly resin acids. It is proposed that a fatty acid layer exists between the resin acids and triglycerides and is sufficiently mobile to move between them. The addition of salt ($CaCl_2$) was found to affect the mobility of molecules at the core of the colloid.

ADDRESSES OF THE AUTHORS:
Roland Lee[1] **(**rolandl@utas.edu.au**), Karen Stack**[1] **(**Karen.Stack@utas.edu.au**), Trevor Lewis**[1] (Trevor.Lewis@utas.edu.au), **Gil Garnier**[2] (gil.garnier@eng.monash.edu.au), **Desmond Richardson**[3] (des.richardson@norskeskog.com), **M.Francesa Ottavianni**[4] (maria.ottavianni@uniurb.it), **Steffen Jockusch**[5] (sj67@columbia.edu), and **Nicholas J. Turro**[5] (njt3@columbia.edu)
[1)] School of Chemistry, University of Tasmania, Private Bag 75, Hobart, 7001,Tasmania, Australia
[2)] Australian Pulp and Paper Institute, Department of Chemical Engineering, Monash University, Monash, Victoria, Australia
[3)] Process Chemistry, Norske Skog Paper Mills (Australia) Ltd, Boyer 7540, Tasmania, Australia
[4)] Department of Earth, Life and Environmental Sciences, University of Urbino, Italy
[5)] Department of Chemistry, Columbia University, USA
Corresponding author: Karen Stack

The wood extractives released from wood during the pulping process have been a major source of deposits for numerous decades. These wood extractives are hydrophobic, and as such form colloidal particles in water, which can aggregate and form deposits called "pitch". The pitch problem continues to be a significant problem for paper manufacturers as paper mills increase system closure and process water recycling in order to reduce water consumption. Increased water recycling results in higher concentrations of wood resins and also salts that destabilise the colloids.

The relative composition of the wood extractives plays a major role in their colloidal stability and determines the deposition tendency and reactivity of the wood resin colloid (Sihvonen et al. 1998, Qin et al. 2003, Qin et al. 2004, McLean et al. 2005, Strand et al. 2011). Different woods are known to have different compositions. *Pinus radiata* contains significant amounts of resin acids while *Picea abies*, also known as spruce, contains very little resin acids and significant amounts of triglycerides (Back, Allen 2000).

A two-layered model for the colloid structure for both *pinus* and spruce wood extracts has been proposed (Qin et al. 2003, Nylund et al. 1998 and Vercoe et al. 2005). This model of the wood extractive colloid depicts the particles as having an inner hydrophobic core consisting of the non-polar components, such as steryl esters and triglycerides, and an outer layer of resin acids and fatty acids (as shown in *Fig 1*). An average-sized colloidal droplet of spruce thermomechanical pulp (TMP) was proposed to have a diameter of 0.24 μm for the interior domain and the thickness for the outer film to be less than 0.01 μm (Qin et al. 2003).

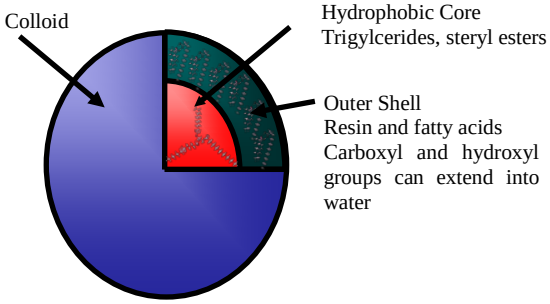

Fig. 1: Two-layered model of the pitch colloid, with non-polar core containing triglycerides and a polar shell made up of fatty acids and resin acids (Vercoe et al. 2005).

The outer layer of the pitch colloid has been reported as determining the surface properties of the resin particles (Nylund et al. 1998, Qin et al. 2003). Nylund et al. (1998), with the use of surface tension measurements, showed that the carboxylic acid head groups of the resin acids and fatty acids orientate to the supernatant solution on account of the extensive acid-base reaction between the colloid and the supernatant solution. Vercoe et al. (2004) showed computationally that different bonding occurred between the fatty acids and the aromatic dehydroabietic acid compared to the other resin acids.

The model, however, does not sufficiently explain some of the trends between pitch problems and triglyceride

levels observed in the paper mill and laboratory (McLean 2003, Stack et al. 2011). Further work is needed to determine if the model needs modifications. In particular the microstructure of the outer polar shell of the pitch colloid has not been elucidated, and the effect of the triglycerides on the surface properties is unexplored.

A number of techniques are available that allow for the structure of colloids to be investigated. For example, several groups have used electron paramagnetic resonance (EPR) to elucidate microenvironments of emulsions, micelles, and other colloidal systems (Fukuda, et al. 2001, Pregetter et al. 1999, Weber et al. 1996, White et al. 2007, Wines et al. 2005 Subramanian et al. 2000). The most common approach is the examination of the changes to the spectra for the free radical spin probe, as the colloidal matrix is changed. Nitroxides, such as 2-(14-carboxytetradecyl)-2-ethyl-4,4-dimethyl-3-oxazolidinyloxy (16-DOXYL stearic acid) and other such free radical probes in aqueous solution, show an isotropic three-line spectrum that is characteristic of highly mobile nitroxide radicals (Weber et al. 1996). Changes in the macroenvironment of a colloid will affect the microenvironment that contains these probes and thus affect the spectrum's amplitude, peak width and shape. The changes to these specific spectrum characteristics can be interpreted in order to better understand alterations to the microscopic environments within the colloid.

With the use of EPR, it is possible to gain information about a number of key physiochemical properties, such as the colloid's chemical substructure, the effect on the chemicals' molecular mobility due to changes in the chemical makeup of these substructures, polarities within the colloid and the changes in the viscosity within these different regions (Weber et al. 1996, White et al. 2007, Wines et al. 2005). Weber et al. (1996) noted through changes to the free movement nitroxide EPR spectrum, that the viscosity of micelle cores could be up to 30 times more viscous than the water phase and 10 to 20 times higher than the mobility of ions near the colloid surface. These viscosities were calculated from the molecular mobility parameter (rotational correlation time) for radical species within the relevant microenvironment and will change as the surfactant chain length and the atomic number of the counter ion are altered. This molecular mobility parameter was also used by Zielinska et al. (2008) to assess the polarity and the viscosity for microemulsions of *N*-alkyl-*N*-methygluconamides as water-in-oil and oil-in-water with *n*-alcohols or *iso*-alcohols as co-surfactants. Other groups have used the molecular mobility parameter in a similar manner to gain a better comprehension of colloidal structures and systems (Wines et al. 2005, Robinson et al. 1999, Chen et al. 2008, Fan et al. 2000, Livshits et al. 1998, Santiago et al. 2007, Livshits, Marsh 2000, Livshits et al. 2003).

At high local concentrations of radicals in solution, the EPR spectra can be affected due to Heisenberg spin exchange. Heisenberg spin exchange is a dynamic isotropic effect due to the collision of radicals at high local concentration. An increase in the local concentration of radicals will result in an increase in the spin – spin exchange and is related to the formation of aggregates of nitroxides in suspension. Nitroxides with a long chain carbon tail also behave as surfactants, and therefore, tend to aggregate in solution at a critical micelle concentration (Ottaviani et al. 1996).

In this paper, the internal geometry of the wood resin colloids formed during the pulping process is examined by placing two different EPR probes of varying polarity into the colloid. This was done to assess the proposed models of the pitch colloids in relation to coordination of the triglycerides, fatty acids and resin acids within the colloid and the alterations pertaining to the addition of salt to the solution.

Materials and Methods

Model Wood Resins

Model wood resins were prepared from oleic acid (technical grade, 90% purity, Sigma-Aldrich), trilinolenin (95% purity, Sigma-Aldrich,) and abietic acid (technical grade, 75% purity, Fluka). *Fig 2* shows the chemical structure of these model compounds.

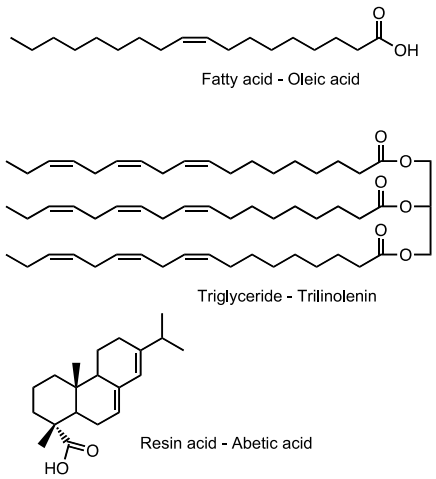

Fig. 2: Chemical structure of model compounds of wood extractive components used in this study.

Extracted Wood Resins

Extracted wood resins (pitch) were collected via soxhlet extraction for 8 hours with hexane (≥99.8% Sigma-Aldrich) of thermomechanical pulp (TMP) from *Pinus radiata*, collected from the primary refiners at Norske Skog, Boyer, Tasmania. The hexane was removed by rotary evaporation and the resulting wood resin was stored at -24°C until required. Table 1 gives the composition of the extracted (real) wood resins as determined by gas chromatography.

Table 1: Composition of hexane extracted (real) wood resins from pinus radiata TMP pulp.

Compound class	Chemical composition (mg/g dry fibre)
Fatty acid	1.5
Resin acid	6.2
Triglycerides	5.9

Pitch Preparation

Aqueous dispersions of thermomechanical pulp (TMP) components were prepared by dissolving the model components or the extracted wood resins with the nitroxide spin labels (for EPR experiments) in acetone (99.5% purity, Chem-Supply) and adding to distilled water at pH adjusted to 5.5. The dispersion was dialyzed using cellulose membrane tubing with a molecular mass cut off of 12,000 amu (Sigma-Aldrich D9402-100FT), to remove acetone. The wash water was pH adjusted with HNO_3 (0.5 M, BDH) to 5.5, and changed every hour for the first 5 hrs and then after 24hrs.

Stock solutions of electrolytes were prepared in distilled water. Constant volumes were added to the EPR solution with desired concentration of stock solutions, such that the final volume had the required concentration of $CaCl_2$, (BDH, 99.8% $CaCl_2$ purity).

EPR Spin Probes

The nitroxide Surfactant-NO (*Fig 3*) was synthesized according to a previous procedure (Bales, Stenland 1992). Non-polar-NO (*Fig 3*) was synthesized from 1,4-dimethylnaphthalene (Futamura, Zong 1992, Barluenga et al.1979, Barluenga et al. 1983).

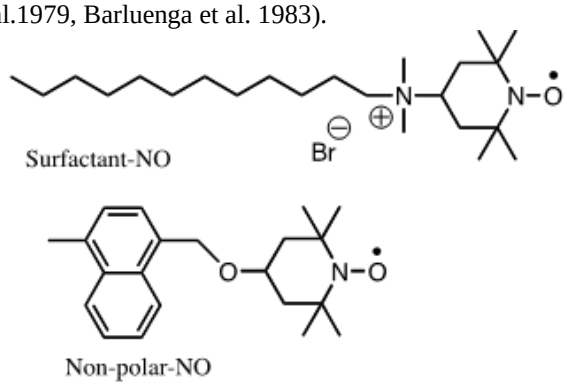

Fig 3: Chemical structure of nitroxide probes used.

EPR Procedures

EPR spectra were recorded on a Bruker EMX spectrometer operating at X band (9.5 GHz) using 1 mm (inner diameter) glass tubes as sample containers. Computation of spectra was accomplished by utilization of the computation program by Budil and Freed (Earle et al. 1996) which takes into account the relaxation process and therefore allows the EPR line shape to be correctly computed. The main parameters extracted from the spectral analysis are:

(a) the g_{ii} components of the **g** tensor for the coupling between the electron spin and the magnetic field;

(b) the A_{ii} components of the coupling tensor between the electron spin and the nuclear nitrogen spin, **A**. For comparison purposes the average value $\langle A_N \rangle = (A_{xx} + A_{yy} + A_{zz})/3$, whose increase is related to an increase in environmental polarity of the radicals, is reported;

(c) the correlation time for the rotational motion of the probe, τ. The Brownian diffusion model ($D_i = 1 / (6\tau_i)$) was assumed in the computation. In this case the main component of the correlation time for motion is the perpendicular one, τ_{perp}, which is thereafter termed, for simplicity, τ. An increase in this parameter corresponds to a decrease in the radical mobility that, in turn, reflects the interactions of the radical with molecules in its surroundings.

In cases where the spectra constitute two spectral components due to spin probes in two motionally different environments, the subtraction of experimental spectra at different relative intensities of the two components is undertaken to extract each component and compute it to obtain the mobility and polarity parameters characteristic of each probe environment. The relative percentages of the two probe populations were obtained from double integration of each component. All EPR experiments were completed with the use of model wood resin components.

Hydrophobisation of glass slides

Glass cover slips (40 mm by 20 mm) were hydrophobised by silylation with 50% hexane (≥99.8% Sigma-Aldrich), 25% pyridine (≥99% Sigma-Aldrich) and 25% trichloromethylsilane (TMCS) (≥99%, Sigma-Aldrich). Slides were placed in solution for 20 min at 60^{O}C, then removed from solution and rinsed with acetone.

Surface tension measurements

Hydrophobic slides were dipped for 10 min into acetone solution of model wood resin components or extracted wood resins, removed from the solution and either placed into H_2O or allowed to air dry.

An Analite surface tension meter (based on the Wilhelmy plate method) was used to measure the surface tension of water with the coated glass slides. The force (F) on the coated length of glass slide due to the adhesion of water was determined from *Eq 1*.

$$\gamma = \frac{F}{2L \cdot \cos\theta} \qquad [1]$$

where F is the force acting on the Wilhelmy plate and is referred to as the Surface Adhesion Force, L is the length of the slide (40 mm) and 2L is the perimeter of the slide at the contact line of the slide with water (neglecting the slide thickness), θ is the contact angle and γ is the surface tension of water (mN/m) when in contact with the glass slide.

Results and Discussion

A series of experiments were undertaken to assess the changes to the EPR spectra of nitroxides when placed within model pitch colloids. To better understand the different regions within the wood resin colloid and the effect of chemical composition on the structure of the colloid, two different probes, the surfactant type Surfactant-NO and Non-polar-NO, were chosen (*Fig 3*). Due to its non-polar nature, it is predicted that the Non-polar-NO would more readily move with the non-polar components of the colloid. This would enable the interactions that the triglycerides and steryl esters undergo within the colloidal matrix and the effect other components have on their mobility to be studied. On the other hand, due to its polar head group and surfactant-type tail, Surfactant-NO would interact with the colloid in a similar manner as the fatty acids. The interaction of the

fatty acids and the bulk components within the colloid could then be determined. This would give an indication of the colloidal shell microstructure, and improve the understanding of the interaction between the fatty acids and the surrounding bulk solution.

The EPR spectrum obtained from the addition of Non-polar-NO to abietic acid, a resin acid found in wood resins, is shown in *Fig 4*. The spectrum depicts a characteristic isotropic three-line EPR spectrum of a freely rotating nitroxide (Weil et al. 1994). The presence of the EPR spectrum shows that nitroxides are still present in solution following dialysis. Given their respective molecular masses, if free in solution, they would be removed through the dialysis with 12,000 amu cellulose tubing. The results suggest that the colloid formed by the resin acid in solution has a relatively large interior volume, in which the molecular mobility of the nitroxide radical is not affected by the abietic acid.

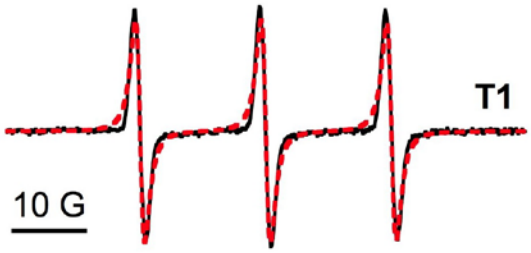

Fig 4: Experimental (black) and computed (red) EPR spectrum of Non-polar-NO at the center a colloid made up of resin acids only (T1) (Colloidal make up and relevant spectrum details can be found in Table 2).

Fig 5 shows EPR spectra of the Non-polar-NO in the presence of pitch colloids made up of resin acid, fatty acid and different amounts of triglyceride. Significant changes occur in the EPR spectra as the amount of triglyceride added to the colloid increases. The presence of two spectral components contributing to T4 spectrum is evident. The second component (broad component) was extracted by subtracting spectrum T1 (absence of fatty acid and triglyceride) from spectrum T2 or T4. This procedure led to calculation of the relative percentages of the two components in the spectra. These components were computed separately to obtain parameters, such as the rotational correlation time τ and coupling constant A_N (see Table 2).

The two spectral components indicate that the probe can be found in two different microenvironments in the colloid. The second spectral component, evident with increasing triglyceride addition, was found to have a higher correlation time τ and smaller coupling constant A_N. The reduced coupling constant and increased correlation time of this second spectral component indicates a less polar and more viscous microenvironment of the radical. As the concentration of the triglyceride increases, the coupling constant further decreases and the percentage of the NO molecules in the less polar microenvironment increases. At the highest level of triglycerides (T4) about 30% of the non-polar nitroxides were found to reside in a highly viscous (τ = 0.53 ns) less polar environment (A_N =15.8 G).

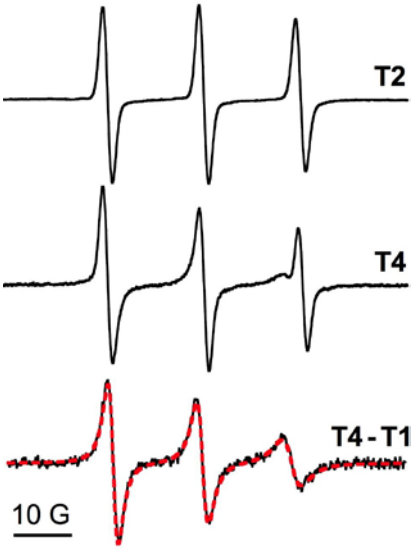

Fig 5: EPR spectra of Non-polar-NO in pitch colloids with variation in the concentration of triglycerides (Colloidal make up and relevant spectrum details can be found in Table 2). Subtracted EPR spectrum (black) of the low mobility component of Non-polar-NO that was generated by subtracting spectrum T1 from spectrum T4. The red line shows the simulated spectrum

Table 2: Colloidal makeup and parameters obtained from the EPR spectra for Non-polar-NO due to changes in the concentration of triglycerides at pH 5.5.

Non-polar-NO	Resin acids (mg/L)	Fatty acids (mg/L)	Triglycerides (mg/L)	τ (ns)	$\langle A_N \rangle$ (G)	%
T1	50	0	0	0.009	17	100
T2	50	16	51.7	0.009	17	78.5
				0.7	16.3	21.5
T4	50	16	246	0.009	17	68.5
				0.53	15.8	31.5

EPR experiments with Surfactant-NO were also performed. It was expected that this surfactant-type nitroxide would interact with the colloid in a similar manner as the fatty acids thus allowing the influence of the fatty acids on the colloid structures to be probed with Surfactant-NO. *Fig 6* (top) shows the EPR spectrum of Surfactant-NO in the presence of resin acid, but without fatty acid and triglycerides (sample F1). The presence of the EPR signal within the sample F1, following dialysis, indicates that Surfactant-NO nitroxides are present and have penetrated the colloids that are formed from abietic acid. Furthermore, as there is no line broadening or amplitude reduction noted for Surfactant-NO when placed in a colloid of resin acid, it can be assumed that its mobility is unaffected by the presence of resin acid in solution. In previous work, surfactant-type nitroxides similar to Surfactant-NO have been observed to form micelles in solution (Ottaviani et al. 1996). As a result of nitroxide molecules being moved into close proximity to each other via this aggregation process, Heisenberg spin exchange has been noted (Porel et al. 2010). However, for the spectra of Surfactant-NO within abietic acid, no spin-spin exchange is seen in *Fig 6*, and, as such, aggregates of the surfactant type nitroxide (Surfactant-NO) are probably not present in solution.

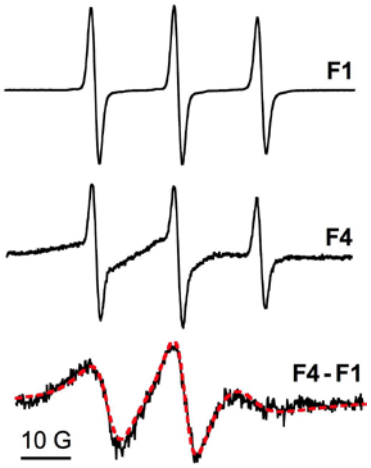

Fig 6: EPR spectra (F1 and F4) of Surfactant-NO in pitch colloids of different compositions. Colloidal makeup and relevant spectrum details can be found in Table 3. Lower spectrum: Subtracted EPR spectrum (black) of the low mobility component of Surfactant-NO that was generated by subtracting spectrum F1 from spectrum F4. The red line shows the simulated spectrum

Addition of triglycerides to the resin acid colloid did not cause any noticeable changes to the spectrum of Surfactant-NO, such as line broadening due to reduction in the mobility of the Surfactant-NO within the colloid. This indicates that Surfactant-NO does not interact with triglycerides under our conditions, which is in sharp contrast to the Non-polar-NO.

Upon addition of increasing amounts of fatty acid to the colloidal matrix, a second spectral component appeared (see *Fig 6*, bottom, for the second component obtained by subtracting spectrum F1 – absence of fatty acid - from spectrum F4). Table 3 summarizes the spectral parameters (τ, A_N, and %) extracted from the computation of the two spectral components. The second spectral component showed a higher rotational correlation time with respect to the first one suggesting a more viscous microenvironment. In addition, the coupling constant of this second spectral component is reduced, indicating a less polar environment. This is consistent with Surfactant-NO residing in the fatty acid residue. From the EPR spectra, it is noted that a significant amount of Surfactant-NO is located within the fatty acid residue and is not interacting with the resin acids. This is consistent with a colloid model, where fatty acids form an independent shell and are separate from the resin acids.

In order to ascertain if the fatty acids make up the outer layer of the colloid or if they are contained within the resin acids, adhesion force measurements were performed. For these experiments hydrophobic glass cover slips were coated with the colloidal components and assessed for their interaction with water. The surface adhesion force for water in contact with a hydrophobic glass slide coated with different pitch components was calculated using surface tension measurements and *Eq 1*. The results in *Fig 7*, show that both the resin acids and fatty acids are more hydrophilic than the hydrophobic glass, as is noted from their higher adhesion force with the solution. However, the resin acids notably have a higher affinity for the water compared to the fatty acid. The surface adhesion force of the pure resin acid with water is the same as that displayed by both the combined resin and fatty acids and the extracted wood resins (real pitch) on the surface. The similarity in the surface adhesion force between the pure resin acid on hydrophobic glass and the combined mixtures of fatty acids (Fa) and resin acids (Ra) suggests that the outer surface of the pitch colloids is made up of mostly resin acids.

Table 3: Colloidal make up and parameters obtained from the EPR spectra for the addition of Surfactant-NO to the colloids at pH 5.5.

Surfactant-NO	Resin acids (mg/L)	Fatty acids (mg/L)	Triglycerides (mg/L)	τ (ns)	$\langle A_N \rangle$ (G)	%
F1	50	0	0	0.05	16.7	100
F2	50	16	0	0.05	16.7	100
F3	50	16	51.7	0.05	16.7	100
F4	50	400	52	0.05	16.7	64.5
				2.65	16.1	35.5
F5	50	790	52	0.05	16.7	33
				2.47	15.9	67

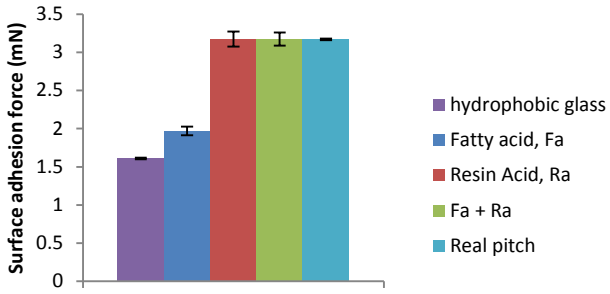

Fig 7: Surface adhesion force with hydrophobic glass and the colloidal components.

The addition of salt, such as $CaCl_2$, to the supernatant solution is assumed to only affect the surface of the colloid in contact with solution. Depending on the rate of coagulation, salt should also influence the rate at which different components within the colloid can move. It is thought that the outer shell of the colloid will be most affected. However, as noted from transmittance microscope images shown in *Fig 8*, the colloid is seen to undergo changes in the size distribution as the composition of the colloid changes but very little change in the size and appearance of the colloid occurs with the addition of $CaCl_2$.

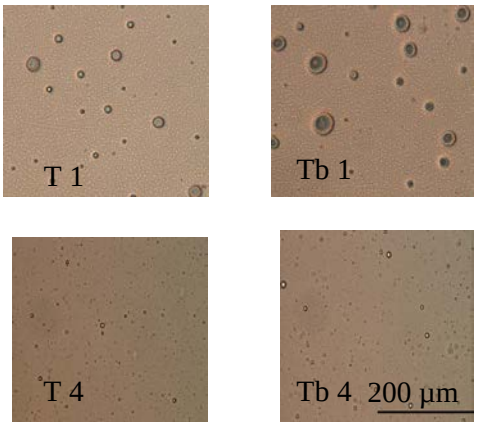

Fig 8: Transmittance microscope image of model pitch colloid particles at 40 x magnification, Left: no electrolytes in solution (Table 2 gives composition of colloids), Right: 2 mM $CaCl_2$ in supernatant solution (Table 4 gives composition of colloids).

To better understand the effect of salt on the structure of the colloid, and hence how the colloidal make up can effect deposition, EPR experiments were performed using Non-polar-NO and Surfactant-NO as probes in the presence of $CaCl_2$. Table 4 shows the colloidal makeup and relevant spectral details for EPR experiment using Non-polar-NO for samples with the addition of 2 mM $CaCl_2$ to the solution. In general, the parameters (τ, A_N, and %) extracted from the EPR spectra with increasing triglyceride concentration follow the same trend as in the absence of salt (Table 2). With increasing concentration of triglyceride a new spectral component appears, where Non-polar-NO resides in a less polar environment with increased viscosity.

As was noted by other groups (Wines et al. 2007, Zielinska et al. 2008, Chen et al. 2008, Ottavini et al. 1998) the viscosity within the microenvironments present in the colloid can be influenced by alterations to the makeup of the colloid or solution. Variations in the colloid's viscosity will result in changes to the mobility of nitroxides and therefore its EPR spectrum. *Fig 9* shows the effect that the addition of triglycerides to the colloid has on the rotational correlation time, the molecular mobility parameter in the presence and absence of 2mM $CaCl_2$. An increase in correlation time corresponds to an increase in viscosity of the microenvironment and a decrease in the molecular mobility of the nitroxide. It is noted from *Fig 9* and Table 4 that following the initial decrease in mobility, as the concentration of triglycerides in the colloid increases, the mobility of molecules in the centre of the colloid begins to increase and the effect is slightly greater in the presence of 2mM $CaCl_2$. The reasons for this behaviour is not clear and needs further investigation.

Fig 10 shows the effect of the addition of fatty acids in the absence and presence of salt (2 mM $CaCl_2$) on the mobility of Surfactant-NO as measured by the correlation time of rotational motion of the probe. It can be seen that the mobility of Surfactant-NO in the fatty acid mobile phase is not influenced by the addition of salt to the solution over the concentration range of fatty acids investigated.

Table 4: Colloidal makeup and parameters obtained from the EPR spectra for Non-polar-NO due to changes to the concentration of triglycerides following the addition of 2 mM of $CaCl_2$ to solution at pH 5.5.

Non-polar-NO + $CaCl_2$	Resin acids (mg/L)	Fatty acids (mg/L)	Triglycerides (mg/L)	τ (ns)	$<A_N>$ (G)	%
TB1	50	0	0	0.02	17.0	100
TB2	50	16	51.7	0.02	17.0	81.5
				0.73	16.2	18.5
TB4	50	16	246	0.02	17.0	55
				0.44	15.8	45

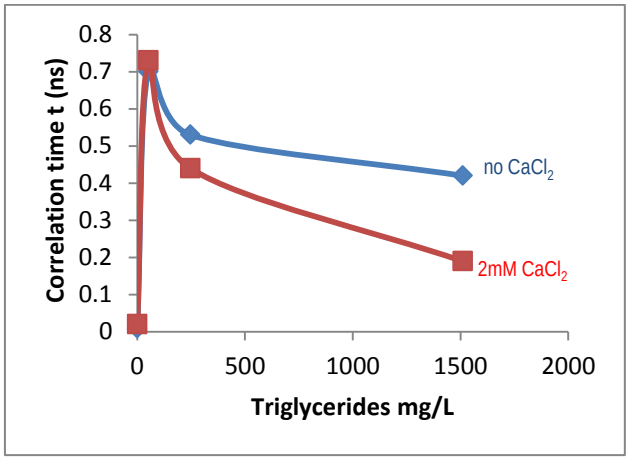

Fig 9: Effect of triglyceride concentration on the correlation time of Non-polar-NO nitroxide radicals in the center of the pitch colloids in the absence and presence of 2mM $CaCl_2$ in the supernatant solution. See Tables 2 and 4 for colloid composition.

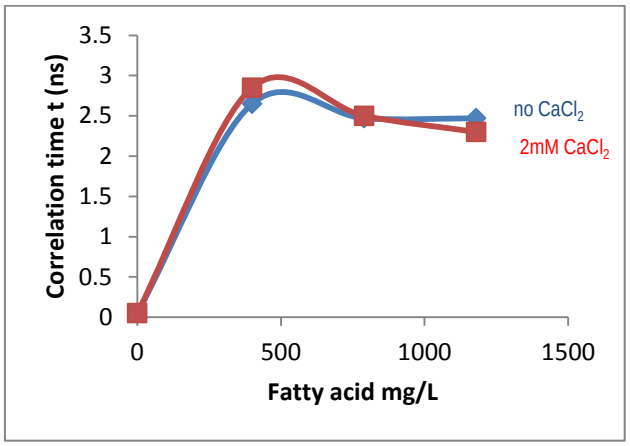

Fig 10: Effect of fatty acid on the mobility of Surfactant-NO nitroxide radicals in the fatty acid shell of the pitch colloids in the absence and presence of 2 mM $CaCl_2$. See Table 3 for colloid composition.

Conclusions

EPR measurements have confirmed that the triglycerides and other non-polar components of the colloid are located in the colloid core, as previously proposed. Surface tension measurements and EPR measurements suggest that the outer layer of the colloid is composed of mostly resin acids. It is proposed that the fatty acids form a mobile layer existing between the hydrophobic core of triglycerides and steryl esters and the outer shell of resin acids. As the triglyceride level changes in the colloid the fatty acid layer moves: at low triglycerides the fatty acids exist closer to the core of the colloid while at high levels of triglycerides in the core, the fatty acids are pushed into the resin acid shell. This modification to the colloid model helps to understand the observed dependence of the colloid behaviour on the triglyceride levels.

The addition of electrolytes to solution affects the mobility of molecules at the colloidal core. However, the mobility of the fatty acid mobile phase is unaffected by this addition.

Acknowledgements

Many thanks to the Australian Research Council and to Norske Skog for funding (LP0882355). The authors at Columbia thank the National Science Foundation of the U.S. for financial support through Grant NSF-CHE-07-17518.

Literature

Back, E. L., Allen, L. H. (2000): Pitch control, wood resin and deresination, Tappi Press, Atlanta.

Bales, B., Stenland, C. (1992): The spin probe-sensed polarity of sodium dodecyl sulfate micelles is proportional to the one-fourth power of the surfactant concentration, Chem. Phys. Lett., 200, 475-482.

Barluenga, J., Alonso-Cires, L., Asensio, G. (1979): Mercury(II) oxide/tetrafluoroboric acid - a new reagent in organic synthesis; a convenient diamination of olefins, Synthesis, 12, 962-964.

Barluenga, J., Ortiz, F. Palacios, F., Gotor, V. (1983): Reactions of ketimines and ethyl phenylpropiolate. Synthesis of 4-oxodihydropyridines, Synthetic Commun., 13, 411-417.

Chen, J., Jayaraj, N., Jockusch, S., Ottaviani, M. F., Ramamurthy, V., Turro, N. (2008): An EPR and NMR study of supramolecular effects on paramagnetic interaction between a nitroxide incarcerated within a nanocapsule with a nitroxide in bulk aqueous media, J. Am. Chem. Soc., 130, 7206-7207.

Earle, K., Budil, D., Freed, J. (1996): Millimeter wave electron spin resonance using quasioptical techniques, Adv. Magn. Opt. Reson., 19, 253-323.

Fan, A., Turro, N., Somasundaran, P. (2000): A study of dual polymer flocculation, Colloids Surf. A, 162, 141-148.

Fukuda, H., Goto, A., Toshioka, H., Goto, R., Morigaki, K., Walde, P. (2001): Electron spin resonance study of the pH induced transformation of micelles to vesicles in an aqueous oleic acid/oleate system, Langmuir, 17, 4223-4231.

Futamura, S., Zong, Z.-M. (1992): Photobromination of side-chain methyl groups on arenes with N-bromosuccinimide – Convenient and selective syntheses of bis(bromomethyl)- and (bromomethyl)methylarenes, B. Chem. Soc. Jpn, 65, 345-348.

Livshits, V., Pali, T., Marsh, D. (1998): Relaxation time determinations by progressive saturation EPR: effects of molecular motion and Zeeman modulation for spin labels, J. Magn. Reson., 133, 79-91.

Livshits, V., Marsh, D. (2000): Spin relaxation measurements using first-harmonic out-of-phase adsorption EPR signals: rotational motion effects, J. Magn. Reson., 145, 84-94.

Livshits, V., Dzikovski, B., Marsh, D. (2003): Anisotropic motion effects in CW non-linear EPR spectra: relaxation enhancement of lipid spin labels, J. Magn. Reson., 162, 429-442.

McLean, D. S. (2003), The effect of wood extractive composition on pitch deposition, PhD thesis, School of Chemistry, University of Tasmania, Hobart, Tasmania, Australia

McLean, D. S., Stack, K. R., Richardson, D. E. (2005): The effect of wood extractives composition, pH and temperature on pitch deposition, Appita J., 58(1), 52-55.

Nylund, J., Sundberg, K., Shen, Q., Rosenholm, J. (1998): Determination of surface energy and wettability of wood resins, Colloids Surf. A., 133, 261-268.

Ottaviani, M. F., Cossu, E., Turro, N., Tomalia, D. (1995): Characterisation of starburst dendrimers by electron paramagnetic resonance. 2. Positively charged nitroxide radicals of variable chain length used as spin probes, J. Am. Chem. Soc., 117, 4387-.

Ottaviani, M. F., Turro, N., Jockusch, S., Tomalia, D. (1996): Characterization of starburst dendrimers by EPR. 3. Aggregational processes of a positively charged nitroxide surfactant, J. Phys. Chem., 100, 13675-13686.

Porel, M. Ottaviani, M. F., Jockusch, S., Jayaraj, N., Turro, N., Ramamurthy, V. (2010): Suppression of spin–spin coupling in nitroxyl biradicals by supramolecular host–guest interactions, Chem. Commun., 46, 7736-7738.

Pregetter, M., Prassel, R., Schuster, B., Kriechbaum, M., Nigon, F., Chapman, J., Laggner, P. (1999): Microphase separation in low density lipoproteins, J. Biol. Chem., 274, 1334-1341.

Qin, M., Hannuksela, T., Holmbom, B. (2003): Physio-chemical characterisation of TMP resin and related model mixtures, Colloids Surf. A., 221(13), 243-254.

Qin, M., Hannuksela, T., Holmbom, B. (2004): Deposition tendency of TMP resin and related model mixtures, J. Pulp Pap. Sci., 30(10), 279-283.

Robinson, B., Mailer, C., Reese, A. (1999): Linewidth analysis of spin labels in liquids, J. Magn. Reson., 138, 199-201.

Santiago, P., Neto, D., Barbosa, L., Itra, R., Tabak, M. (2007): Interaction of meso-tetrakis (4-sulfnatophenyl) porphyrin with cationic CTAC micelles investigated by small angle X-ray scattering (SAXS) and electron paramagnetic resonance (EPR), J. Colloid Interf. Sci., 316, 730-740.

Sihvonen, A. L., Sundberg, K., Sundberg, A., Holmbom, B. (1998): Stability and deposition tendency of colloidal wood resin, Nord. Pulp Paper Res. J.,13(1), 64-67.

Stack, K.R., Lee, R., Zhang, J., Lewis, T.W., Garnier, G., Richardson, D.E. (2011): Colloidal and deposition behaviour of pinus radiate extractives and model colloid systems, 16th ISWFPC, Tianjin, China, 1243-1248.

Strand, A., Sundberg, A., Vähäsalo, L., Holmbom, B. (2011): Influence of pitch composition and wood substances on the phase distribution of resin and fatty acids at different pH levels, J. Disp. Sci. Technol., 32, 702-709.

Subramanian, R., Huang, Y., Zhu, S., Hrymak, A., Pelton, R. (2000): Electron spin resonance study and reactive extrusion of polyacrylamide and polydiallyldimethylammmonium chloride, J. Appl. Polym. Sci., 7, 1154-1164.

Sundberg, K., Pettersson, C. Eckerman, C., Holmbom, B. (1996): Preparation and properties of a model dispersion of colloidal wood resin from Norway spruce, J. Pulp Pap. Sci., 22, 248-252.

Vercoe, D., Stack, K., Blackman, A., Richardson, D. (2004): An innovative approach characterising the interactions leading to pitch deposition, J. Wood Chem. Technol., 24(2), 115-137.

Vercoe, D., Stack, K., Blackman, A., Richardson, D. (2005): A multicomponent insight into the interactions leading to wood pitch deposition, Appita J., 58(3), 208-213.

Weber, S., Wolff, T., von Bunau, G. (1996): Molecular mobility in liquid and in frozen micellar solution: EPR spectroscopy of nitroxide free radicals, J. Colloid Interf. Sci., 184, 163-169.

Weil, J., Bolton, J., Wertz, J. (1994): Electron paramagnetic resonance : elementary theory and practical applications, Wiley-Interscience, NewYork.

White, G., Ottignon, L., Georgiou, T., Kleanthous, C., Moore, G., Thomson, A., Oganesyan, V. (2007): Analysis of nitroxide spin label motion in a protein-protein complex using multiple frequency EPR spectroscopy, J. Magn. Reson., 185, 191-203.

Wines, T., Somasundaran, P., Turro, N., Jockusch, S., Ottaviani, M. F. (2005): Investigation of the mobility of amphiphilic polymer- AOT reverse microemulsion systems using electron spin resonance, J. Colloid Interf. Sci., 285, 318-325.

Zielinska, K., Wilk, K., Jezierski, A., Jesionowski, T. (2008): Microstructure and structural transition in microemulsions stabilised by aldonamide-type surfactants, J. Colloid Interf. Sci., 321, 408-417.